



Photonic Integrated Circuit Tutorial

Jonathan Klamkin

Electrical and Computer Engineering Department

University of California Santa Barbara

klamkin@ece.ucsb.edu

PIC Training NYC

October 19, 2015

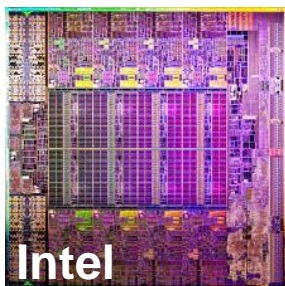
Outline

- **Photonic Integrated Circuits (PICs) background**
- **Integrated passives**
 - Waveguide basics
 - Passive components
 - Example building blocks
- **Integrated actives**
 - Lasers and semiconductor optical amplifiers (SOAs)
 - Modulators
 - Photodetectors
- **Integration platforms and manufacturing**

Photonic Integrated Circuit

Integrated Circuit:

an electronic circuit whose **components** are manufactured in one flat piece of semiconductor material



Transistors

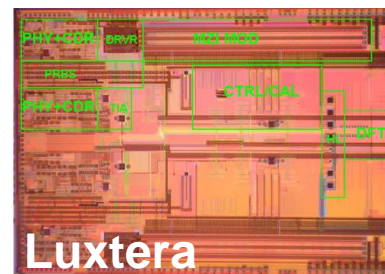
Capacitors

Resistors

Inductors

Photonic Integrated Circuit:

a photonic circuit whose **components** are manufactured in one flat piece of [semiconductor] material



Lasers

Couplers

Modulators

Filters

Photodetectors

Attenuators

Optical amplifiers

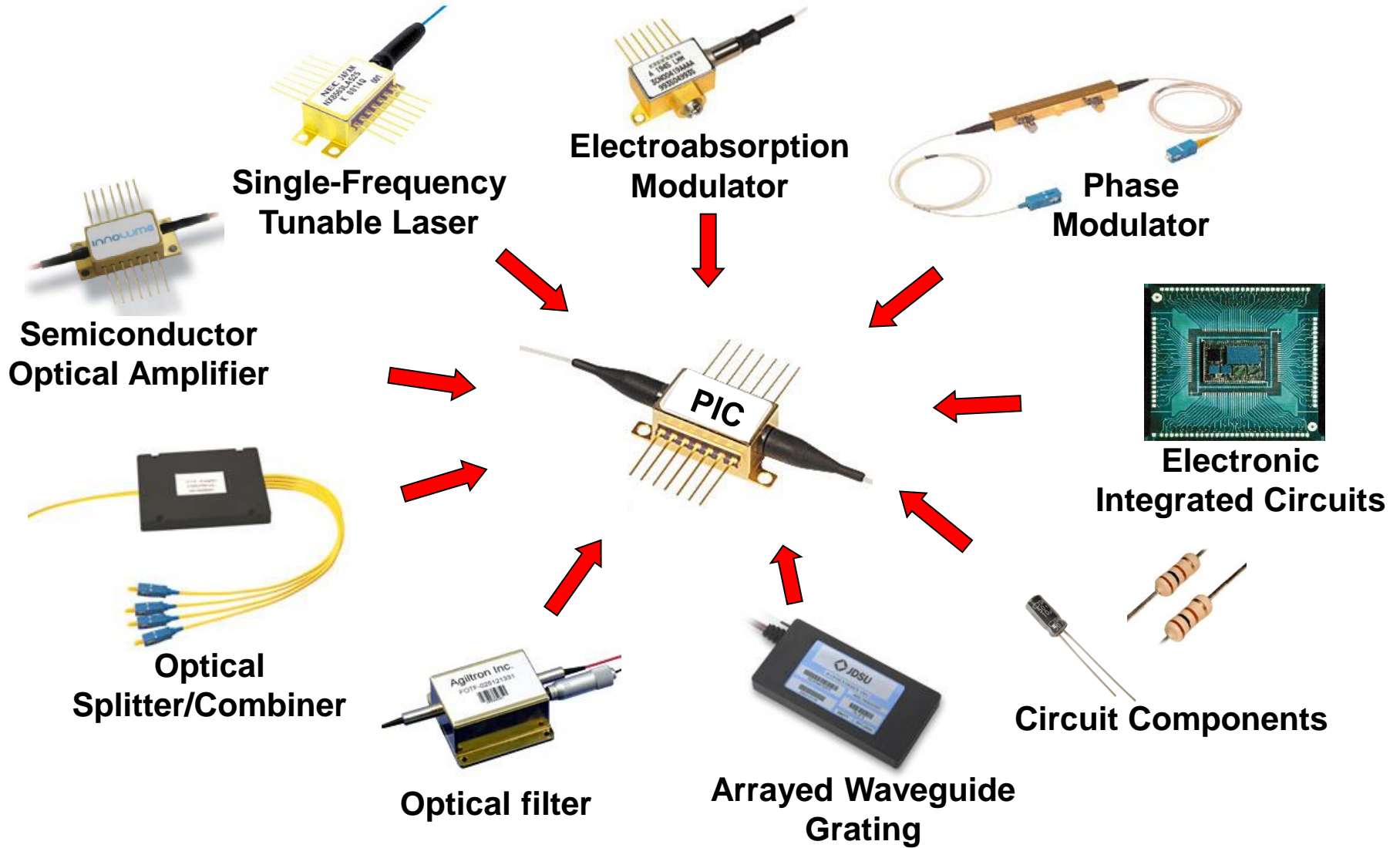
Isolators

Control electronics

Mode converters

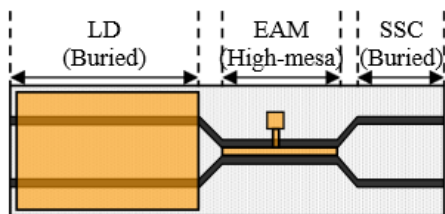
Photonics: generation, emission, transmission, modulation, signal processing, switching, amplification, detection and sensing of light

Photonic Integrated Circuit



Photonic Integrated Circuit Complexity

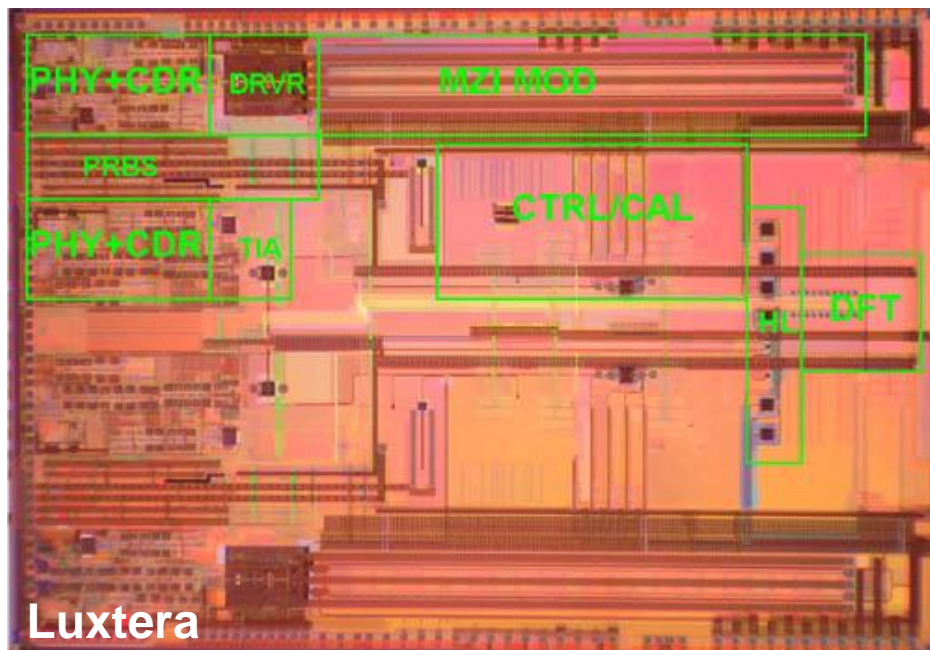
Integrated 28 Gb/s Externally Modulated Laser



Mitsubishi Electric

DFB laser and high-speed EAM

Luxtera 10 Gb/s Optical Transceiver

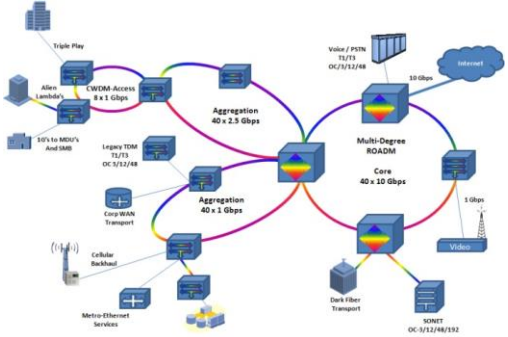


Luxtera

Optical modulators, photodetectors, integrated electro-optical signal conditioning, clock and data recovery, control and calibration circuitry

PIC Applications

Telecommunications



Fiber sensors



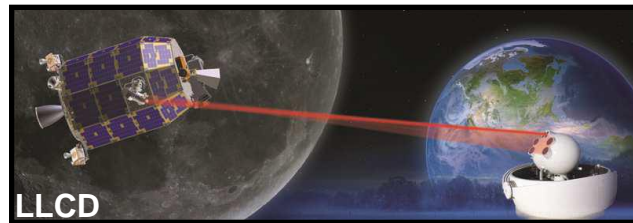
Antenna remoting



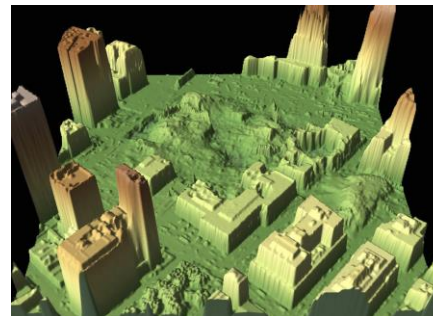
Data communications



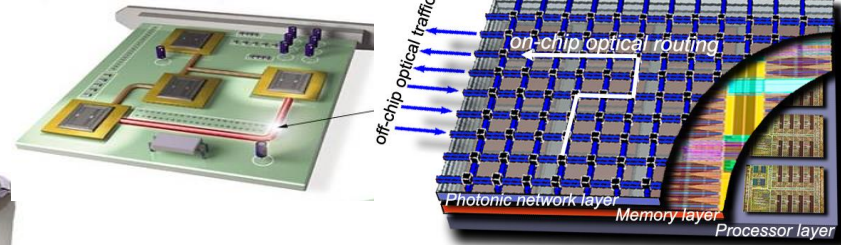
Free-space laser comm.



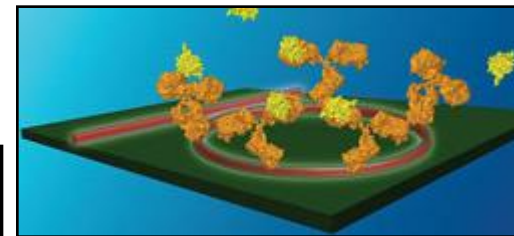
LIDAR



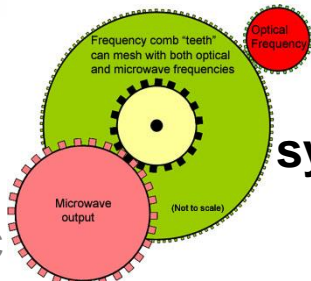
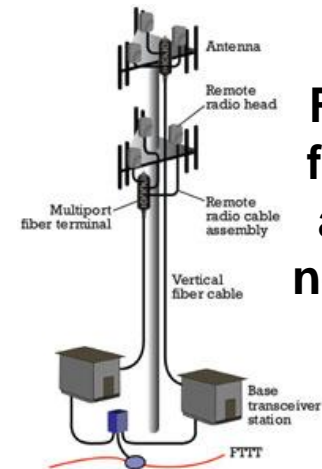
High performance computing



Biophotonic sensors



RF over fiber for access networks

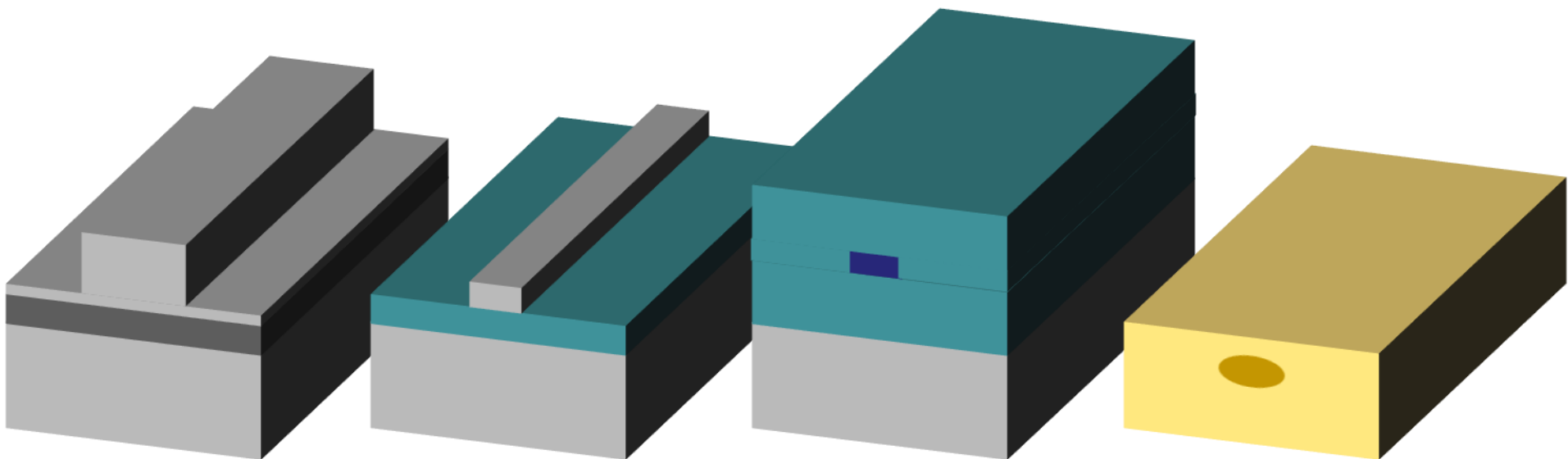


Optical synthesizer

Motivation for Photonic Integration

- **High chip functionality**
- **Low cost and high volume production**
- **Low size, weight and power (SWaP)**
- **Less fiber-to-chip and chip-to-fiber coupling**
- **Improved performance**
- **Better reliability**
- **Scalability**
- **Stability**

PIC Materials



Indium phosphide (InP)

- $\Delta = 5-10\%$
- Small devices ($\sim\mu\text{m}-\text{mm}$)
- Lasers, modulators, SOAs, photodetectors, passives

Silicon on insulator (SOI)

- $\Delta = 40-45\%$
- Small devices ($\sim\mu\text{m}$)
- Modulators, photodetectors, passives

SiO₂, SiON, Si₃N₄ (PLC)

- $\Delta = 0.5-20\%$
- Large devices ($\sim\text{mm}-\text{cm}$)
- Passives

Lithium niobate (LiNbO₃)

- $\Delta = 0.5-1\%$
- Large devices ($\sim\text{mm}-\text{cm}$)
- Modulators, passives

• Index contrast = $\Delta = (n_{core}^2 - n_{cladding}^2)/(2n_{core}^2)$

• Typical waveguide architectures shown

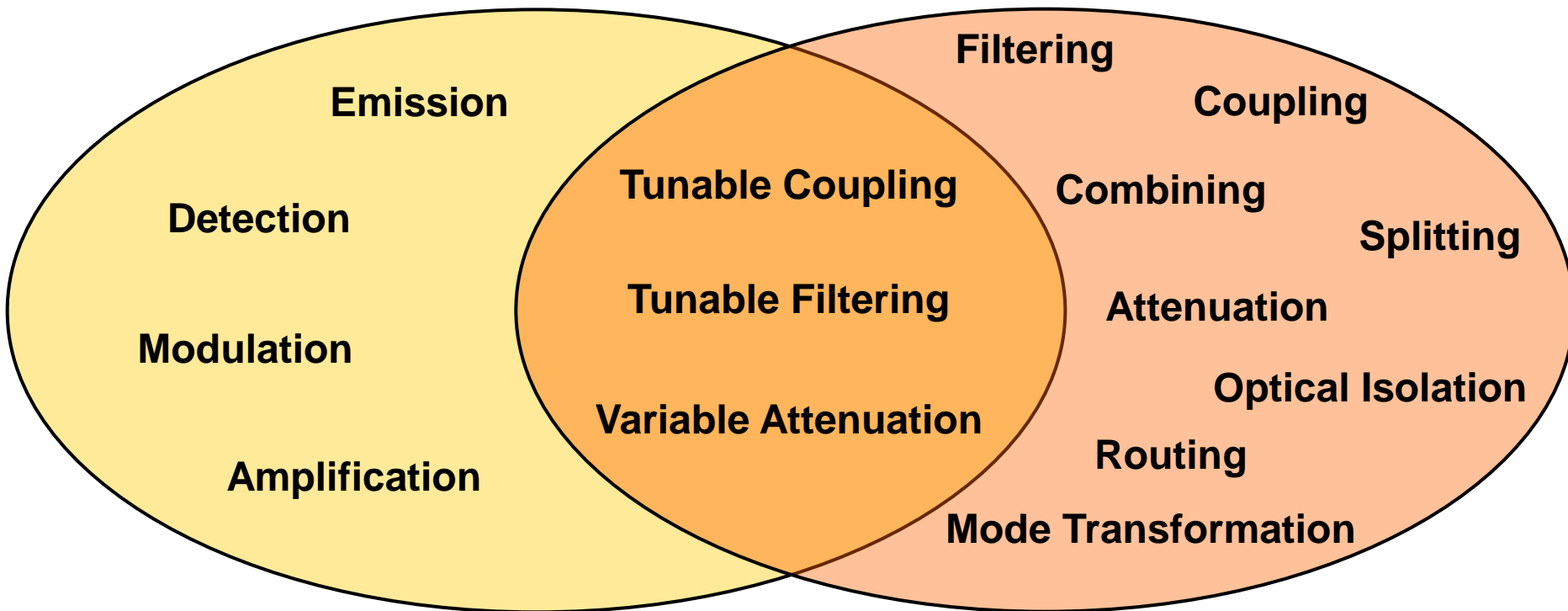
Active and Passive Photonic Functions

Active

Passive

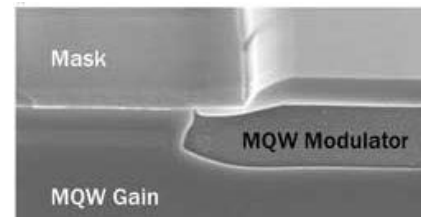
Variable function that responds to external actuation or control

Fixed and constant function



Types of Photonic Integration

- **Monolithic**: More than one photonic component integrated on a common substrate



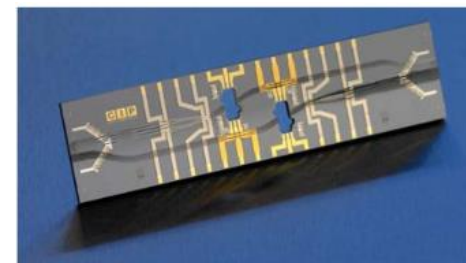
Y. Akulova, et al., Photonics Spectra, 2013

- **Heterogeneous**: Merging traditionally incompatible photonic material systems on a common substrate to exploit unique material properties



M. -C. Tien, et al., Optics Express, 2011

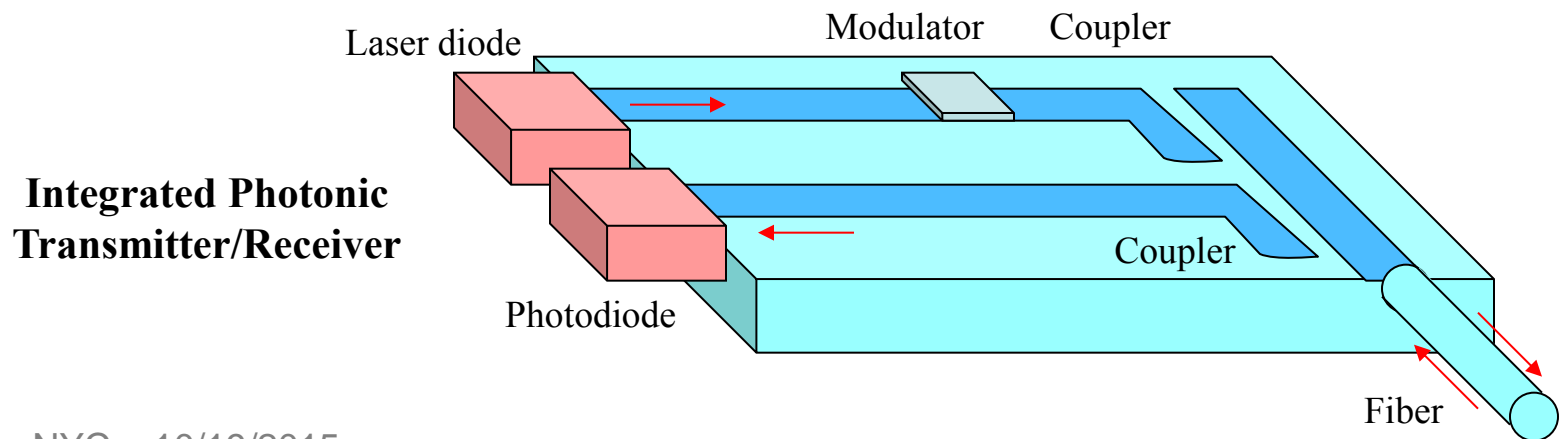
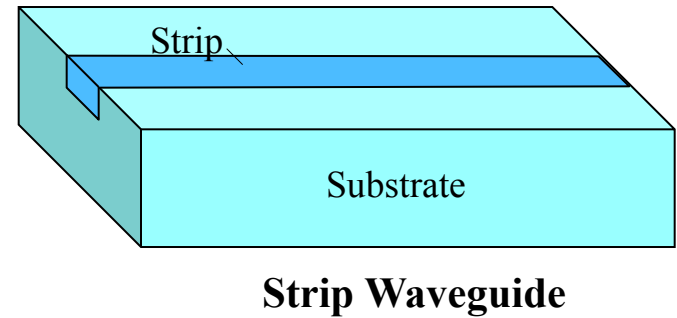
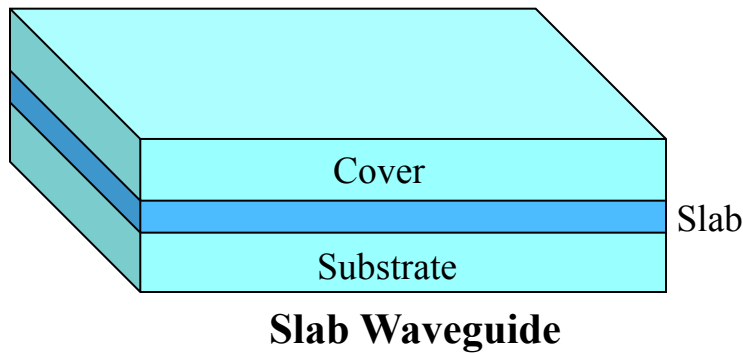
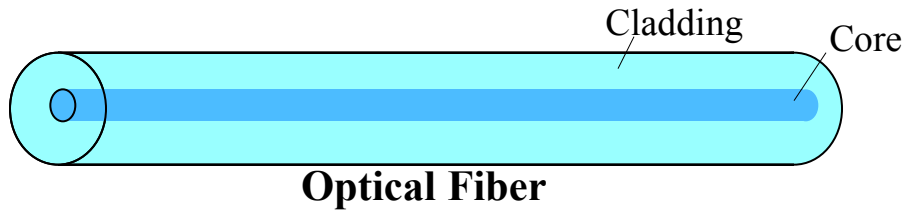
- **Hybrid**: Close integration of discrete photonic chips whereby light is coupled from one chip to the other



A. Poustie, IPNRA, 2007

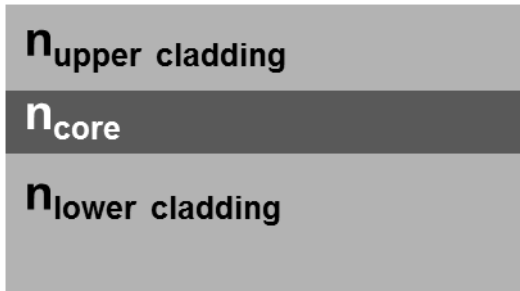
Passives

Waveguides



Waveguides

Planar Slab



Ridge



Rib



Buried Rib



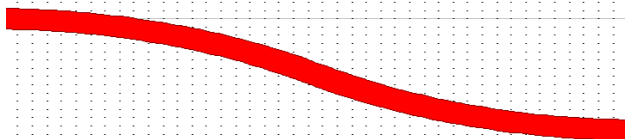
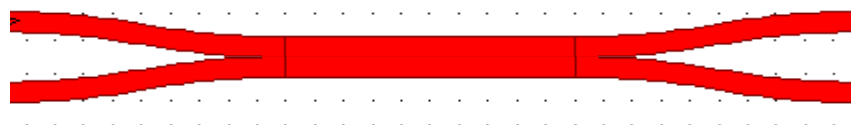
Buried Channel/Strip



Deep Ridge



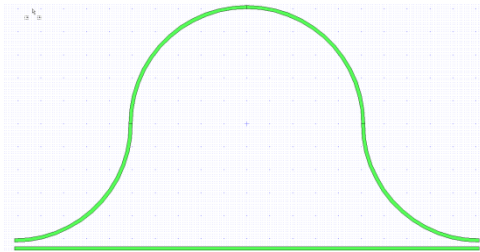
Passives: Photonic Interconnects

Curve/bend**S-bend****Flare****Taper****Y-branch****Directional coupler****Multimode interference coupler**

- **Passive components interconnect active components**
- **Passive components have other functionalities:**
 - Bend can filter higher order modes
 - Multimode interference coupler (MMI) splits incoming field and produces phase shift
 - Active components also built from waveguide structures

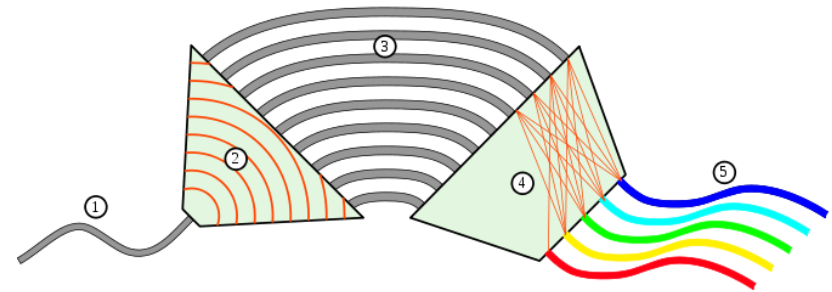
Integrated Passive Components

1x8 MMI Coupler

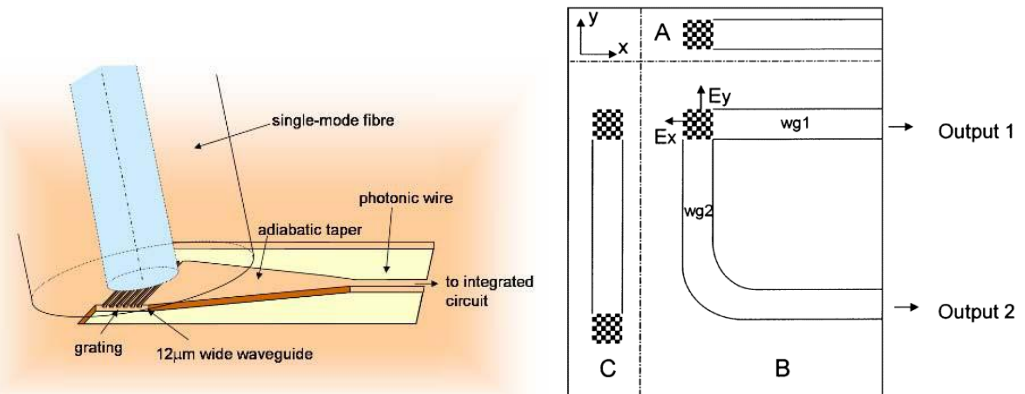


Integrated Delay Line (IDL)

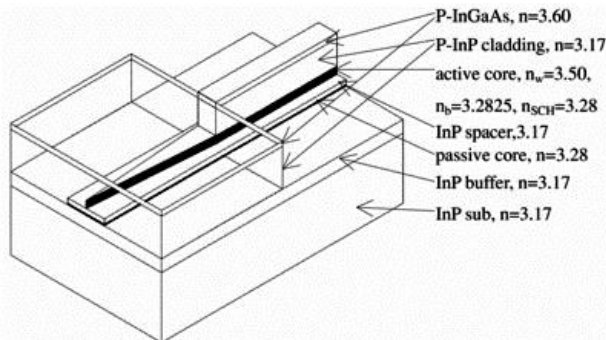
Arrayed Waveguide Grating (AWG)



Grating Coupler

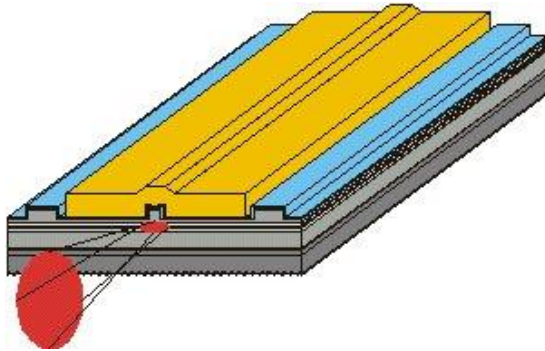


Spot Size Converter

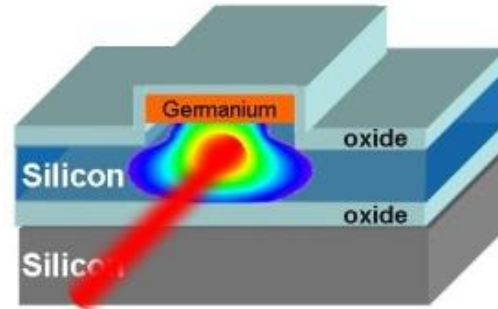


Integrated Active Components

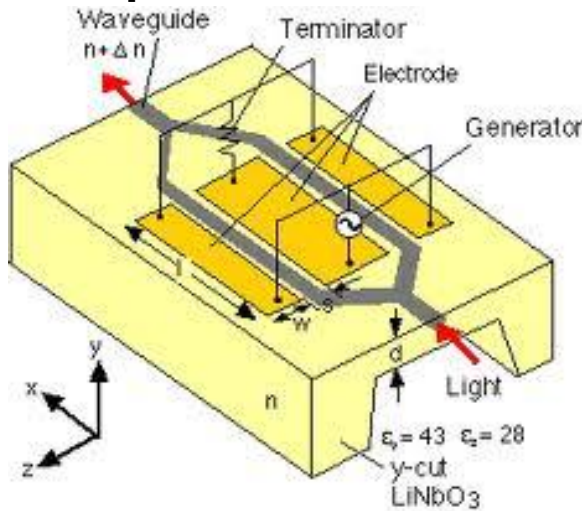
Semiconductor laser



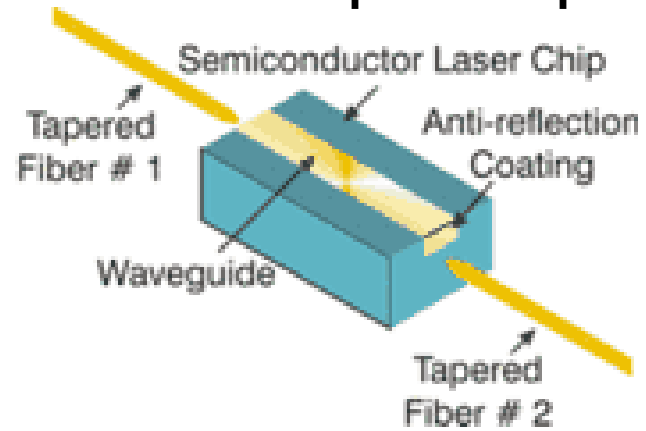
Photodiode



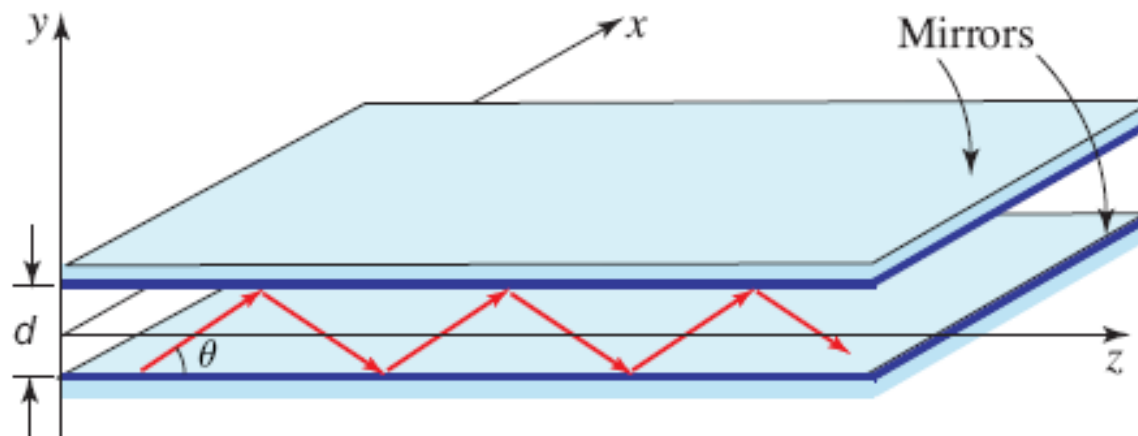
Optical modulator



Semiconductor optical amplifier

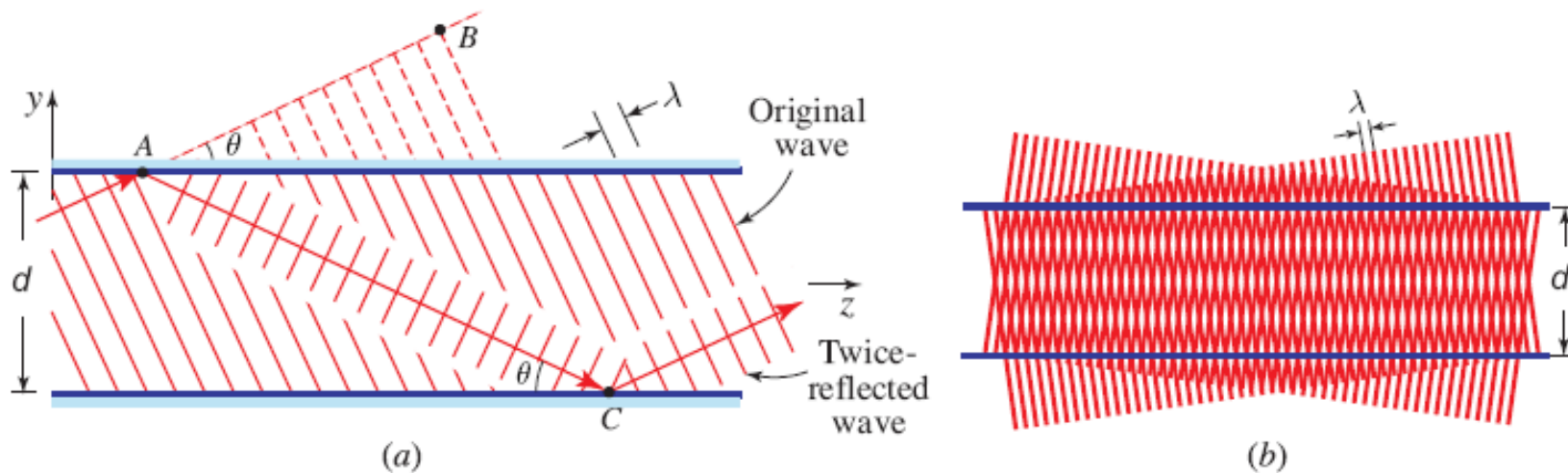


Waveguides: How do we guide light?



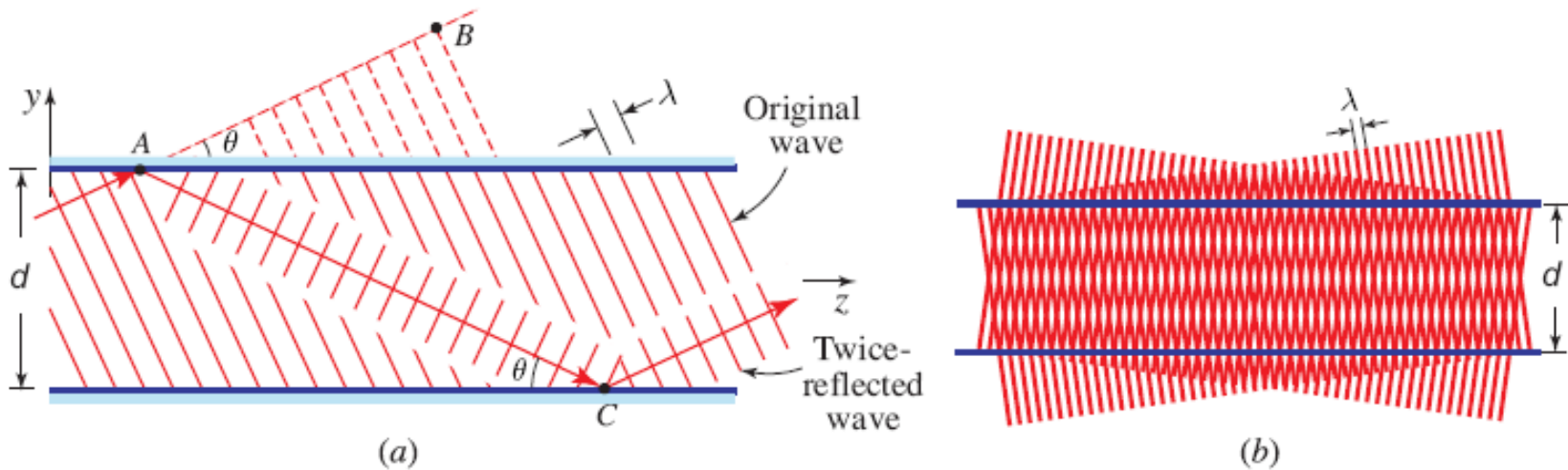
- Start with a simple planar-mirror waveguide
 - Not realistic but a good introduction to dielectric waveguides to introduce the concept of **guided modes**
- Apply E&M analysis by assigning each ray a TEM plane wave
- The total field is then the sum of these plane waves
- Subject to these conditions:
 - Wave is polarized in x and lies in y - z plane
 - Each reflection induces a π -phase shift but amplitude and polarization are maintained (perfect mirror)

Planar Mirror Waveguides



- Self-consistency condition: As wave reflects twice, it reproduces itself so as to yield only two distinct plane waves
 - Original wave must interfere with itself constructively (only certain fields satisfy this condition → eigenfunctions or modes)
- Modes are the fields that satisfy self-consistency condition
 - **Modes** are the fields that maintain the same transverse distribution and polarization at all locations along the waveguide axis

Planar Mirror Waveguides



Phase shift from A to B must equal (or differ by integer multiple of 2π) phase shift from A to C (which undergoes two reflections); recall: $\varphi = kl$ (for plane wave)

$$\Delta\varphi = \underbrace{2\pi AC/\lambda - 2\pi}_{\text{Reflected wave}} - \underbrace{2\pi AB/\lambda}_{\text{Original wave}} = 2\pi q, \quad q = 0, 1, 2, \dots$$

$$AC = d / \sin \theta \quad AB = (d / \sin \theta)(\cos 2\theta)$$

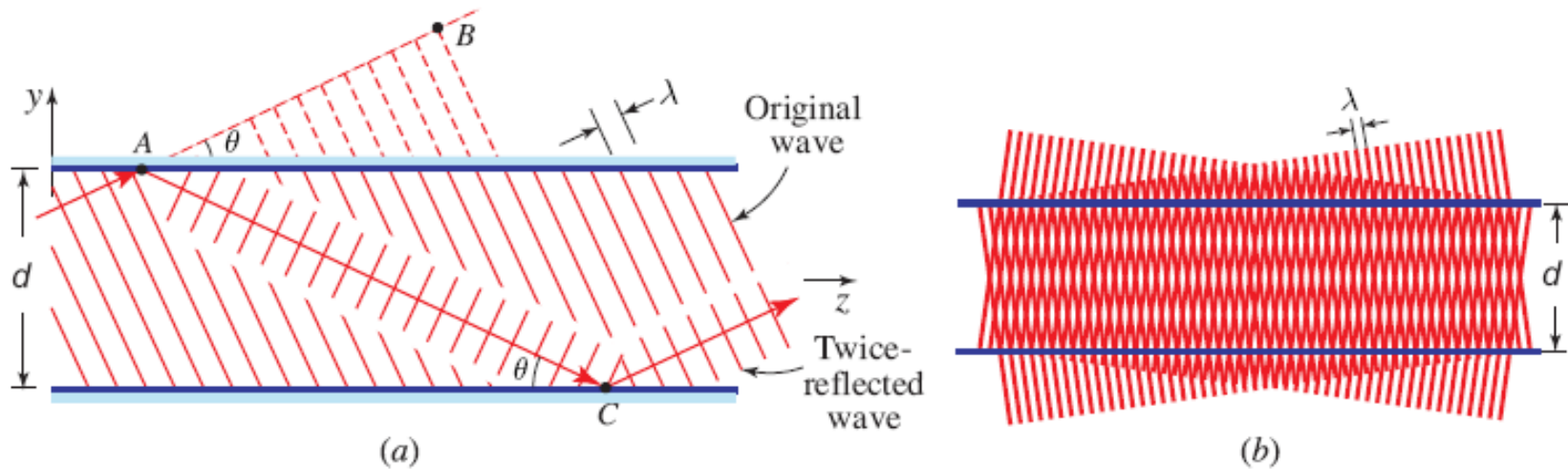
$$\cos(2\theta) = 1 - 2 \sin^2(\theta)$$

$$AC - AB = 2d \sin \theta \quad \Rightarrow$$

$$(2\pi/\lambda)2d \sin \theta = 2\pi m, \quad m = 1, 2, \dots$$

where $m = q + 1$

Planar Mirror Waveguides



$$(2\pi/\lambda)2d \sin\theta = 2\pi m, \quad m = 1, 2, \dots$$

Self-consistency therefore satisfied for certain values of $\theta = \theta_m$ (bounce angles)

$$\sin\theta_m = m\lambda/2d, \quad m = 1, 2, \dots$$

- Each θ_m corresponds to a mode
- $m = 1 \rightarrow$ first or fundamental mode (has smallest angle)

y component of the propagation constant

$$k_y = nk_o \sin\theta$$

quantized form:

$$k_{ym} = nk_o \sin\theta_m = (2\pi/\lambda)\sin\theta_m$$

$$k_{ym} = m\pi/d, \quad m = 1, 2, 3, \dots$$

- Therefore k_{ym} are spaced by π/d
- Phase shift for one round trip (vertical distance of $2d$) must be multiple of 2π
- Note dependence on d (only confined in vertical)

Propagation Constants

The sum (or difference) of the two distinct waves (that traveling at angle $+\theta$ and that traveling at angle $-\theta$) has component $\exp(-jk_z z)$

The propagation constant of the guided wave is $\beta \equiv k_z = k \cos \theta$.

Thus β is quantized with values

$$\beta_m = k \cos \theta_m$$

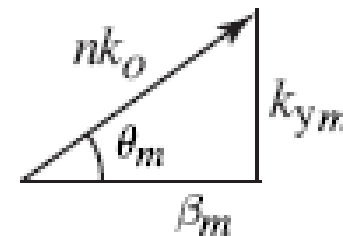
$$\beta_m^2 = k^2 (1 - \sin^2 \theta_m)$$

$$\sin \theta_m = m \frac{\lambda}{2d}$$



$$\beta_m^2 = k^2 - \frac{m^2 \pi^2}{d^2}$$

Dispersion relation



Higher order modes travel with smaller propagation constants.

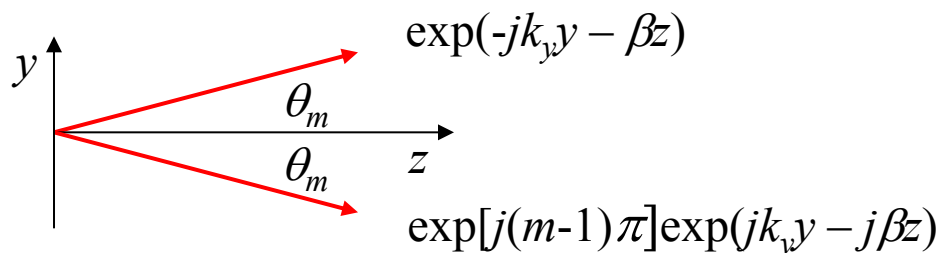
Field Distributions

The phase shift encountered when a wave travels a distance $2d$ (one round trip) in the y direction, with propagation constant k_{ym} , must be a multiple of 2π . ($k_{ym} 2d = m2\pi$)

- Recall: total field in waveguide is sum of upward and downward TEM plane waves
- When the self-consistency condition is satisfied, the phases of the upward and downward plane waves at points on the z axis differ by half the round-trip phase shift $q\pi$, $q = 0, 1, \dots$, or $(m - 1)\pi$, $m = 1, 2, \dots$
- So waves add for odd m and subtract for even m

There are therefore symmetric modes, for which the two plane-wave components are added, and antisymmetric modes, for which they are subtracted.

General principle: the modes of every symmetric structure can be classified as ODD or EVEN with respect to a symmetry axis



TE Modes

Consider first TE modes, such that the electric field is in the x direction

Upward wave component: $A_m e^{-jk_{ym}y - j\beta_m z}$

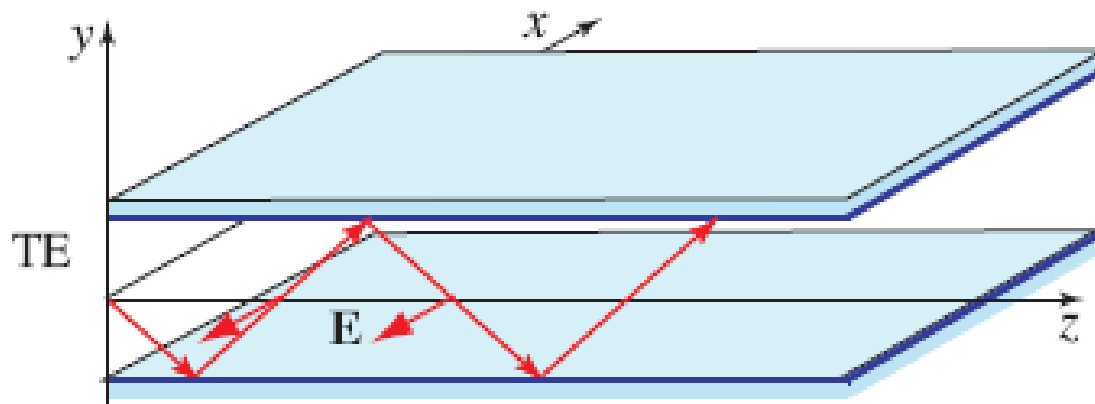
Downward wave component: $e^{j(m-1)\pi} A_m e^{jk_{ym}y - \beta_m z}$

At $y = 0$ the two waves differ in phase by $(m - 1)\pi$.

Total field:

Symmetric modes (m odd) \rightarrow components add $E_x(y, z) = 2A_m \cos(k_{ym}y)e^{-j\beta_m z}$

Asymmetric modes (m even) \rightarrow components subtract $E_x(y, z) = 2jA_m \sin(k_{ym}y)e^{-j\beta_m z}$



Complex Field Amplitudes

Transverse electric field, x -polarized

Write in this form:

$$E_x(y, z) = a_m u_m(y) \exp(-j\beta_m z)$$

Amplitude of the mode

$$a_m = \sqrt{2d} A_m \quad \text{Odd } m$$

$$a_m = j\sqrt{2d} A_m \quad \text{Even } m$$

Transverse distributions

$$u_m(y) = \begin{cases} \sqrt{\frac{2}{d}} \cos\left(m\pi\frac{y}{d}\right), & m = 1, 3, 5, \dots \\ \sqrt{\frac{2}{d}} \sin\left(m\pi\frac{y}{d}\right), & m = 2, 4, 6, \dots, \end{cases}$$

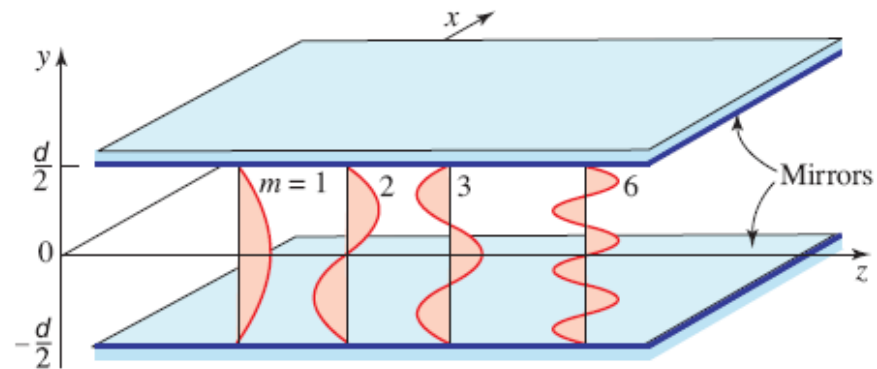
\downarrow
 $k_{my} y$

Transverse distributions have been normalized

$$\int_{-d/2}^{d/2} u_m^2(y) dy = 1.$$

And can be shown to be orthogonal

$$\int_{-d/2}^{d/2} u_m(y) u_l(y) dy = 0, \quad l \neq m,$$



Complex Field Amplitudes

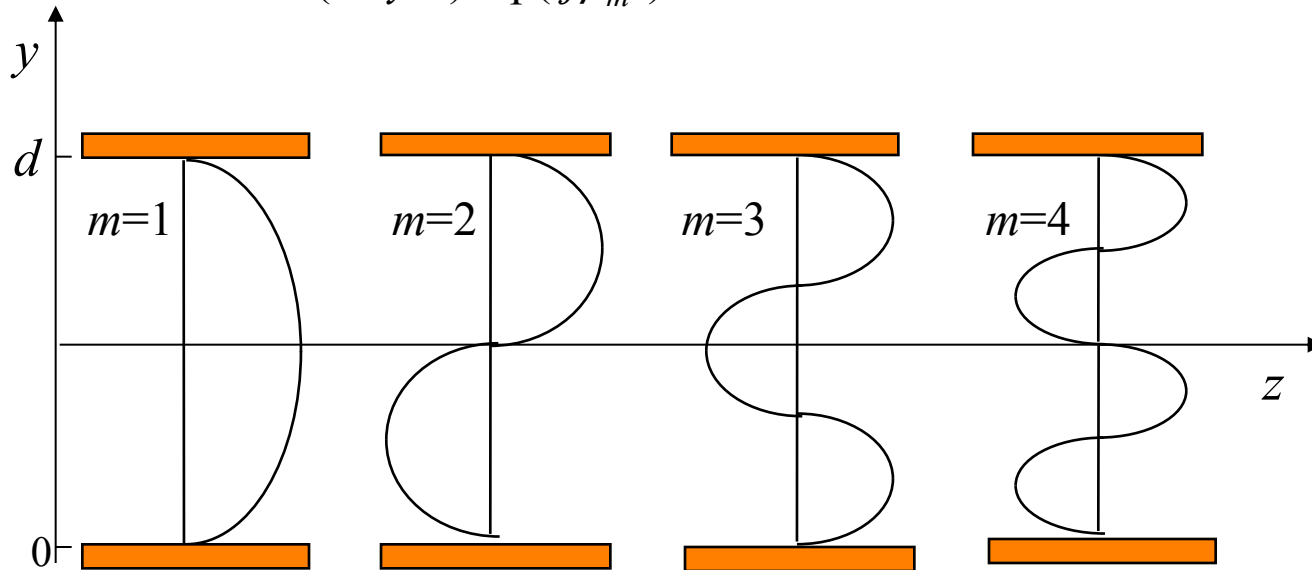
Field distributions

$$\cos(m\pi y/d)\exp(-j\beta_m z)$$

m odd

$$\sin(m\pi y/d)\exp(-j\beta_m z)$$

m even



Take Home Messages

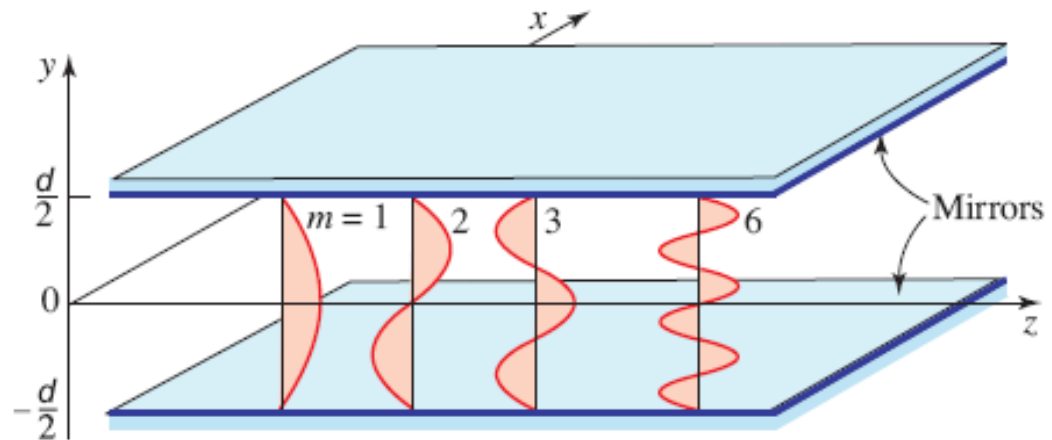
- Each mode can be viewed as a standing wave in the y direction, traveling in the z direction.
- Modes of large m vary in the transverse plane at a greater rate, k_y , and travel with a smaller propagation constant β .
- Field vanishes at mirror boundary ($y = \pm d/2$) for all modes, so the boundary conditions are always satisfied.

$$m = 1, 2, 3, \dots$$

$$\sin \theta_m = m \frac{\lambda}{2d}$$

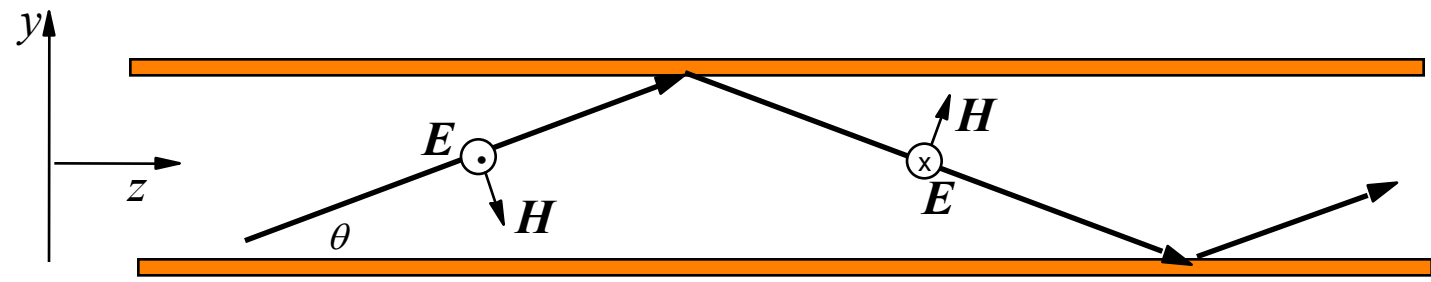
$$k_{ym} = m \frac{\pi}{d}$$

$$\beta_m = k \cos \theta_m$$

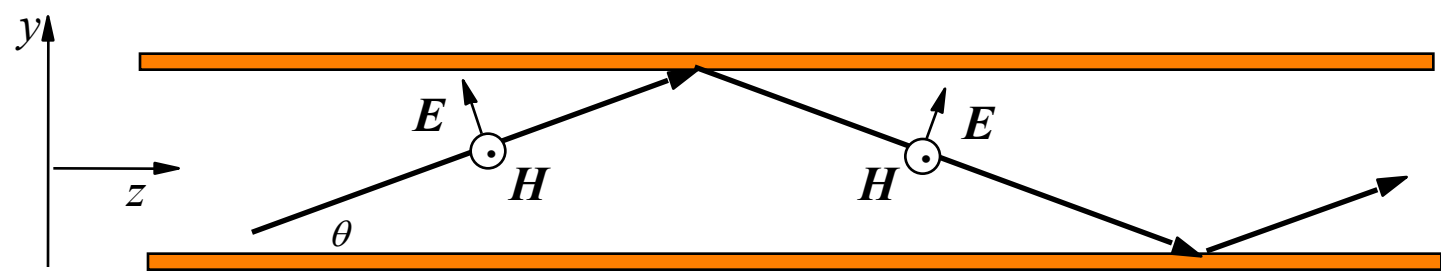


TE Versus TM Modes

| | | | |
|----------|-------|-----------------------------------|----------|
| TE Modes | E_x | $\cos(m\pi y/d)\exp(-j\beta_m z)$ | m odd |
| | | $\sin(m\pi y/d)\exp(-j\beta_m z)$ | m even |



| | | | |
|----------|-------|-----------------------------------|----------|
| TM Modes | E_z | $\cos(m\pi y/d)\exp(-j\beta_m z)$ | m odd |
| | | $\sin(m\pi y/d)\exp(-j\beta_m z)$ | m even |

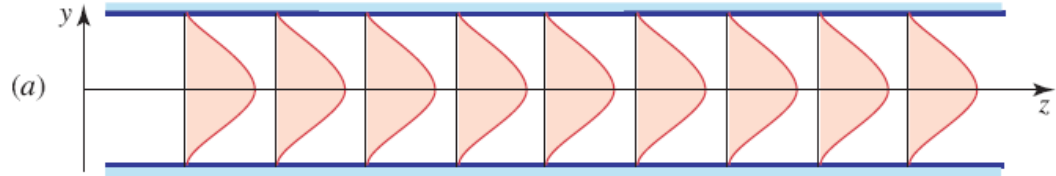


Now there are E components in the y and z directions.
 The z component behaves exactly as the x component of a TE mode.

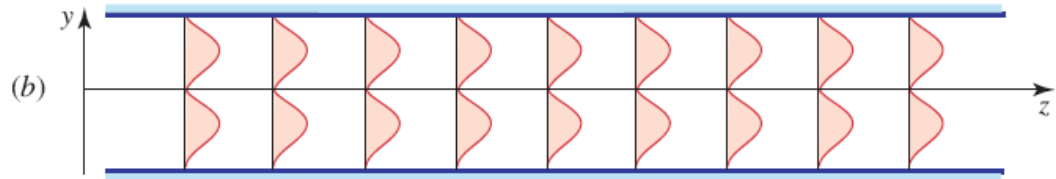
Multimode Fields

Waveguide may support several modes (more than one mode satisfy boundary conditions)

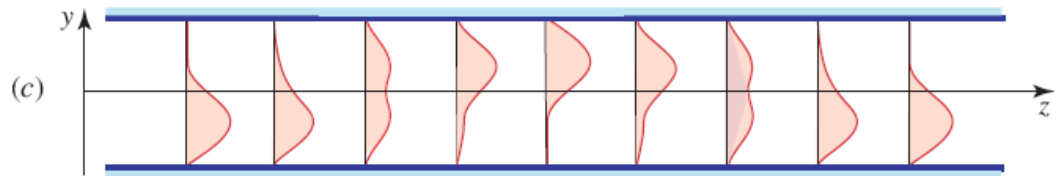
$$E_1(y, z) = u_1(y)\exp(-j\beta_1z)$$



$$E_2(y, z) = u_2(y)\exp(-j\beta_1z)$$



$$E_{TOT}(y, z) = u_1(y)\exp(-j\beta_1z) + u_2(y)\exp(-j\beta_1z)$$



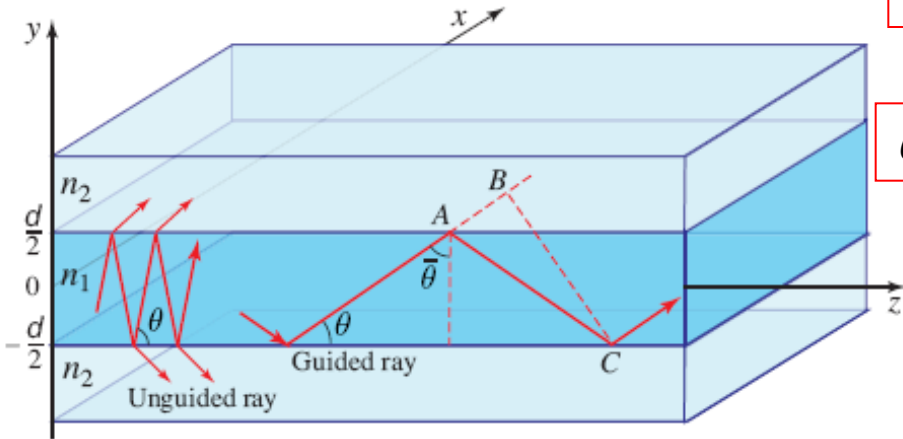
Arbitrary field polarized in the x direction and satisfying the boundary conditions can be written as a **weighted superposition of the TE modes**:

$$E_x(y, z) = \sum_{m=0}^M a_m u_m(y) \exp(-j\beta_m z),$$

Optical power divided among modes and power distribution is position dependent

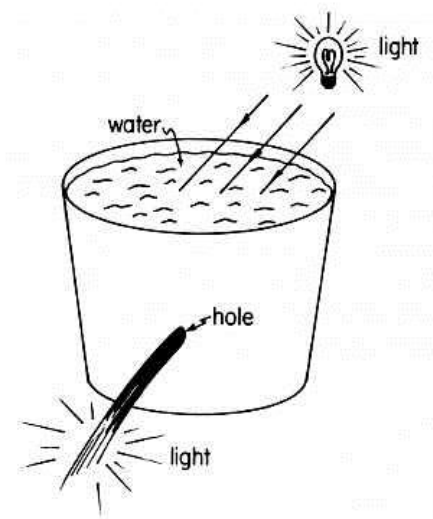
Planar Dielectric Waveguides

Dielectric slab waveguide



$$n_1 > n_2$$

$$\theta_c = \sin^{-1}(n_2/n_1)$$



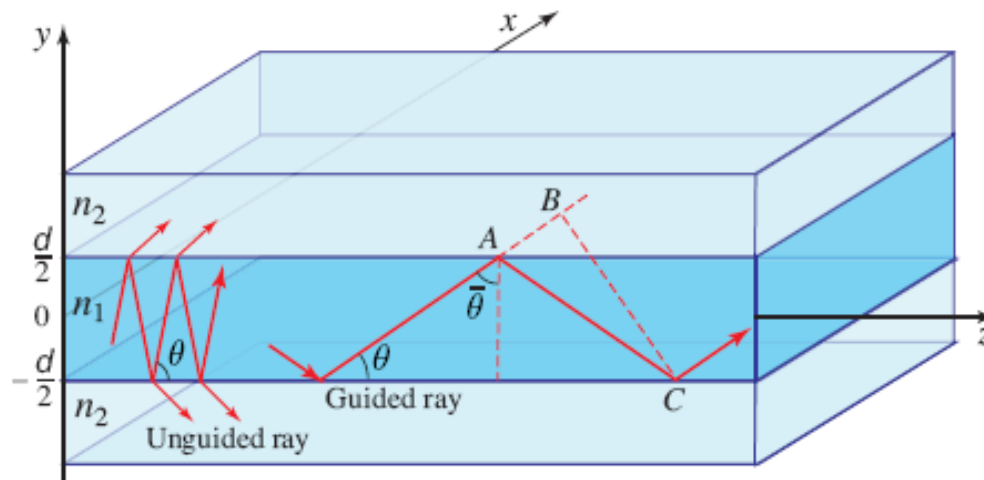
- The dielectric waveguide has an inner medium (core or slab) with refractive index n_1 larger than that of the outer medium (cladding or cover/substrate) n_2
- The electromagnetic wave is trapped in the inner medium by total internal reflection at an angle θ greater than the critical angle $\theta_c = \sin^{-1}(n_2/n_1)$
- Waves making larger angles refract therefore losing a portion of power at each reflection (so eventually vanish)

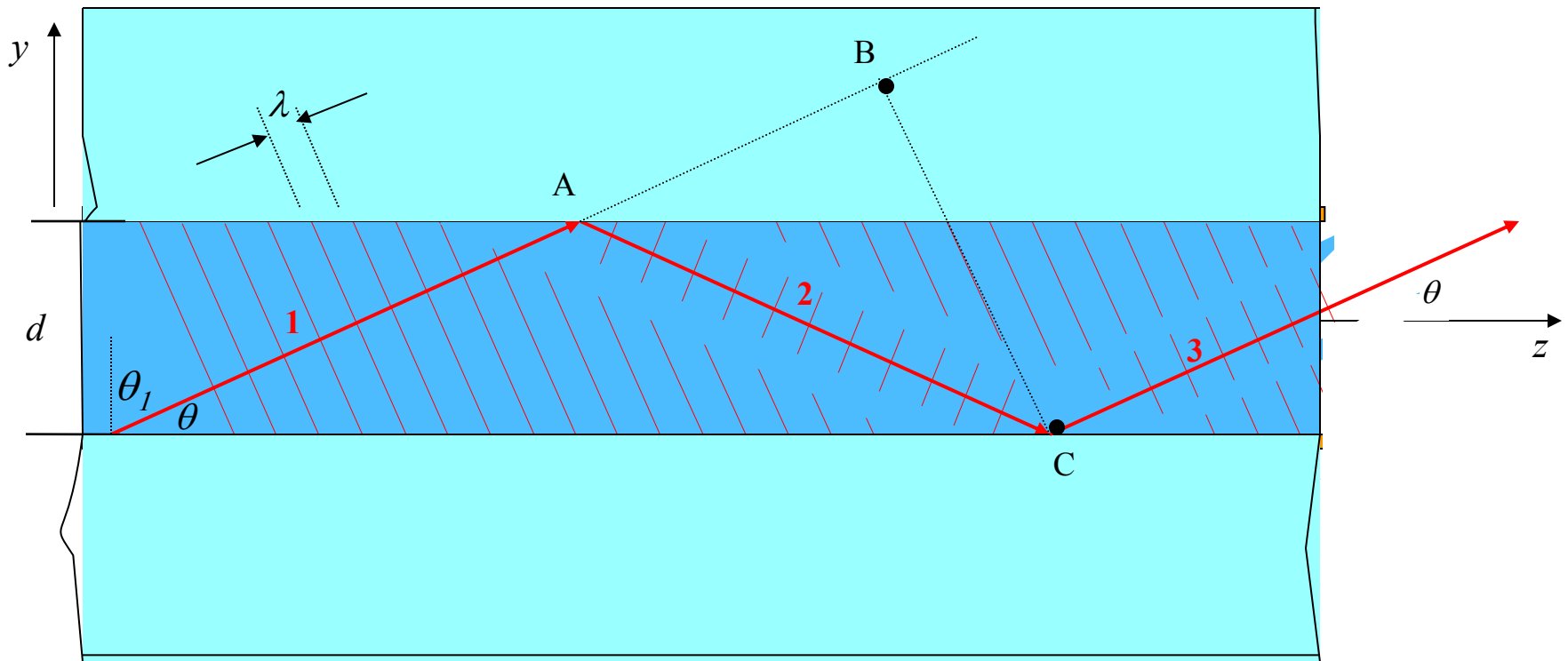
Guiding condition:

$$\bar{\theta} > \theta_c \quad \text{or } \theta \text{ is smaller than the complement of the critical angle } \bar{\theta}_c = \pi/2 - \sin^{-1}(n_2/n_1) = \cos^{-1}(n_2/n_1)$$

Planar Dielectric Waveguides

- To determine the waveguide modes, solutions to Maxwell's equations can be reached in the core and cladding regions where appropriate boundary conditions are imposed
- Here apply similar approach to that for planar mirror waveguide
 - Write a solution in terms of **TEM plane waves bouncing** between surfaces of the slab
 - Apply **self-consistency condition** to determine θ_m , β , u_m , v_g





Self consistency: Wave 1 at B has the same phase as wave 3 at C (wave reproduction)

$$\frac{2\pi}{\lambda} 2d \sin \theta - 2\varphi_r = 2\pi m,$$

$AC - AB$ two reflections

$$m = 0, 1, 2, \dots$$

φ_r = phase introduced by **total internal reflection**
(replaces π from planar-mirror waveguide)

$$2k_y d - 2\varphi_r = 2\pi m.$$

Determine TE Modes

Guiding (self-consistency) condition:

$$\frac{2\pi}{\lambda} 2d \sin \theta - 2\varphi_r = 2\pi m$$

Phase shift for TE
(from analysis of
reflection at boundary):

$$\tan \frac{\varphi_r}{2} = \sqrt{\frac{\sin^2 \bar{\theta}_c}{\sin^2 \theta} - 1}$$

$$\theta_1 = \pi/2 - \theta$$

$$\theta_c = \pi/2 - \bar{\theta}_c$$

Rewrite self-consistency
equation in this form:

$$\tan \left(\pi \frac{d}{\lambda} \sin \theta - m \frac{\pi}{2} \right) = \tan(\varphi_r / 2)$$

- This is a transcendental equation for $\sin \theta$
- \rightarrow plot both sides
- Solutions yield the bounce angles

Determine TE Modes

Self-consistency condition (TE modes):

$$\tan\left(\pi \frac{d}{\lambda} \sin \theta - m \frac{\pi}{2}\right) = \sqrt{\frac{\sin^2 \bar{\theta}_c}{\sin^2 \theta} - 1}$$

LHS

RHS

In this plot:

$$\sin \bar{\theta}_c = 8 \frac{\lambda}{2d}$$

$$M = 9$$

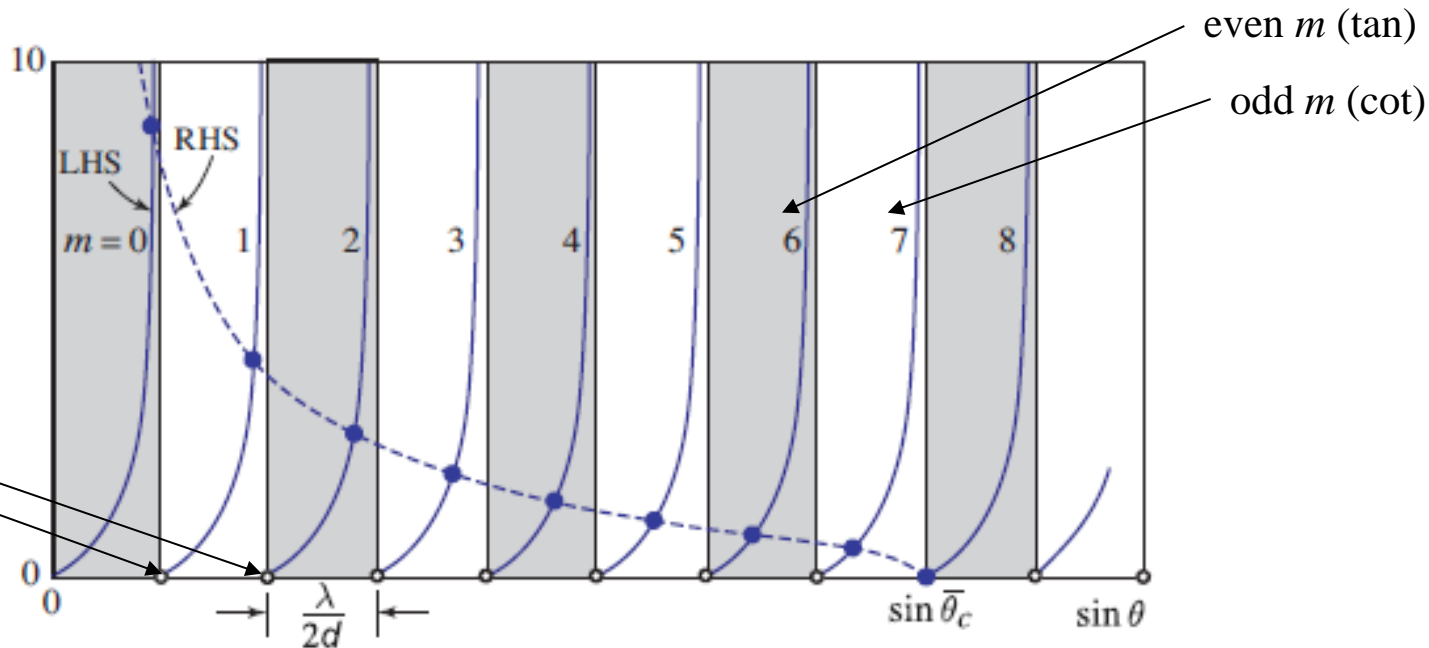
Crossings yield the bounce angles θ_m of the guided modes

For planar-mirror:

$$\varphi_r = \pi$$

$$\Rightarrow \tan(\varphi_r / 2) = \infty$$

$$\sin \theta_m = m\lambda / 2d$$

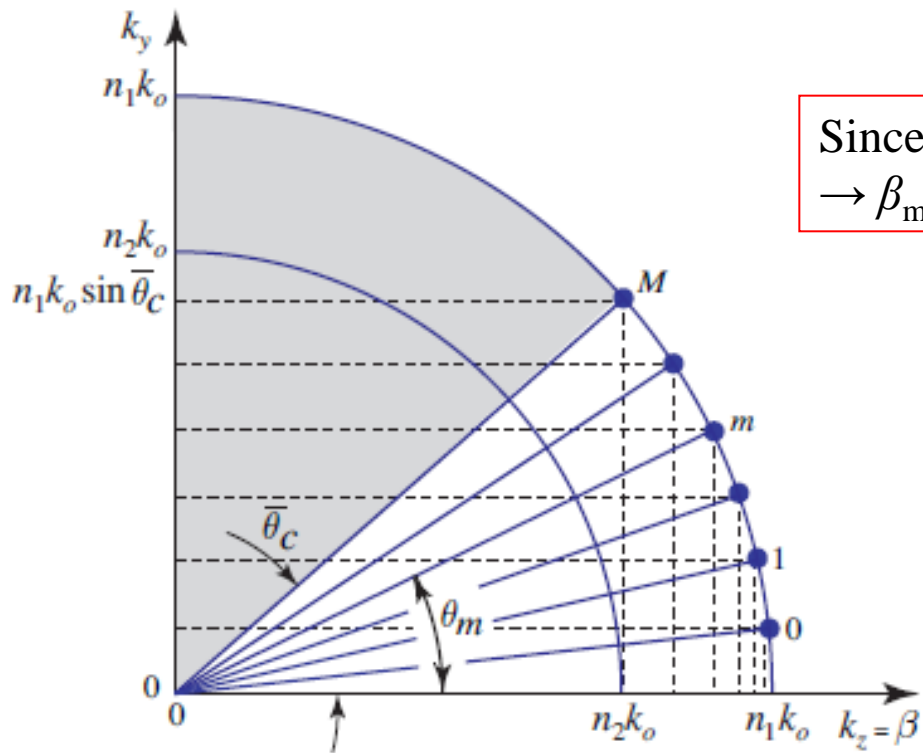


$$\theta_m \text{ are between } 0 \text{ and } \bar{\theta}_c$$

Propagation Constants

z-components of wavevectors are the propagation constants

$$\beta_m = n_1 k_0 \cos \theta_m.$$



Since $\cos \theta_m$ lies between 1 and $\cos \bar{\theta}_c = n_2/n_1$
 $\rightarrow \beta_m$ lies between $n_2 k_0$ and $n_1 k_0$

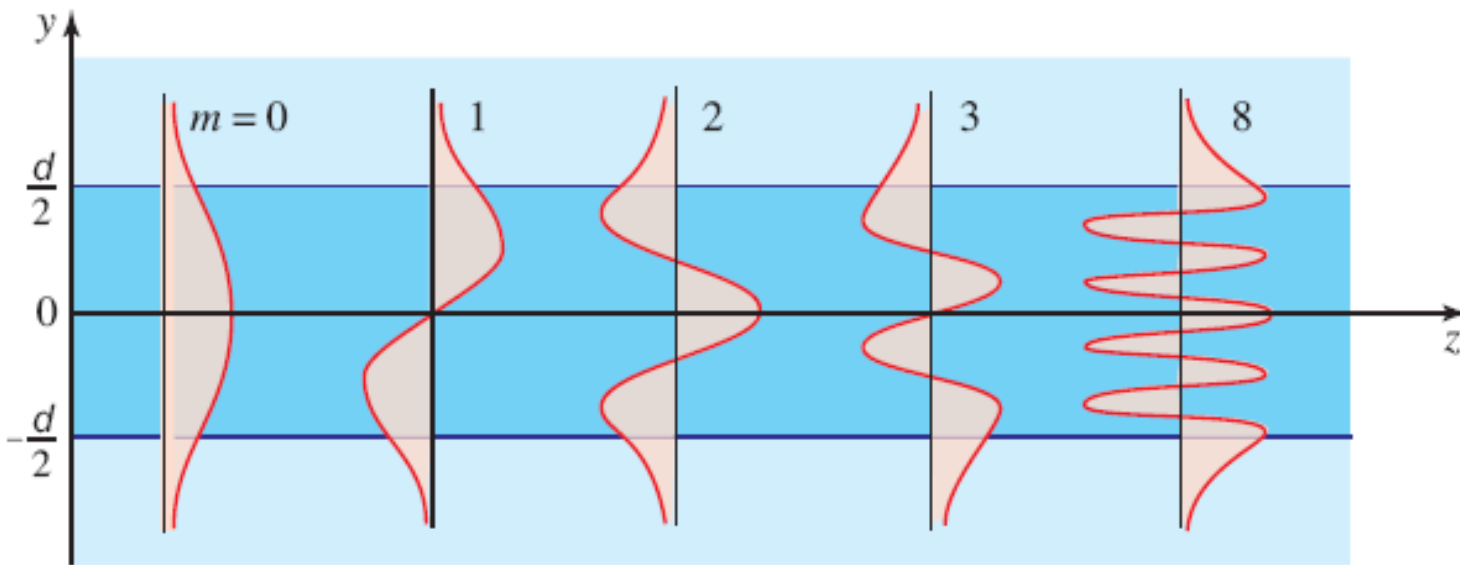
Guiding condition

$$n_2 k_0 < \beta_m < n_1 k_0$$

Field Distributions

Concept of internal and external fields

$u_m(y)$ functions



Forward-looking observation:

Higher order modes leak more into upper and lower cladding layers

TE Internal Fields

- The field inside the slab is composed of two TEM plane waves traveling at angles θ_m and $-\theta_m$ with wavevector components $(k_x, k_y, k_z) = (0, \pm n_1 k_0 \sin \theta_m, n_1 k_0 \cos \theta_m)$.
- At the center of slab, these fields have same amplitude and phase shift ($m\pi$, i.e. half of a round trip)
- Arbitrary field is superposition over all the modes:

$$E_x(y, z) = \sum_m a_m u_m(y) \exp(-j\beta_m z),$$

where $\beta_m = n_1 k_0 \cos \theta_m$.

$$u_m(y) \propto \begin{cases} \cos\left(2\pi \frac{\sin \theta_m}{\lambda} y\right), & m = 0, 2, 4, \dots \\ \sin\left(2\pi \frac{\sin \theta_m}{\lambda} y\right), & m = 1, 3, 5, \dots, \end{cases} \quad -\frac{d}{2} \leq y \leq \frac{d}{2},$$

Proportionality constant to be determined by matching the fields at the boundaries


Note: field distributions are harmonic but do not vanish at boundaries

TE External Fields

The external field must match the internal field at all boundary points $y = \pm d/2$.

Substitute $E_x(y, z) = a_m u_m(y) \exp(-j\beta_m z)$

into $(\nabla^2 + n_2^2 k_o^2) E_x(y, z) = 0,$

 $\frac{d^2 u_m}{dy^2} - \gamma_m^2 u_m = 0, \quad \gamma_m^2 = \beta_m^2 - n_2^2 k_o^2.$

For guided waves $\beta_m > n_2 k_o \longrightarrow \gamma_m^2 > 0$ therefore exponential solutions

$$u_m(y) \propto \begin{cases} \exp(-\gamma_m y), & y > d/2 \\ \exp(\gamma_m y), & y < -d/2. \end{cases}$$

Proportionality constants determined by matching internal and external fields at $y = d/2$ and using normalization.

Extinction coefficient/decay rate

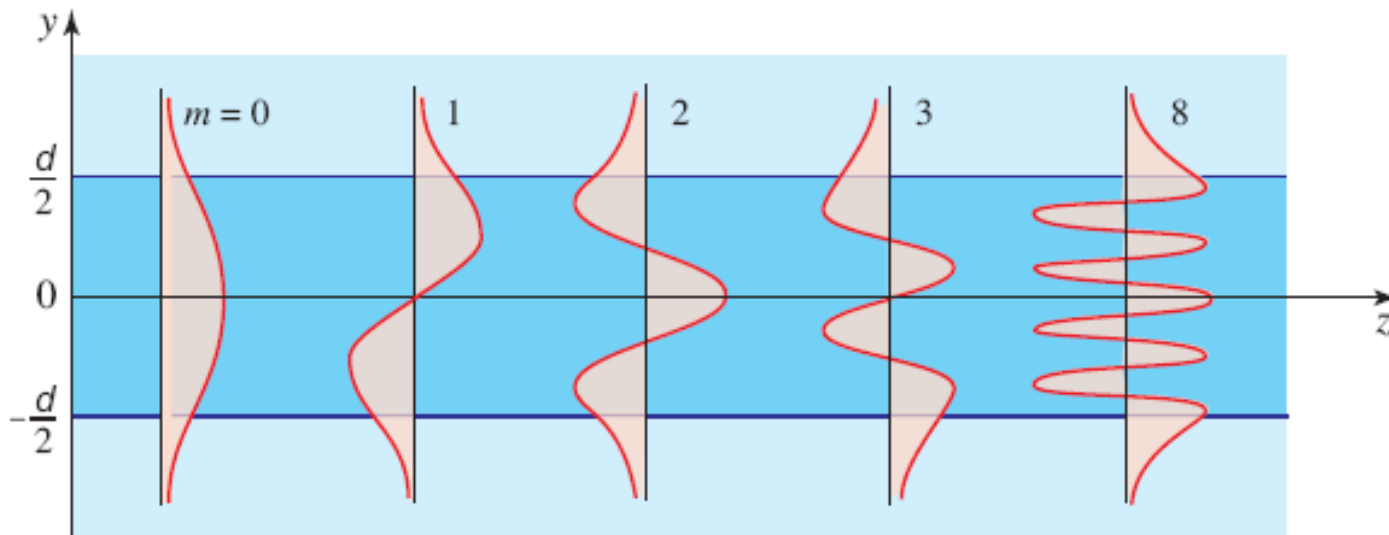
$$\gamma_m = n_2 k_o \sqrt{\frac{\cos^2 \theta_m}{\cos^2 \theta_c} - 1}.$$

As mode number increases, γ_m decreases and modes penetrate more into cladding and substrate

Optical Confinement Factor

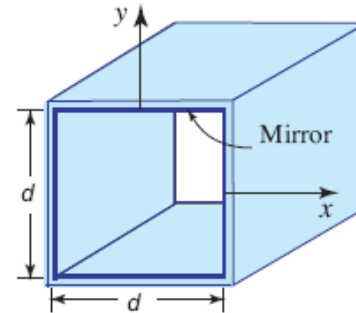
Ratio of power in slab to total power

$$\Gamma_m = \frac{\int_0^{d/2} u_m^2(y) dy}{\int_0^\infty u_m^2(y) dy}$$



Rectangular Mirror Waveguide

- Start with square mirror waveguide of width d
- As for planar case, light guided by multiple reflections at all angles
- For plane wave (with wavevector (k_x, k_y, k_z)) to satisfy self consistency, must have (i.e. self-consistency in both dimensions)



- Then determine β from:

$$2k_x d = 2\pi m_x, \quad m_x = 1, 2, \dots$$

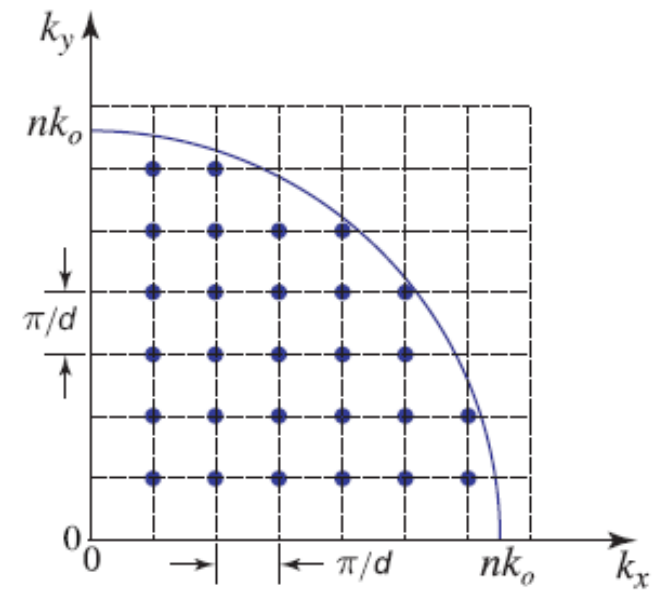
$$2k_y d = 2\pi m_y, \quad m_y = 1, 2, \dots,$$

$$k_x^2 + k_y^2 + \beta^2 = n^2 k_0^2$$

- k_x, k_y, k_z (β) therefore have discrete values
- Each mode identified by indices m_x, m_y
 - As shown in plot, all integer values permitted as long as $k_x^2 + k_y^2 \leq n^2 k_0^2$
- Number of modes (per polarization) (M large):

$$M \approx \frac{\pi}{4} \left(\frac{2d}{\lambda} \right)^2 NA^2$$

Compared to 1-D waveguide, we see multiplication of degrees of freedom



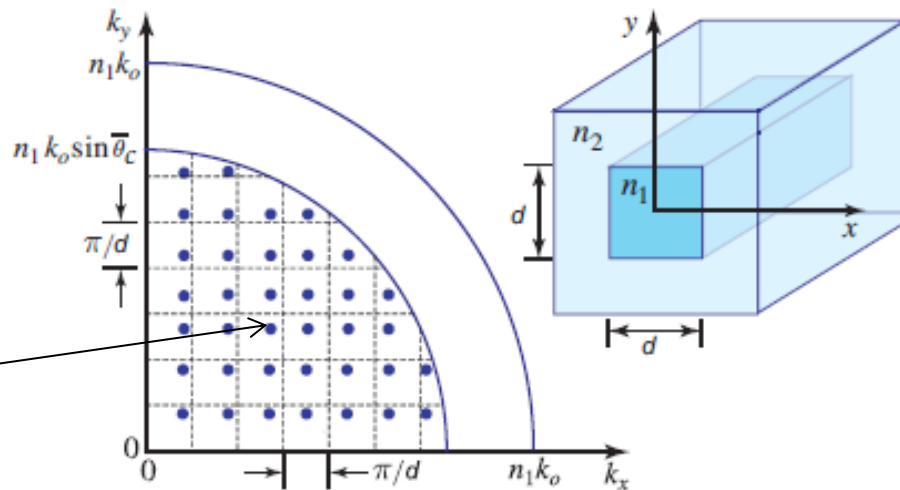
Rectangular Dielectric Waveguide

The components of the wavevector must satisfy:

$$k_x^2 + k_y^2 \leq n_1^2 k_0^2 \sin^2 \bar{\theta}_c$$

$$\bar{\theta}_c = \cos^{-1} \frac{n_2}{n_1}$$

- Now k_x and k_y lie within reduced area
- Can determine values using phase shifts (φ) as for planar case



Note: Unlike the mirror waveguide, k_x and k_y of modes are not uniformly spaced.

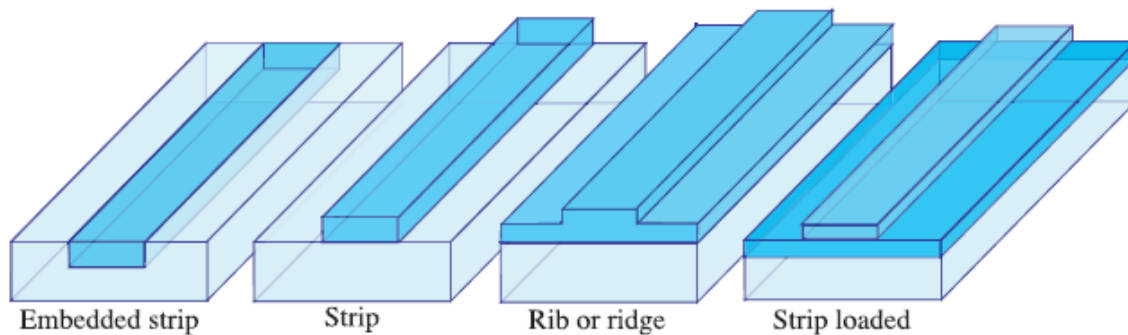
However, two consecutive values of k_x (or k_y) are separated by an average value of π/d (the same as for the mirror waveguide)

Number of modes (each polarization)

$$M \approx \frac{\pi}{4} \left(\frac{2d}{\lambda_0} \right)^2 (\text{NA})^2,$$

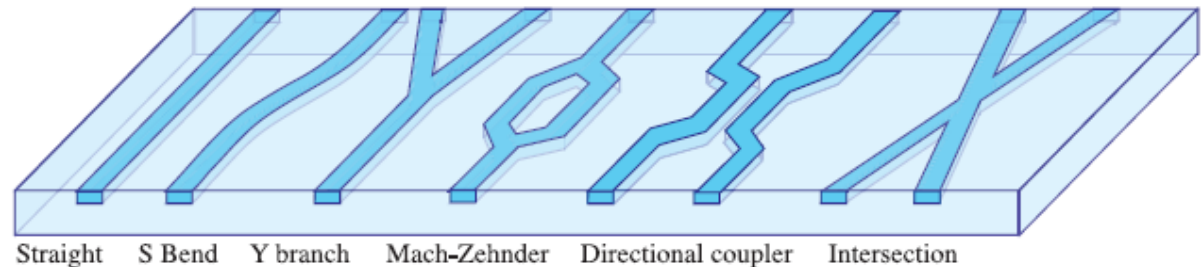
$$\text{NA} = \sqrt{n_1^2 - n_2^2}$$

Waveguide Geometries



Basic waveguide geometries

Basic waveguide functions

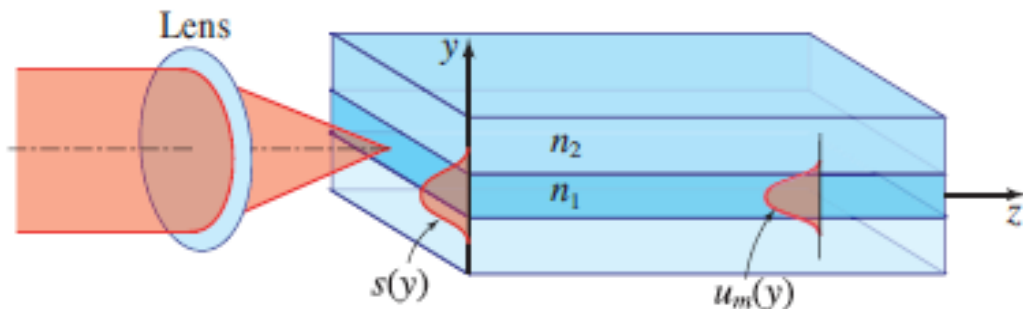


The exact analysis of these geometries is not trivial and approximations are needed

See: *Fundamentals of Optical waveguides*, K. Okamoto, Academic Press, 2000

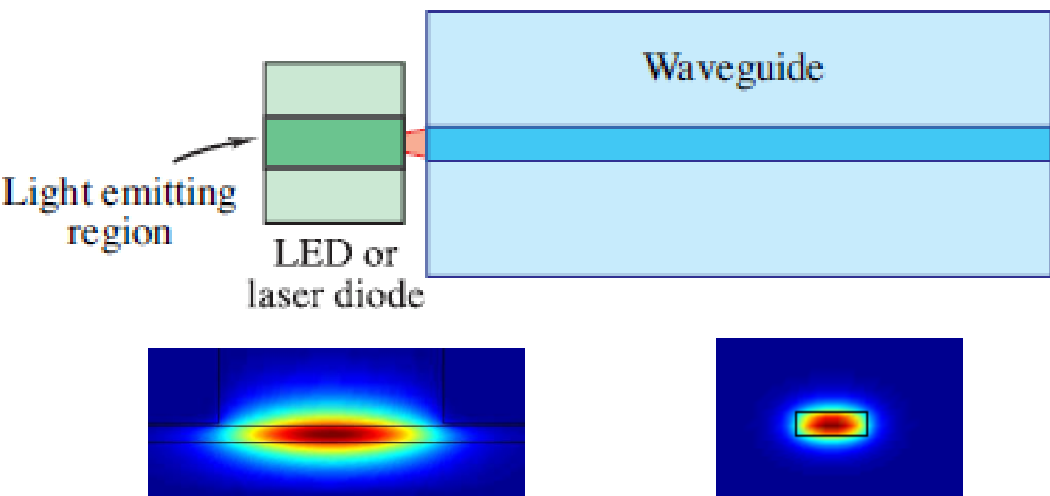
Waveguide Coupling for Integration

Fiber-to-chip coupling

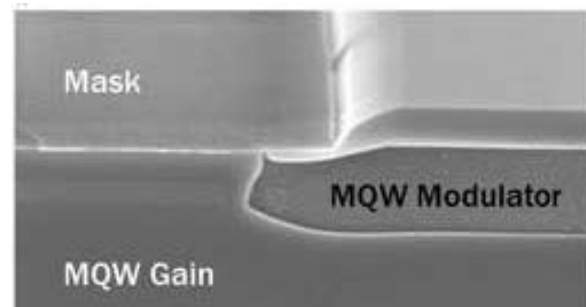


These are coupling problems
 → mode matching problems

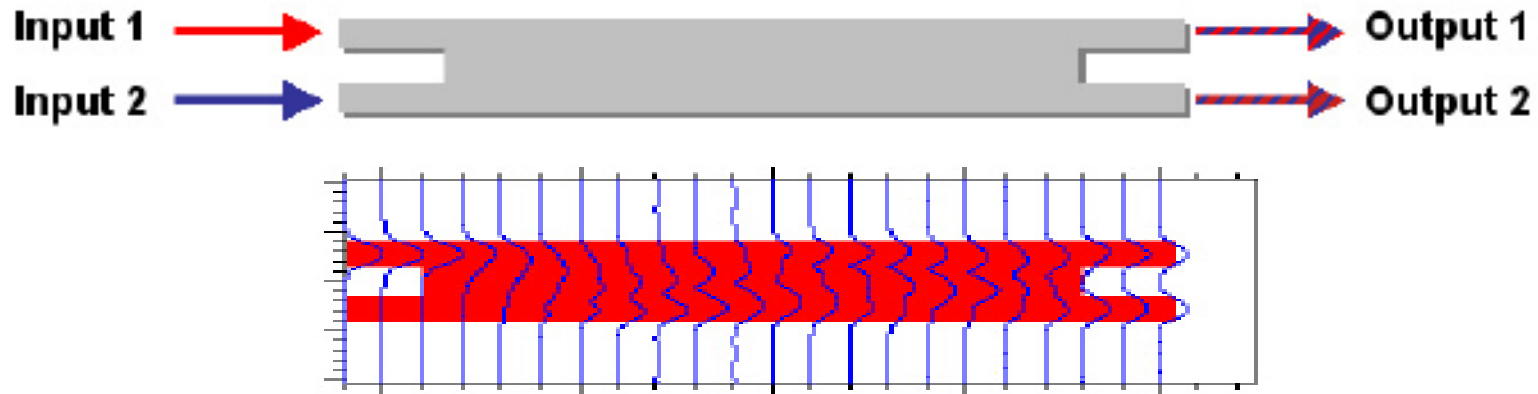
Butt-coupling from emission source to waveguide



On-chip coupling

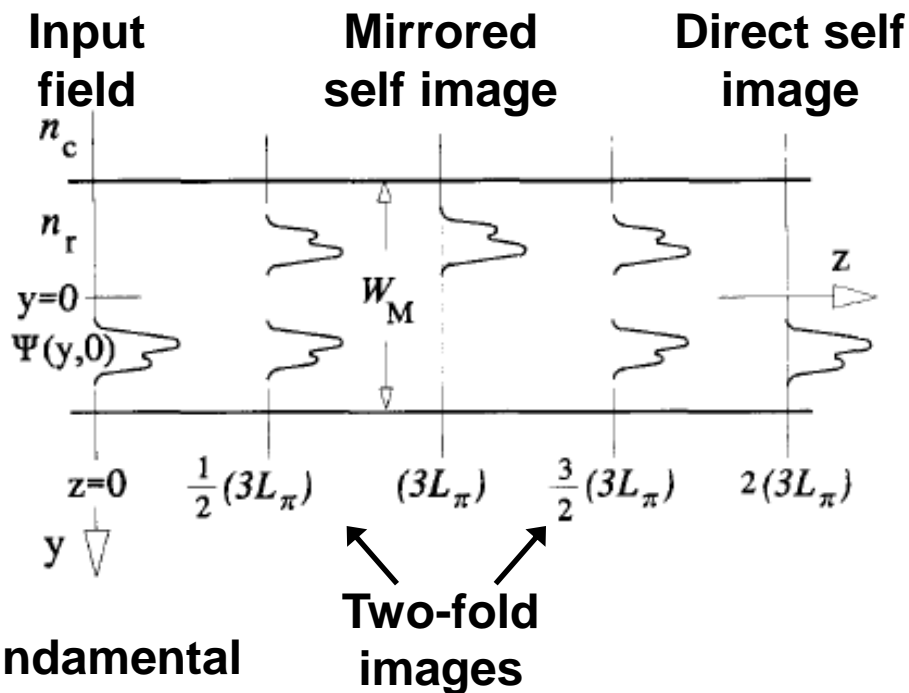


Multimode Interference (MMI) Coupler



- MMI coupler consists of a multimode region and input and output access waveguides that are nominally single mode
- Input field excites guided modes of multimode waveguide producing images of input field at periodic intervals along the direction of propagation (this is called self imaging)
- For 50:50 coupler, choose multimode region length so that two images of equal amplitude are produced at output waveguides

Principle of Self Imaging



Beat length of fundamental and second order mode

$$L_\pi = \frac{\pi}{\beta_0 - \beta_1} \simeq \frac{4n_r W_e^2}{3\lambda_0}$$

Field profile

$$\Psi(y, L) = \sum_{\nu=0}^{m-1} c_\nu \psi_\nu(y) \exp \left[j \frac{\nu(\nu+2)\pi}{3L_\pi} L \right]$$

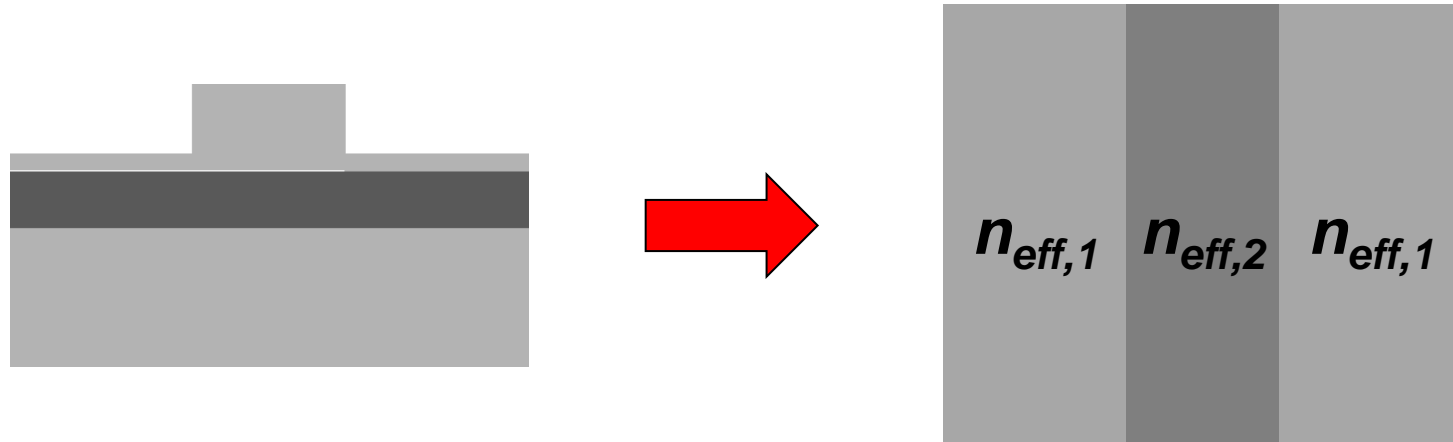
Mirrored image of input field at:

$$z = p(3L_\pi) \quad \text{with } p = 0, 1, 2, \dots$$

Two-fold imaging of input field at:

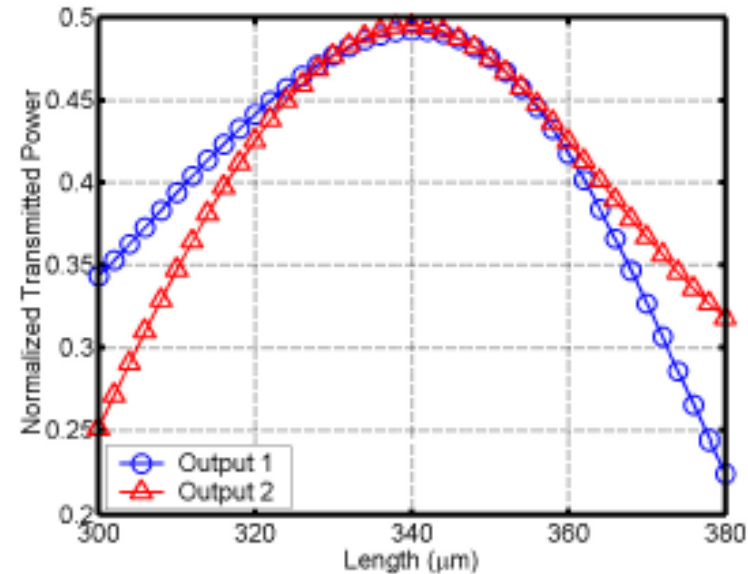
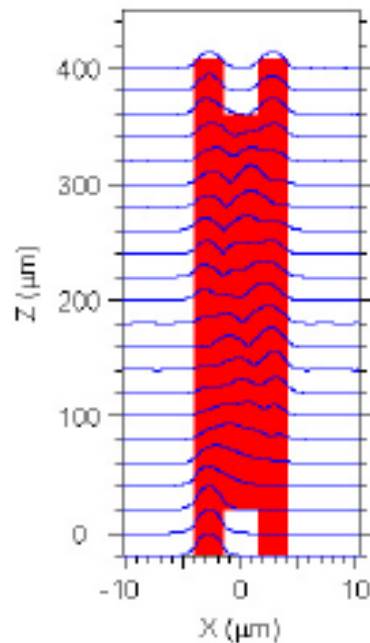
$$z = \frac{p}{2}(3L_\pi) \quad \text{with } p = 1, 3, 5, \dots$$

MMI Coupler Design



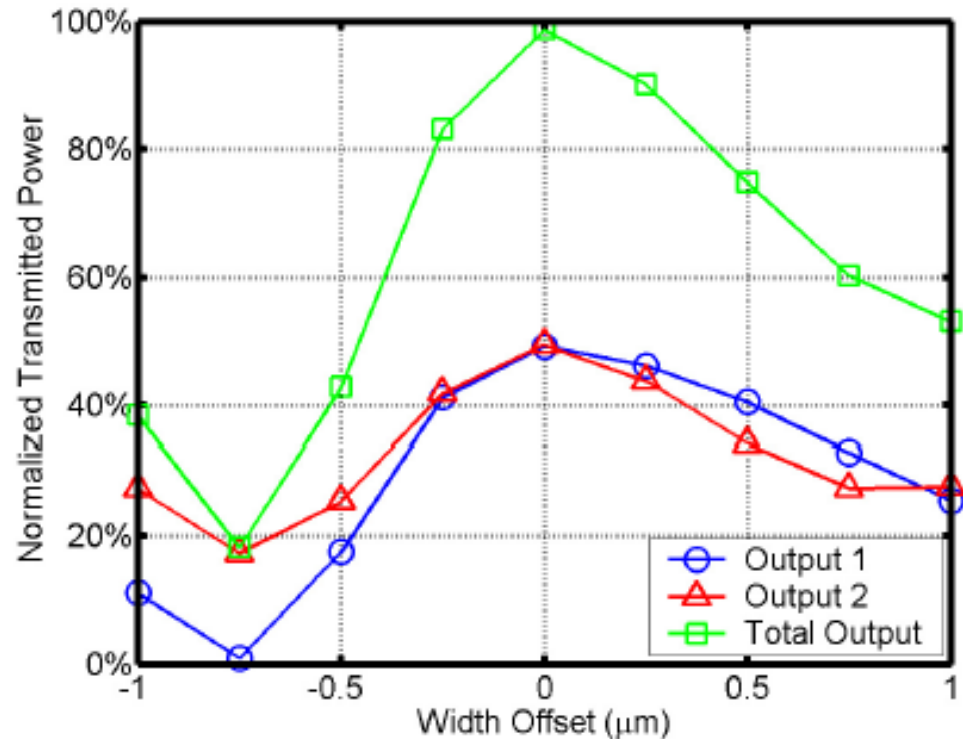
- First simplify the problem by applying the effective index method (2D \rightarrow 1D)
- Then use BPM simulation to design coupler
- Note: This works well for lower index contrast platforms (InP), but not so well for high index contrast (SiPh) – for high index contrast, best not to approximate

MMI Coupler Design



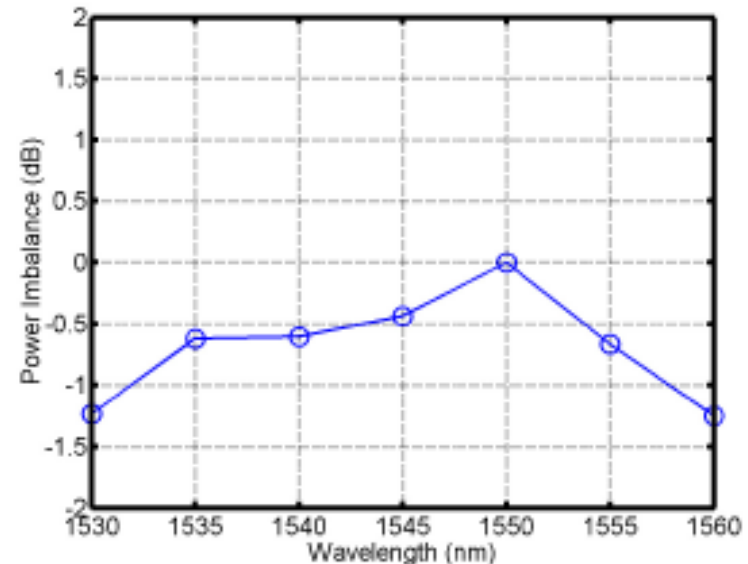
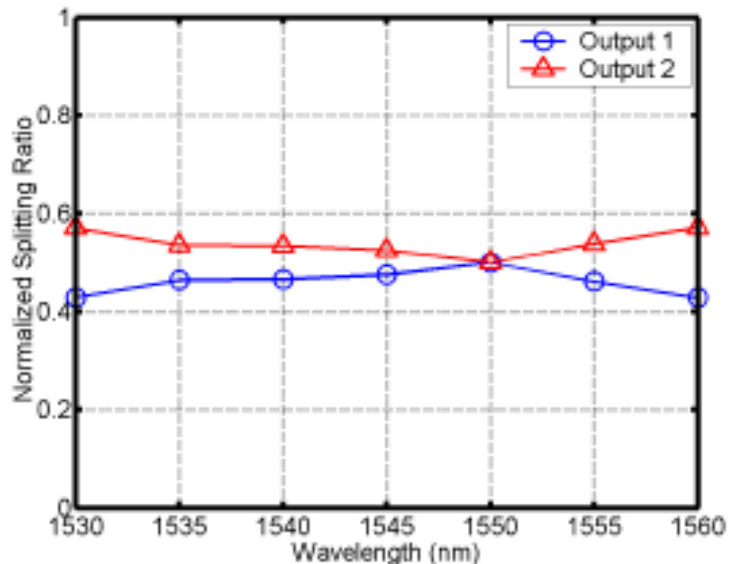
- Using BPM simulation tool, launch light at one input and monitor the two outputs while varying the MMI region length
- For 50:50 splitting, this 8- μm -wide MMI coupler requires a length of 340 μm
- Why did we use 8 μm for the width of the MMI region?

MMI Coupler Design



- To understand sensitivity, simulate the transmission as a function of MMI region width variation
- How would the above simulation influence your design?

MMI Coupler Performance



- What is the splitting ratio at 1530 nm?
- Power imbalance = $10\log_{10}(P_{OUT,1}/P_{OUT,2})$
- Why is it important to 'dial-in' your MMI coupler design with experiment?
 - Think about what parameters we used for simulation
- How can we increase the design tolerance?

Compact MMI Coupler



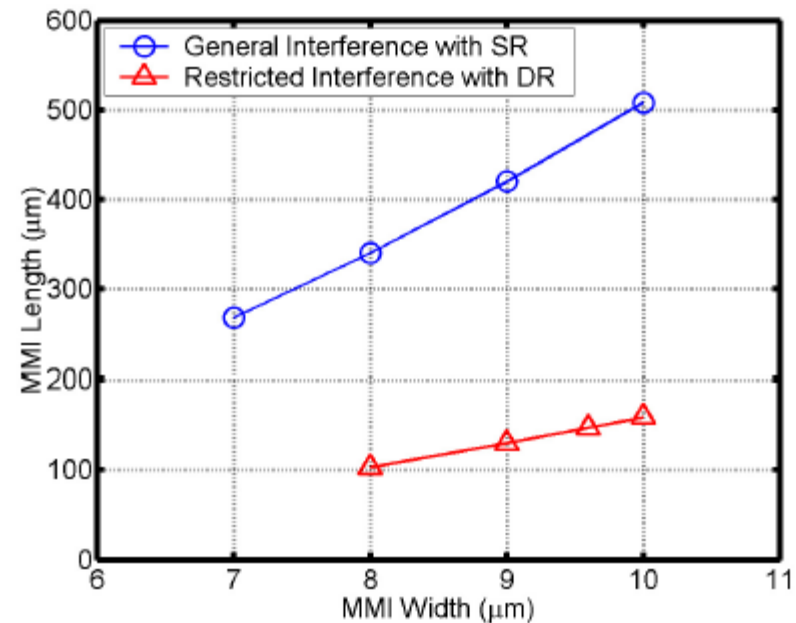
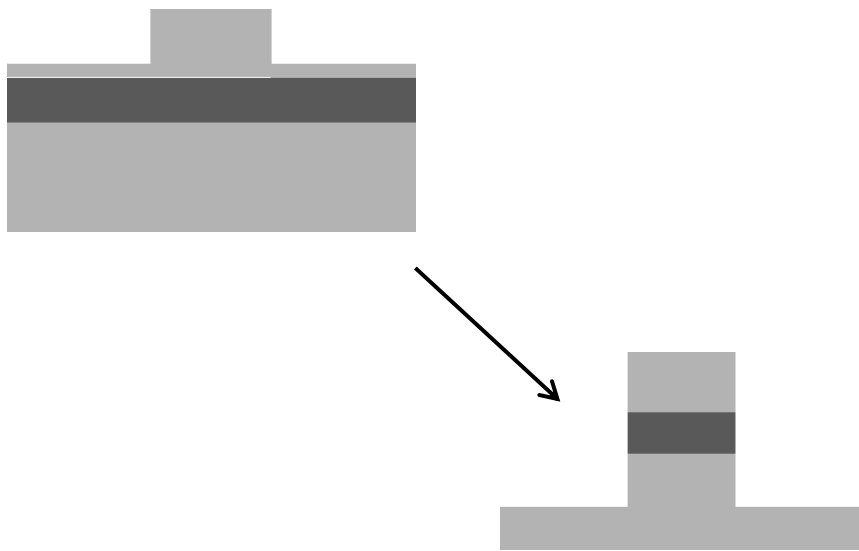
- The previous MMI coupler utilized what is known as a general interference, which means that no restrictions were placed on the number of modes excited in the MMI region.
- If instead excite only some of the modes, then the length for 50:50 splitting is shorter
 - If don't excite every third mode length is a factor of three shorter
- To achieve this selective excitation, can launch an even symmetric input field with access waveguides at $\pm W_e/6$

Compact MMI Coupler



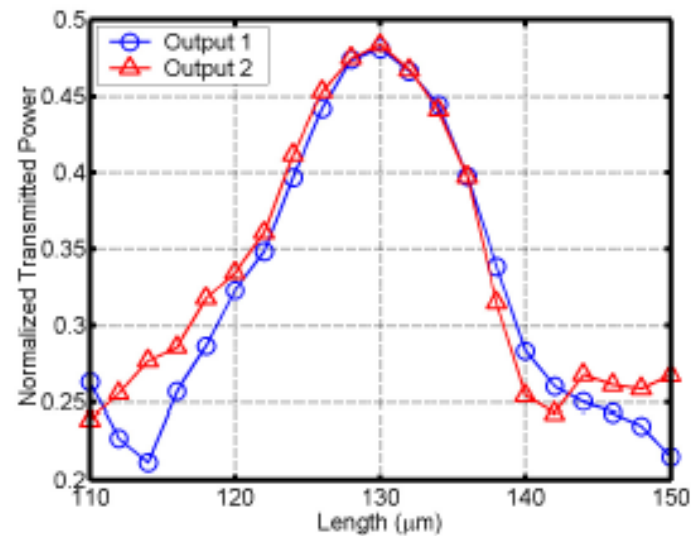
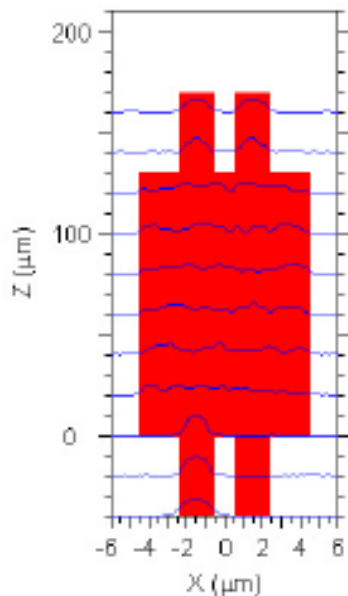
- The catch is that we are placing the access waveguides closer together and exciting fewer modes, which can affect the imaging quality
- Using same ridge structure as before, feasible MMI region width is $10.5 \mu\text{m}$ (for access waveguide spacing), but imaging quality is poor
- To still maintain compactness but improve the design, we can use a more highly confined waveguide architecture
 - Better imaging quality because more modes are confined
 - Smaller access waveguides so narrow MMI region

Compact MMI Coupler



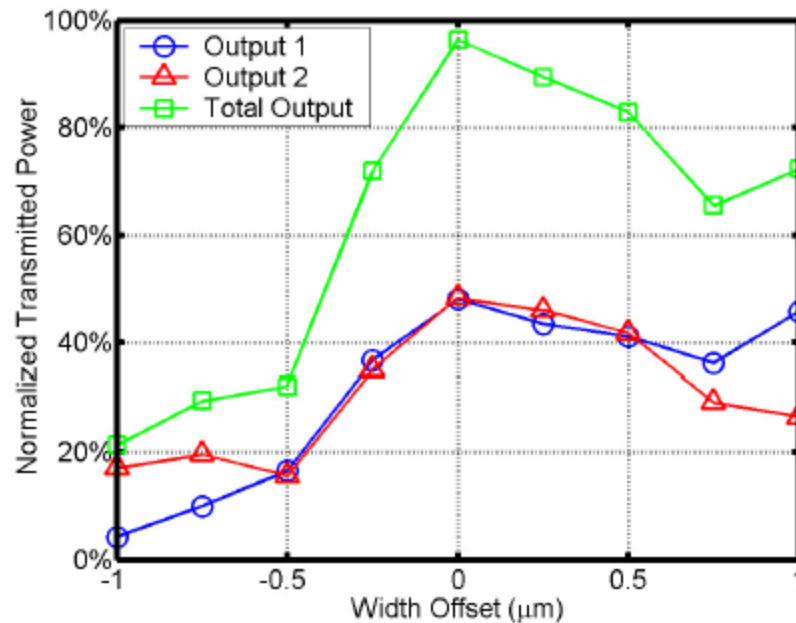
- Ridge to deep ridge for higher confinement
- Simulation shows reduction in length achieved using restricted interference

Compact MMI Coupler Design



- Simulate new structure, but effective index method does not work as well for highly confined waveguides
- Instead use 3D BPM and wait longer for the simulation

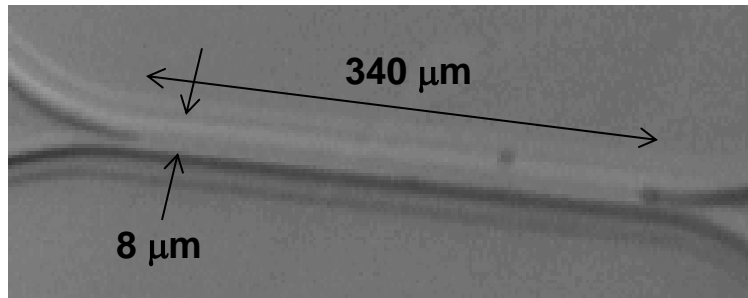
Compact MMI Coupler



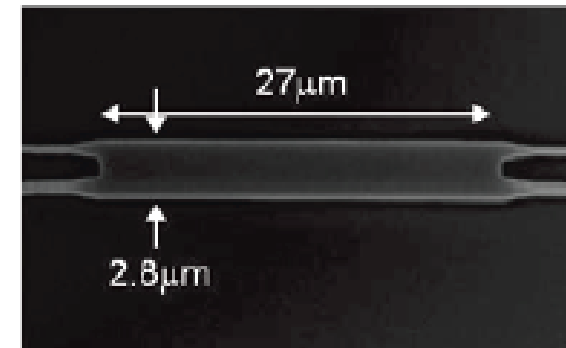
- **To understand sensitivity, simulate the transmission as a function of MMI region width variation**

MMI Coupler Comparison

InP MMI Coupler



SiPh MMI Coupler

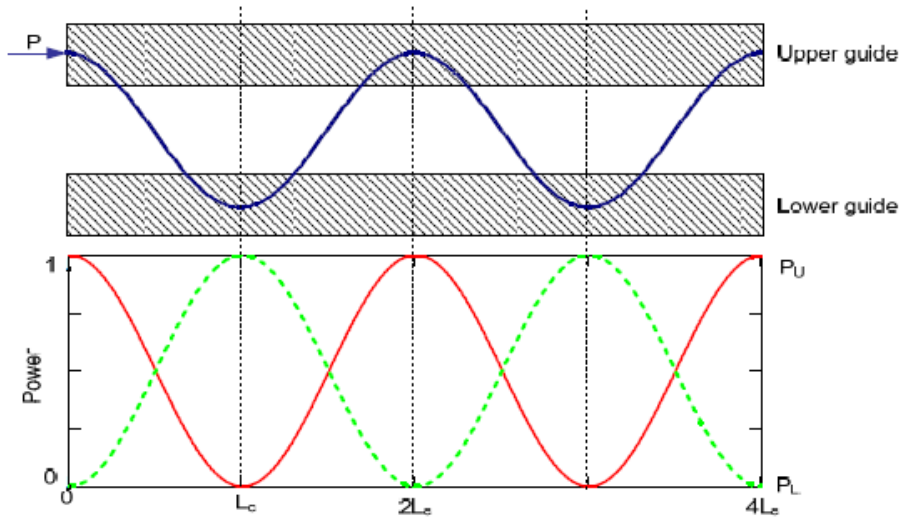
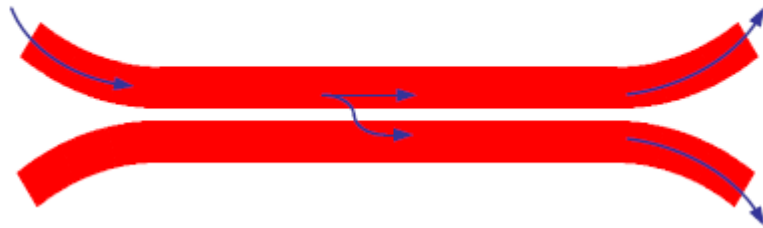


- **SiPh is a higher index contrast platform**
- **Multimode region can be small and still support sufficient number of modes for imaging quality**

Directional Coupler

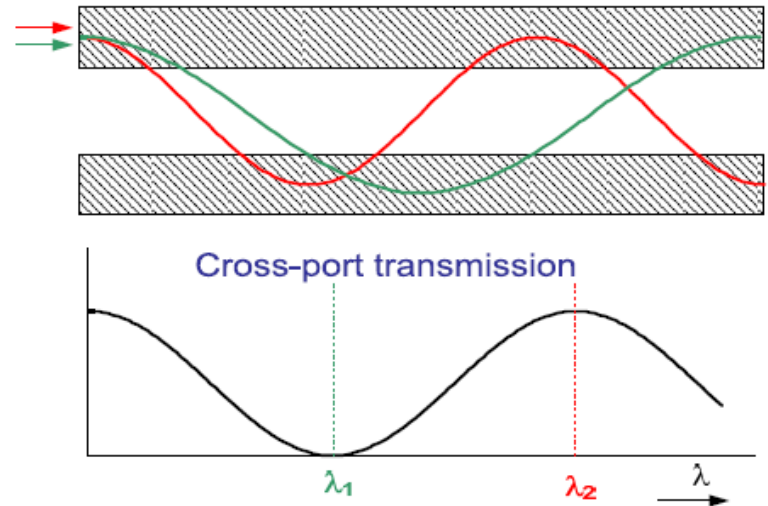
1x2 splitter or 2x2 coupler

in out

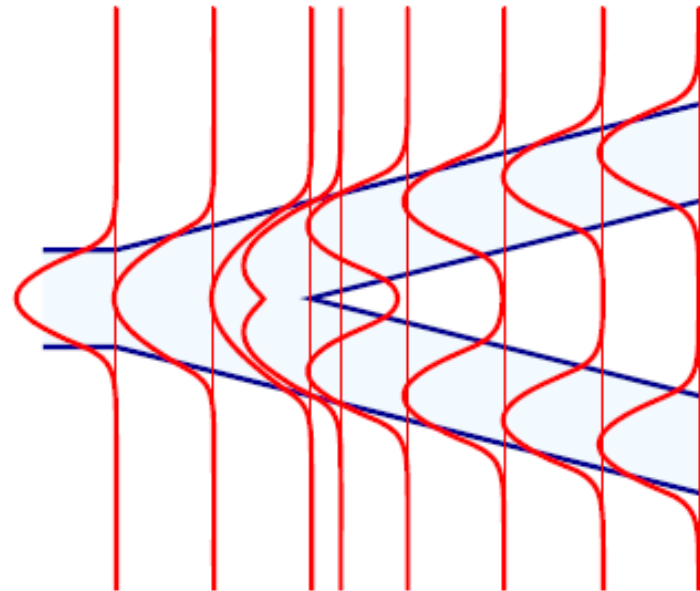
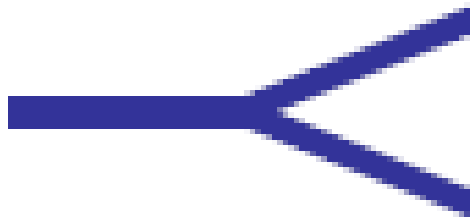


*Jeppix

Duplexer



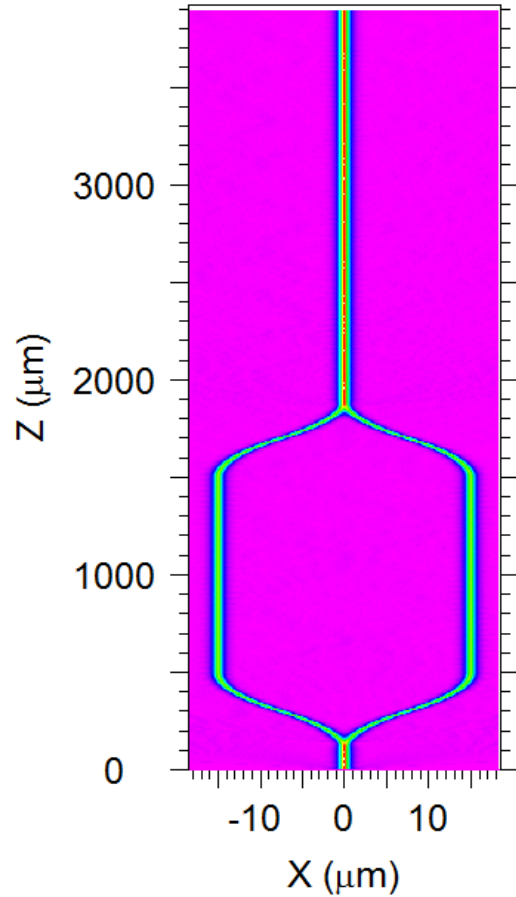
Y-Branch



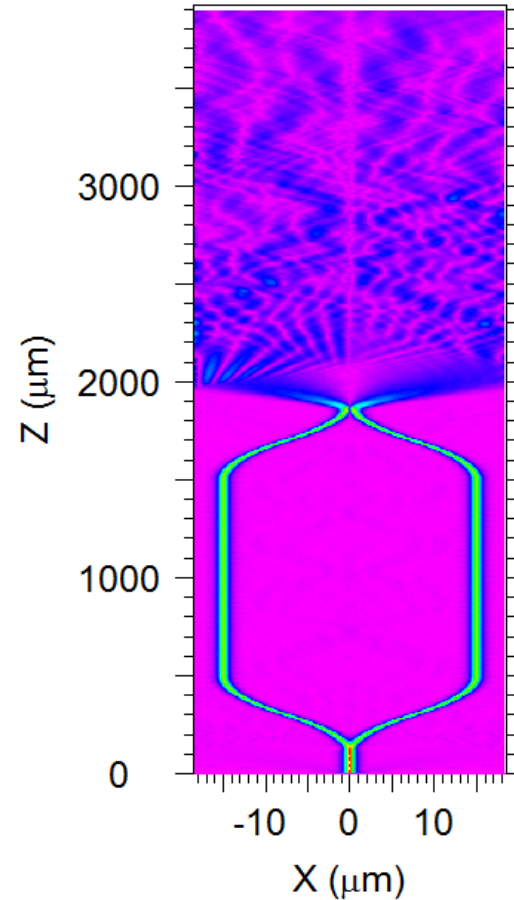
**Jeppix*

Mach-Zehnder Modulator/Switch

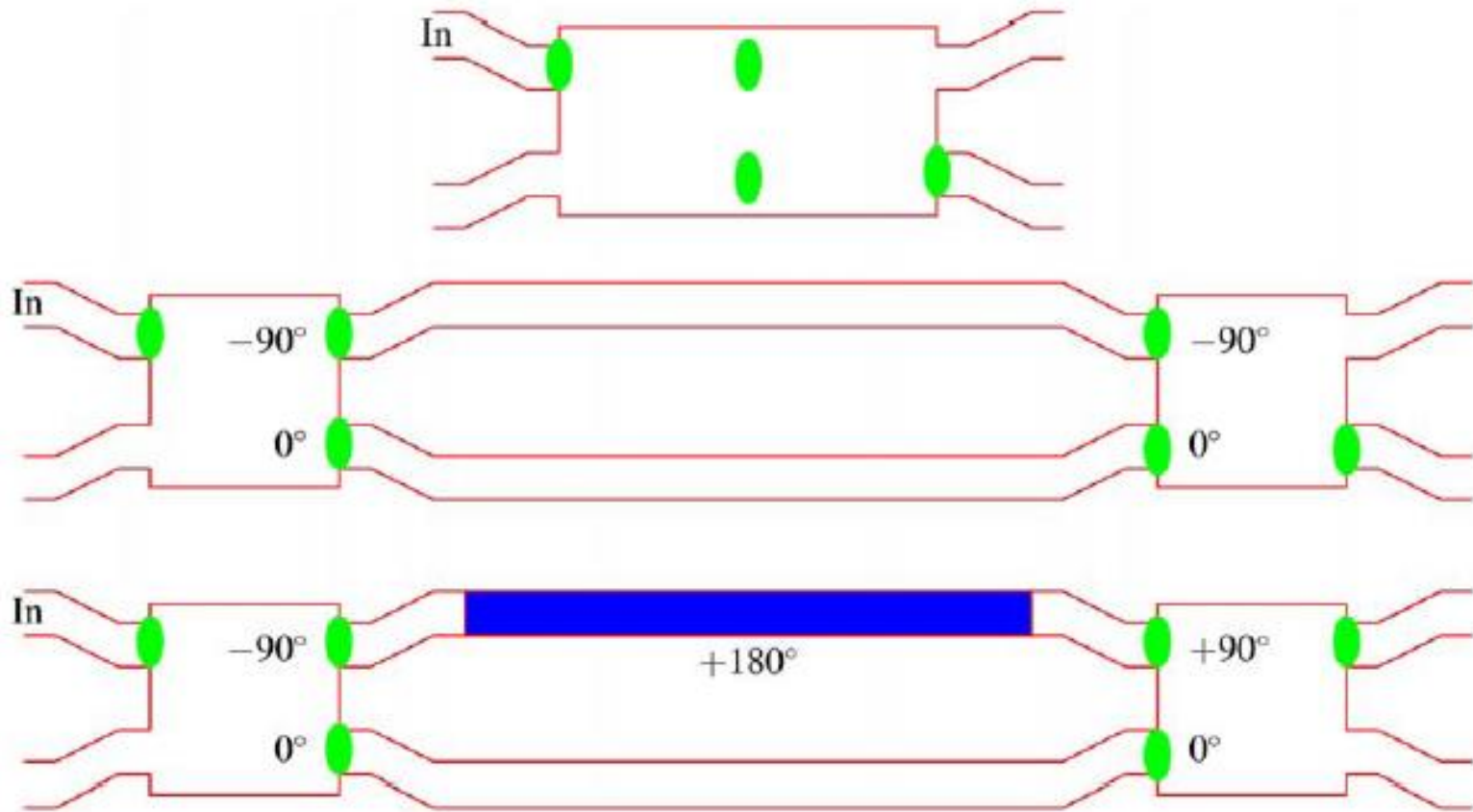
Constructive Interference



Destructive Interference

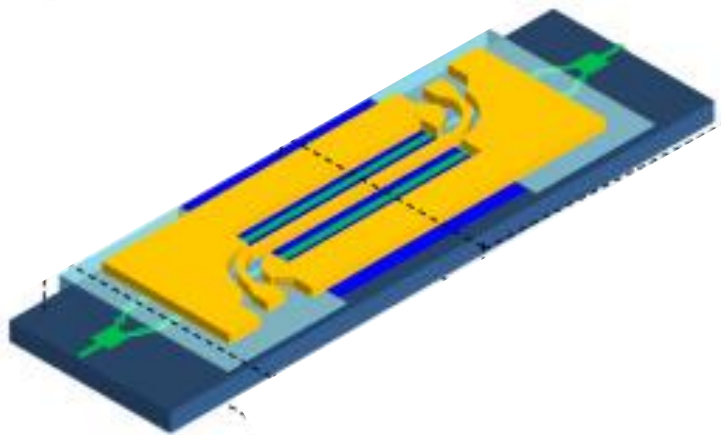


Mach-Zehnder Modulator/Switch

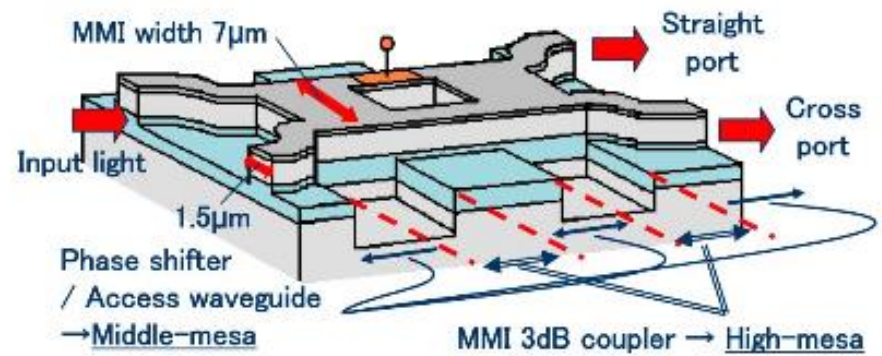


*Jeppix

Mach-Zehnder Modulator/Switch

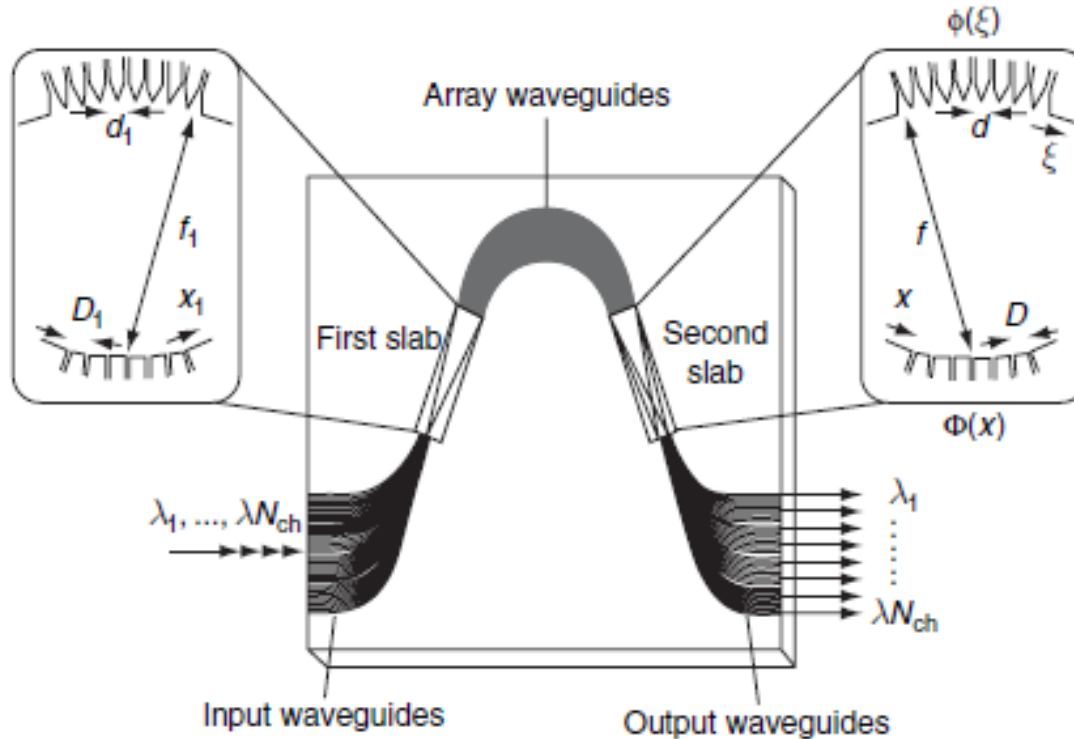


Y. Ogiso, et al., OE, 2014



Y. Ueda, et al., PTL, 2009

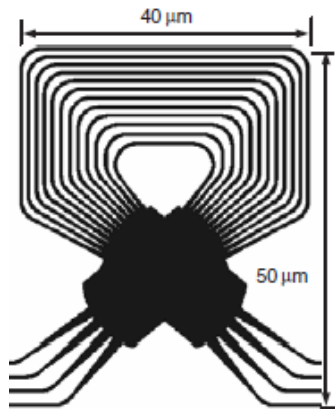
Arrayed Waveguide Grating (AWG)



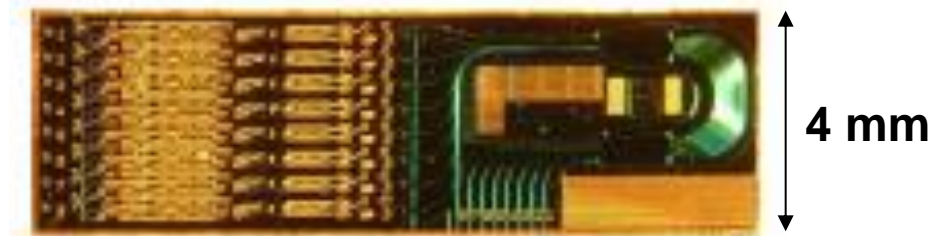
- **AWG consists of input and output waveguides, star couplers, and an array of waveguides with fixed path difference between neighbors**
- **It is essentially a MZI with more than two waveguides**
- **Field from input waveguide illuminates waveguides in array through star coupler, then fields interfere constructively in one of the output ports**

AWG Examples

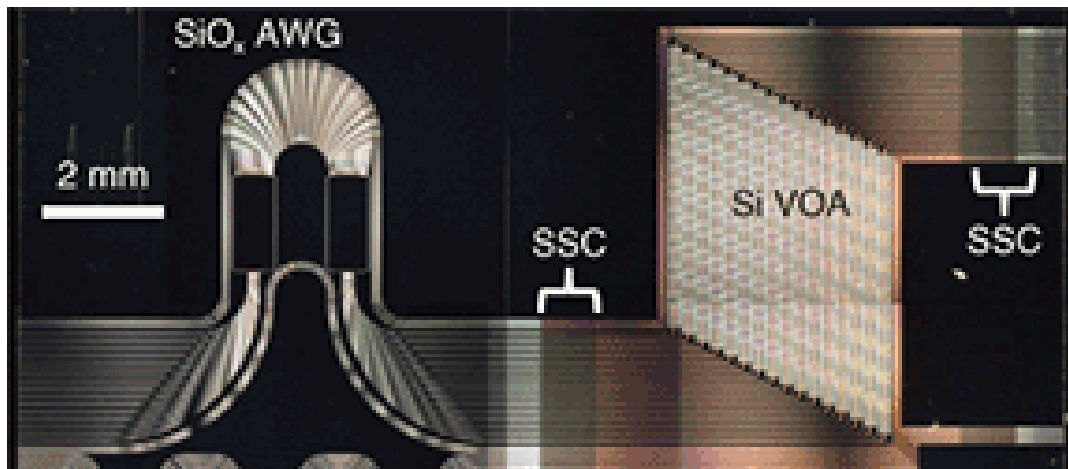
Si



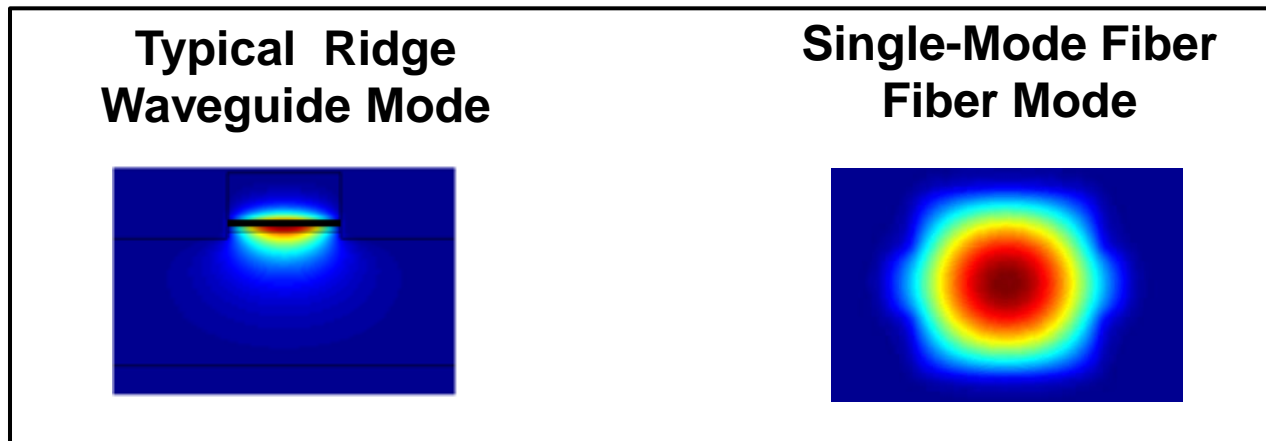
InP



SiO_x



Spot-Size Converter

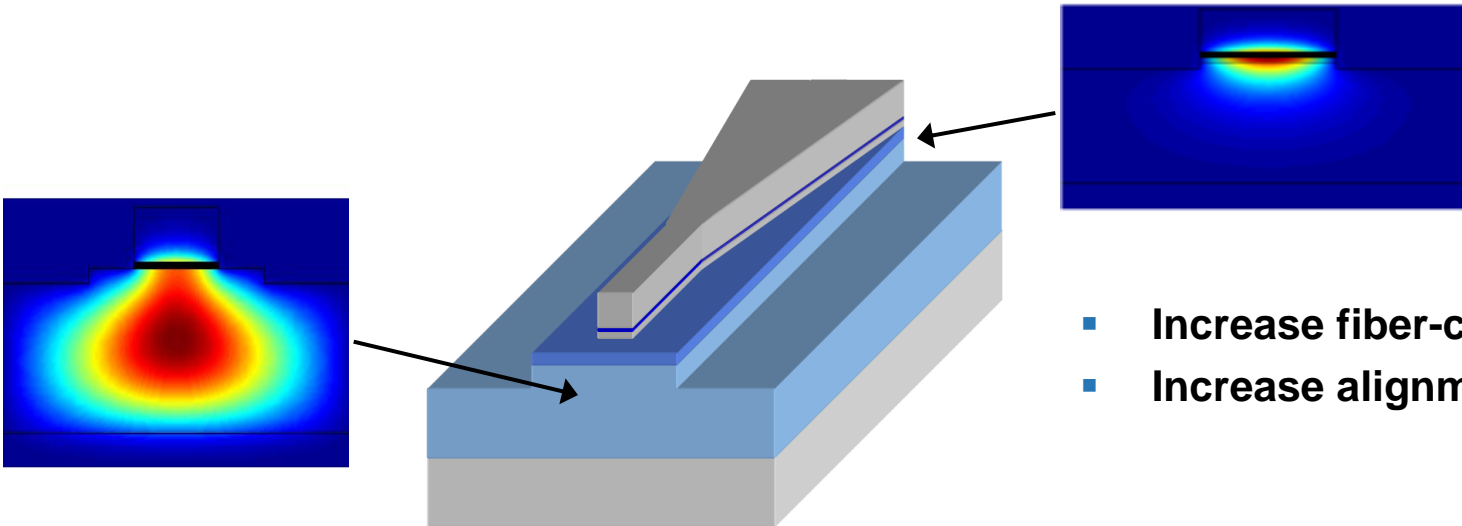
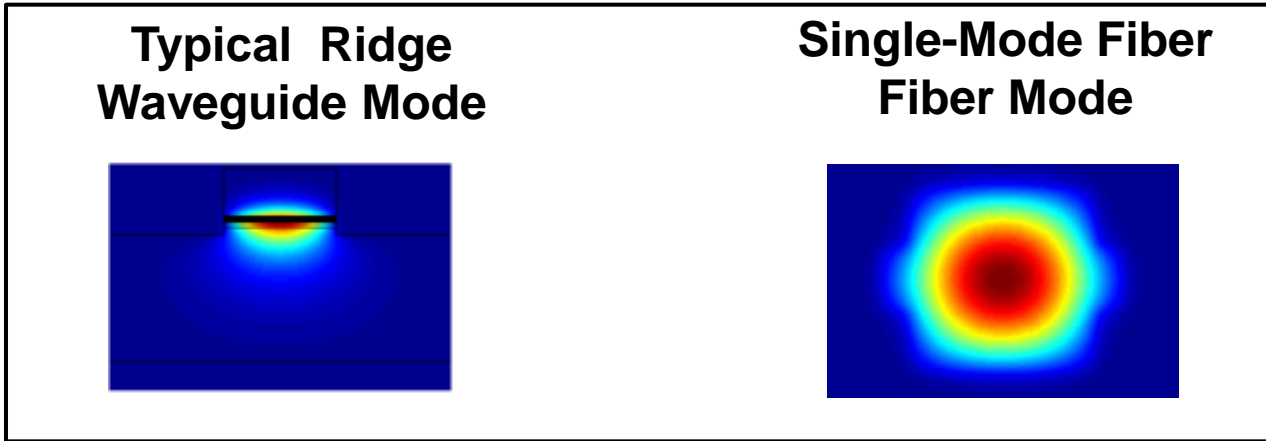


Index contrast = 1-45%
Mode size $\sim 1 \mu\text{m} \times 3 \mu\text{m}$ (InP)
Mode size $\sim 0.3 \mu\text{m} \times 0.5 \mu\text{m}$ (Si)

Index contrast = 0.1-0.3%
Mode size $\sim 10 \mu\text{m} \times 10 \mu\text{m}$

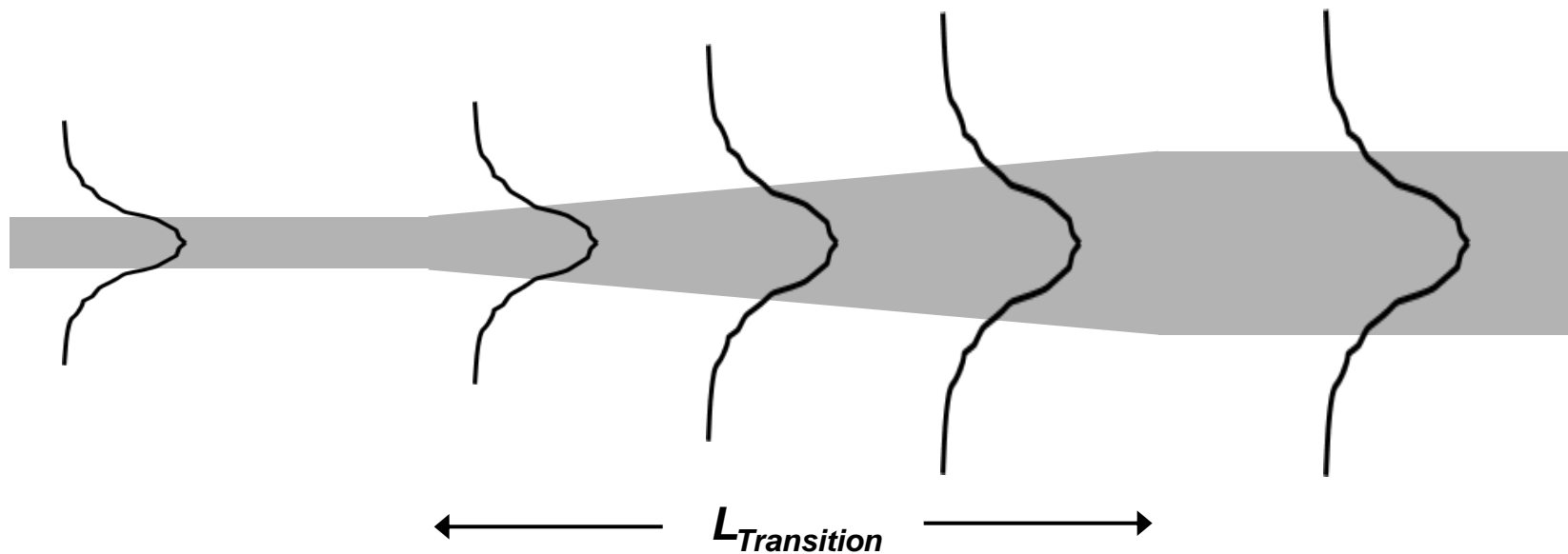
- Lensed fibers or microlenses can transform mode size
- Complex optics or wedged fibers can alter shape but complicated to build and align
- Need to solve both size and asymmetry problem

Spot-Size Converter



- Increase fiber-coupling efficiency
- Increase alignment tolerance

Adiabatic Transition



- An adiabatic transition occurs gradually with respect to distance along the propagation direction such that power is not transferred to other modes

Spot-Size Converters

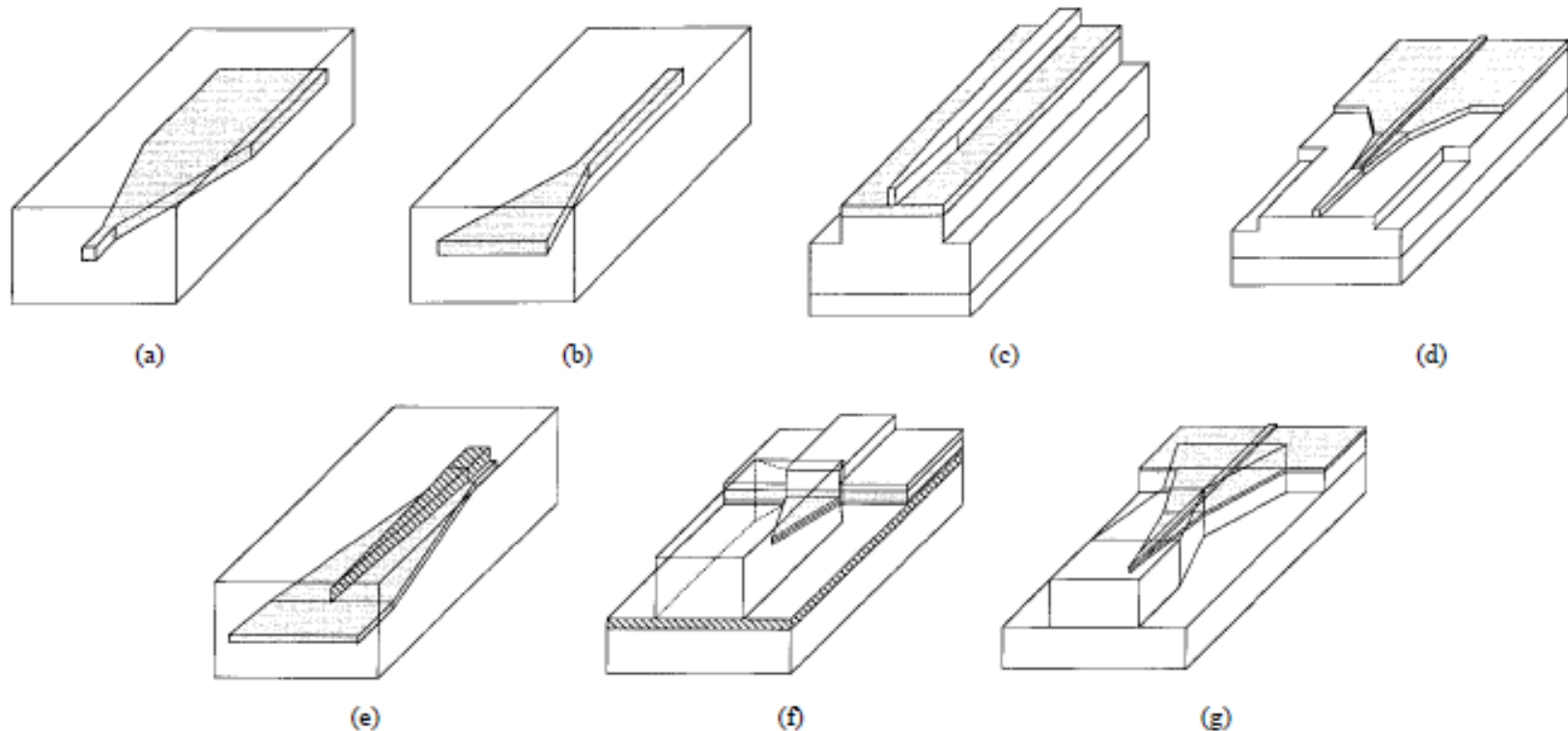


Fig. 2. Lateral taper designs. (a) Lateral down-tapered buried waveguide. (b) Lateral up-tapered buried waveguide. (c) Single lateral taper transition from a ridge waveguide to a fiber-matched waveguide. (d) Multisection taper transition from a ridge waveguide to a fiber-matched waveguide. (e) Dual lateral overlapping buried waveguide taper. (f) Dual lateral overlapping ridge waveguide taper. (g) Nested waveguide taper transition from a ridge waveguide to a fiber-matched waveguide.

- **Horizontal tapers easy to make but sensitive to width variations**

Moerman, et al., IEEE JSTQE, 3(6), 1997

Spot-Size Converters

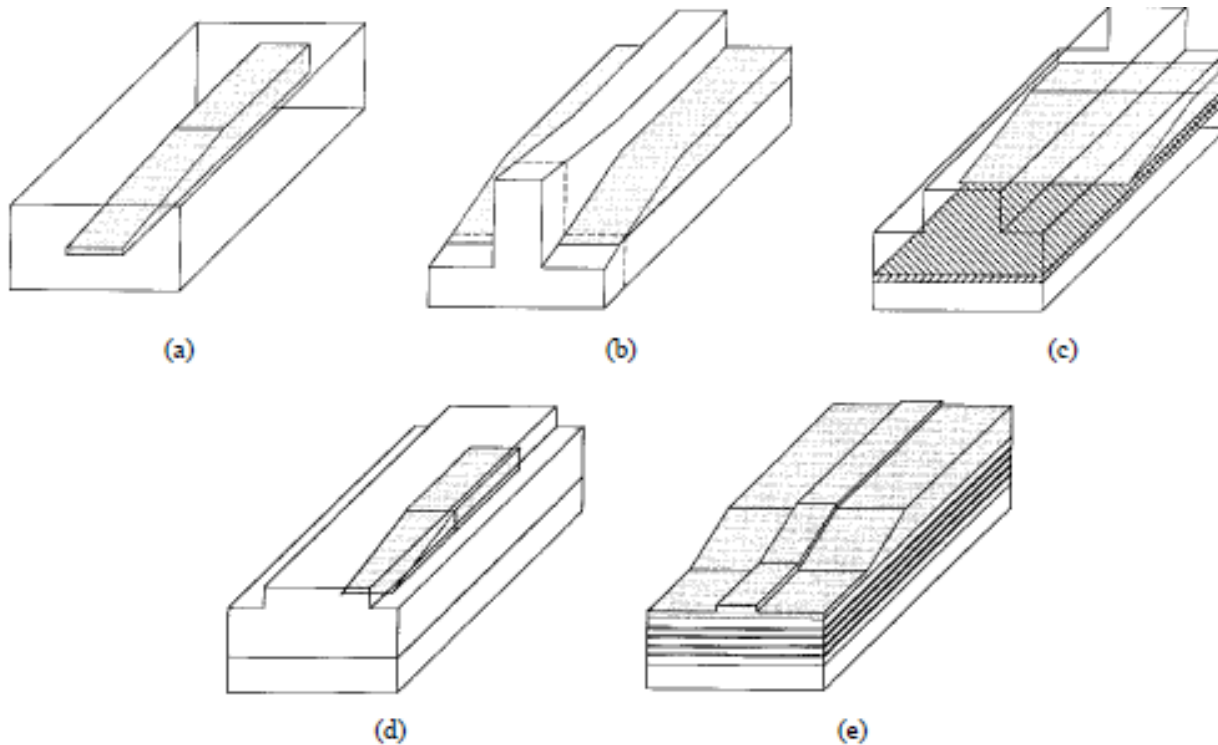


Fig. 3. Vertical taper designs. (a) Vertical down-tapered buried waveguide. (b) Vertical down-tapered ridge waveguide. (c) Vertical overlapping ridge waveguide taper. (d) Vertical overlapping waveguide taper transition from a buried waveguide to a fiber-matched waveguide. (e) Vertical overlapping waveguide taper transition from a ridge waveguide to a fiber-matched waveguide.

- Vertical taper more effective for asymmetric waveguides

Moerman, et al., IEEE JSTQE, 3(6), 1997

Spot-Size Converters

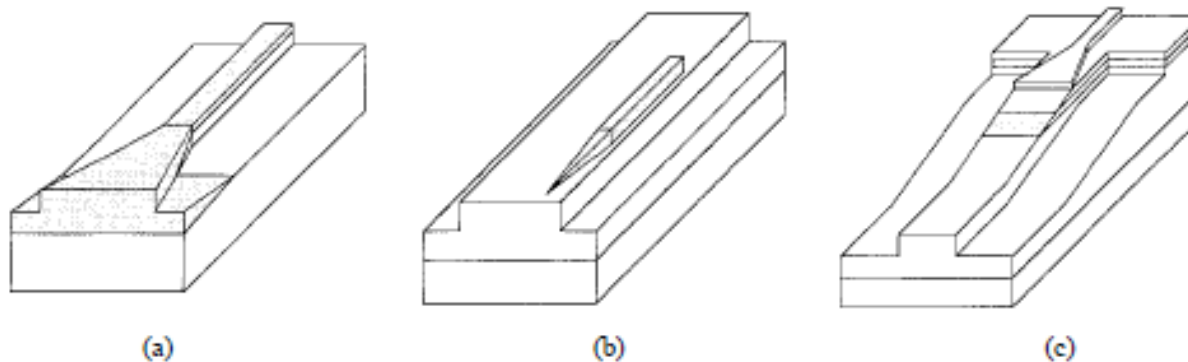
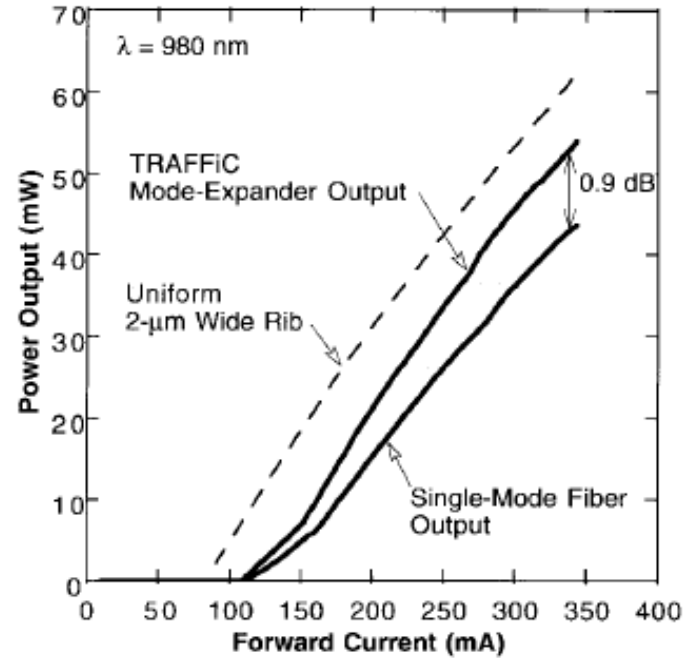
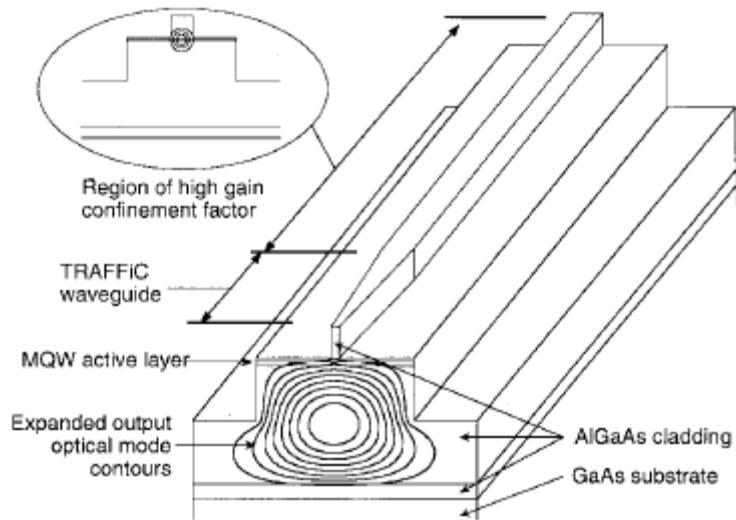


Fig. 4. Combined vertical and lateral taper designs. (a) Combined lateral and vertical ridge waveguide taper. (b) 2-D overlapping waveguide taper transition from a buried waveguide to a fiber-matched waveguide. (c) Overlapping waveguide taper transition with two sections from a ridge waveguide to a fiber-matched waveguide.

- **Combine vertical and horizontal tapers for most effective spot-size conversion**

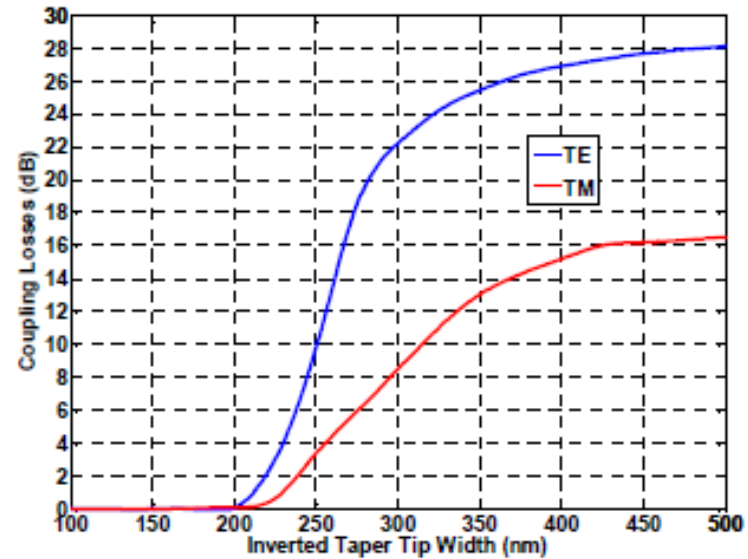
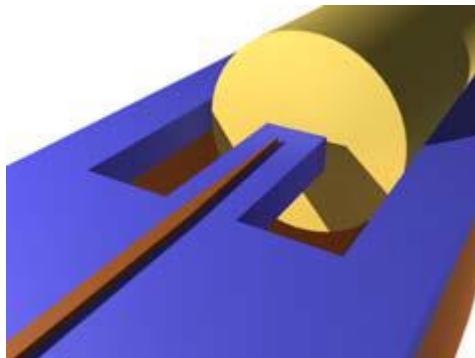
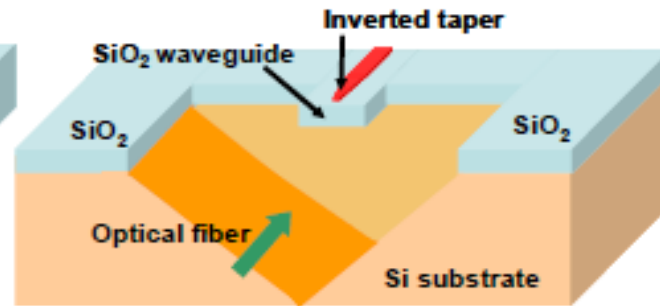
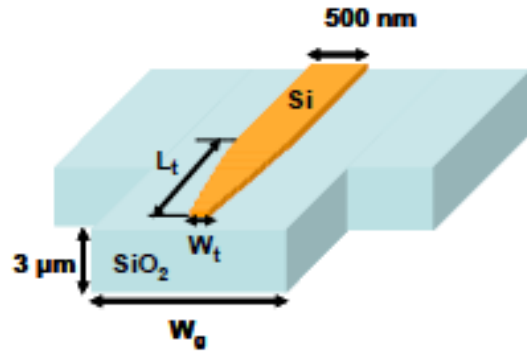
Moerman, et al., IEEE JSTQE, 3(6), 1997

InP SSC Example



Vawter, et al., PTL, 9(4), 1997

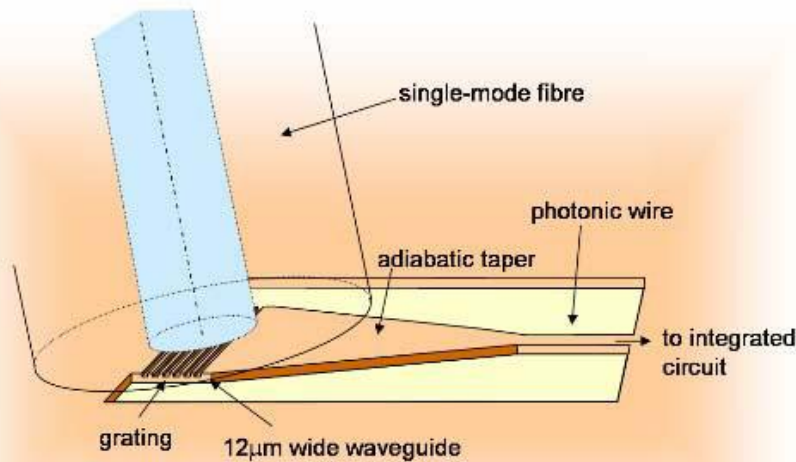
SiPh SSC Example



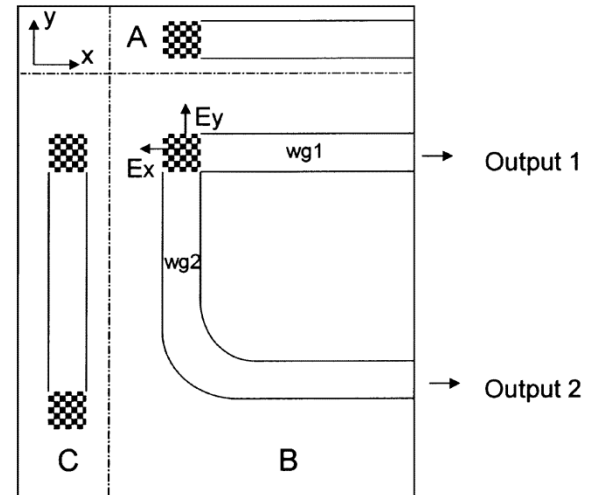
Galan, et al., Optics Express, 15(11), 2007

SiPh Grating Coupler

Vertical Grating Coupler

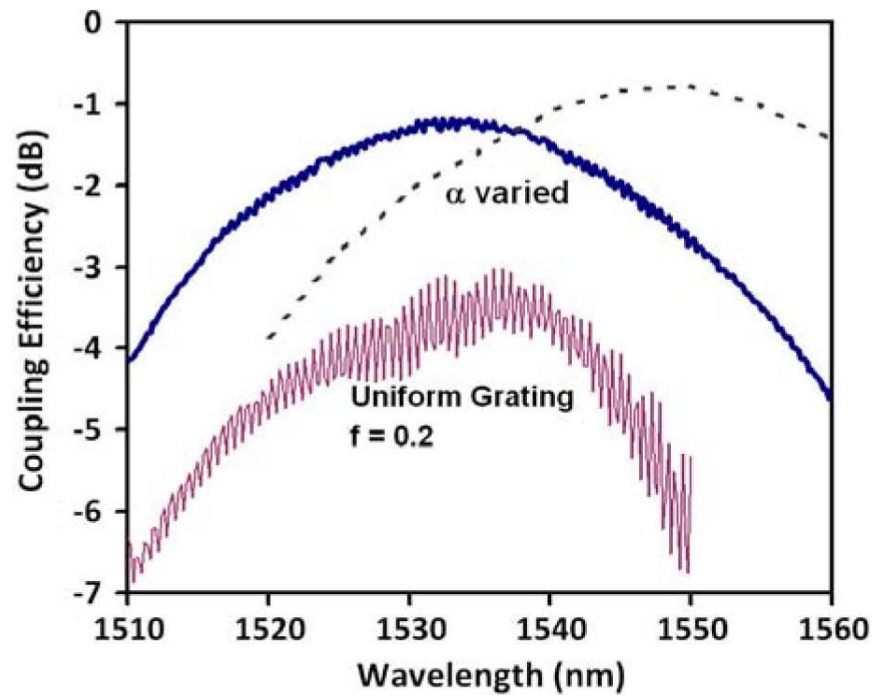
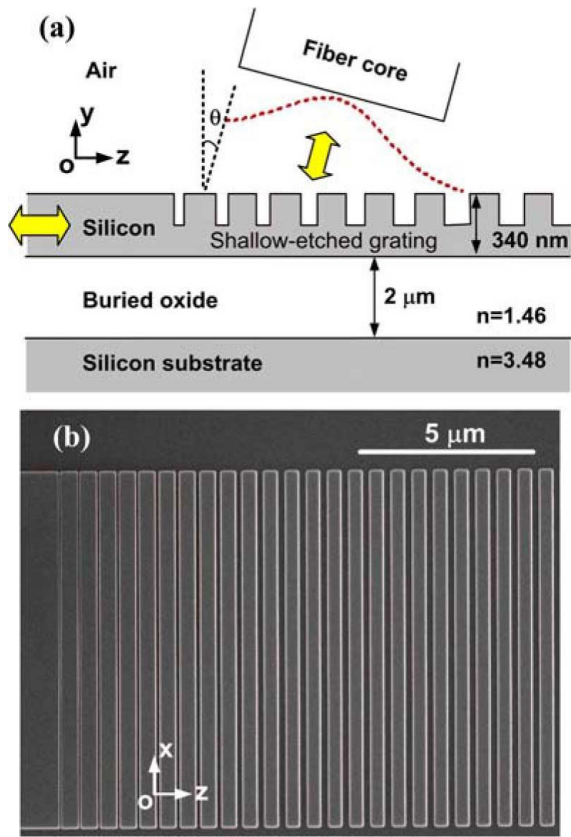


Polarization Diversity



- Do not have to rely on cleaved facets for coupling
- Allows for on-chip testing
- 2D grating allows for polarization diversity

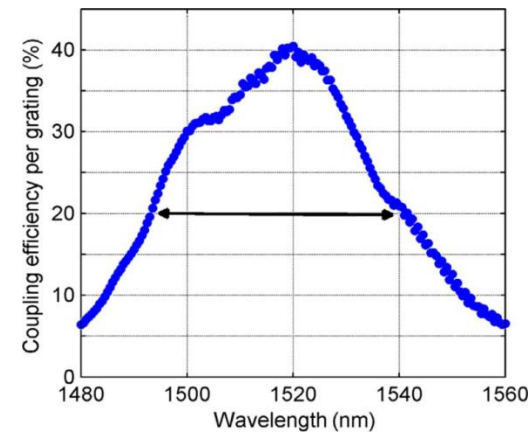
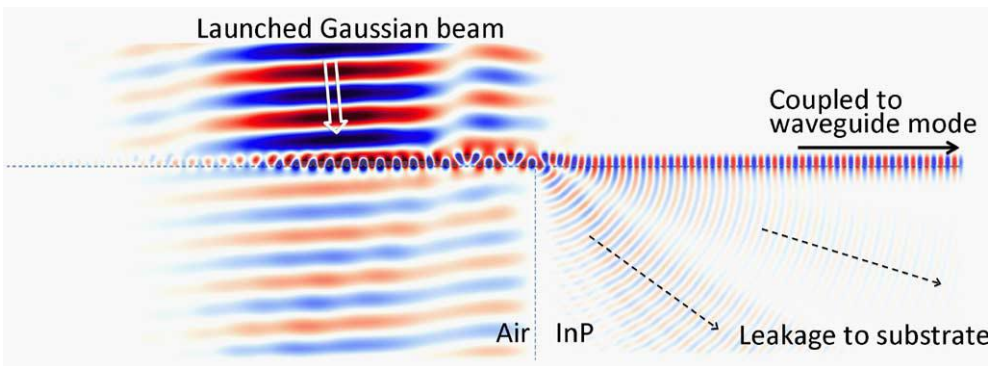
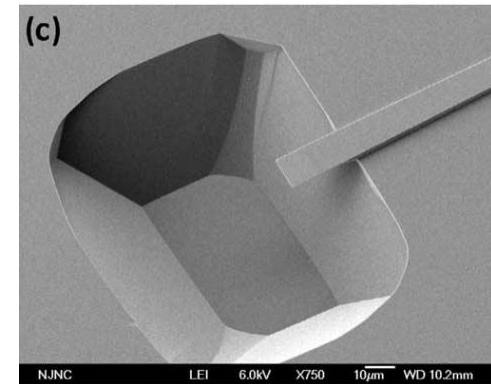
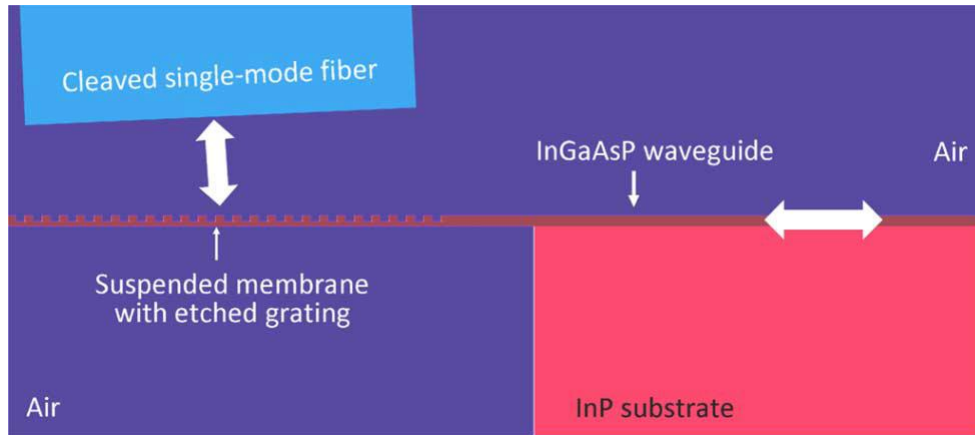
Apodized SiPh Grating Coupler



X. Chen et al., PTL, 22(15), 2010

- High index contrast SOI platform ideal for surface grating coupler
- This example uses apodized grating

InP Grating Coupler

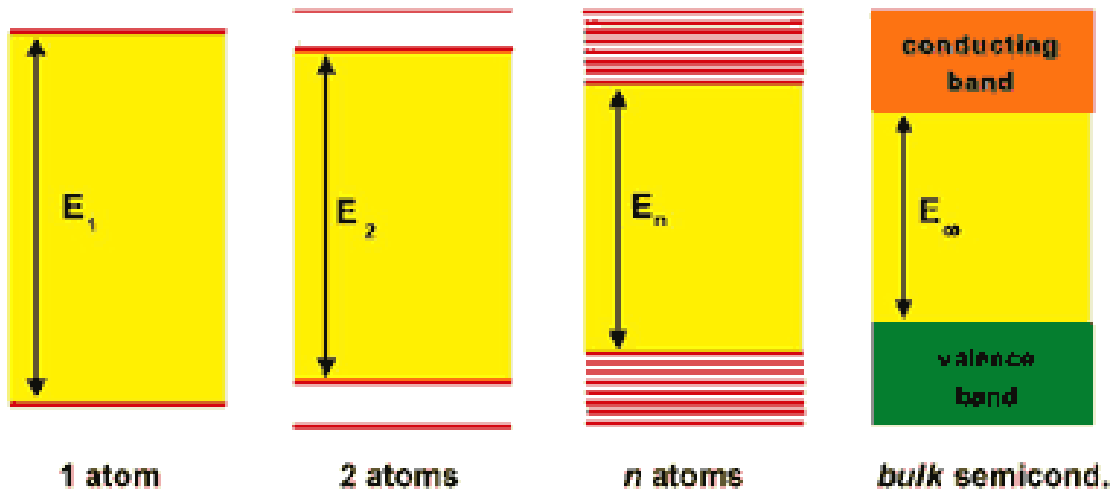


L. Chen et al., PTL, 22(12), 2010

- Grating coupler requires high index contrast
- This work used a suspended membrane for grating

Actives

Energy Bands in Solids

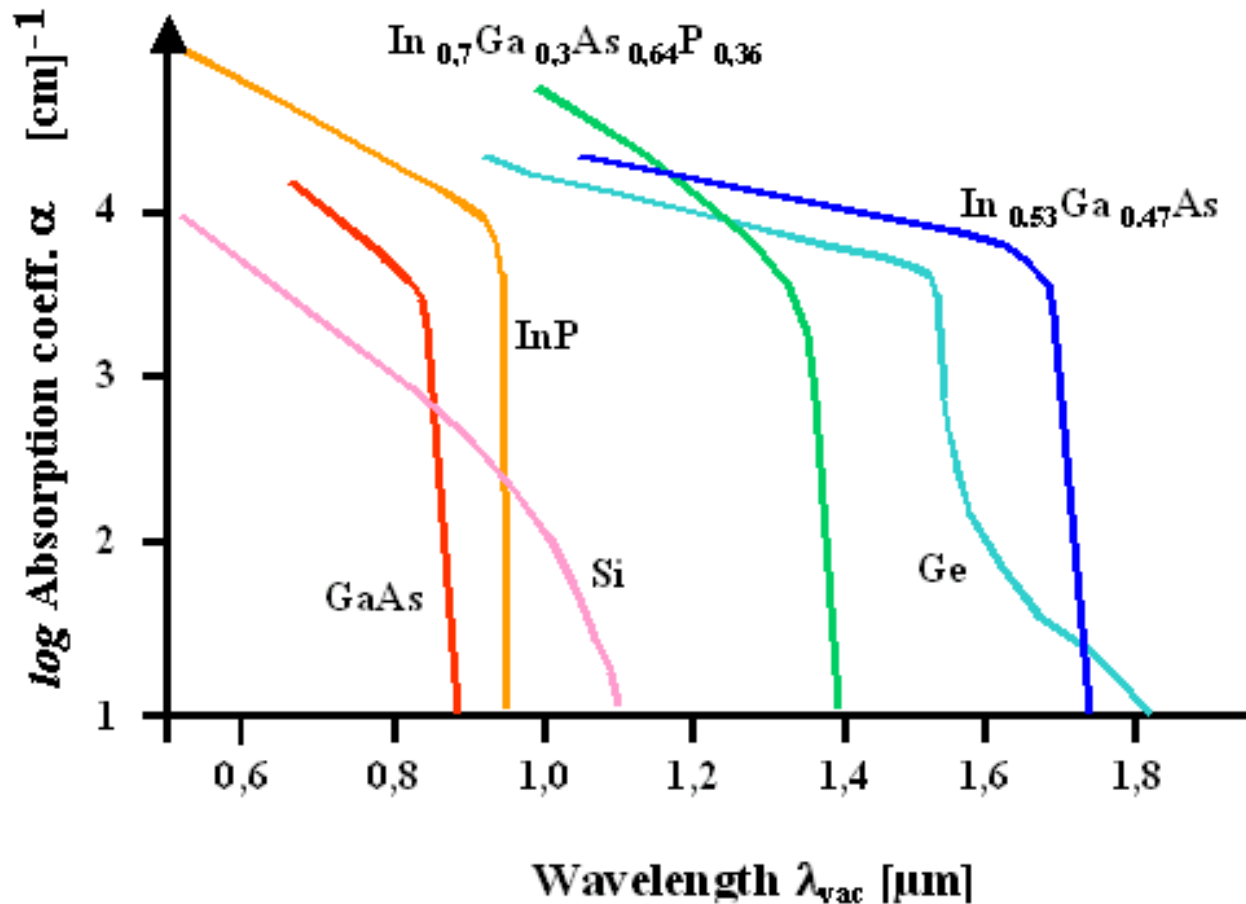


$$E_1 > E_2 > E_n > E_\infty$$

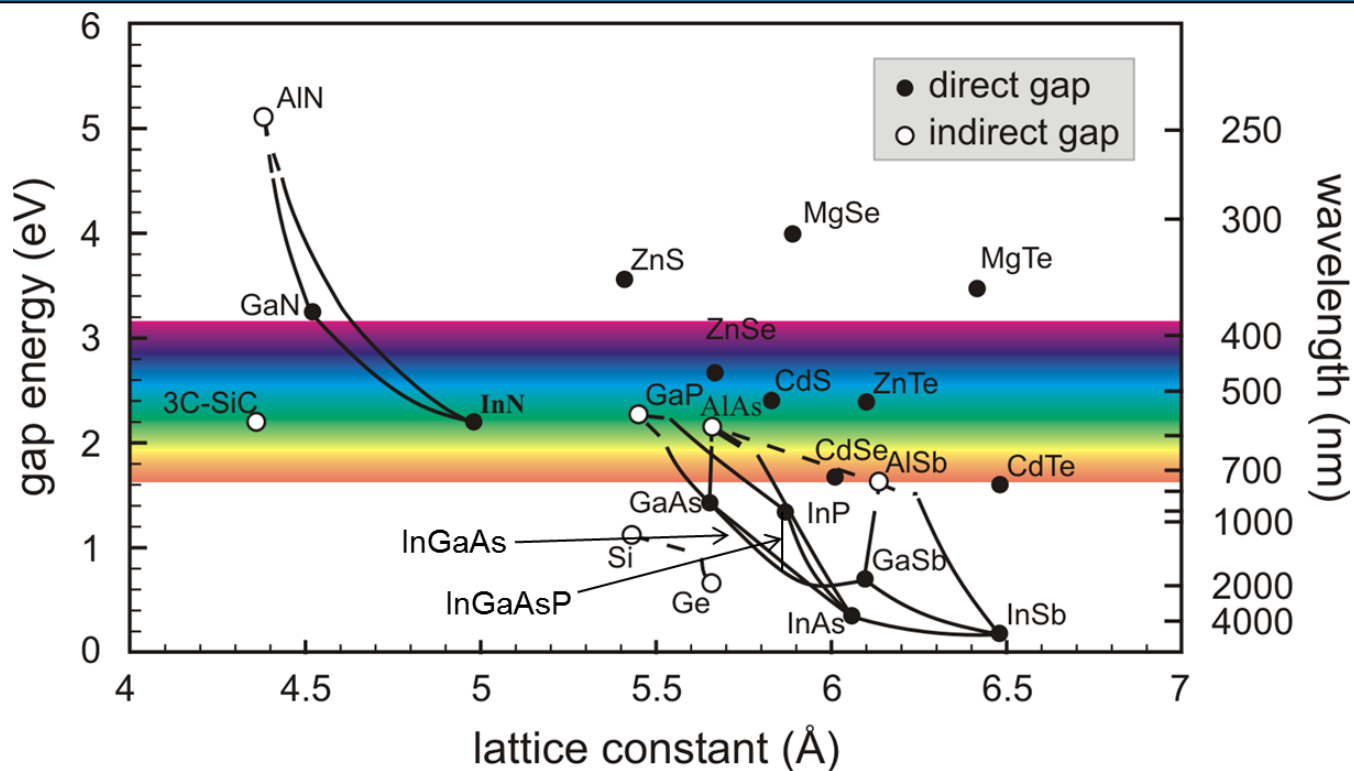
$$E = \frac{hc}{\lambda}$$

- **Optically induced transitions in isolated atoms behave as two-level systems; also nearly the case for gas and solid state lasers**
- **Emitted or absorbed photons will have nearly exact energy E_1**
- **In a solid, covalent bonding nature causes energy levels to broaden into bands (disturbs spectral purity)**

Absorption Spectra of Photonic Materials



Lattice Constants



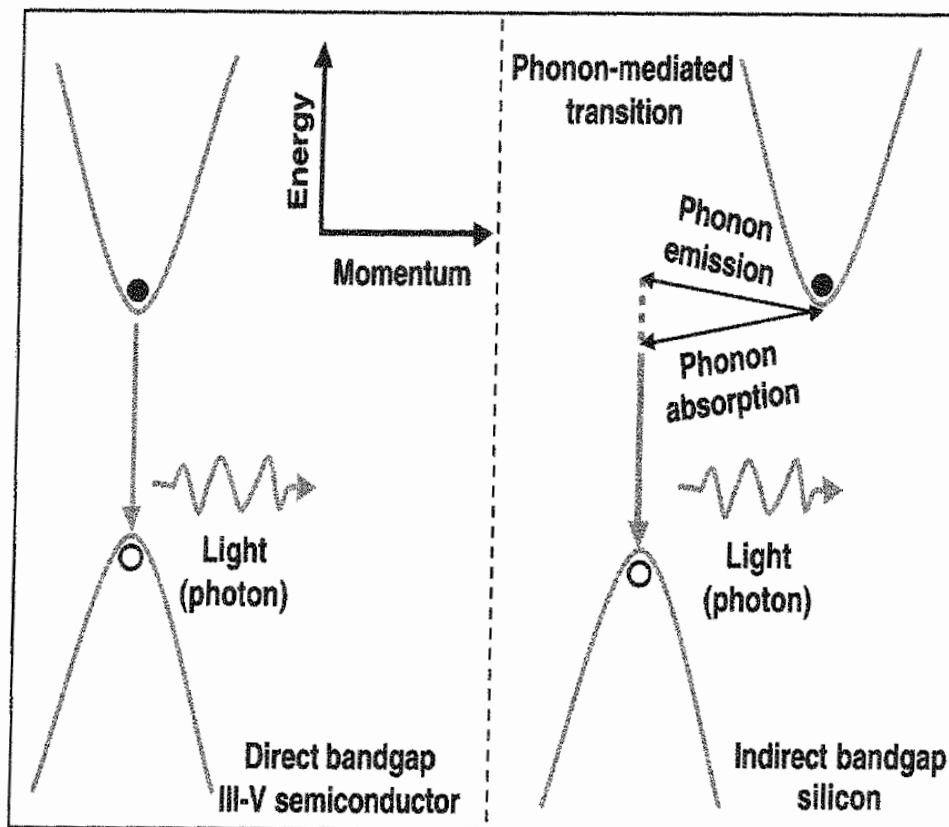
- Only certain substrates available
- InGaAsP can be tuned from ~1.0-1.6 μm , InGaAs ~1.65 μm
- Strain due to lattice mismatch
 - Limits compatibility but some strain may be desirable

Direct Versus Indirect Bandgap

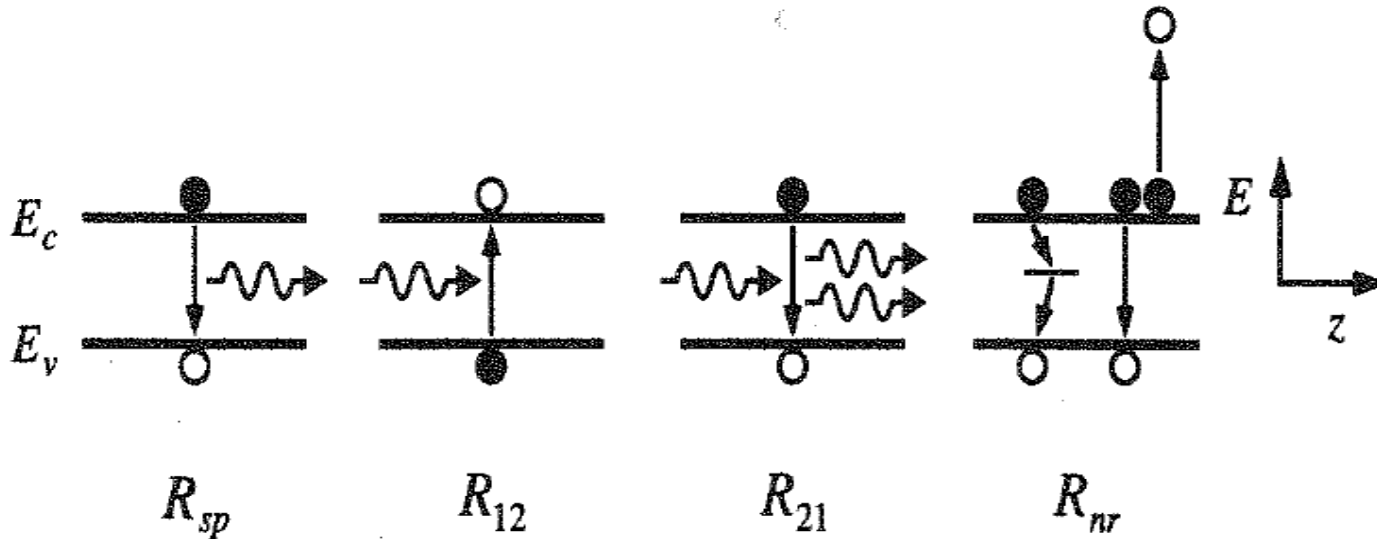
Simplified picture

Conduction Band

Valence Band

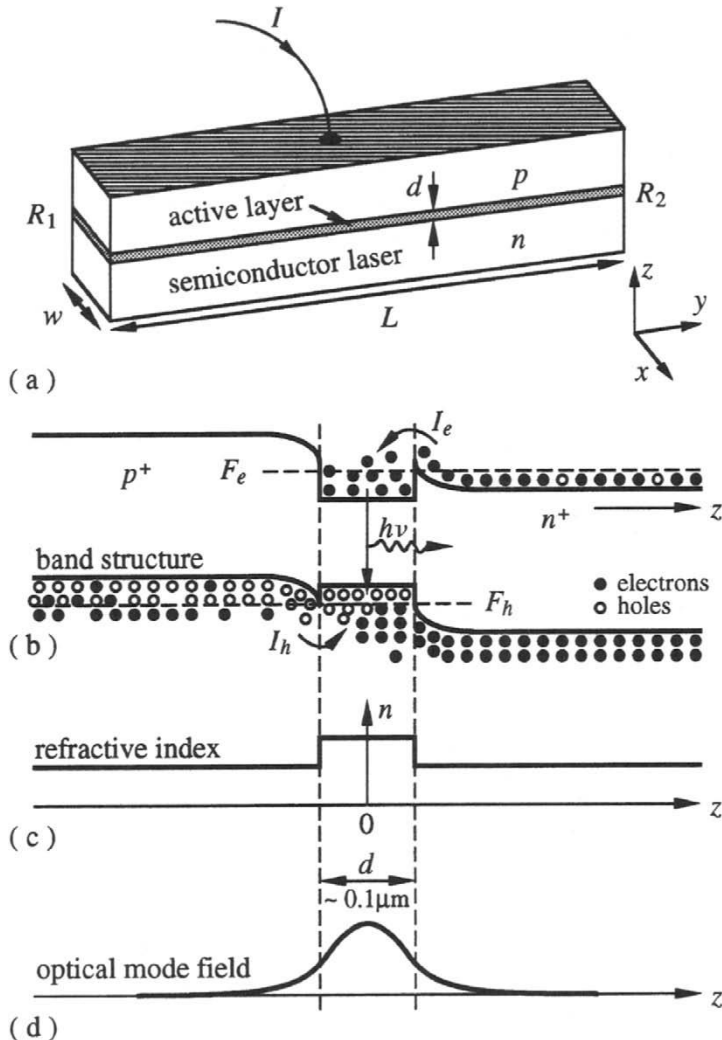


Electronic Transitions



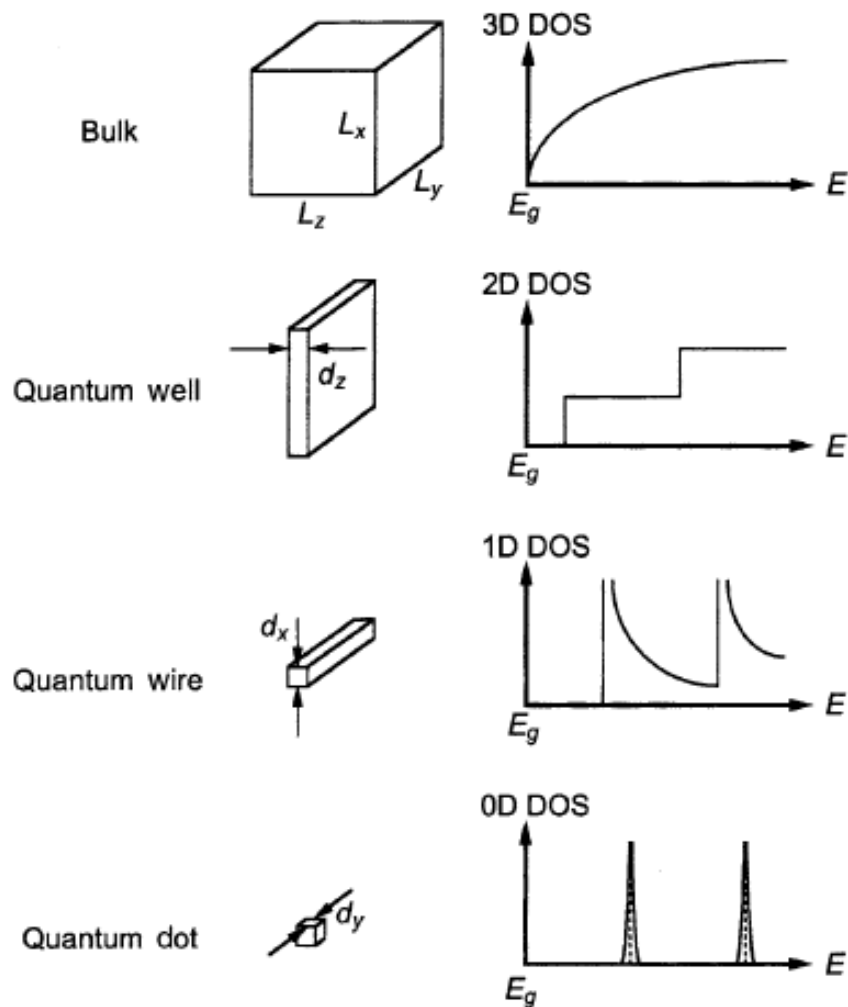
- R_{sp} = spontaneous emission rate (photon emission)
- R_{12} = stimulated generation (photon absorption)
- R_{21} = stimulated recombination (coherent photon emission)
- R_{nr} = nonradiative recombination

Semiconductor Laser Principles



- Semiconductor lasers built as double-heterostructure p-i-n diodes
- i-region is typically the active region of the device
- p- and n-type cladding layers have large bandgap so will not absorb light produced from active region
- Under forward bias, electrons from n-side and holes from p-side injected into active region
- Carriers confined in i-region increasing probability of recombination
- Optical confinement created by index profile

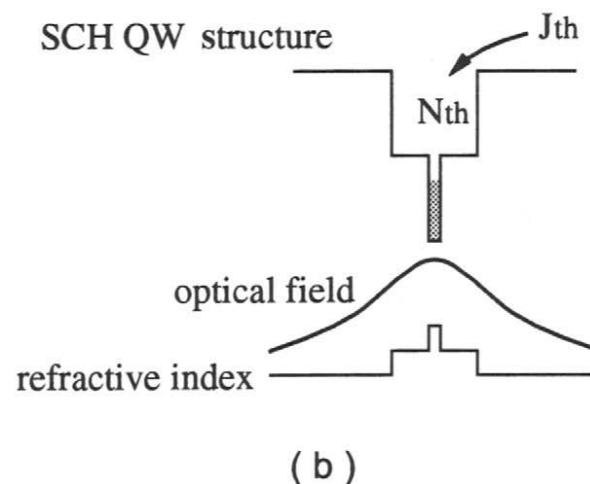
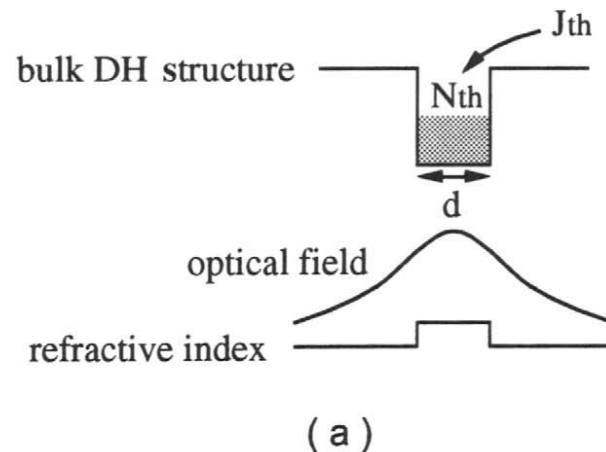
Semiconductor Quantum Well Lasers



- Increase confinement, decrease active volume, threshold current density drops
- Conventional growth techniques allow for uniform planar thin films
 - Quantum wells feasible
 - Wires and dots more difficult
- Try to approach atom-like behavior (recover spectral purity in solids)

Separate Confinement Heterostructure

- If use just one QW or a few QWs, the active region is too thin to confine optical mode
- Do not want to increase the width of the QWs because then approach bulk
- Use a SCH so that optical confinement is the same but electrical confinement is improved



Lateral Confinement

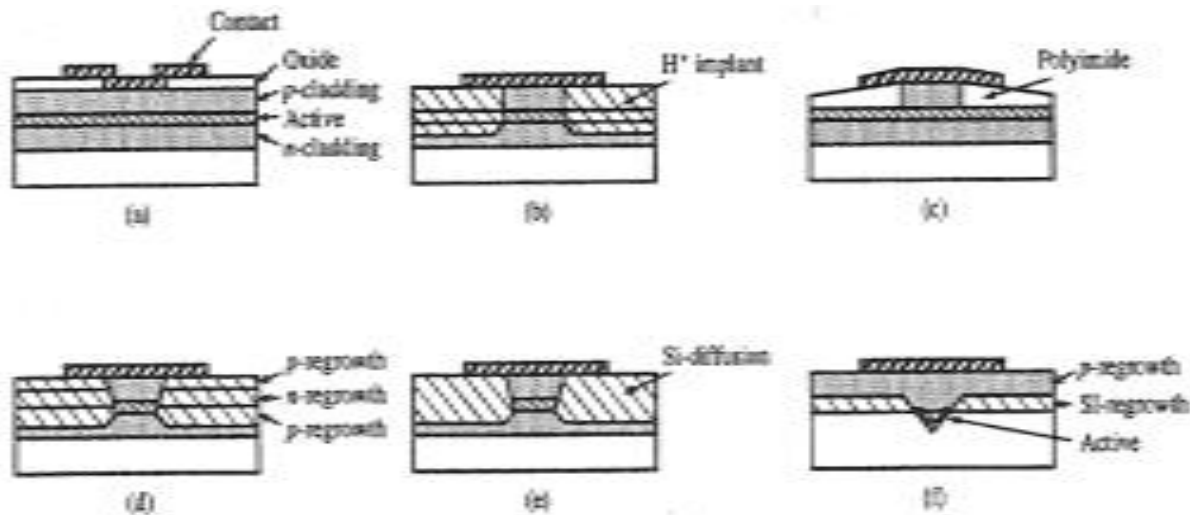
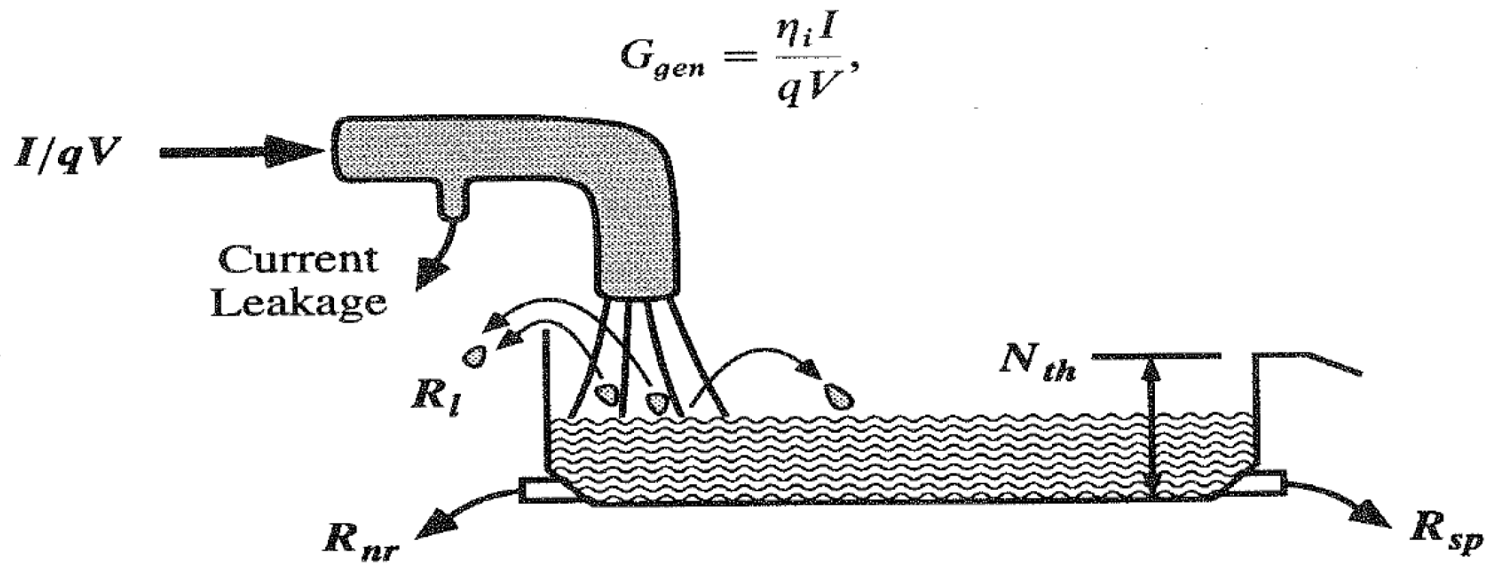


FIGURE 1.13 Lateral confinement structures for heterostructure lasers: (a) oxide-stripe provides current confinement; (b) proton-implant provides current confinement; (c) ridge structure provides current plus photon confinement; (d) etched mesa buried-heterostructure (BH) provides current, photon, and carrier confinement; (e) impurity-induced disordered BH provides current, photon, and carrier confinement; (f) channeled substrate BH provides current, photon, and carrier confinement.

**Coldren and Corzine, Diode Lasers and Photonic Integrated Circuits*

Picture Below Threshold



- I/qV is rate at which carriers are injected into device; η_i is fraction that enters the active region
- R_l (leakage rate), R_{nr} (nonradiative recombination rate), R_{sp} (spontaneous recombination rate) – all per unit volume
- Below threshold shows light emitting diode (LED) behavior

Carrier Rate Equation

$$\frac{dN}{dt} = G_{gen} - R_{rec} \quad \text{Rate equation}$$

$$G_{gen} = \frac{\eta_i I}{qV} \quad R_{rec} = R_{sp} + R_{nr} + R_l + R_{st}$$

$$\frac{dN}{dt} = \frac{\eta_i I}{qV} - \frac{N}{\tau} - R_{st} \quad \text{Rewrite by grouping unstimulated decay processes and defining carrier lifetime}$$

$$\frac{\eta_i I}{qV} = R_{sp} + R_{nr} + R_l \quad \text{Under steady state conditions and neglecting } R_{st} \quad \eta_r = \frac{R_{sp}}{R_{sp} + R_{nr} + R_l}$$

$$P = R_{sp} h\nu V = \eta_i \eta_r \frac{h\nu}{q} I \quad \text{Below threshold, spontaneous emission only}$$

Photon Rate Equation

$$\frac{dN_p}{dt} = \Gamma R_{st} + \Gamma \beta_{sp} R_{sp} - \frac{N_p}{\tau_p}$$

$$N_p + \Delta N_p = N_p e^{g\Delta z}$$

$$e^{g\Delta z} \approx (1 + g\Delta z) \quad \text{small } \Delta z$$

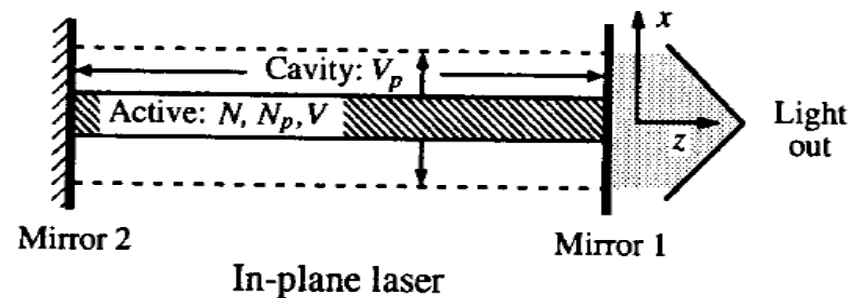
$$\Delta N_p = N_p g v_g \Delta t$$

$$R_{st} = \Delta N_p / \Delta t = N_p g v_g$$

$$\frac{dN}{dt} = \frac{\eta_i I}{qV} - \frac{N}{\tau} - N_p g v_g$$

$$\frac{dN_p}{dt} = \Gamma N_p g v_g + \Gamma \beta_{sp} R_{sp} - \frac{N_p}{\tau_p}$$

- First two terms are photon generation
- Losses characterized by photon lifetime
- Stimulated emission described as gain/length



Reaching Laser Threshold

$$r_1 r_2 e^{-2j\beta_{th}L} = 1$$

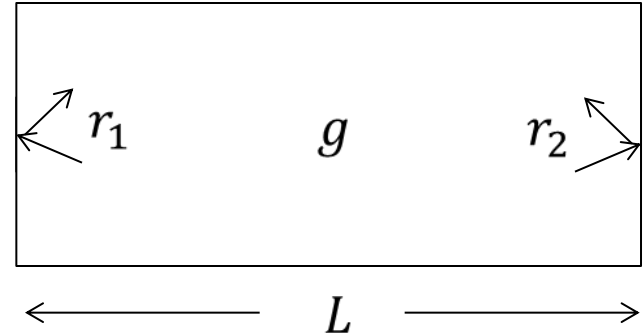
$$\beta = \beta_r + j\beta_i$$

$$\beta = \beta_r + \frac{j}{2} (\Gamma_{xy}g - \langle \alpha_i \rangle_{xy})$$

$$\Gamma_{xy}g_{th}L = \alpha_i L + \ln\left(\frac{1}{r_1 r_2}\right) \quad \text{magnitude}$$

$$\Gamma g_{th} = \langle \alpha_i \rangle + \frac{1}{L} \ln\left(\frac{1}{R}\right)$$

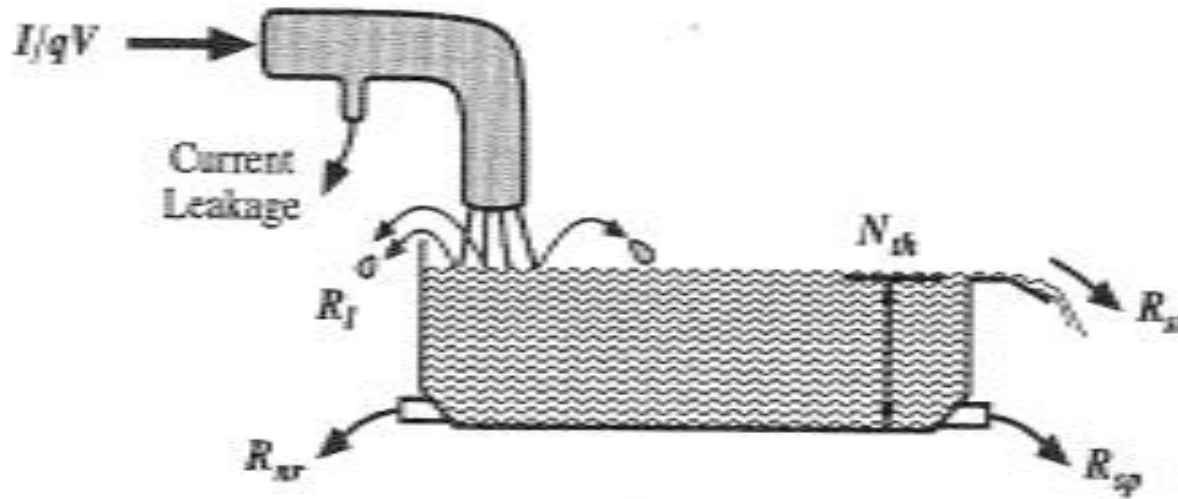
$$\lambda_{th} = \frac{2}{m} [nL] \quad \text{phase}$$



- To reach threshold, gain must overcome all losses
- Electric field must replicate itself after one round trip

- Phase part provides modal wavelength

Picture Above Threshold



- Steady state gain $g =$ value at threshold, g_{th}
- Carrier density N clamps at N_{th}

Threshold and Above Threshold

$$\frac{\eta_i I_{th}}{qV} = (R_{sp} + R_{nr} + R_l)_{th} = \frac{N_{th}}{\tau}$$

$$\frac{dN}{dt} = \eta_i \frac{(I - I_{th})}{qV} - N_p g v_g$$

$$N_p = \frac{\eta_i (I - I_{th})}{q v_g g_{th} N_p}$$

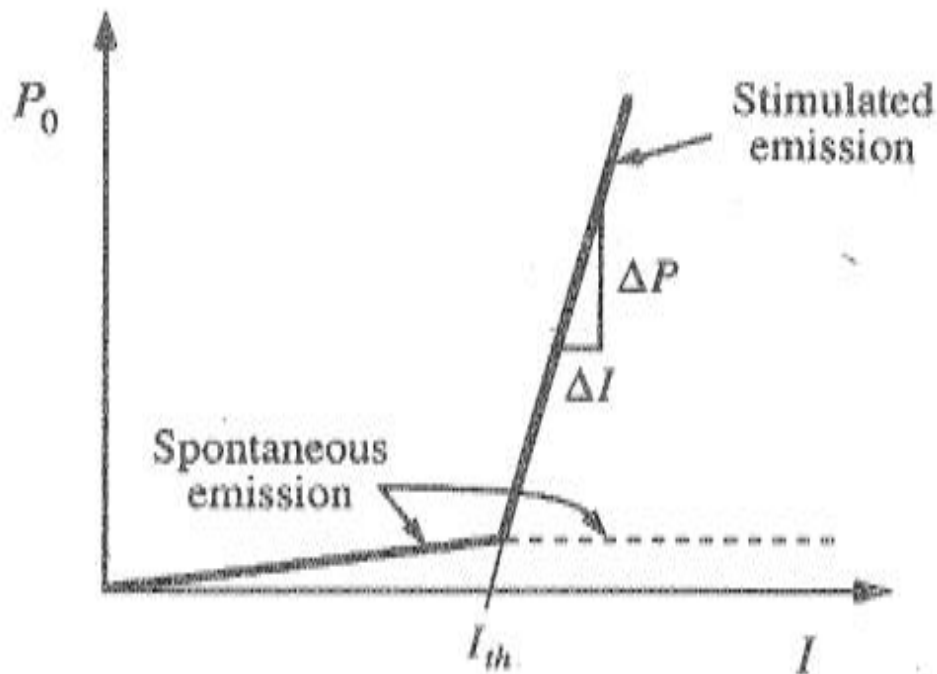
$$P_{OUT} = v_g \alpha_m N_p h \nu V_p$$

$$P_{OUT} = \eta_d \frac{h \nu}{q} (I - I_{th})$$

- Using below threshold rate equation just at threshold
- Understanding what terms clamp at threshold to write rate equation for above threshold
- At steady state
- Power = photon density*photon energy*cavity volume*mirror loss rate

$$\eta_d = \frac{\eta_i \alpha_m}{\langle \alpha_i \rangle + \alpha_m}$$

Lasing Characteristic



- Light current (LI) measurements extremely useful for characterizing laser diode properties:
 - Differential quantum efficiency, injection efficiency, internal loss (latter two using different length lasers)

$$\eta_d = \frac{\eta_i \alpha_m}{\langle \alpha_i \rangle + \alpha_m}$$

Direct Modulation

- How can we modulate laser light?
- External modulation can dynamically change the intensity or phase of the laser light
- Can we directly modulate the laser itself?

$$I = I_0 + I_1 e^{j\omega t}$$

I_0 Bias current above threshold

$$N = N_0 + N_1 e^{j\omega t}$$

I_1 Small signal ac current

$$N_p = N_{p0} + N_{p1} e^{j\omega t}$$

$$N_p(t) \rightarrow P_{OUT}(t)$$

Direct Modulation

- Coupling between N_1 and N_{p1} has relaxation resonance frequency ω_R
- Use rate equations to solve for frequency response

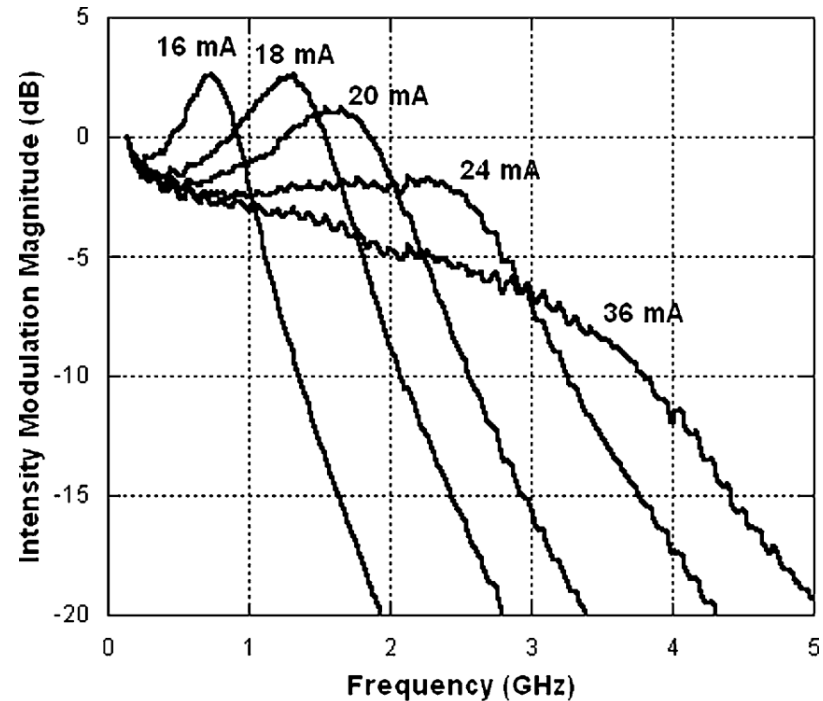
$$\frac{P_{ac}(\omega)}{I_1(\omega)} = \frac{\eta_d h\nu/q}{1 - (\omega - \omega_R)^2 + j(\frac{\omega}{\omega_R}) \left[\omega_R \tau_p + \frac{1}{\omega_R \tau} \right]}$$

Solve for 3-dB frequency

$$f_{3\text{ dB}} \approx \frac{1.55}{2\pi} \left[\frac{\Gamma v_g a \eta_i}{h\nu V \eta_d} \right]^{\frac{1}{2}} \sqrt{P_{OUT}}$$

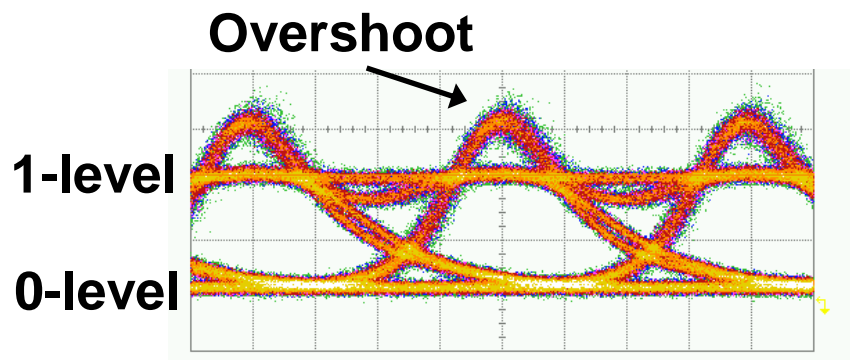
- Increasing power level increases modulation bandwidth (BW)
- BW enhancement limited by: increased damping of resonance and thermal rollover

Measured Laser Frequency Response



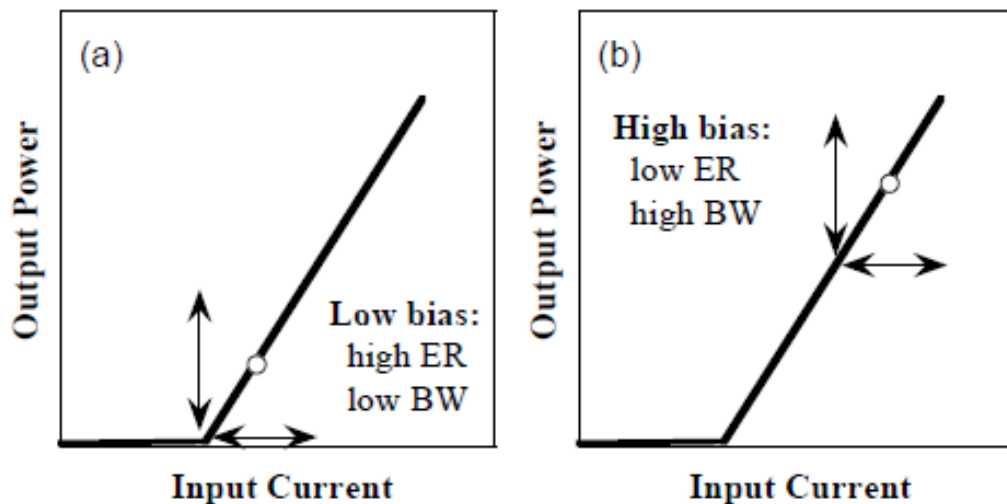
Large Signal Direct Modulation

2.5 Gb/s OOK NRZ eye diagram



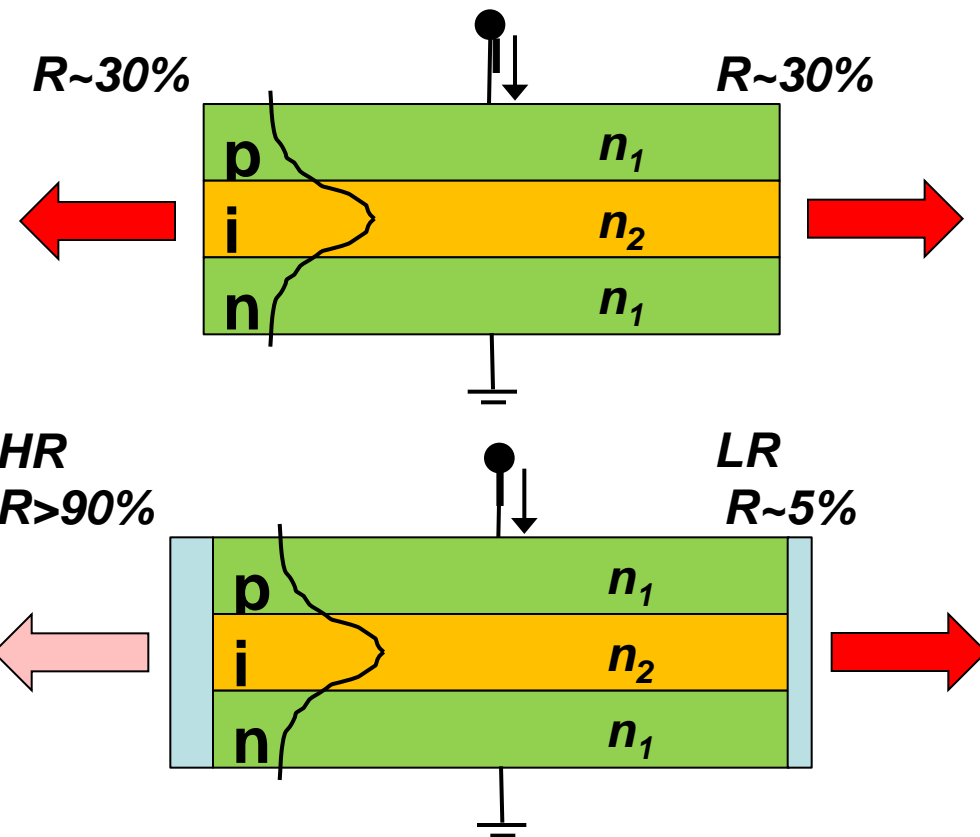
Extinction Ratio (ER) = P_1/P_0

Bias Optimization



- Modulation depth/BW tradeoff for small signal modulation
- ER/BW tradeoff for large signal modulation
- Direct modulation BW typically limited to 10 GHz
- Some demonstrations beyond 30 GHz
- Optical injection locking implored for even higher BW

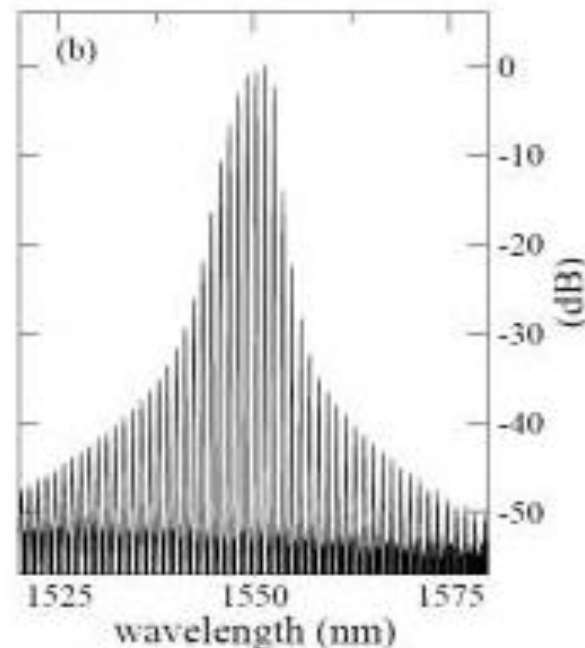
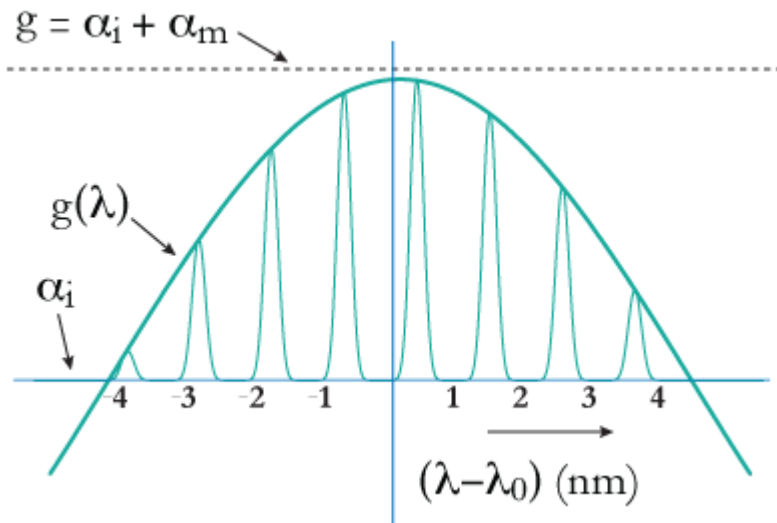
Facet Reflectivity



High Reflectivity (HR) Coating
 Low Reflectivity (LR) Coating
 Anti-Reflection (AR) Coating

- Typical cleaved InP facets have reflectivity $\sim 30\%$
- Equal power emitted from both facets
- Collecting power from both facets is challenging
- If power is important, coat facets so that most of light is emitted from single facet

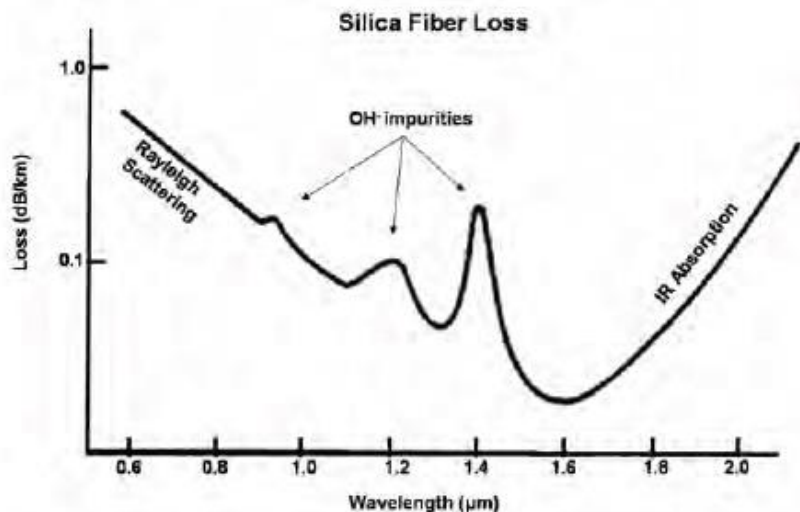
Fabry-Perot Lasing Spectrum



- Typical QW gain spectrum is broad (50-100 nm)
- FP spectrum has many modes within the gain spectrum (500- μm long 1.55- μm laser has cavity mode spacing of 0.388 nm,)
- When reach threshold condition (gain overcomes loss) the gain spectrum narrows but does not collapse into single longitudinal mode

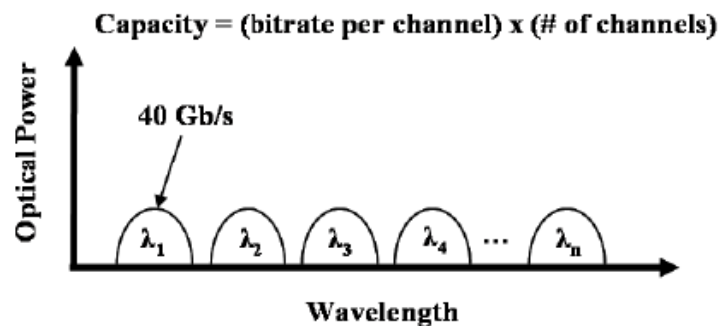
Optical Fiber Communications

Loss Spectrum for Silica Single Mode Fiber



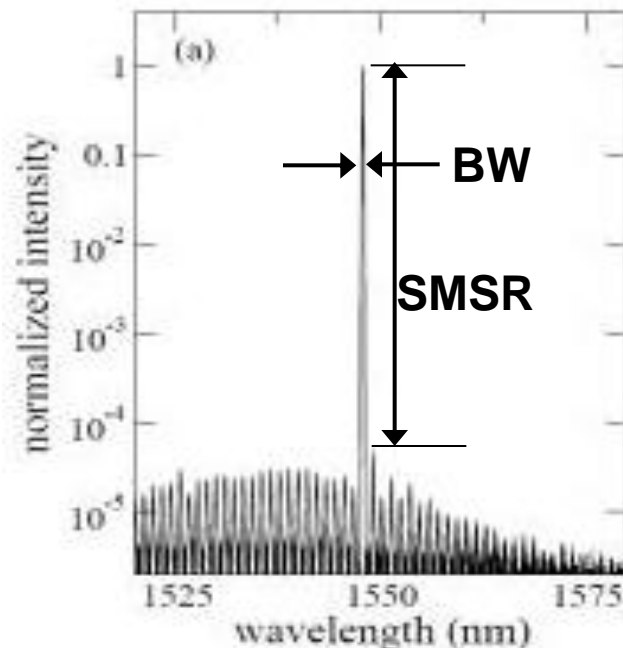
- Extremely low loss near 1.55 μm
- ~15 THz of bandwidth available in low loss region
 - S-band: 1492 – 1530 nm
 - C-band: 1530 – 1570 nm
 - L-band: 1570 – 1612 nm

Wavelength Division Multiplexing (WDM) Spectrum



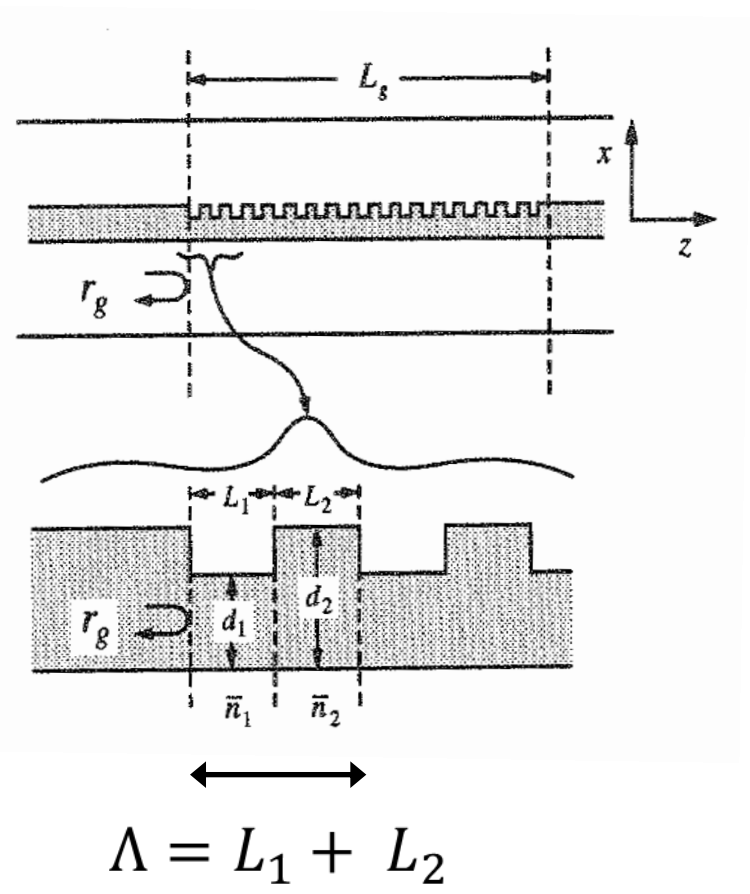
- WDM increases fiber utilization
 - 40 channels, 100 GHz spacing, 40 Gb/s per channel \rightarrow 1.6 Tb/s
- Recent efforts focused on phase encoded modulation formats to increase capacity further

Desired Spectrum



- Lasing in a single longitudinal mode or narrow band
- Side mode suppression ratio (SMSR) is ratio of primary mode power to next strongest mode power
- Spectral bandwidth (BW) quoted as 3-dB, 10-dB or 20-dB of peak power

Gratings



- Distributed Bragg reflector (DBR) can be used for single-longitudinal mode or narrow-band operation
- Reflections from each discontinuity add up exactly in phase at the Bragg frequency

$$\Lambda = \frac{\lambda_B}{2n}$$

- Period of grating should be ~240 nm for operation at 1.55 μm

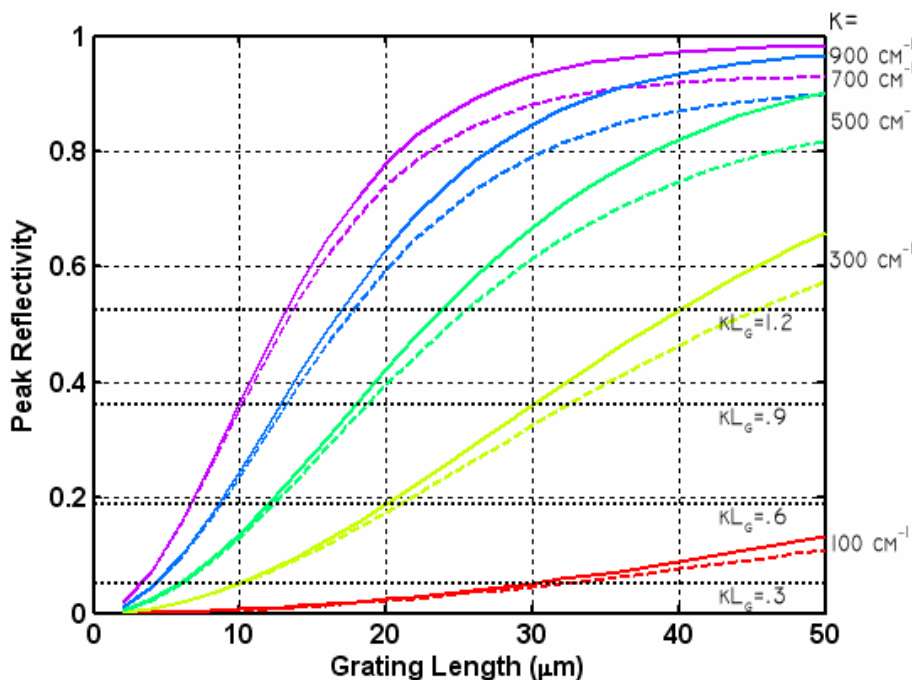
Gratings

$$r_g \approx \tanh(2mr)$$

$$\kappa = \frac{1}{\Lambda} \frac{\Delta n}{n}$$

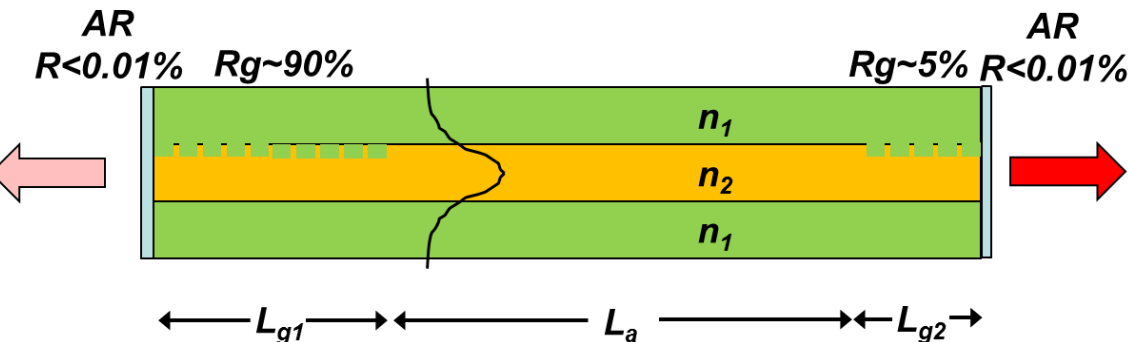
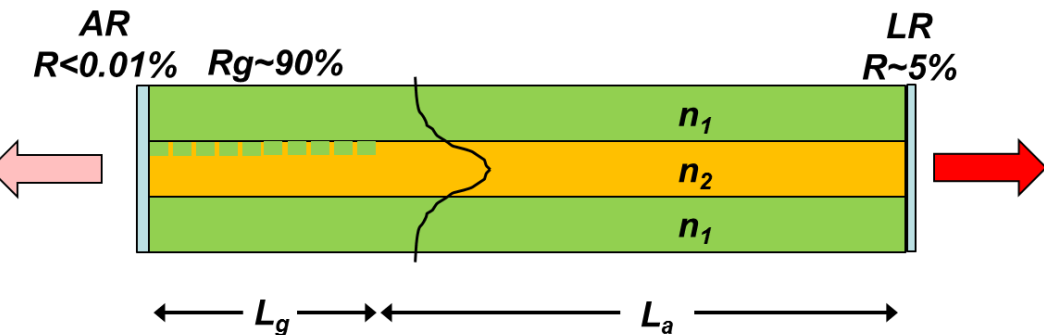
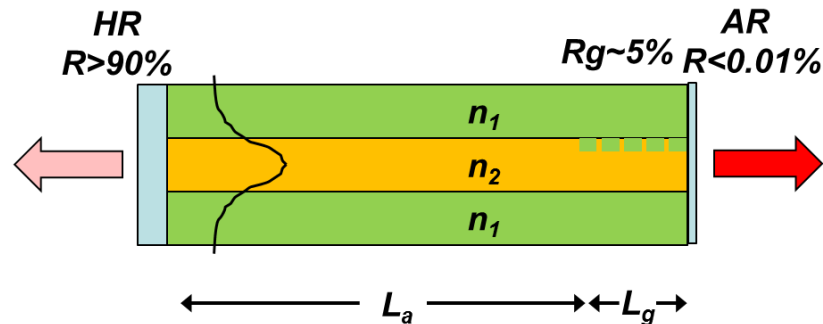
$$\approx \tanh(\kappa L_g)$$

$$\Delta\lambda \sim \Delta n$$



- Grating reflection has spectrum with tanh shape
- Convenient to define coupling coefficient or reflection per unit length
- Typical $\kappa = 100\text{-}300 \text{ cm}^{-1}$
- Value of κ dependent somewhat on fabrication
- Magnitude of reflection depends on coupling strength and length
- Bandwidth depends on index contrast

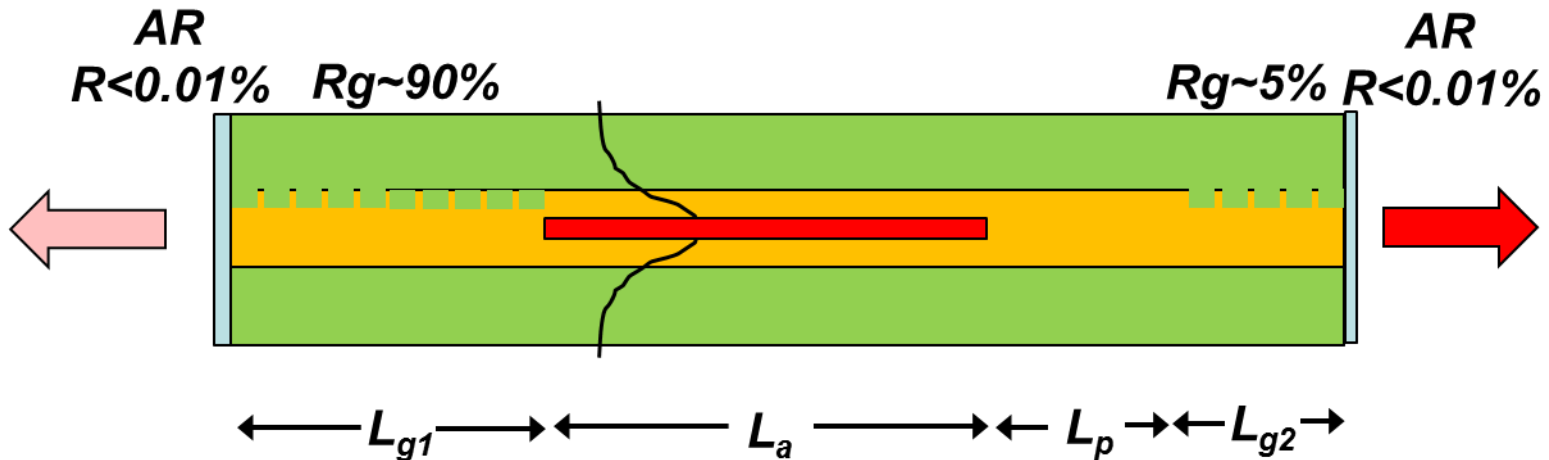
DBR Laser Configurations



- Vary grating length to vary reflectivity
- HR, AR or LR coatings applied depending on configuration
- Could also choose not to coat and have 30% reflection; for which configuration?
- Which is best for a PIC?

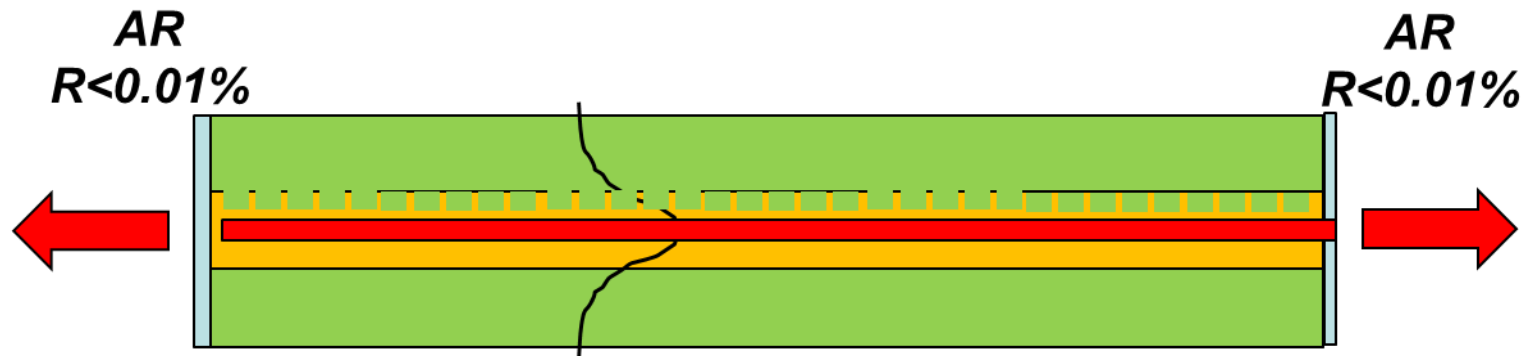
High Reflectivity (HR) Coating
 Low Reflectivity (LR) Coating
 Anti-Reflection (AR) Coating

Four-Section DBR Laser



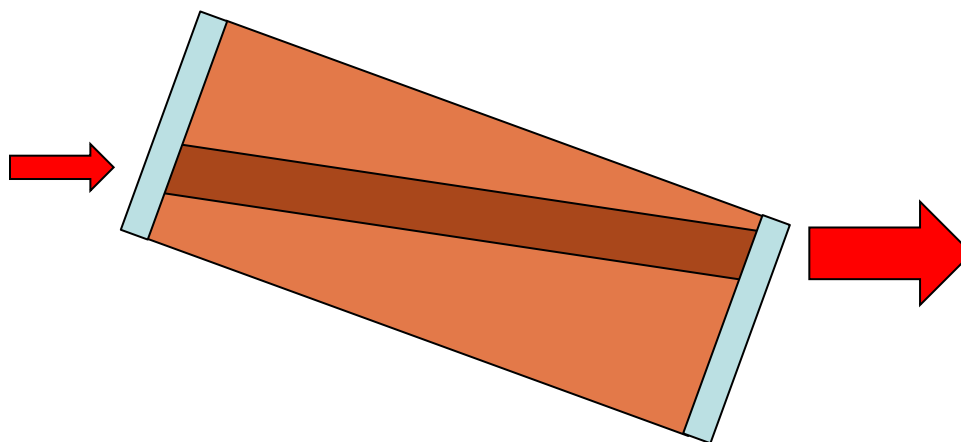
- Four section DBR laser
- Phase section for fine control of cavity modes
- Can maximize output power at different wavelengths

Distributed Feedback (DFB) Laser



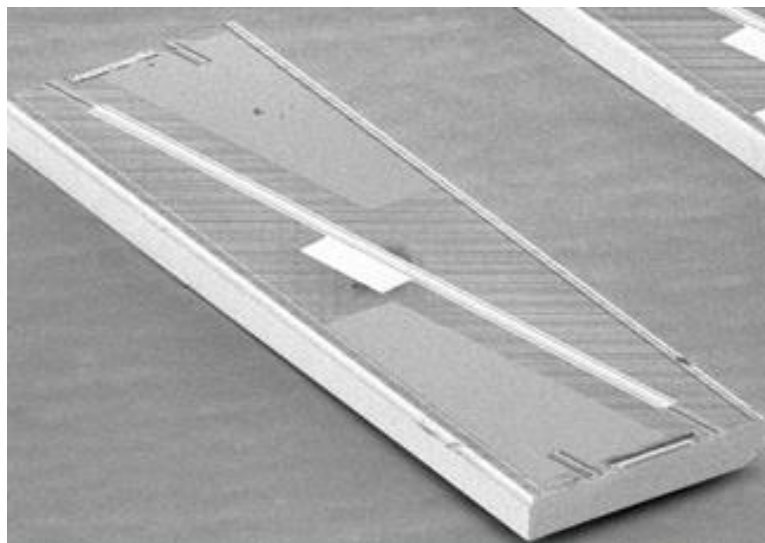
- DFB laser is an all active laser with gratings distributed throughout the active length
- Standard DFB laser with AR coatings has two lasing modes spaced symmetrically about the Bragg wavelength
- Can disturb this degeneracy by incorporating a $\lambda/4$ shift or by cleaving in the right place so net reflection from end out of phase with grating
 - The cleave method is used in industry; yield is at best 50%
 - Not ideal for PIC yield

Semiconductor Optical Amplifier (SOA)



- **Use same or similar material used for laser**
- **Minimize reflections at facet by:**
 - Angle ridge waveguide with respect to facet
 - Apply AR coating

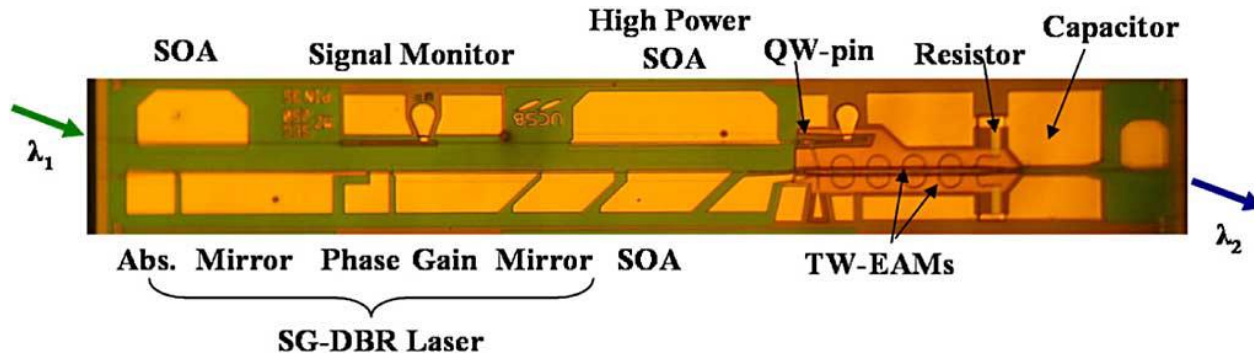
Semiconductor Optical Amplifier (SOA)



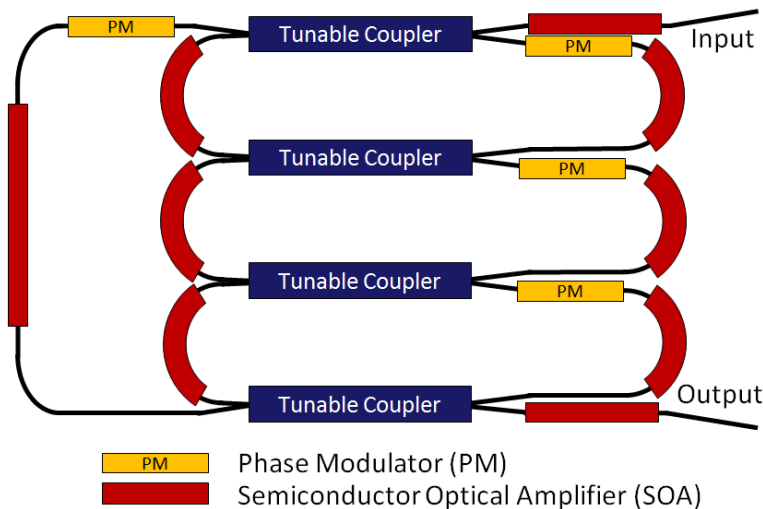
- **Use same or similar material used for laser**
- **Minimize reflections at facet by:**
 - Angle ridge waveguide with respect to facet
 - Apply AR coating

SOAs in PICs

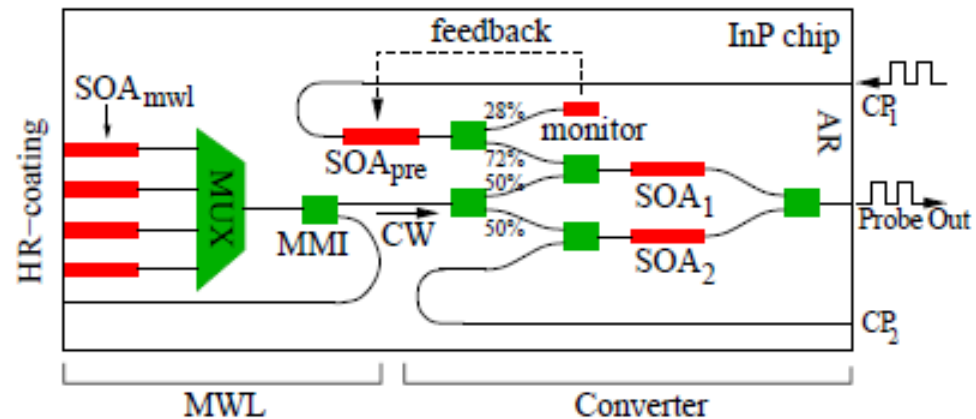
Transceiver



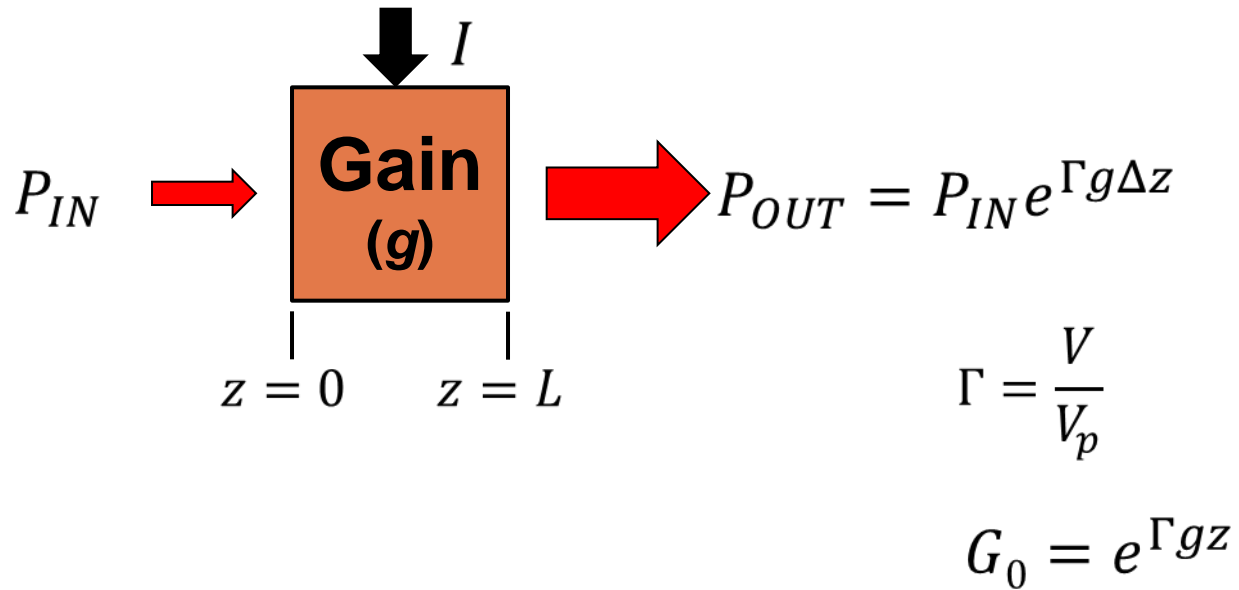
Programmable Filter



Wavelength Converter



SOA Basic Principles



Gain

$$N_p + \Delta N_p = N_p e^{g\Delta z}$$

$$e^{g\Delta z} \approx 1 + g\Delta z \quad \text{for } \Delta z \text{ small}$$

$$\Delta z = v_g \Delta t$$

$$g = \frac{1}{N_p v_g} \frac{\Delta N_p}{\Delta t}$$

$$g = \frac{1}{N_p v_g} (R_{21} - R_{12})$$

R_{21} **Stimulated emission rate**

R_{12} **Stimulated absorption rate**

Gain

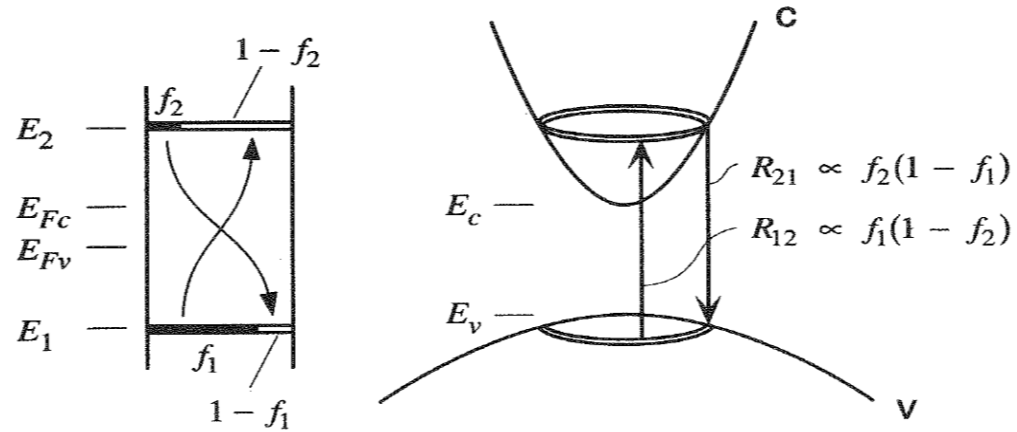
$$R_{12} = R_r f_1 (1 - f_2)$$

$$R_{21} = R_r f_2 (1 - f_1)$$

$$R'_{sp} = R_r^{vf} f_2 (1 - f_1)$$

$$R_{st} = R_{21} - R_{12}$$

$$R_{st} = R_r (f_2 - f_1)$$



$$f_1 = \frac{1}{e^{(E_1 - E_{Fv})/kT} + 1} \quad f_2 = \frac{1}{e^{(E_2 - E_{Fc})/kT} + 1}$$

$$E_{21} = E_g + \frac{\hbar^2 k^2}{2m_c} + \frac{\hbar^2 k^2}{2m_v}$$

$$E_2 = E_c + (E_{21} - E_g) \frac{m_r}{m_c}$$

$$E_1 = E_v - (E_{21} - E_g) \frac{m_r}{m_v}$$

$$\frac{1}{m_r} = \frac{1}{m_c} + \frac{1}{m_v}$$

Gain

$$R_r = \frac{2\pi}{\hbar^2} |H'_{21}|^2 \rho_f(E_{21}) |_{E_{21}=\hbar\omega}$$

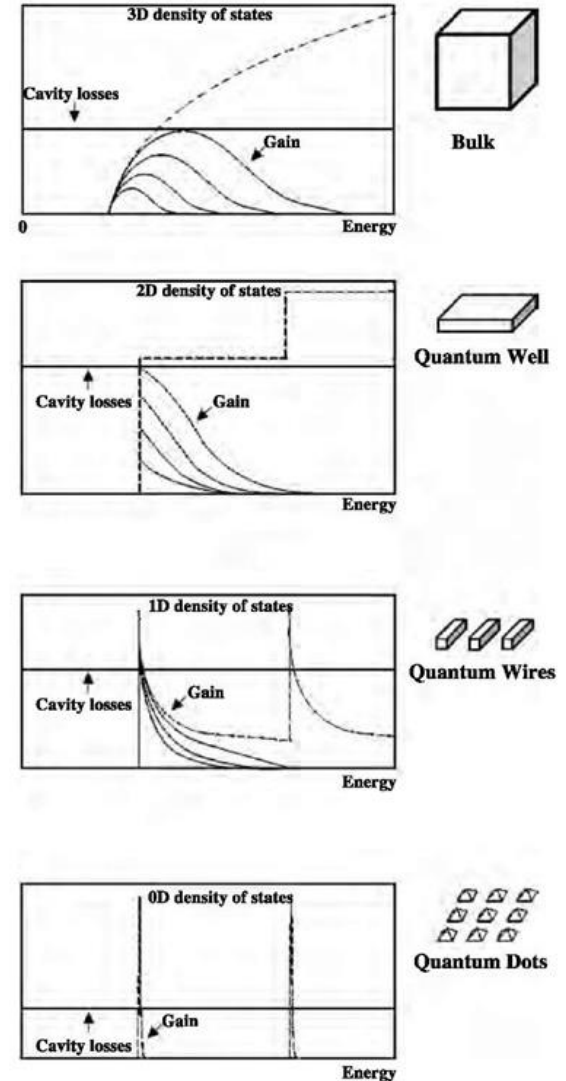
$$H'_{21} = \langle \psi_2 | H'(r) | \psi_1 \rangle = \int_V \psi_2^* H'(r) \psi_1 d^3r$$

$$\rho(E) = \frac{\sqrt{E}}{2\pi^2} \left[\frac{2m}{\hbar^2} \right]^{3/2} \quad \rho(E) = \frac{m}{\pi \hbar^2 dz} \quad \rho(E) = \frac{\rho(k)}{\sqrt{E}} \left[\frac{2m}{\hbar^2} \right]^{1/2}$$

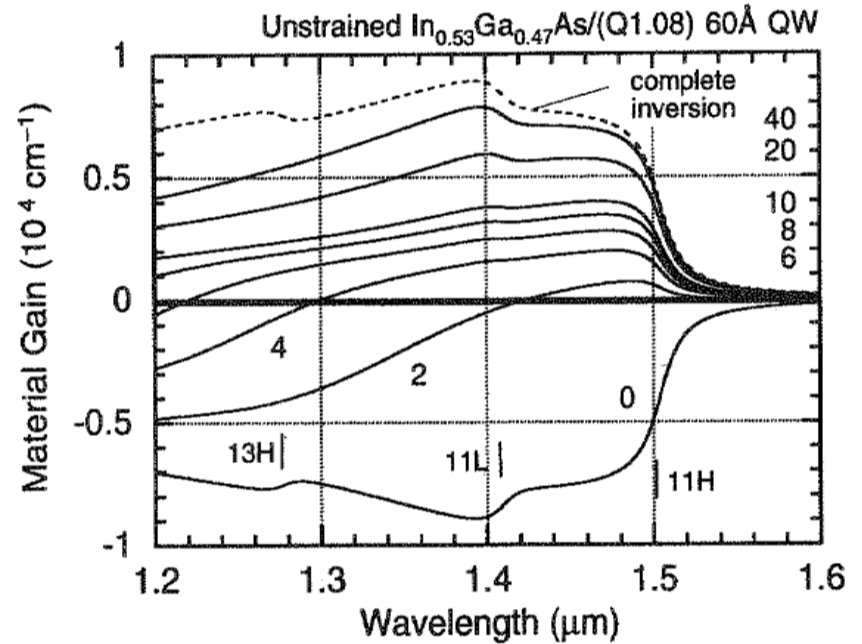
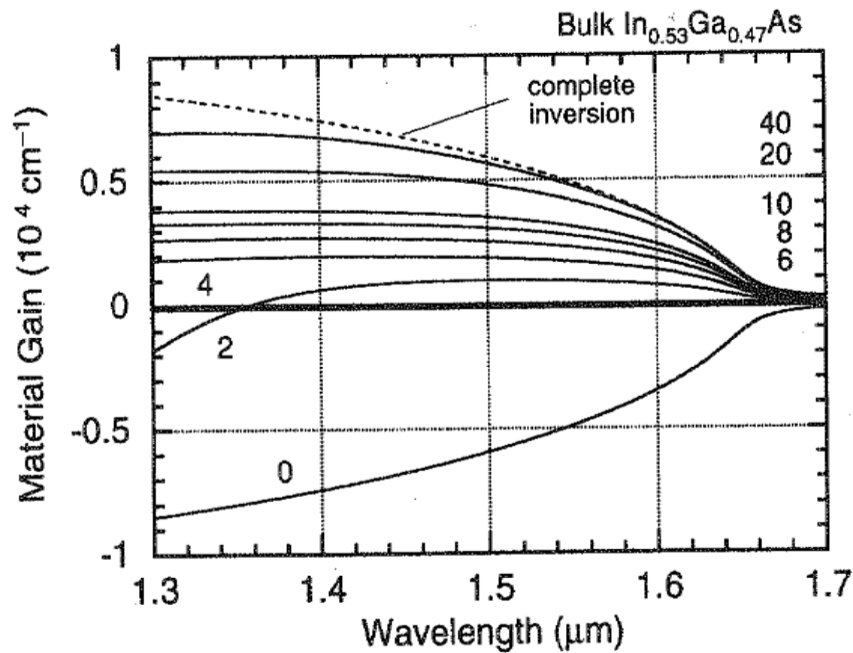
$$g = \frac{1}{N_p v_g} (R_{21} - R_{12}) = \frac{R_r}{N_p v_g} (f_2 - f_1)$$

$$g_{21} = \frac{2\pi}{\hbar^2} \frac{|H'_{21}|^2}{v_g N_p} \rho_f(E_{21}) (f_2 - f_1)$$

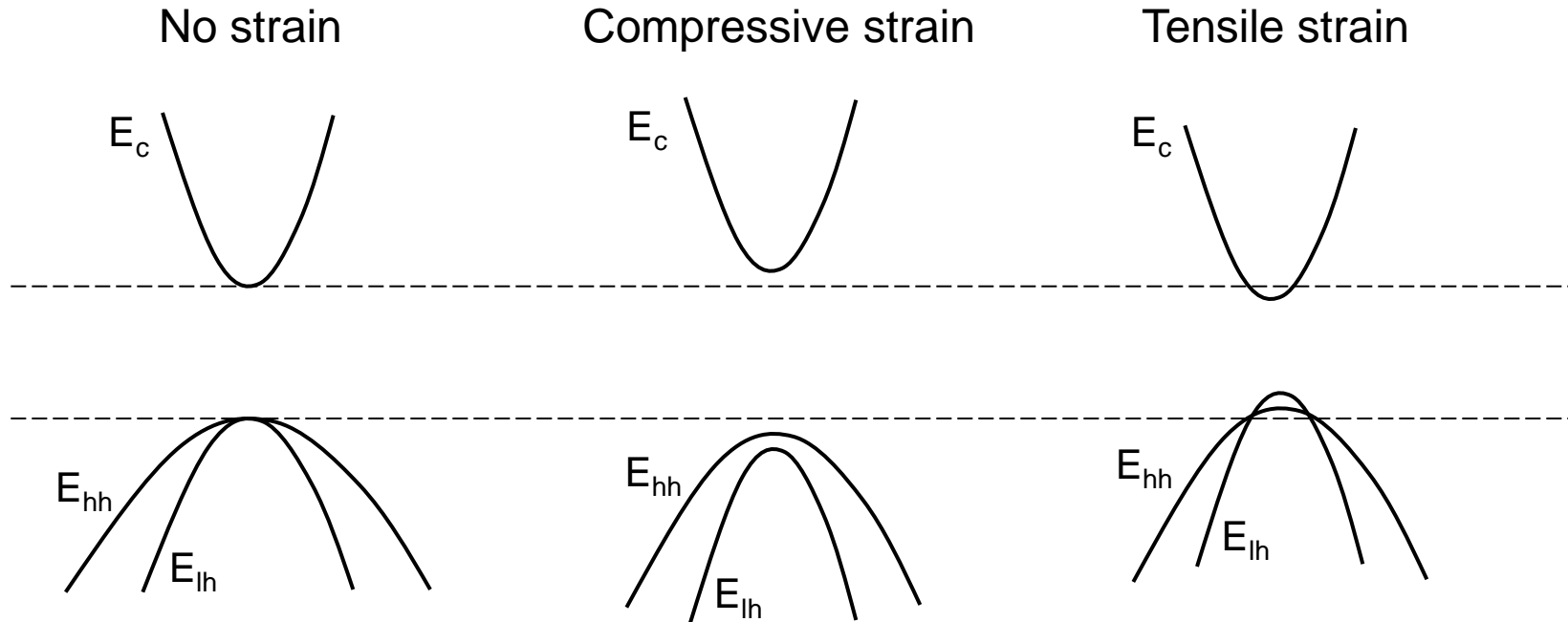
$$g_{21} = \sum_{n_c} \sum_{n_v} g_{21}^{sub}(n_c, n_v)$$



Gain Curves

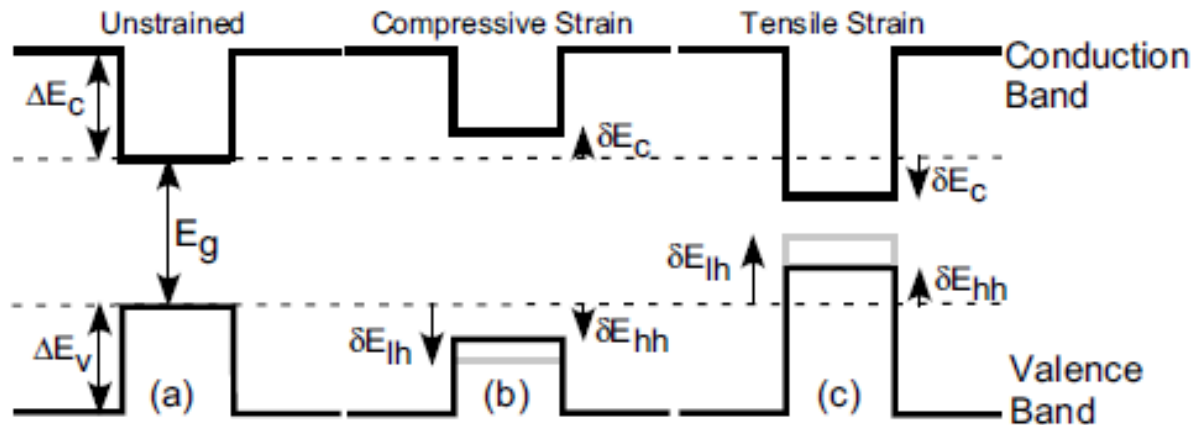


Strain



- **Compressive strain \rightarrow mostly TE gain**
- **Tensile strain \rightarrow TM gain**
- **Valence band shape in particular changes**

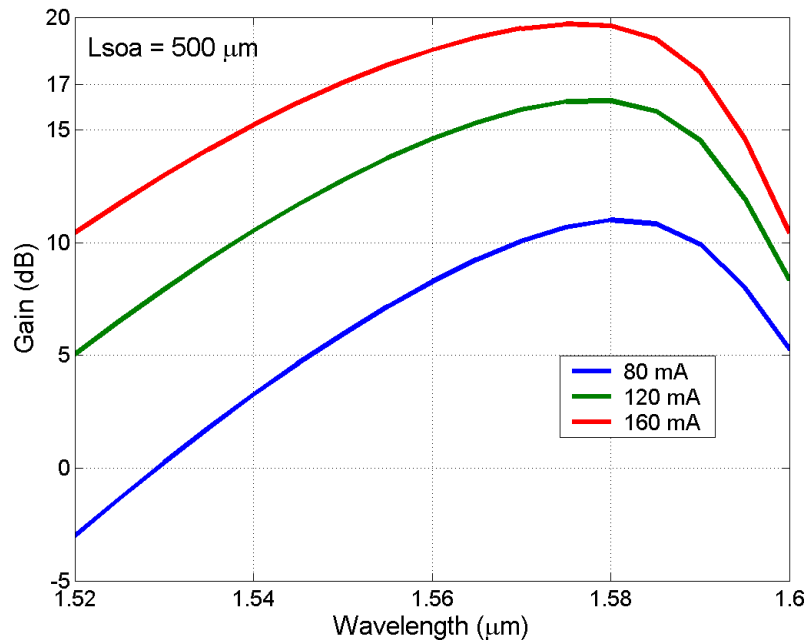
Strain



- Compressive strain \rightarrow mostly TE gain
- Tensile strain \rightarrow TM gain
- Valence band shape in particular changes

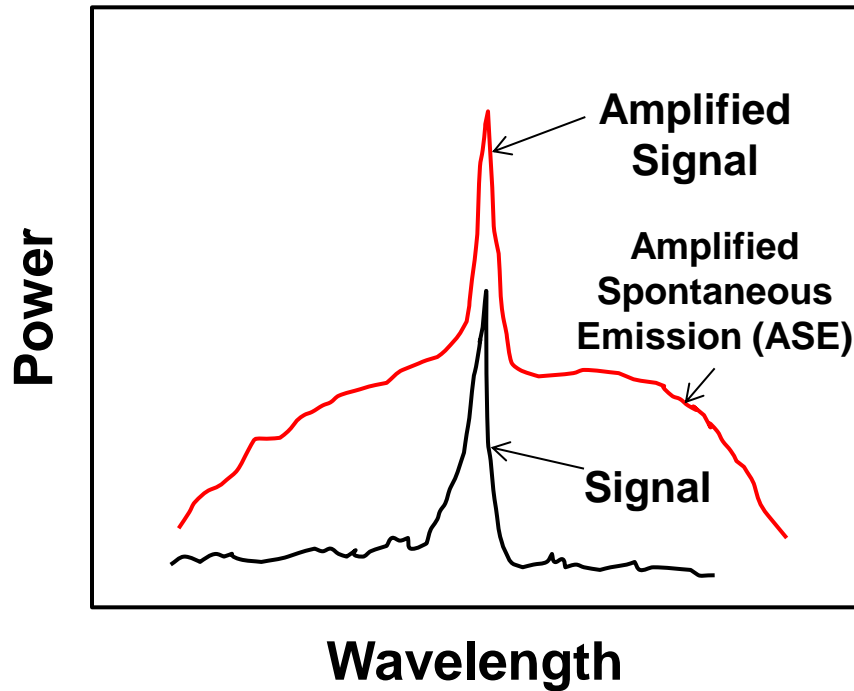
SOA Basic Principles

SOA Gain Spectra

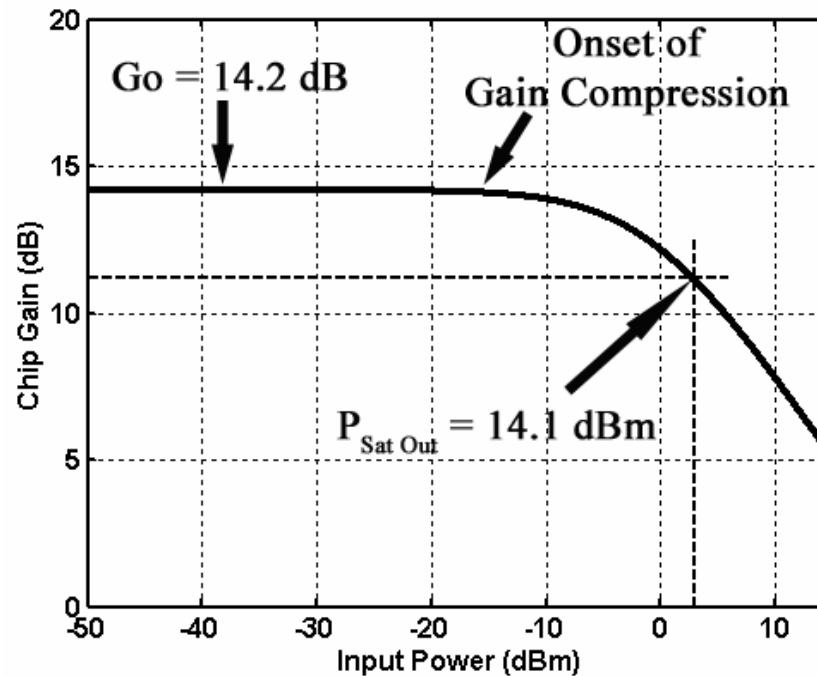


For a fixed SOA length, what is varying to increase the SOA Gain?

SOA Basic Principles

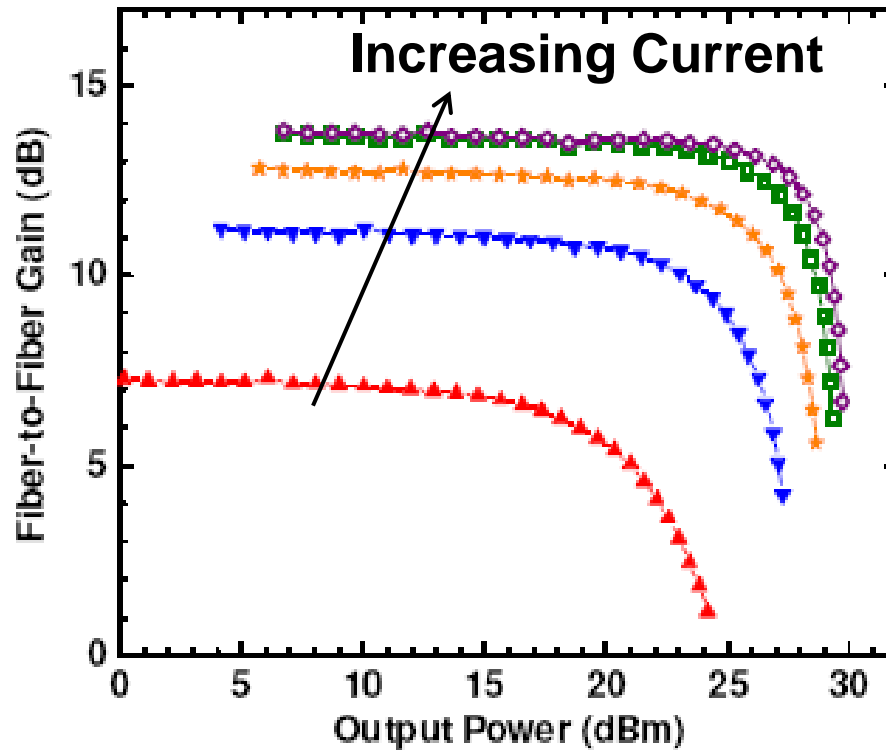


SOA Gain-Saturation Characteristic



- Unsaturated gain, G_0
- Output saturation power, $P_{\text{SAT,OUT}}$

Effect of Temperature



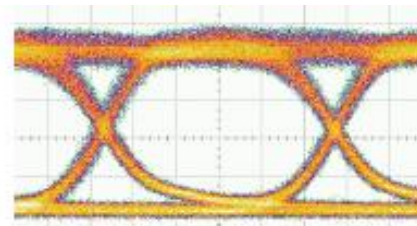
Temperature effects limit the maximum applied current

Saturation Power

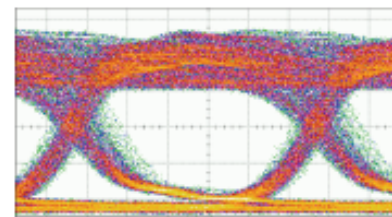
$$g = \frac{g_0}{1 + \frac{P}{P_S}}$$

$$P_S = \frac{wdhv}{a\Gamma\tau} = \frac{V_p hv}{a\tau}$$

Below Saturation



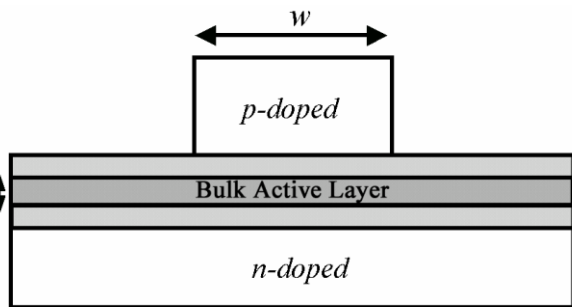
Above Saturation



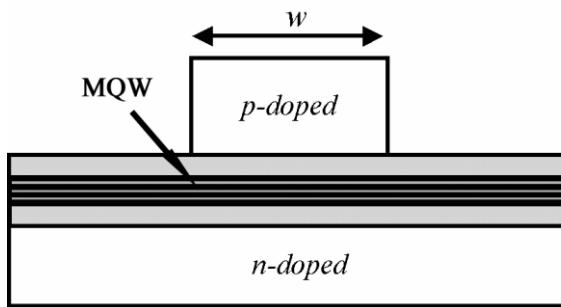
- **SOA saturates at high optical power levels because carriers deplete → causes gain variation**
- **Carrier density/gain recovery time causes pattern effects (carriers quickly deplete and then recover to steady state)**

SOA Active Region Structures

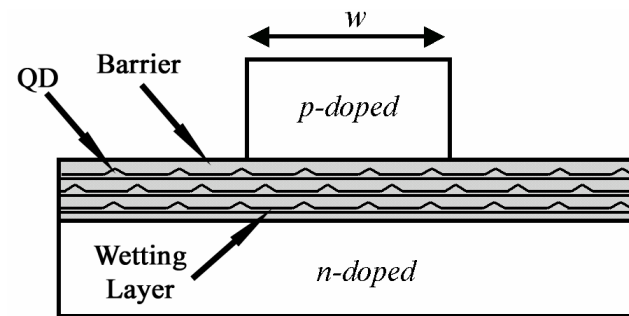
Bulk



Quantum Well (QW)



Quantum Dot (QD)

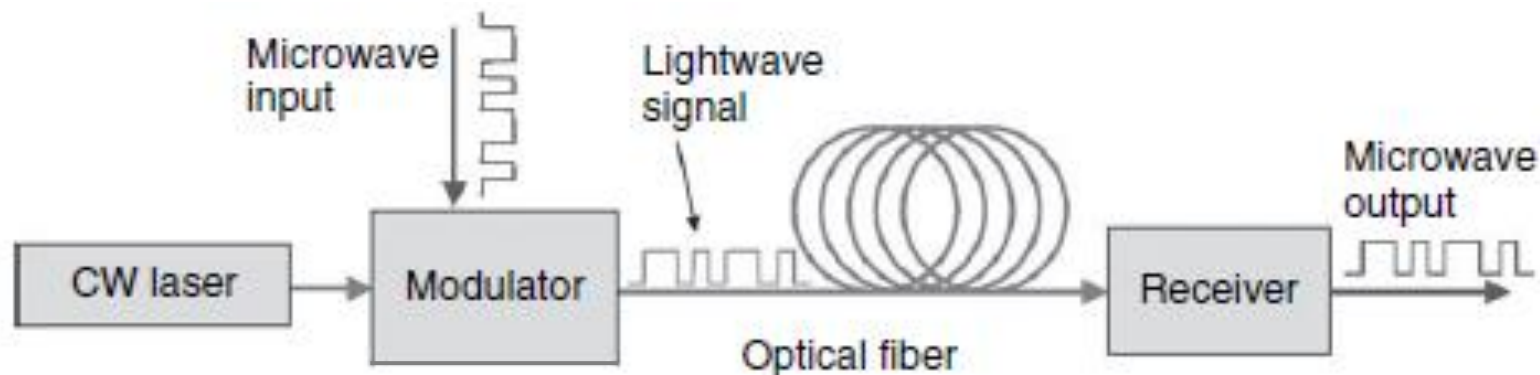


- Broad gain spectrum
- Can have lower gain recovery time

- Narrower gain spectrum
- High differential gain
- Low transparency current density

- Higher differential gain
- Lower transparency condition

External Modulation

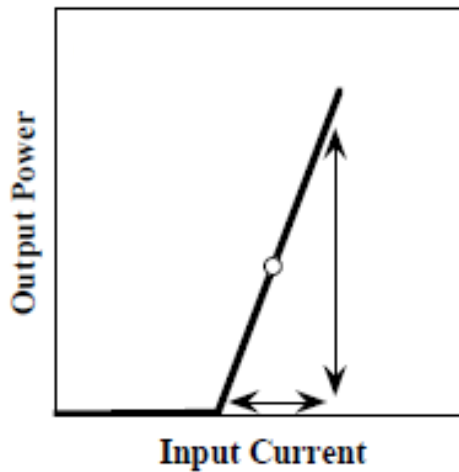


- Externally modulate light from CW laser to convey information onto optical carrier
- System can be viewed as a link with electrical input and electrical output
 - Optical fiber is transmission medium; require E-O and O-E conversion
- But if we can simply directly modulate lasers, then why would we use external modulation?

Direct versus External Modulation

Direct

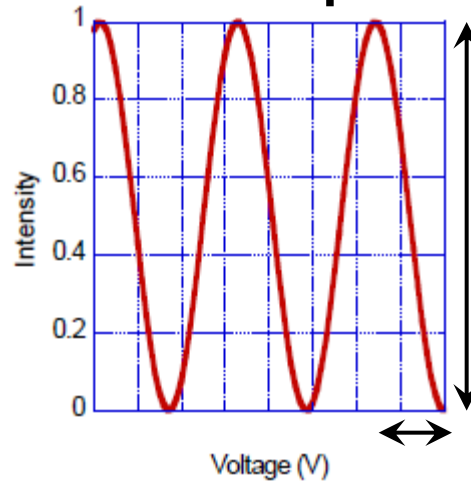
Laser LI Curve



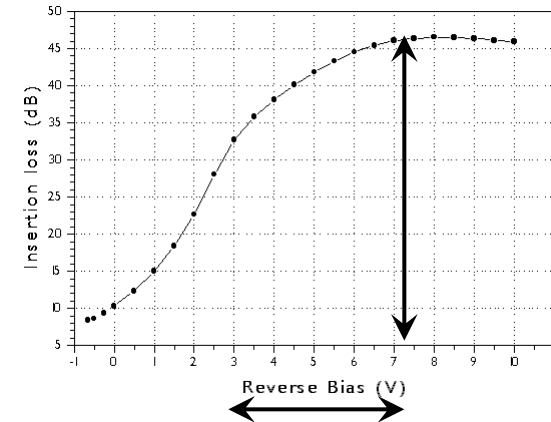
- Simple
- Low cost
- Linear
- High efficiency
- Chirp positive and large
- Speed limited to ~10 Gb/s

External

MZM Response

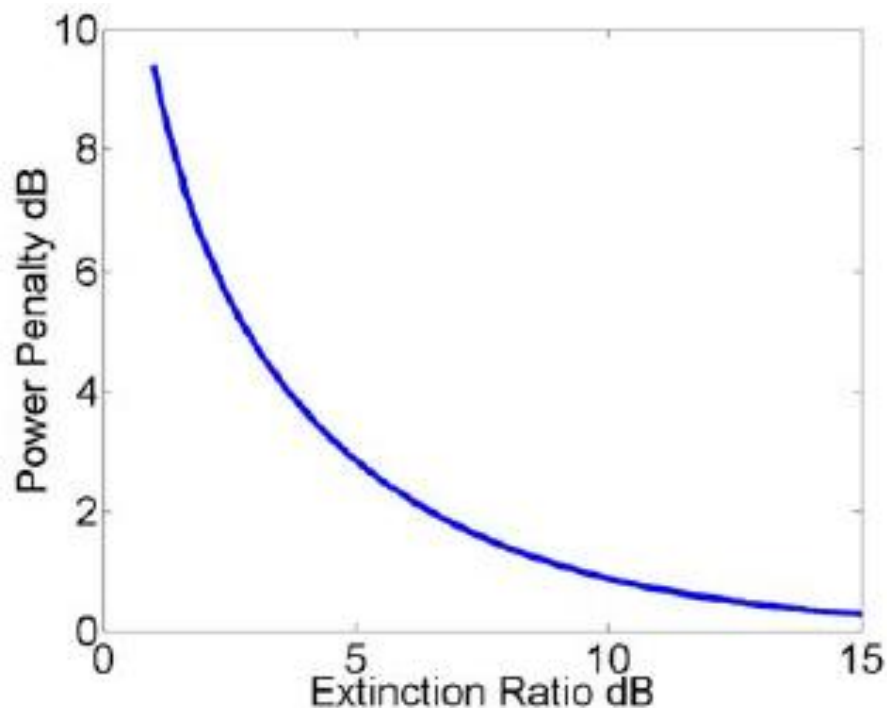


EAM Response



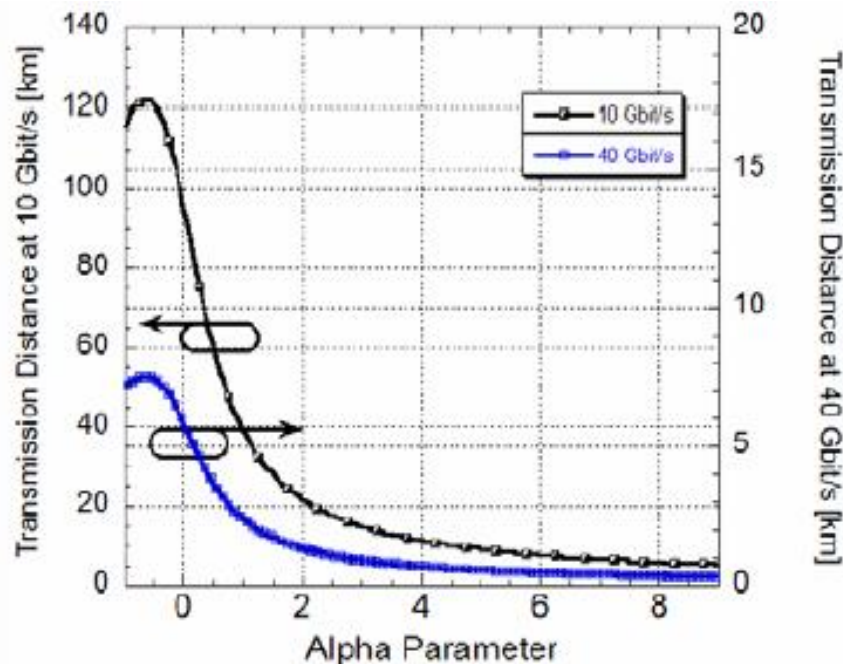
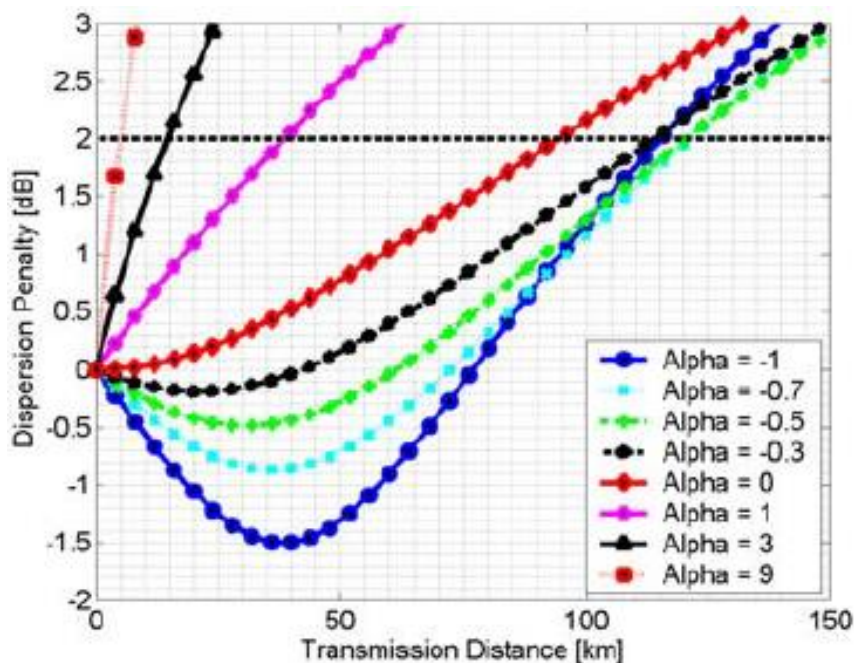
- More complex
- More expensive
- Nonlinear (in intensity)
- High efficiency
- Low, zero and negative chirp
- Speed > 40 Gb/s

Impact of Extinction on System Performance



- **Power penalty is additional power required at receiver for error-free operation**

Impact of Chirp on System Performance

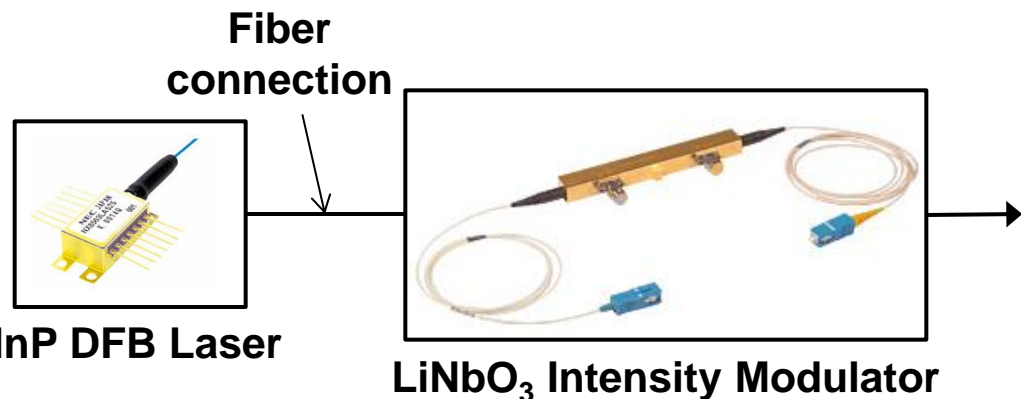


$$\alpha = \frac{d\phi/dt}{E^{-1}dE/dt} = \frac{\Delta n_{real}}{\Delta n_{imaginary}}$$

- Modulator chirp interacts with GVD of fiber; coupled through dispersion penalty, which limits the transmission distance
- Chirp of direct modulation lasers high → complex chirp-managed lasers
- Chirp of external modulators is low and can be zero or negative

Photonic Integration for Laser/Modulator

Discrete Laser/Modulator



- Laser power: 20 mW
- Modulation rate: 40 Gb/s (up to 100 GHz BW)
- Modulator insertion loss: 5 dB
- Modulator efficiency: 3 V
- Extinction Ratio: ~15-30 dB
- Modulator length: ~2 cm

Integrated Laser/Modulator



- Laser power: 20 mW
- Modulation rate: 40 Gb/s (up to 100 GHz BW)
- Modulator insertion loss: 3 dB
- Modulator efficiency: 2 V
- Extinction Ratio: ~10-20 dB
- Modulator length: ~1 mm

**What about integrating InP laser with LiNbO₃ modulator?
What type of integration would this be?**

Electrorefraction versus Electroabsorption

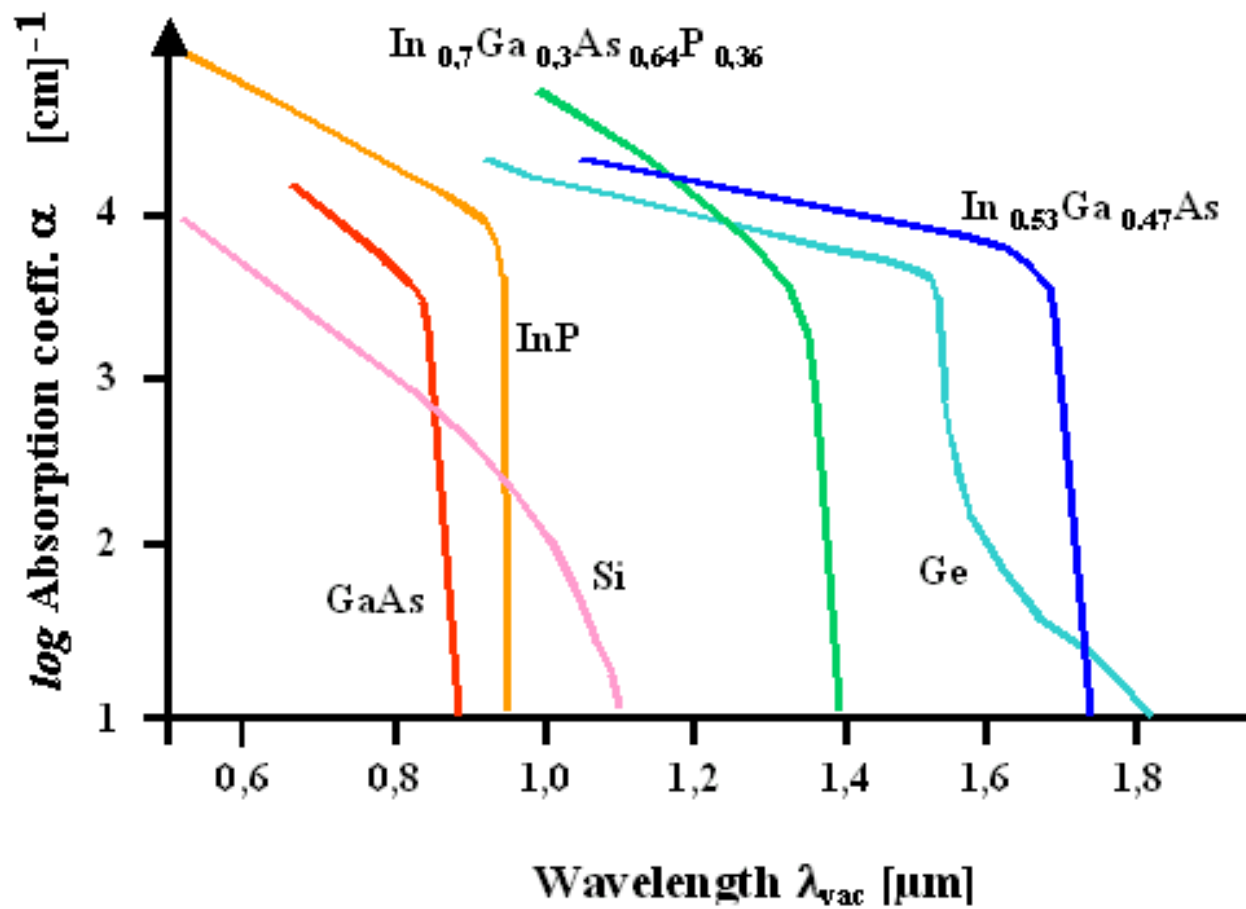
$$n = n_{real} + jn_{imaginary}$$

- **Electrorefraction**: change in real part of refractive index
- **Electroabsorption**: change in imaginary part of refractive index
- The real and imaginary parts are connected through the Kramers-Kronig relation

Modulation Mechanisms

- **Electrorefractive (ER) effects**
 - Pockels effect or linear electro-optic effect ($\Delta n \sim E$)
 - Kerr effect or quadratic electro-optic effect ($\Delta n \sim E^2$)
 - Thermo-optic effect
- **Electroabsorptive (EA) effects**
 - Franz-Keldysh effect (but also ER)
 - Quantum-confined Stark effect (QCSE) (but also ER)
 - Plasma dispersion effect (carrier injection or depletion)
- **Note that EA effects accompanied by ER effects**
 - For EA-based intensity modulator desirable to minimize ER
 - Can use EA for phase modulator; desirable to minimize EA

Regarding EA Effects



Pockels Effect (Linear Electro-optic Effect)

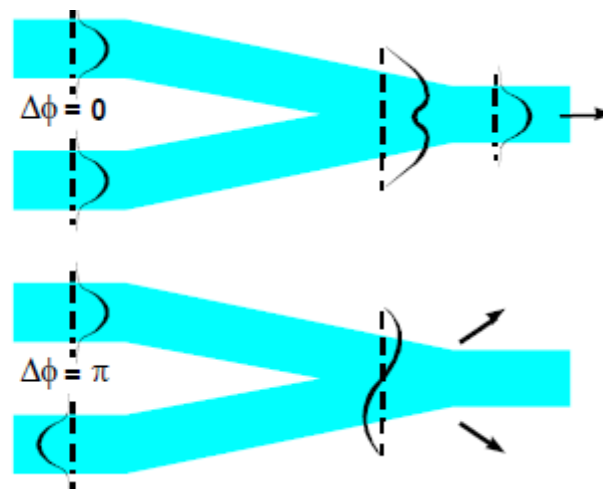
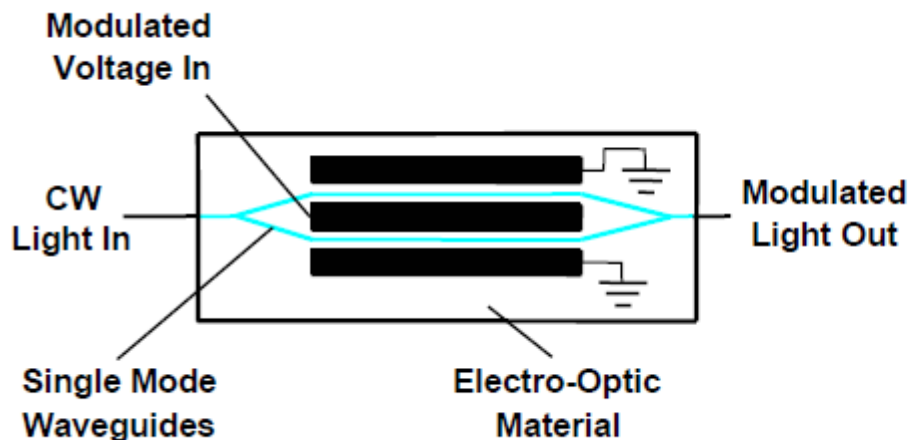
$$\Delta n \sim E$$

$$\Delta n = -r_{33} n_{33} \frac{E_3}{2}$$

For LiNbO₃ r_{33} is most efficient electro-optic coefficient: 30.8e-12 m/V

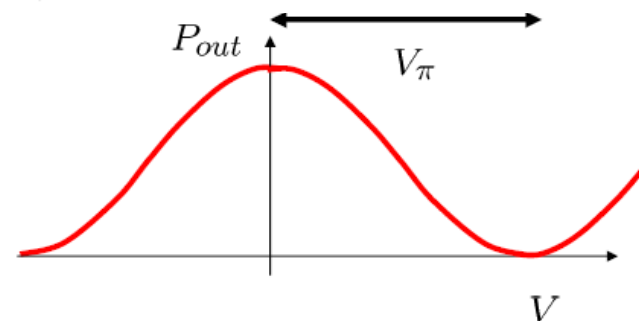
- Δn proportional to applied electric field
- Dependent on direction of applied field with respect to crystal axes; therefore polarization dependent
- Occurs in crystals that do not have inversion symmetry
 - LiNbO₃, GaAs, InP (also poled polymers and glasses)
 - No Pockels effect for Si
- Can build a linear phase modulator

Mach-Zehnder Modulator (MZM)



$$P_{OUT} = P_{IN} \cos^2\left(\frac{\Delta\phi(V)}{2}\right)$$

$$\Delta\phi = \frac{2\pi L}{\lambda} \Gamma \Delta n$$



- Phase modulation translated into intensity modulation using Mach-Zehnder interferometer (MZI)
- Change phase in one arm relative to the other
- Waves interfere at output coupler

Building Electro-optic Modulators



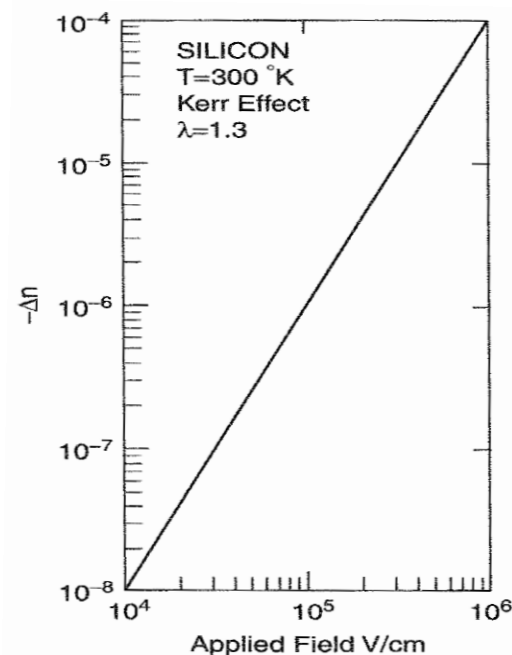
- **GaAs uses typical ridge waveguide structures**
- **LiNbO₃ uses Ti-diffused waveguides**
- **LiNbO₃ favorable for low loss transmission lines**
 - **Used for traveling wave devices for high speed**

Kerr Effect (Quadratic Electro-optic Effect)

$$\Delta n \sim E^2$$

$$\Delta n = s_{33} n_0 \frac{E^2}{2}$$

For Si



- Second-order effect so Δn proportional to square of applied electric field
- s_{33} is Kerr coefficient
- Fairly weak but present in Si
- Larger effect in InP

Electroabsorption

- **Carrier-based effect**
 - Plasma dispersion effect
- **Field-based effect**
 - Franz-Keldysh effect
 - Quantun-Confined Stark effect (QCSE)
- **Used for intensity modulation**
- **Do not want residual phase change because this leads to chirp**

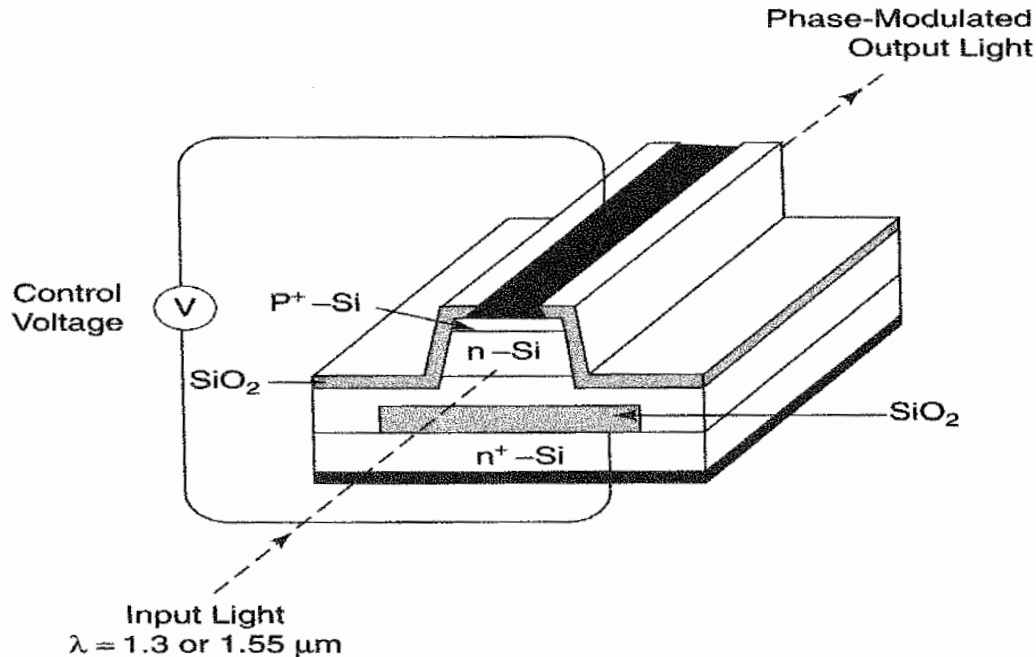
Plasma Dispersion Effect

$$\Delta\alpha = \frac{e^3 \lambda_0^3}{4\pi^2 c^3 \epsilon_0 n} \left(\frac{N_e}{\mu_e (m_{ce}^*)^2} + \frac{N_h}{\mu_h (m_{ch}^*)^2} \right)$$

- Carrier injection or depletion changes the number of free carriers → will lead to change in absorption
- This leads to index change by way of Kramers-Kronig relations

$$\Delta n(\lambda_0, \Delta V) = \frac{\lambda_0^2}{2\pi^2} P \int_0^\infty \frac{\Delta\alpha_{abs}(\lambda_0, \Delta V)}{\lambda_0^2 - \lambda^2} d\lambda$$

Silicon Modulator

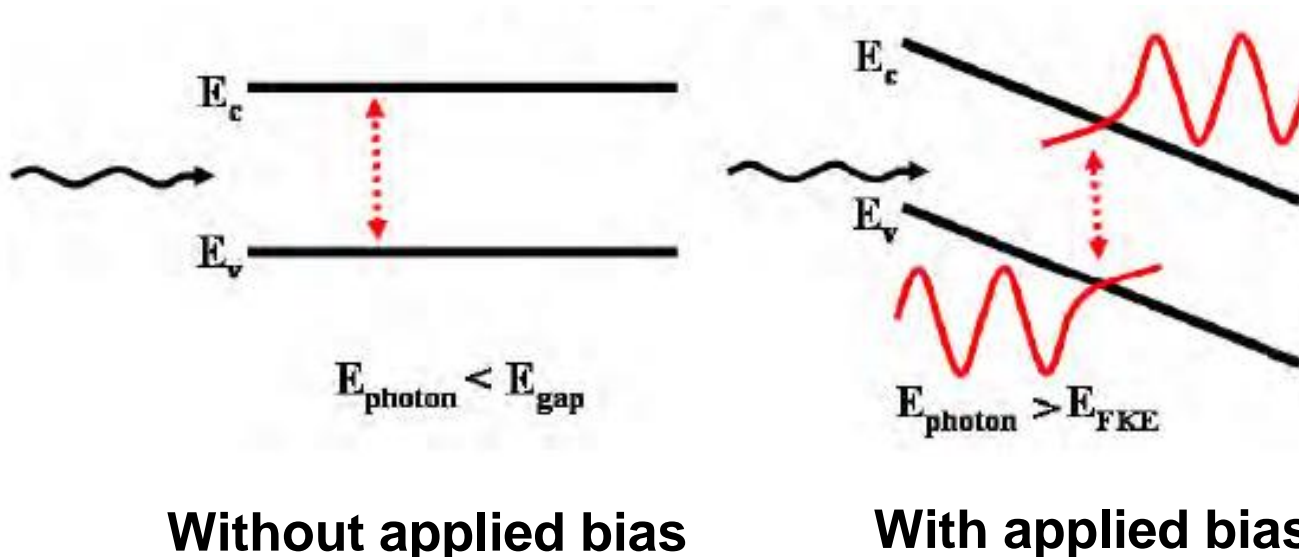


$$\Delta n = \Delta n_e + \Delta n_h = -8.8 \times 10^{-22} \Delta N_e - 8.5 \times 10^{-18} (\Delta N_h)^{0.8}$$

$$\Delta \alpha = \Delta \alpha_e + \Delta \alpha_h = 8.5 \times 10^{-18} \Delta N_e + 6.0 \times 10^{-18} \Delta N_h$$

Speed somewhat limited because relying on carrier lifetime

Franz-Keldysh Effect



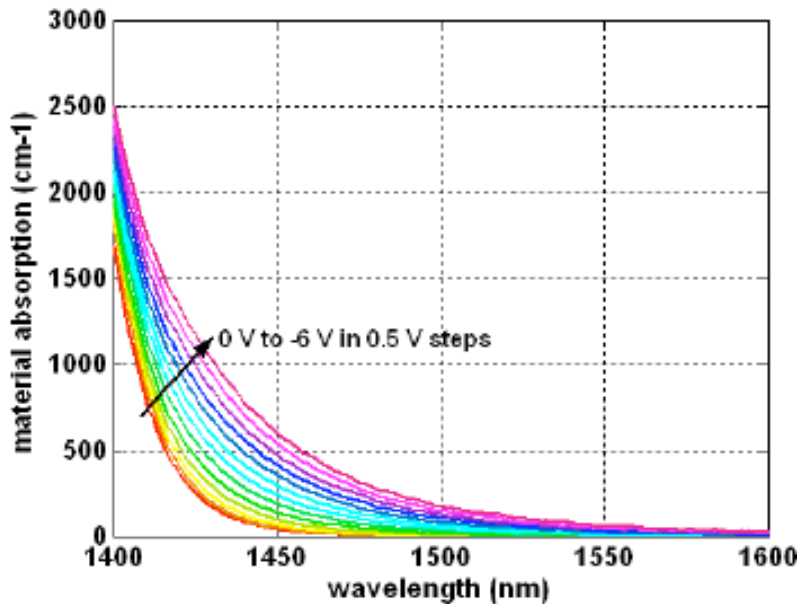
Without applied bias

With applied bias

- Without applied bias, photons with energy $<$ bandgap energy will not be absorbed
- With applied bias, bands tilt and electron and hole wavefunction tails (Urbach tails) overlap with energy $<$ bandgap
 - Photons with energy $<$ bandgap can be absorbed

Franz-Keldysh Effect

Absorption Spectra



Can be used for intensity modulator:

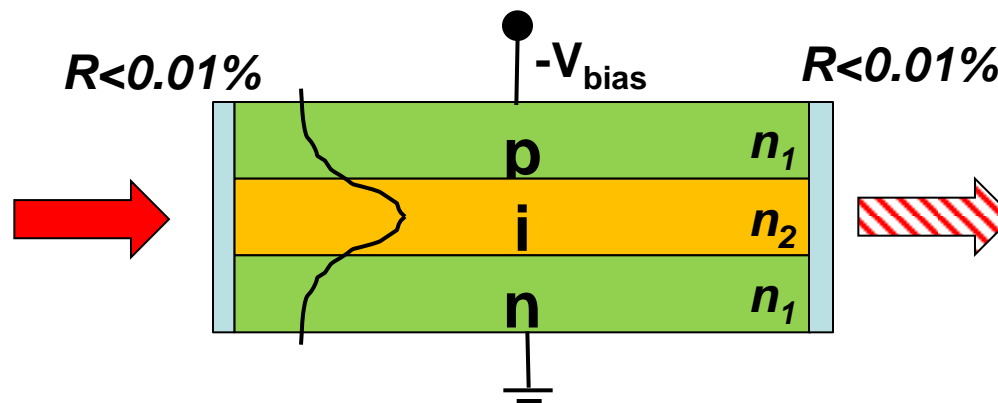
$$P_{OUT} = P_{IN} e^{-\Gamma \Delta \alpha L}$$

Or for phase modulator:

$$\Delta n(\lambda_0, \Delta V) = \frac{\lambda_0^2}{2\pi^2} P \int_0^\infty \frac{\Delta \alpha_{abs}(\lambda_0, \Delta V)}{\lambda_0^2 - \lambda^2} d\lambda$$

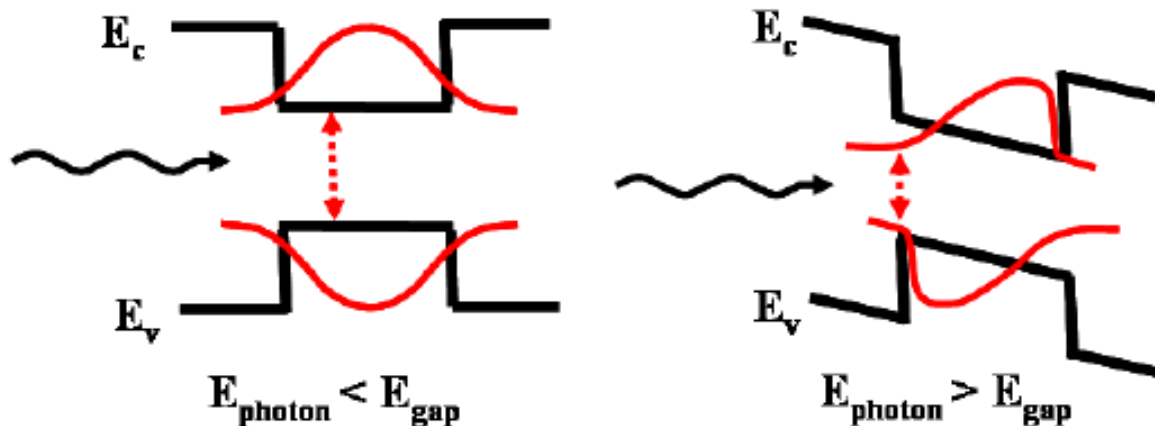
$$\Delta \phi = \frac{2\pi L}{\lambda} \Gamma \Delta n$$

FK Effect Modulator



- Here Γ affects the efficiency of the modulator
- Active area is defined by the field region

Quantum-Confined Stark Effect (QCSE)



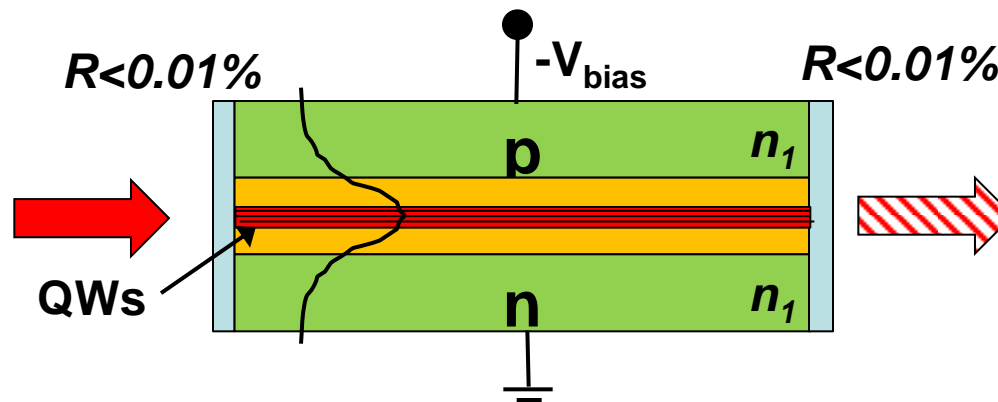
Without applied bias

With applied bias

- In a quantum well, electron and hole wavefunctions are more confined and $E_{21} > E_g$
- Large overlap leads to Coulomb attraction and atomic-like electron-hole pair or exciton
- Photons with energy $>$ exciton energy can be absorbed

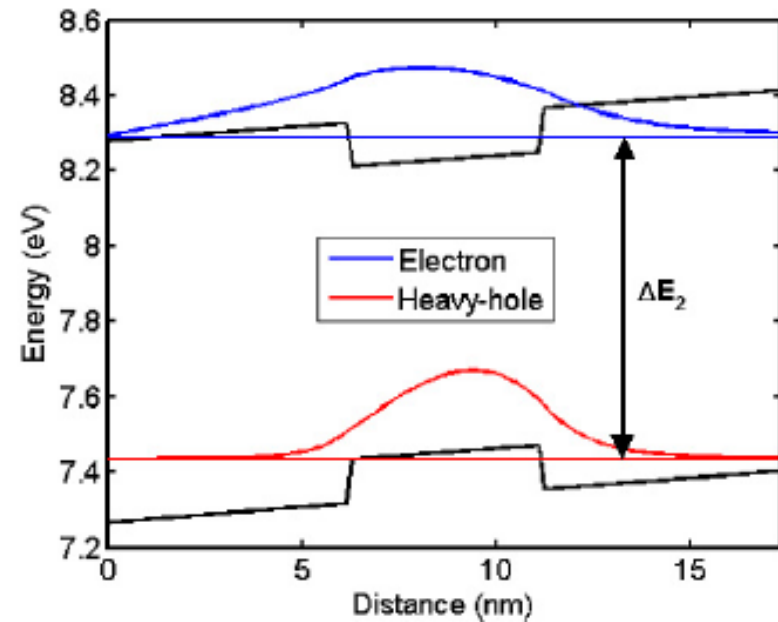
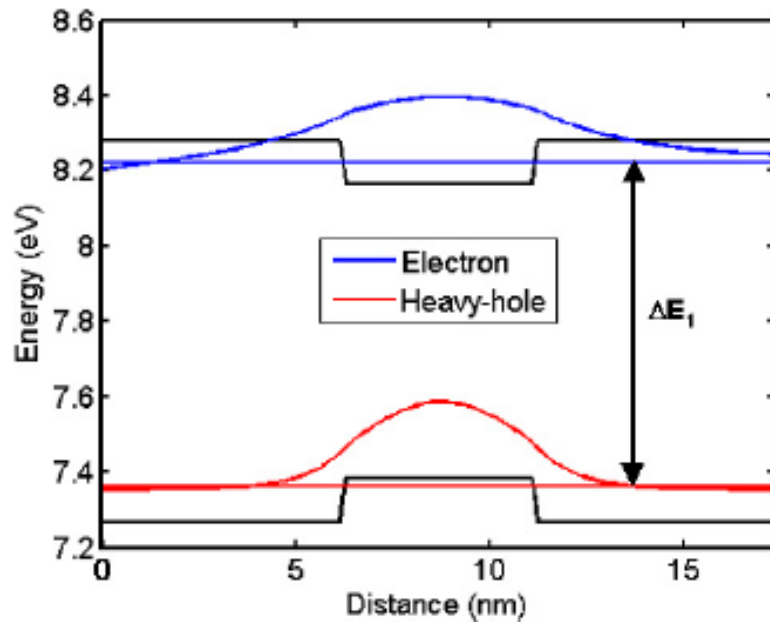
$$E_{exciton} = E_{bulk} + E_{1e} + E_{1h} - E_{binding}$$

QCSE Modulator



- Here Γ affects the efficiency of the modulator
- Active area is defined by the field region (QWs)

Design of QCSE Modulator



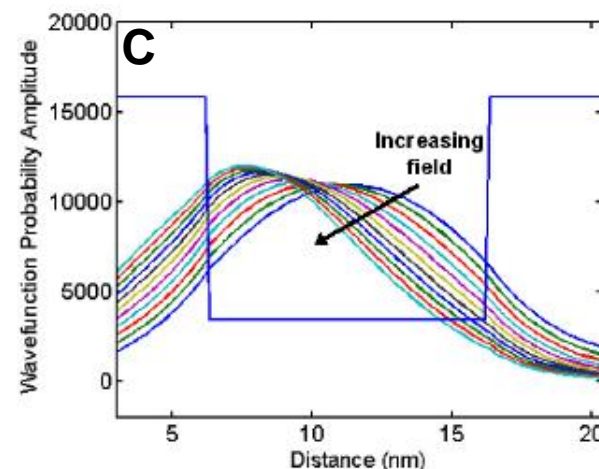
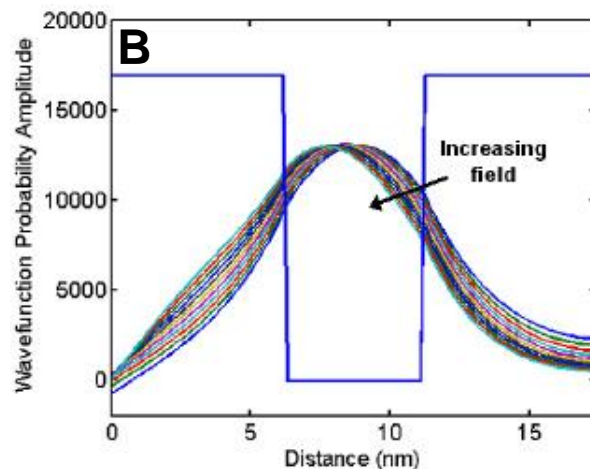
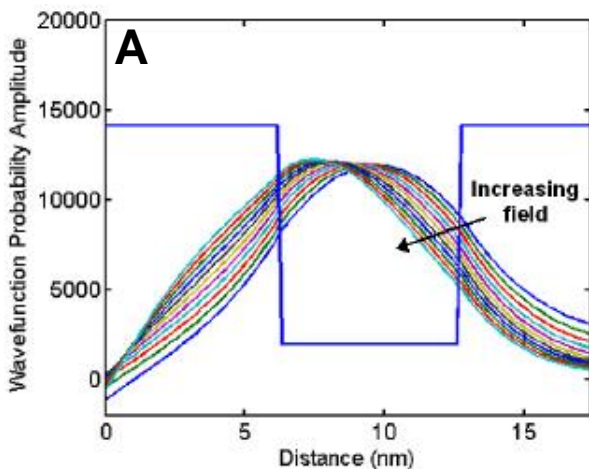
- We are showing the conduction band-heavy hole transition as the lowest energy transition; what does this tell us about the material?

Design of QCSE Modulator

$\Delta E_c = 70$ meV
 $w = 6.5$ nm

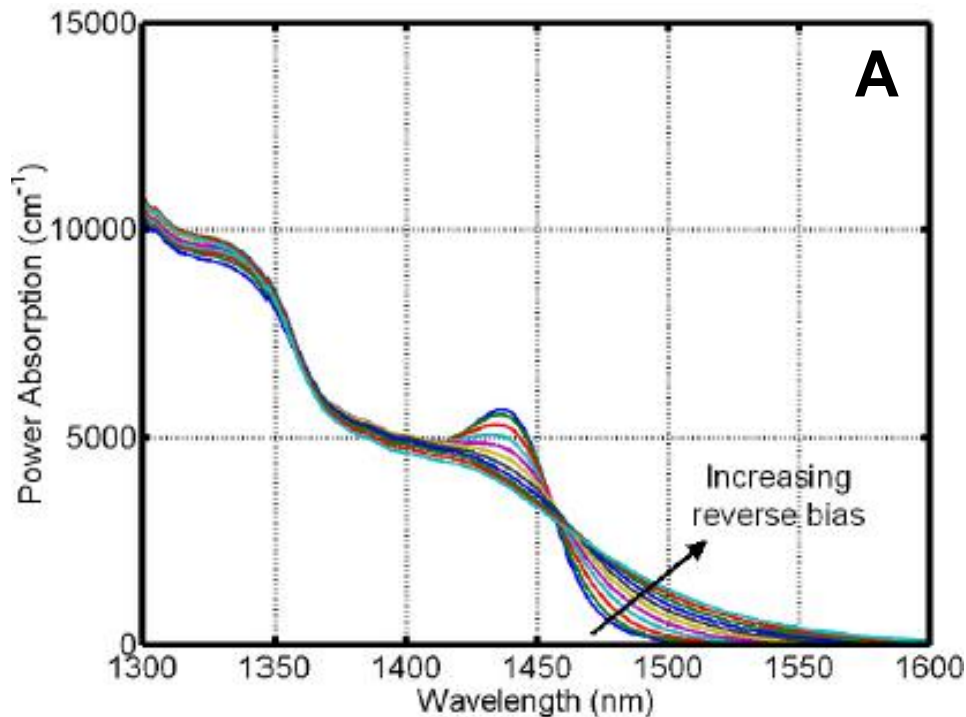
$\Delta E_c = 100$ meV
 $w = 5.0$ nm

$\Delta E_c = 70$ meV
 $w = 10.0$ nm



- Impact of QW width and depth on confinement
- Looking only at conduction band only for simplicity
 - But keep in mind that valence band depth is different; in InGaAsP materials, $\Delta E_c \approx \Delta E_v$
 - Why could this be especially problematic for say an EAM?

Absorption Spectra Analysis

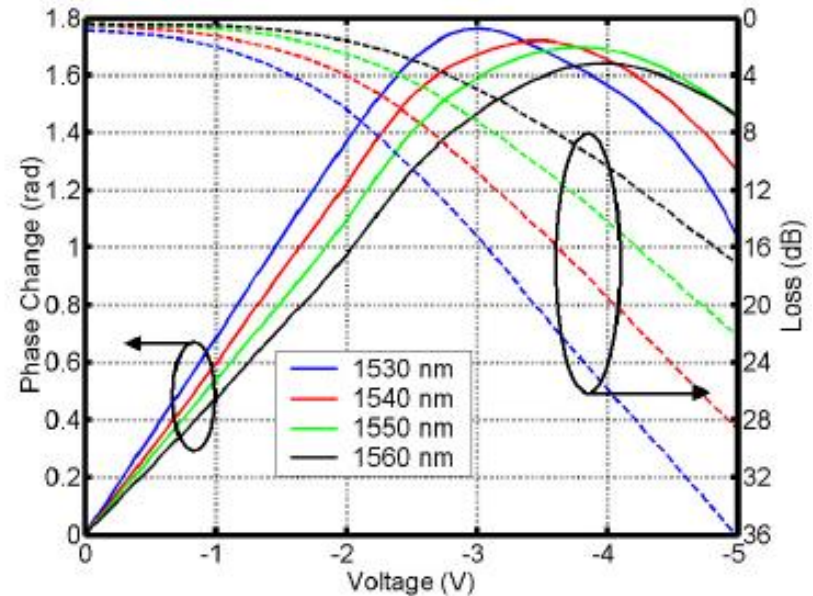
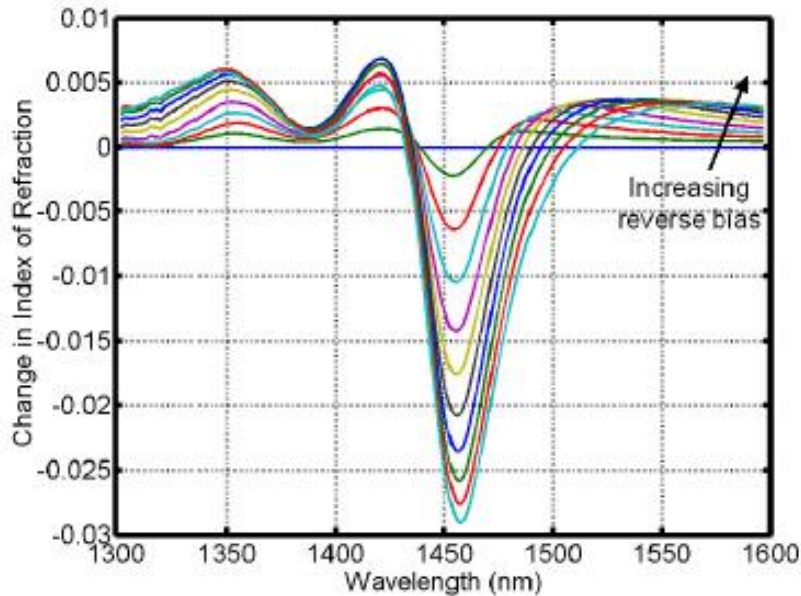


- The peak in absorption at 0 bias is observed in QWs
 - This is the exciton peak
- Why does the exciton peak diminish with increasing bias?
- Presence of exciton peak and impact on shape of absorption spectra influence Kramers-Kronig relation

Kramers-Kronig Relation

$$\Delta n(\lambda_0, \Delta V) = \frac{\lambda_0^2}{2\pi^2} P \int_0^\infty \frac{\Delta \alpha_{abs}(\lambda_0, \Delta V)}{\lambda_0^2 - \lambda^2} d\lambda$$

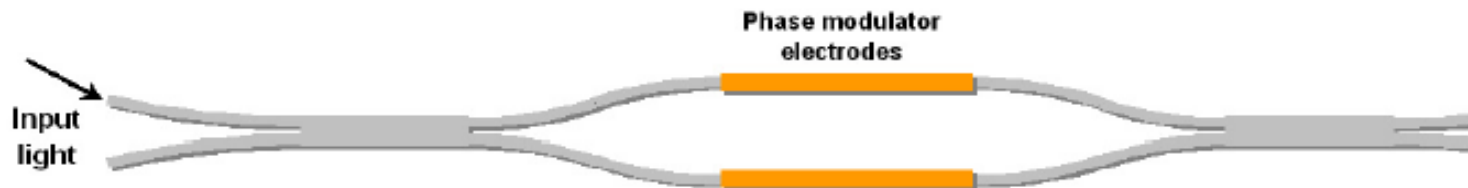
Absorption Spectra Analysis



$$\Delta\phi = \frac{2\pi L}{\lambda} \Gamma \Delta n$$

- Apply Kramers-Kronig and then calculate $\Delta\phi$
- Compare $\Delta\phi$ to $\Delta\alpha$ to understand tradeoff between phase modulation and amplitude modulation
 - What else does this tell us about the modulator performance?

MZM Response



$$E(V_1, V_2) = E_0 \sqrt{SR_{in}SR_{out}} \exp \left\{ - \left(\frac{\Delta\alpha(V_1)}{2} + j\Delta\beta(V_1) \right) L \right\} \\ + E_i \exp \left\{ - \left(\frac{\Delta\alpha(V_2)}{2} + j[\Delta\beta(V_2) + \phi_0] \right) L \right\}$$

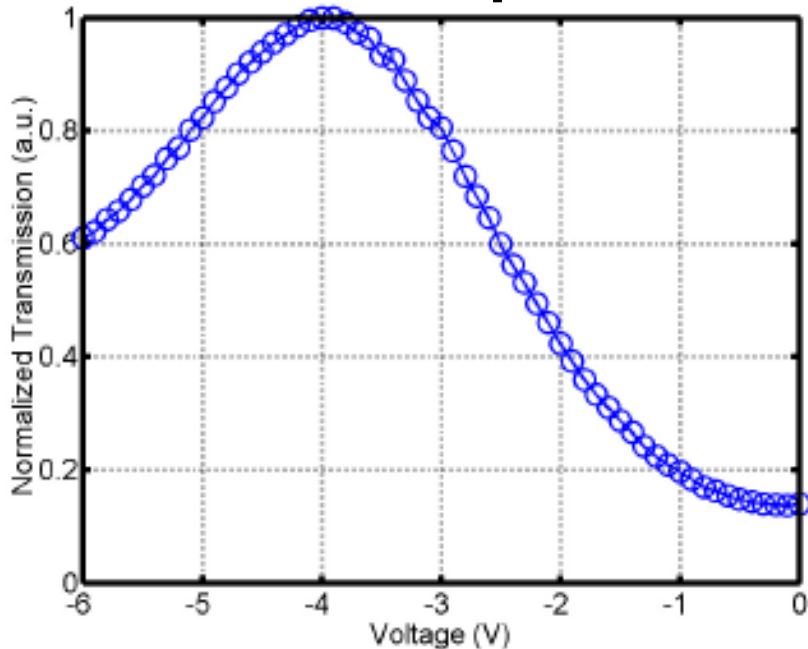
$$E_i = \frac{E_0}{\sqrt{(1 + SR_{in})(1 + SR_{out})}}$$

$$I(V_1, V_2) = |E(V_1, V_2)|^2 \quad \text{What we measure}$$

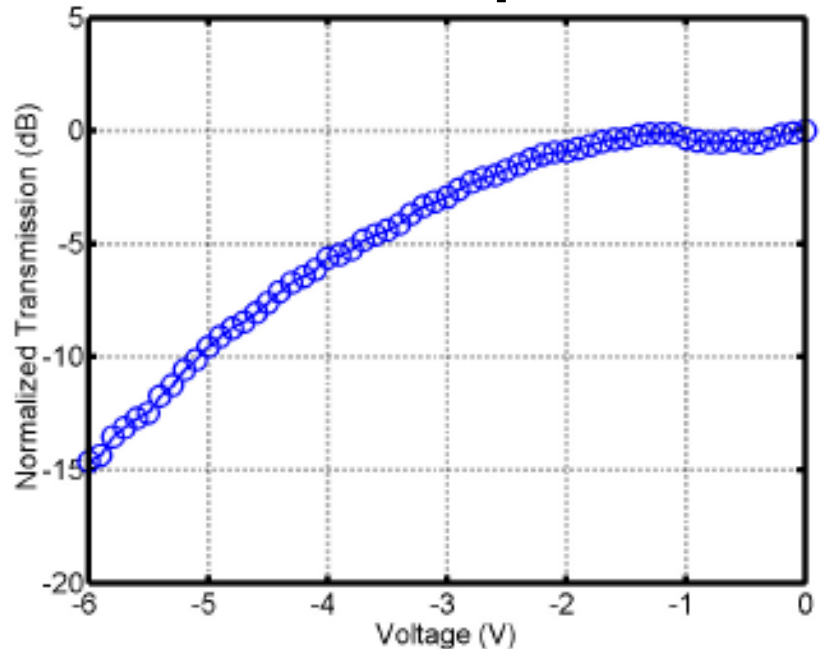
- Interfere two waves in MZI
- Change phase in each arm over some interaction length

MZM and EAM

MZM Response

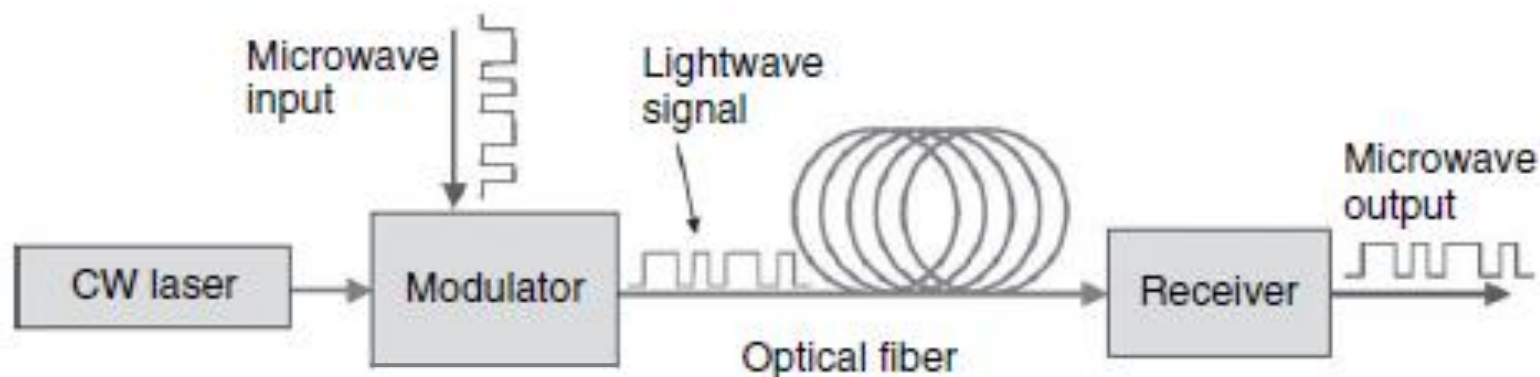


EAM Response



- Extract figures of merit: V_{pi} ? Extinction efficiency?
- What would you use this modulator for?

Photodetectors

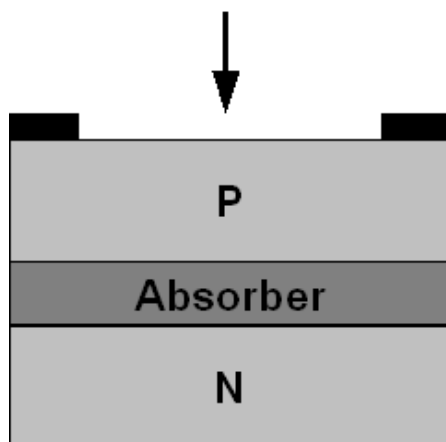


- **Photodetectors used in receivers for optical communications**
- **Photodetectors are O-E converters**
 - Use photodiodes for PICs
 - Absorbed photons generate mobile carriers
 - Convert mW of optical power to mA of current in external circuit
 - When terminated with load, mA of current become mW of electrical power
- **Why perform this O-E conversion?**

Surface Normal Versus Waveguide

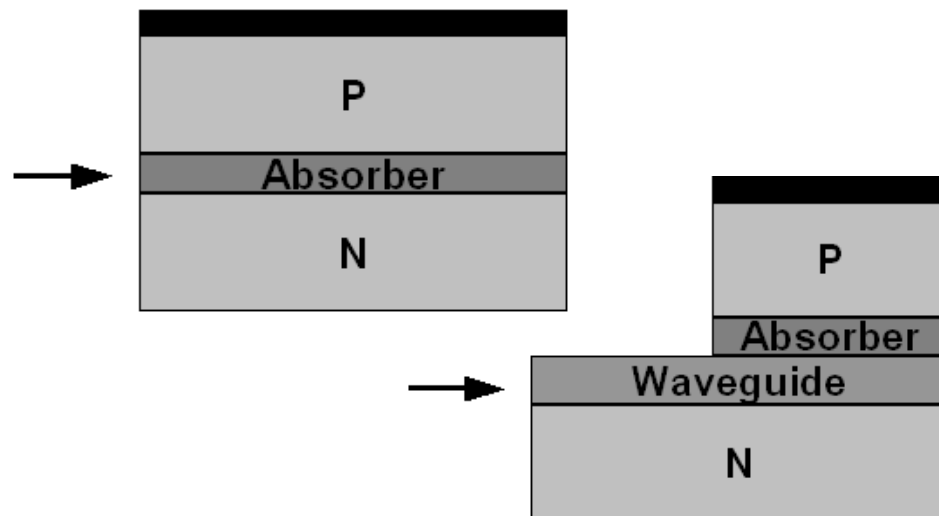
- **Surface normal photodiode**

- Light incident from top or bottom
- Efficiency determined by thickness of absorptive layer
- Bandwidth determined by thickness of absorptive layer (and by active area)



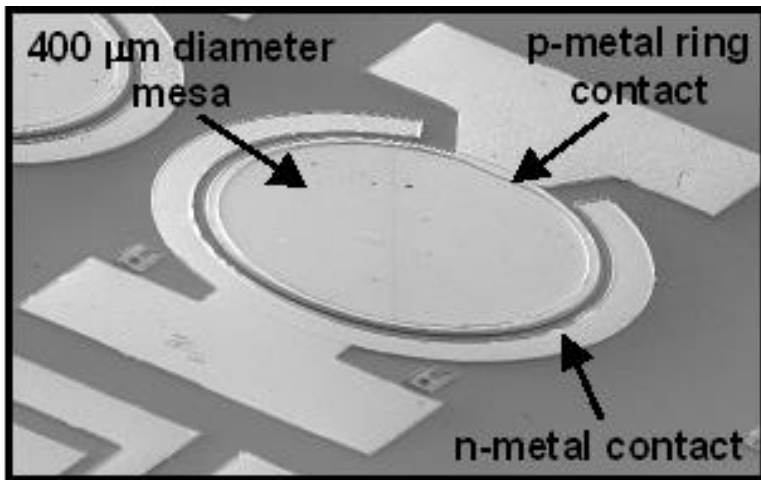
- **Waveguide photodiode**

- Light incident from edge facet
- Efficiency determined by length of device
- Bandwidth determined by thickness of absorptive layer



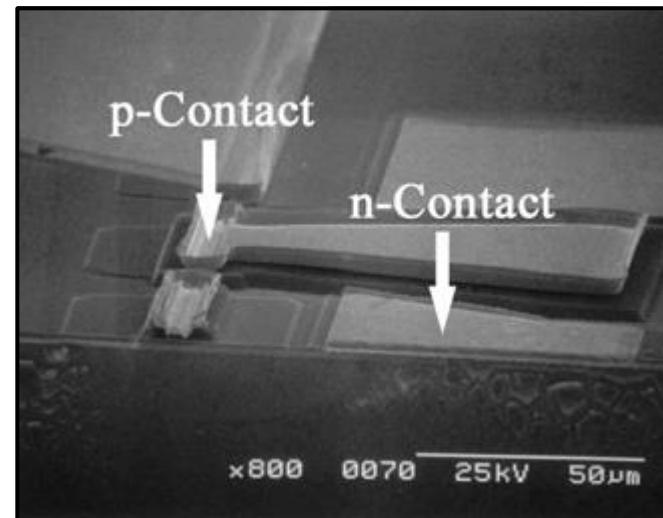
Surface Normal Versus Waveguide

Surface Normal Photodiode



Typical diameter = 5 – 500 μm

Waveguide Photodiode

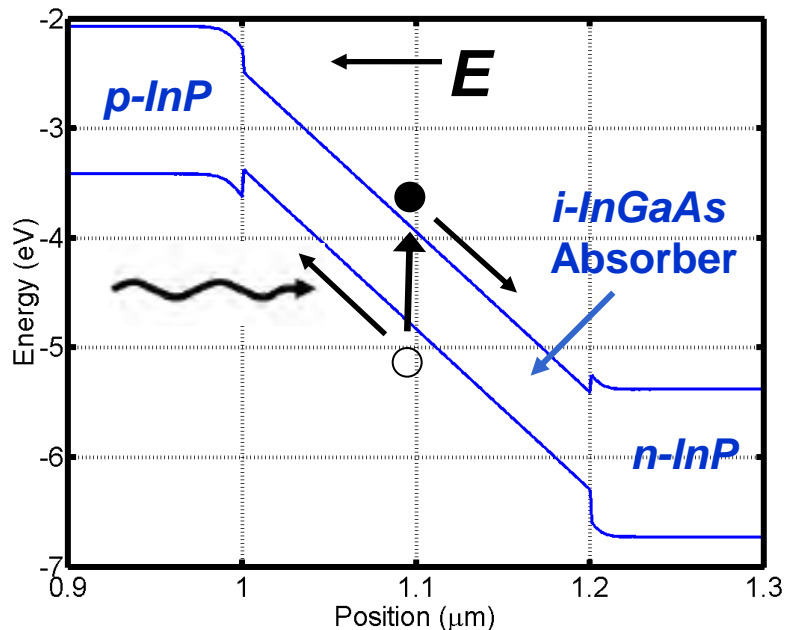


Typical length = 10 – 1000 μm

Typical width = 1 – 5 μm

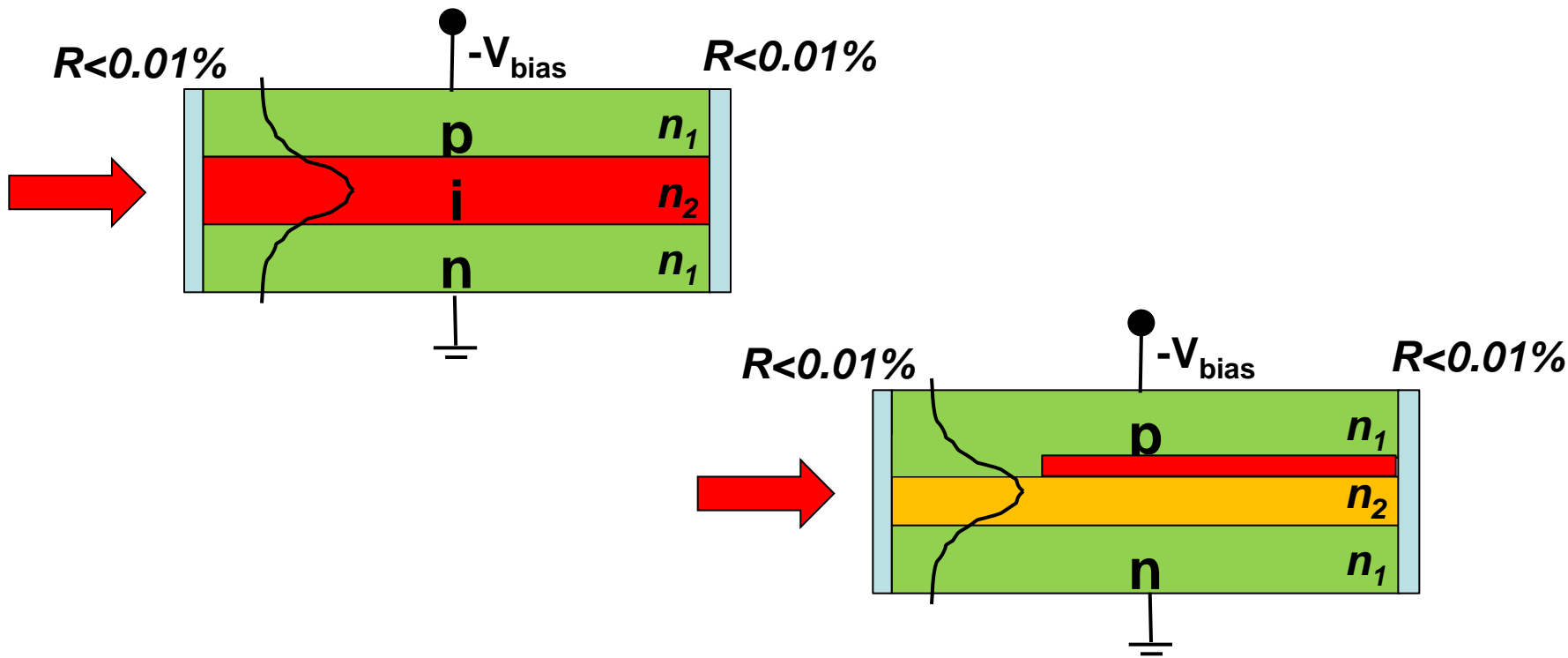
Conventional PIN Photodiode

Band diagram at -2 V



- Absorption in an UID (~intrinsic) depleted photo-absorption layer generates electron-hole pairs
- Both carriers swept out of depletion region by applied field (drift)
- Carriers enter p- and n-type regions where they are majority carriers and settle with dielectric relaxation time (very fast)
 - In this way photogenerated carriers contribute to current in external circuit

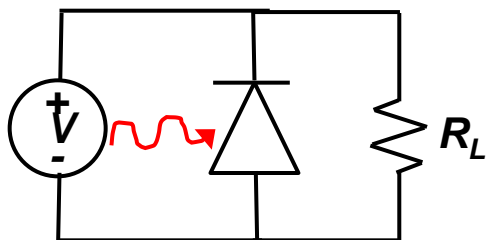
Waveguide Photodetector



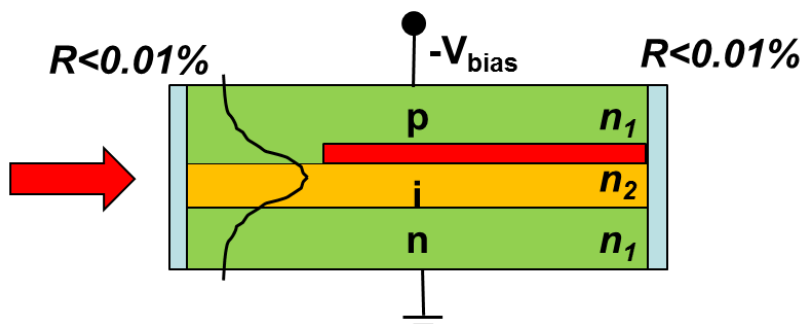
- Γ affects the absorption profile \rightarrow efficiency of the photodetector, also saturation characteristics
- Active area defined by field region where mobile space carriers are present
- So far discussed bulk absorber materials; what other compatible materials/structures could be used for absorption?

Photodetector Bandwidth

Simplified Circuit Model



$$f_{3-dB} = \frac{1}{2\pi \sqrt{(R_L C_j)^2 + \tau_t^2}}$$



$$C = \frac{\epsilon A}{d}$$

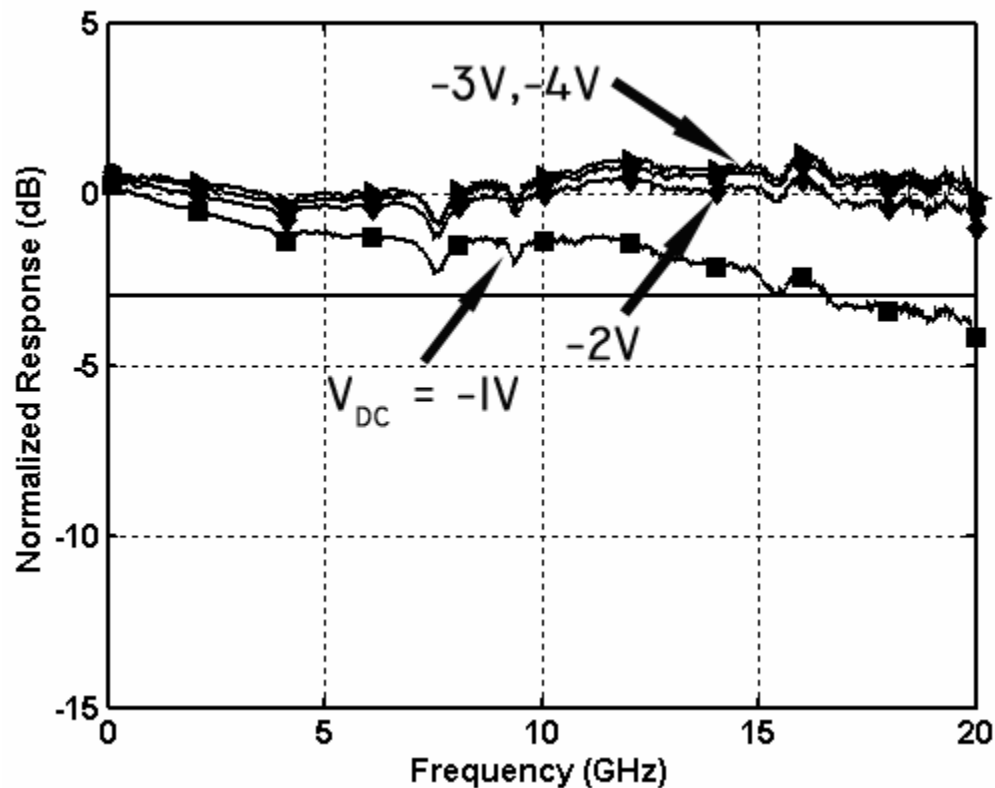
At 50V/cm

$$\tau_{drift,e} = 7 \times 10^6 \text{ cm/s}$$

$$\tau_{drift,h} = 4 \times 10^6 \text{ cm/s}$$

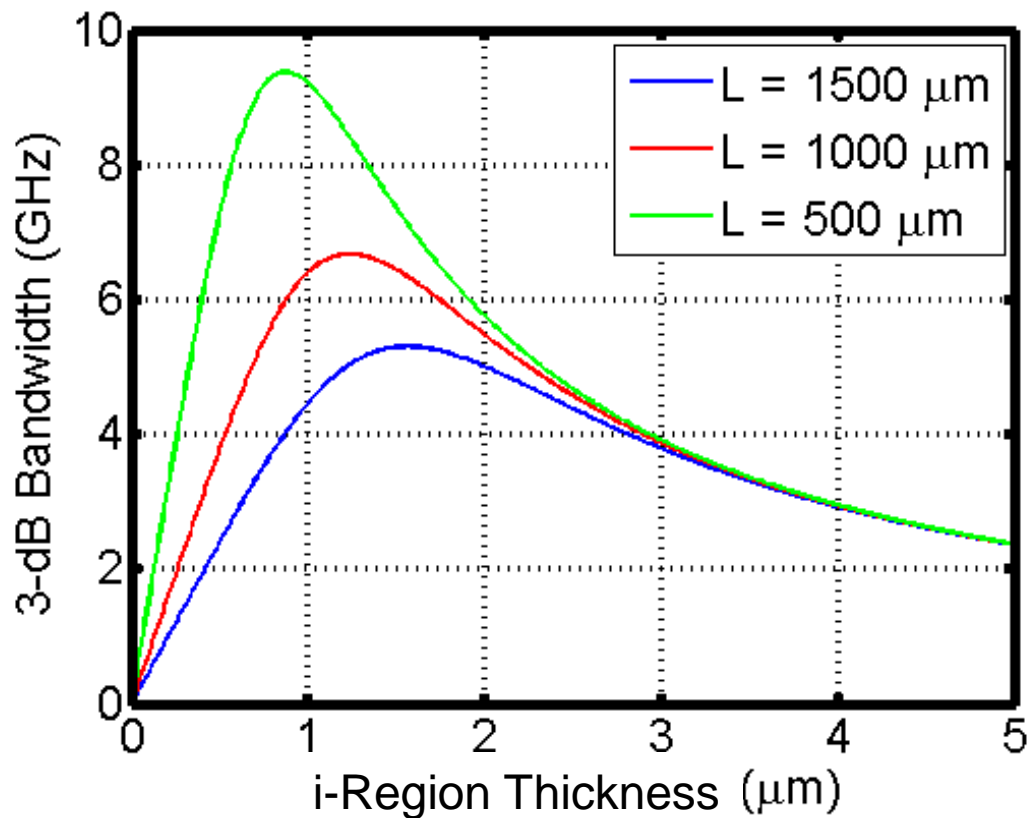
- Bandwidth dependent on parallel plate capacitance, load resistance and carrier transit time
- Parallel plate separation is depletion thickness

Photodetector Bandwidth



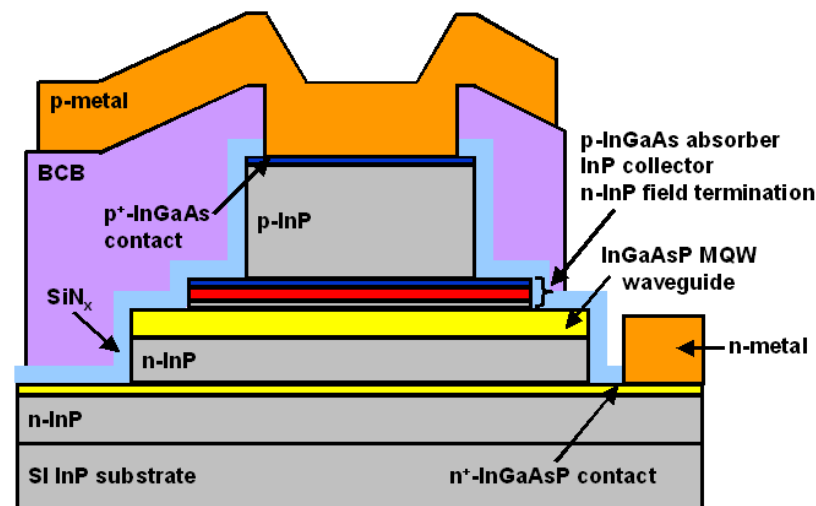
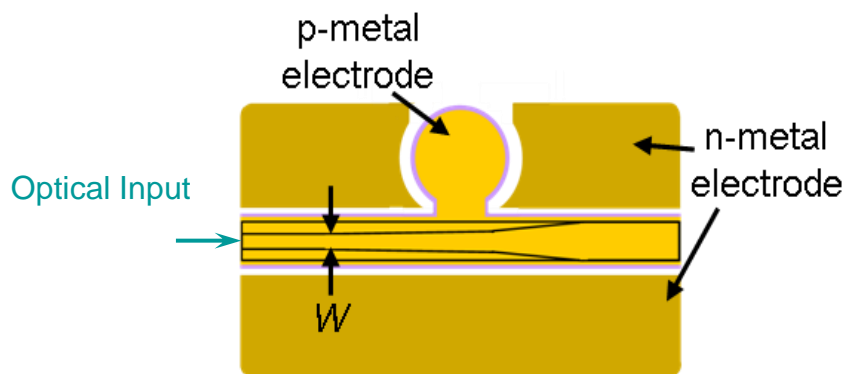
- What is the bandwidth at -1 V bias?
- Why is the bandwidth bias dependent?

RC-Limited versus Transit-Time Limited



- Which is the RC-limited region and which is the transit-time-limited region?

Practical Implementation



- Require metal contact pad to probe or wirebond to; typical diameter is 100 μm
- Problematic in that adds parasitic capacitance
- Solution: insert thick dielectric with low dielectric constant between metal pad and ground plane

Photodetector Efficiency

$$P_{OUT} = P_{IN}e^{-\Gamma\alpha L}$$

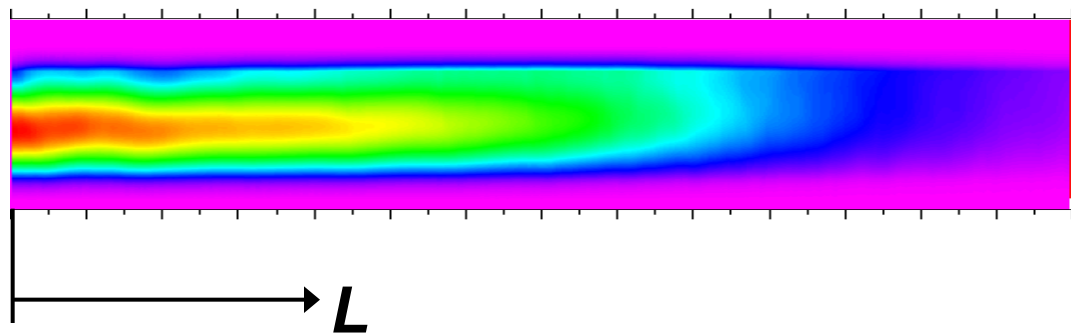
$$\eta_{int} = \frac{P_{IN} - P_{OUT}}{P_{IN}}$$

$$\eta_{int} = 1 - e^{-\Gamma\alpha L}$$

$$R = \eta_{ex} \frac{q}{h\nu} [A/W]$$

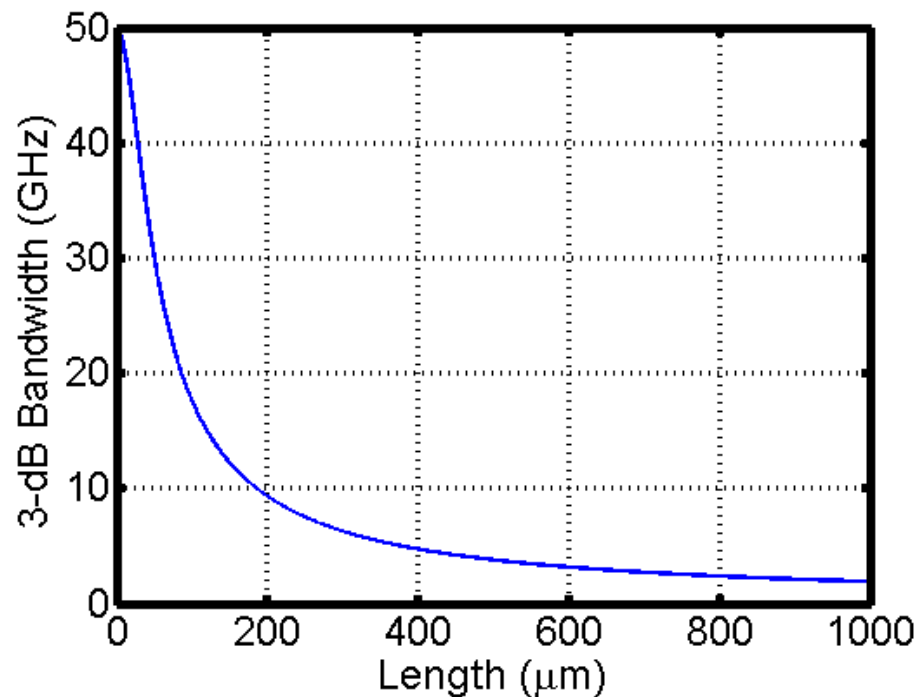
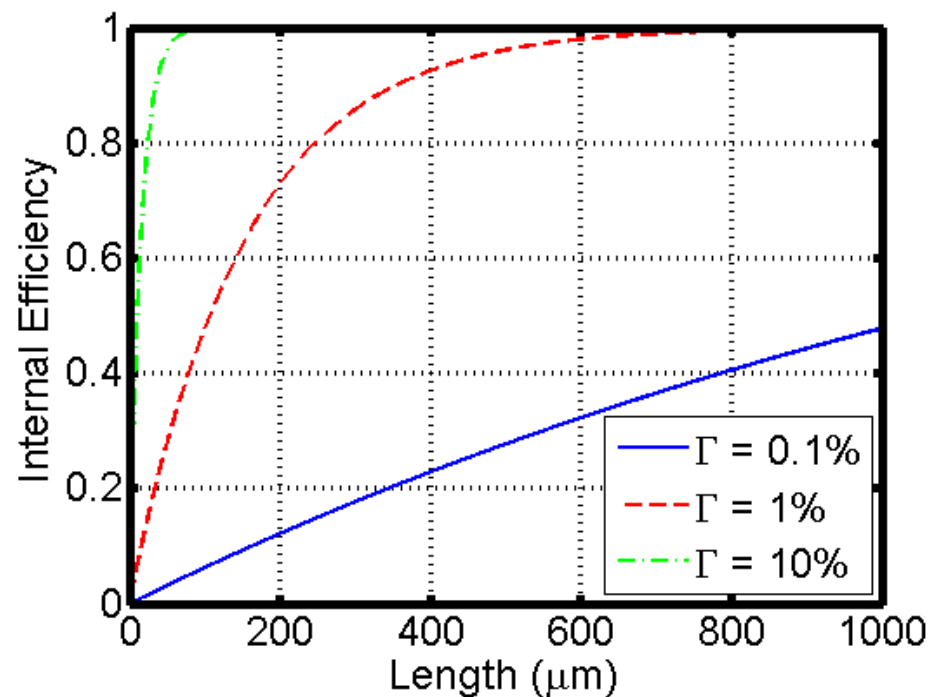
$$\eta_{ex} = \eta_{int}\eta_{coupling}$$

Beam Propagation Method (BPM) Simulation



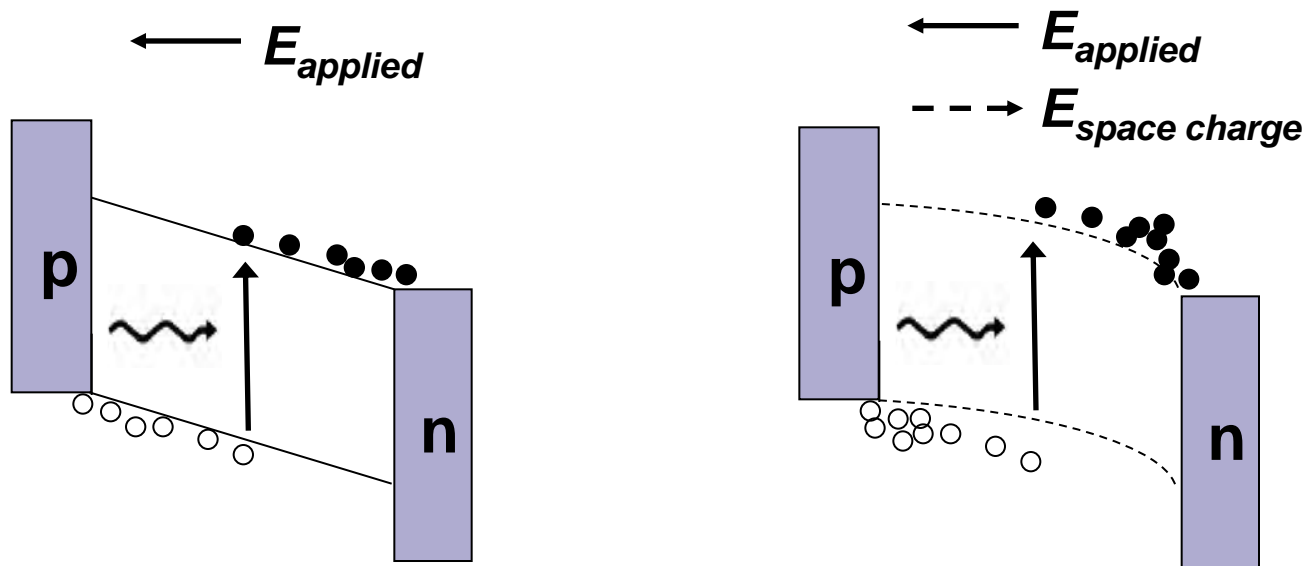
- Exponential absorption profile
- Calculate with knowledge of confinement factor or simulate complex structure

Waveguide Photodiode Design



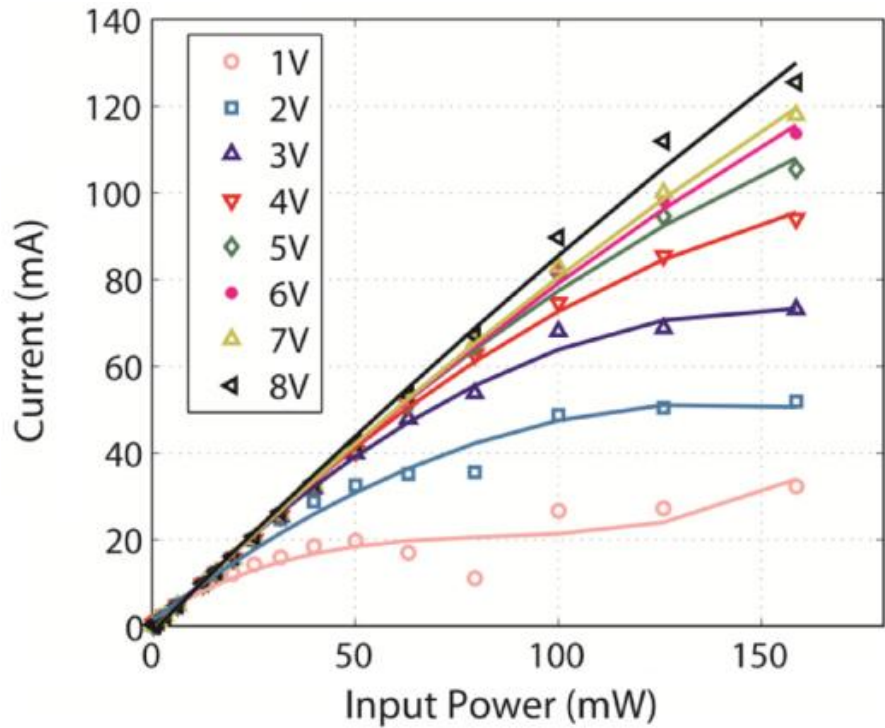
- Vary the length given: active region thickness, material absorption, carrier drift times, 50-ohm load impedance
- What parameter would you change to increase the bandwidth?
- Why could it be problematic to use a high Γ ?

Saturation Induced by Space Charge

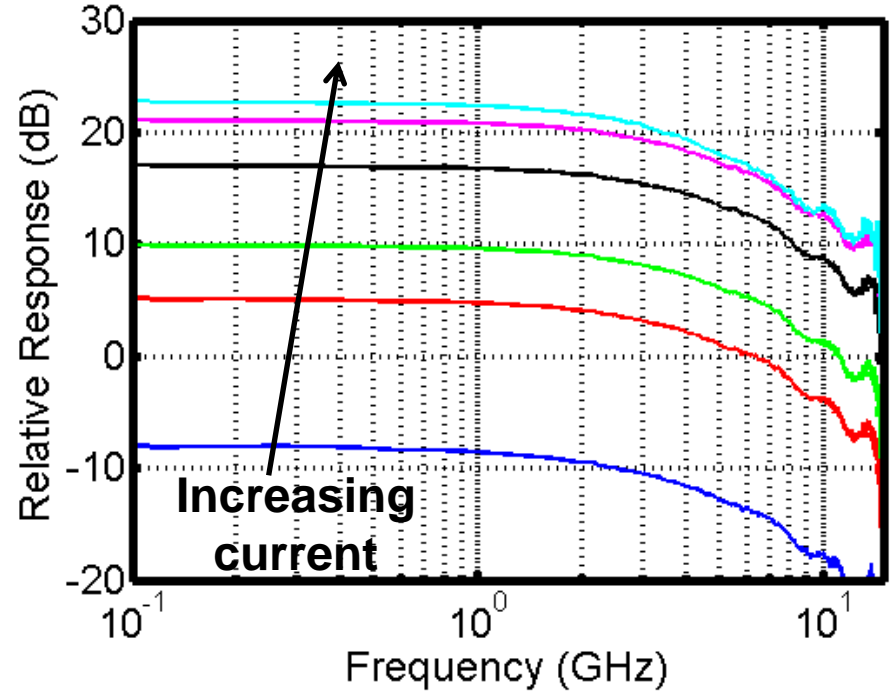


- Mobile space charge accumulation induces a field opposing the applied field
- At high current levels, space-charge field significant and causes saturation of photodiode
 - Depletion region effectively small and carrier velocities lower

Saturation Induced by Space Charge



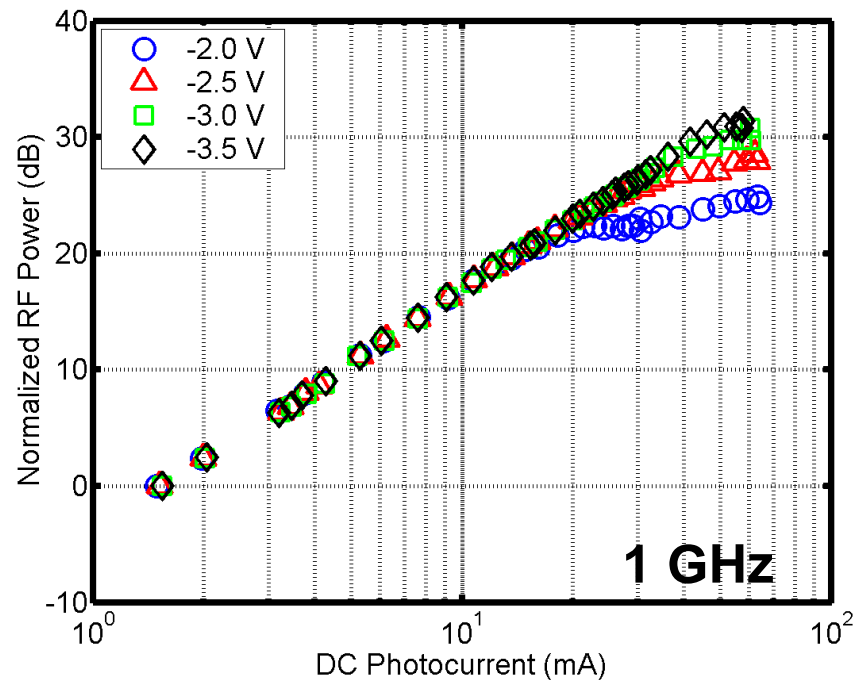
Measured at DC



Bias = -3 V

Saturation Induced by Space Charge

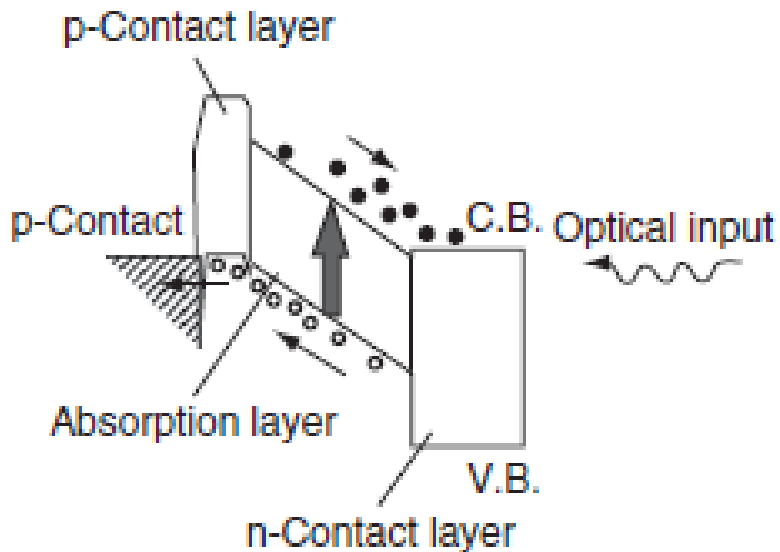
$$P = \frac{1}{2} I^2 R$$



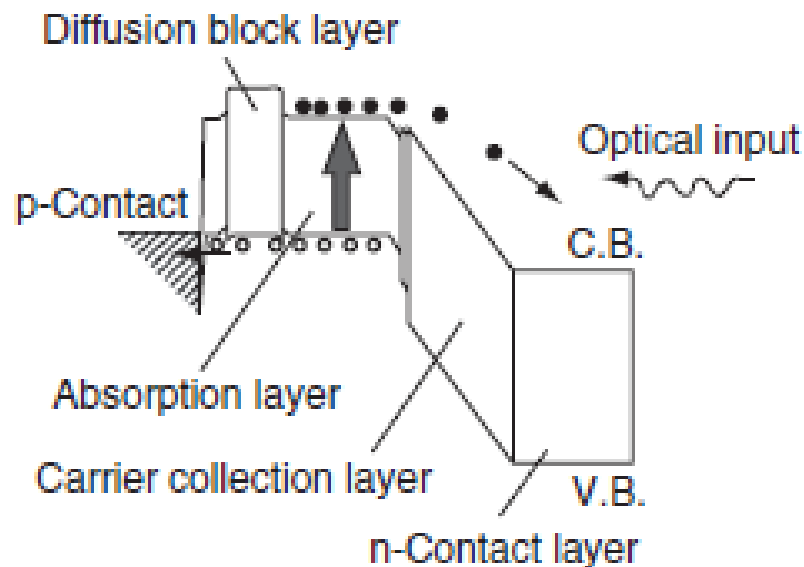
- **1-dB compression current defined by current when power degrades by 1 dB from ideal**
- **Extract from the figure**
- **What would you expect at higher frequency?**

Uni-Traveling-Carrier Photodiode

PIN-PD Band Diagram

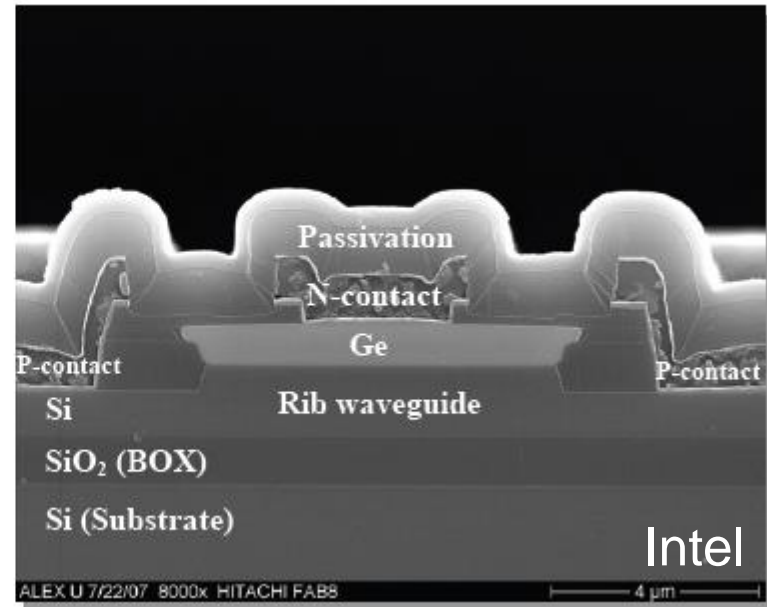
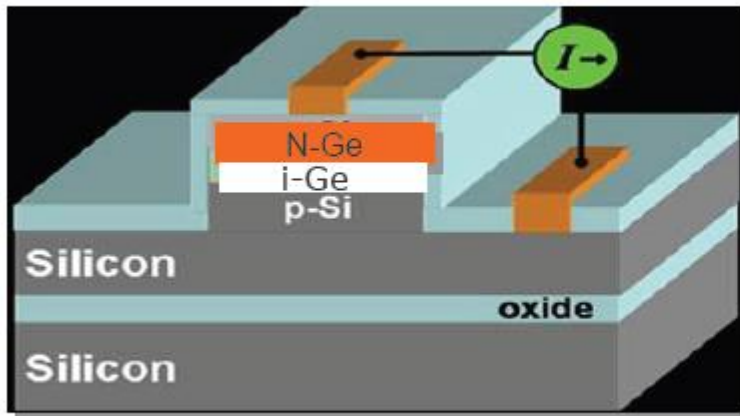


UTC-PD Band Diagram



- **UTC-PD has p-type undepleted absorption layer**
- **Photogenerated electrons diffuse to absorption layer/collection layer interface and are injected into wide-bandgap drift layer then swept out by applied field**
- **Electrons are only active carriers; why is this beneficial?**

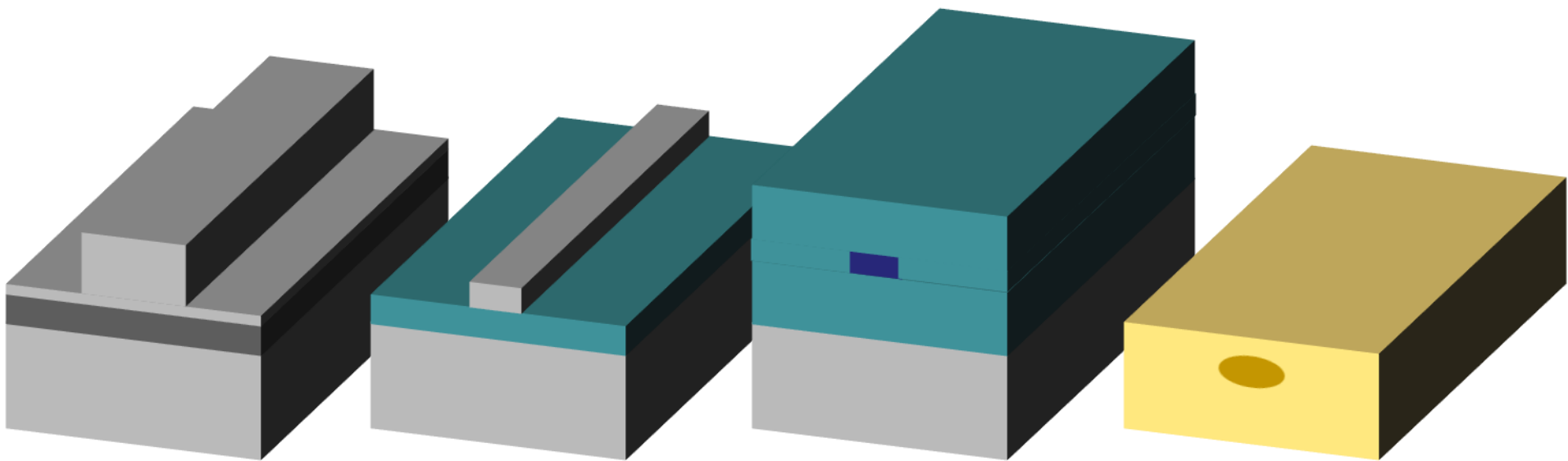
Germanium Photodiode



- Ge on Si photodiode
- Lattice mismatch between Ge and Si large therefore Ge growth challenging

Integration Platforms and Manufacturing

Integrated Photonic Materials



Indium phosphide (InP)

- $\Delta = 5-10\%$
- Small devices ($\sim\mu\text{m}-\text{mm}$)
- Lasers, modulators, SOAs, photodetectors, passives

Silicon on insulator (SOI)

- $\Delta = 40-45\%$
- Small devices ($\sim\mu\text{m}$)
- Modulators, photodetectors, passives

SiO₂, SiON, Si₃N₄ (PLC)

- $\Delta = 0.5-20\%$
- Large devices ($\sim\text{mm}-\text{cm}$)
- Passives

Lithium niobate (LiNbO₃)

- $\Delta = 0.5-1\%$
- Large devices ($\sim\text{mm}-\text{cm}$)
- Modulators, passives

• Index contrast = $\Delta = (n_{core}^2 - n_{cladding}^2)/(2n_{core}^2)$
 • Typical waveguide architectures shown

InP Monolithic Integration Platforms

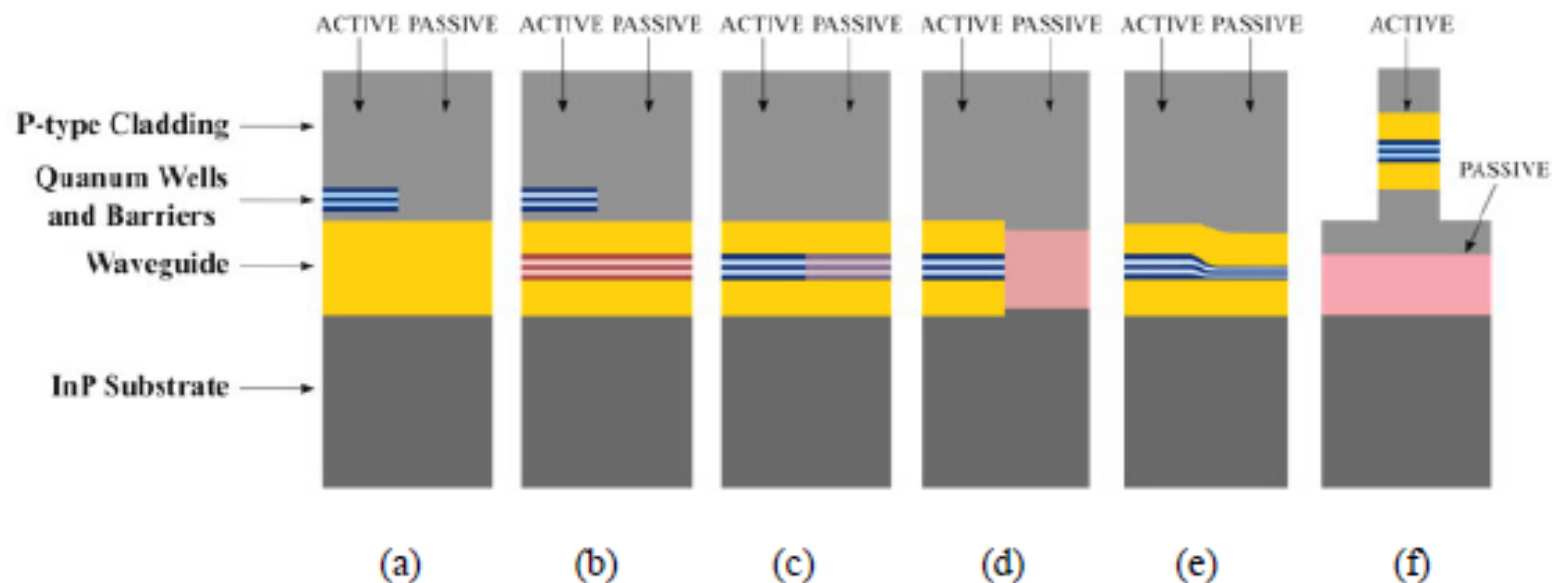
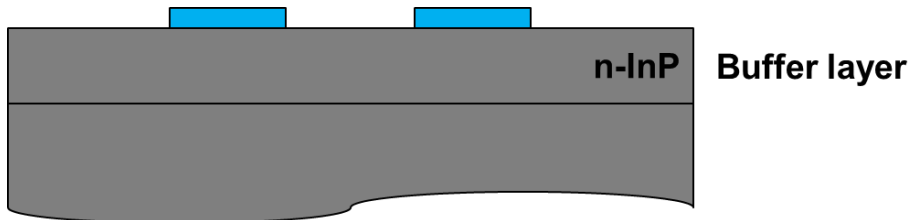
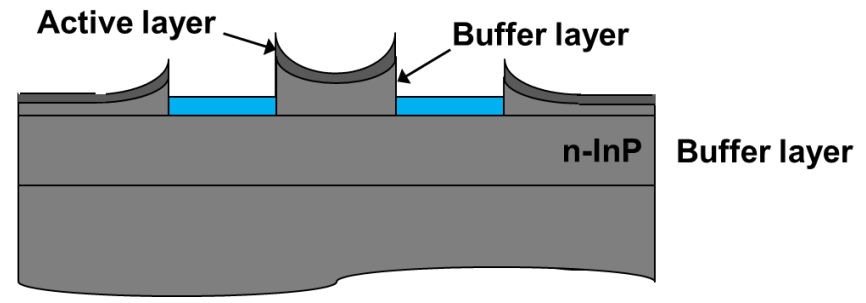


Fig. 2.4 Summary of popular integration platforms: (a) offset quantum well; (b) dual quantum well; (c) quantum-well intermixing; (d) butt-joint regrowth; (e) selective-area growth; and (f) asymmetric twin-waveguide.

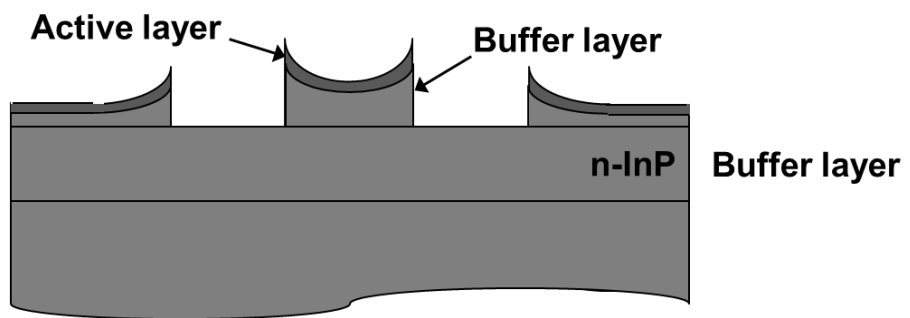
Selective Area Growth (SAG)



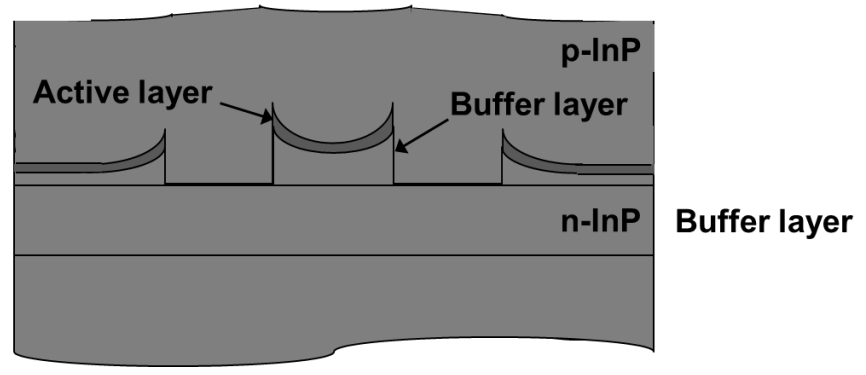
1. Buffer layer growth and mask formation



2. Selective area active region growth

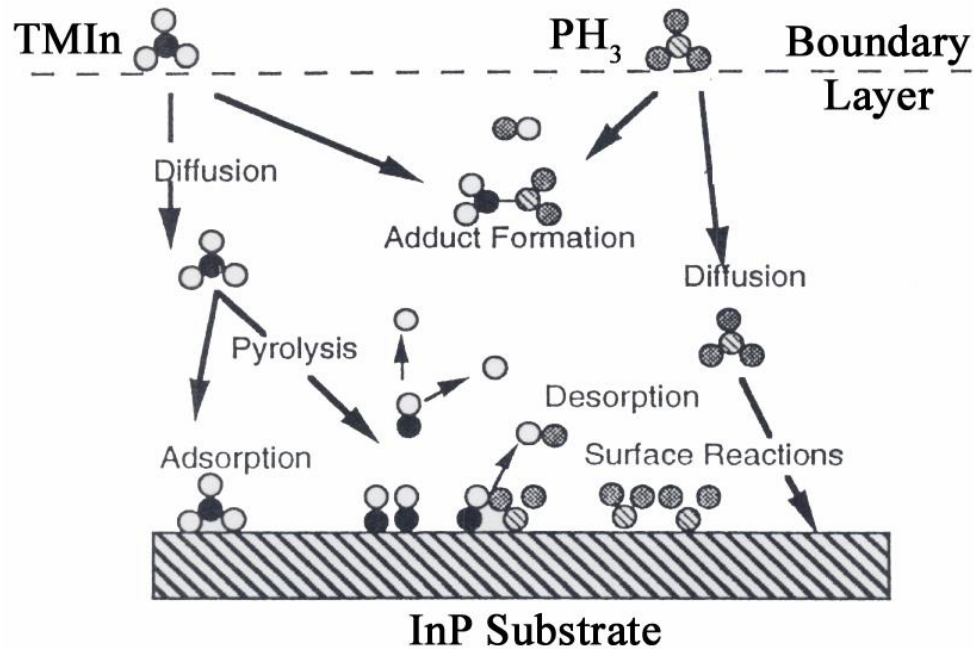


3. Mask removal

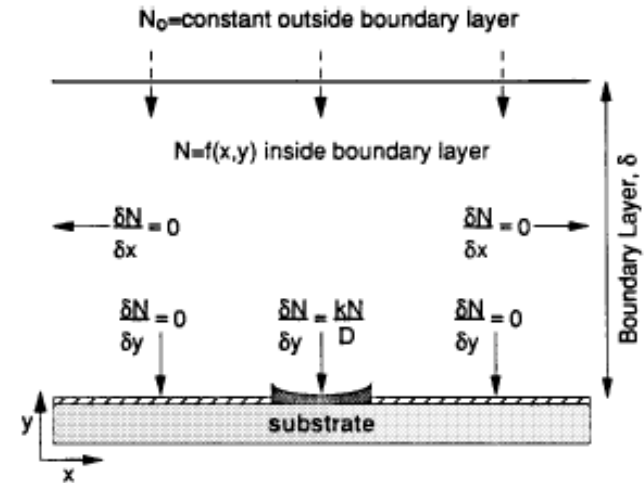
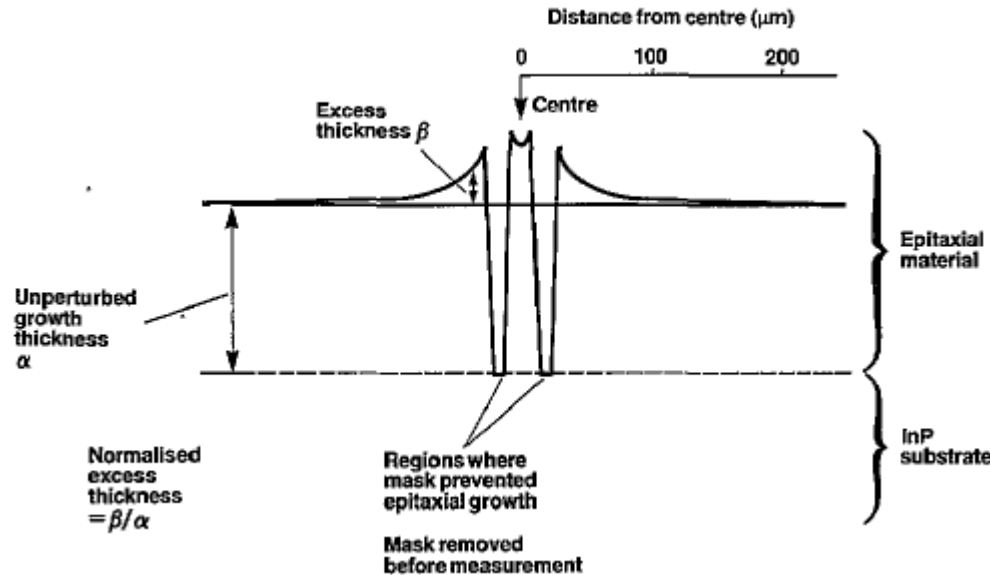


4. Overgrowth

MOCVD Growth Fundamentals

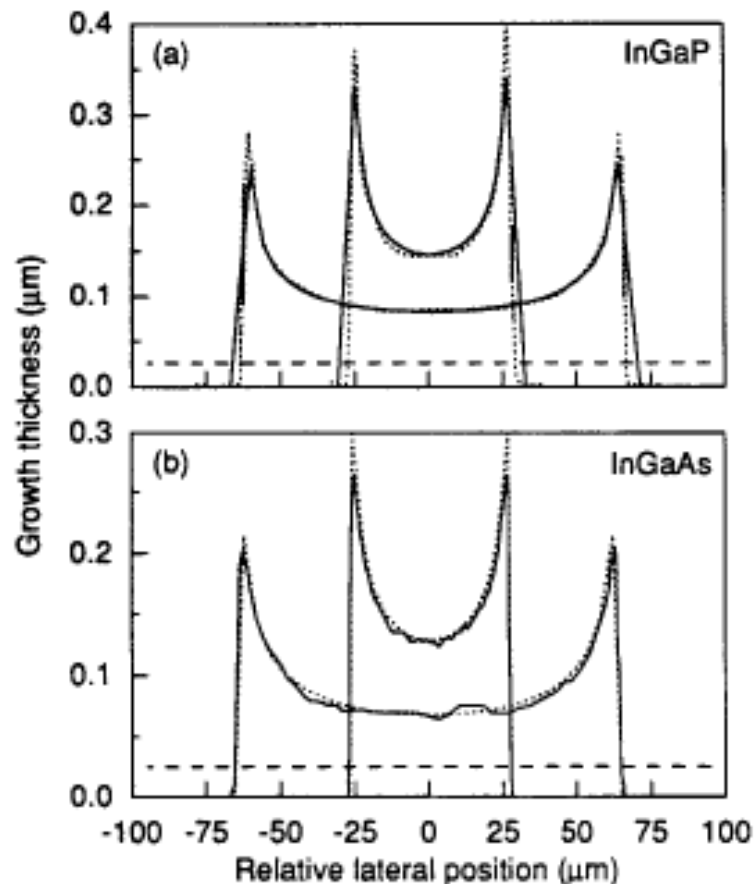


- Under typical growth conditions, the growth rate is controlled by the group III reactant concentration (mass transport regime)
- There exists a boundary layer above the growing surface where the gas volume is stagnant
- Reactants deplete at surface leading to a gradient



- Inside boundary layer lateral variation of group III reactant concentration is induced by growth mask
- Material grows nonuniformly in the vicinity of growth-inhibiting SiO₂ mask; growth rate enhanced

Coleman, et al., IEEE JSTQE 3(3), 1997



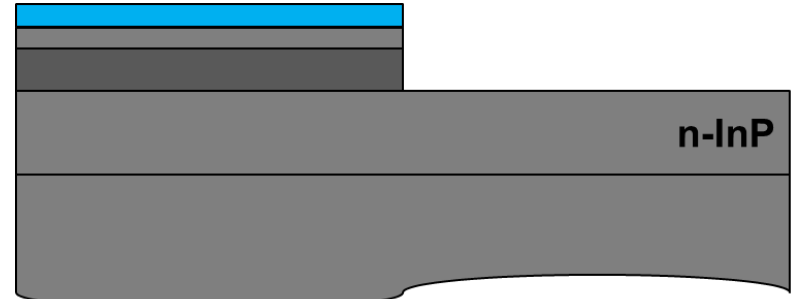
- Measured and predicted thickness profiles
- Mask windows are 50 and 125 μm wide
- Composition is also affected for ternary and quaternary compounds

Coleman, et al., IEEE JSTQE 3(3), 1997

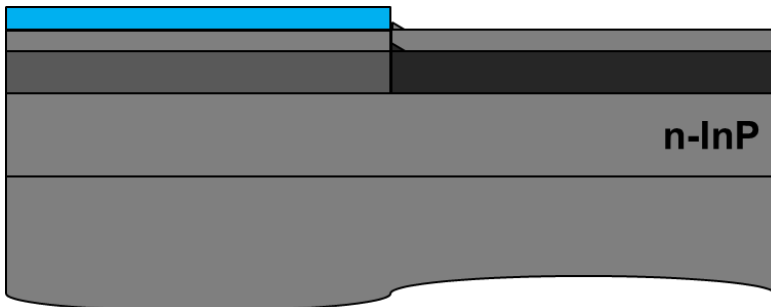
Butt Joint Growth (BJG)



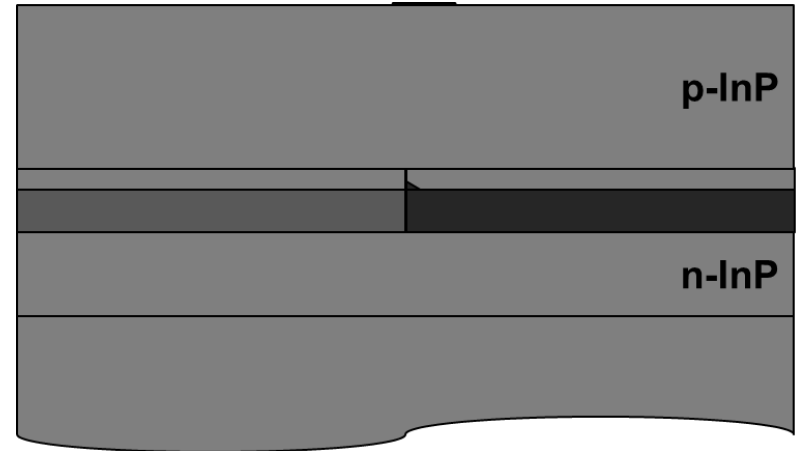
1. Buffer layer and first waveguide growth



2. Mask formation and etch



3. Second waveguide selective area growth



4. Mask removal and upper cladding growth

Etched InP

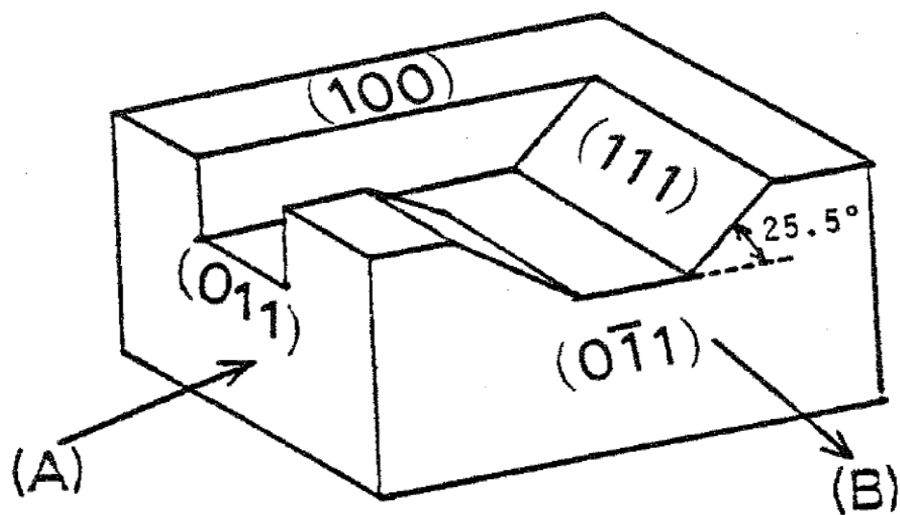
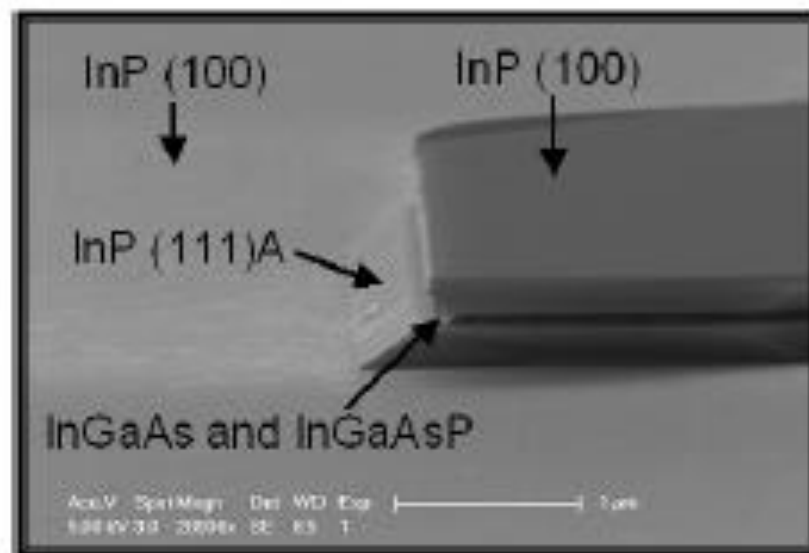


Fig. 3. Schematic diagram of etched pattern with respect to crystal orientation.

Etched InP, InGaAsP



Etched InP

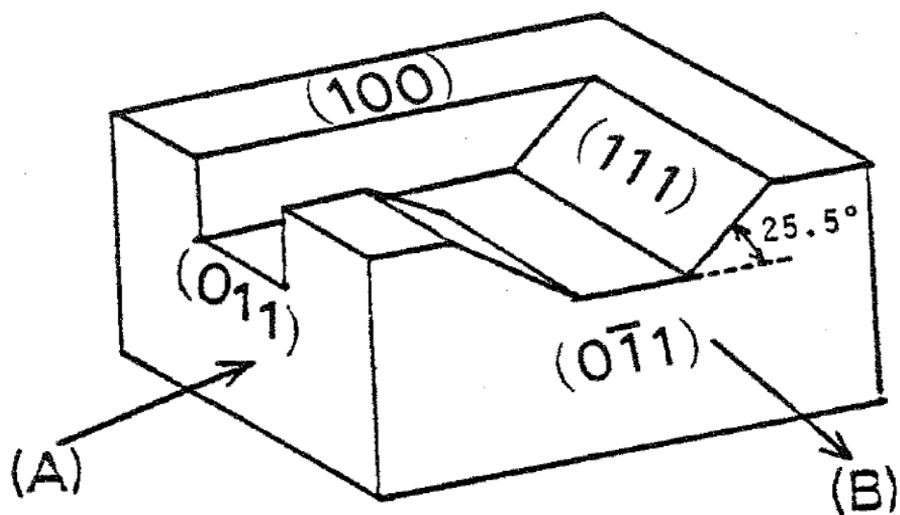
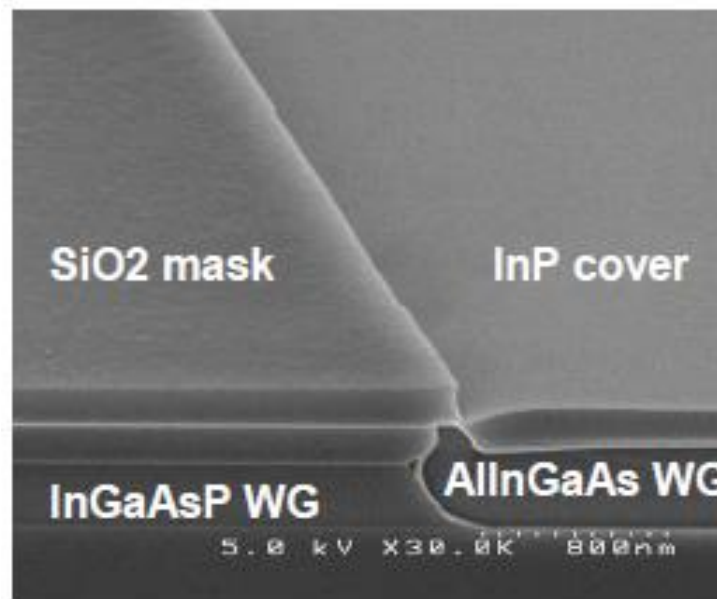


Fig. 3. Schematic diagram of etched pattern with respect to crystal orientation.

Butt-Joint Interface



[110] Direction



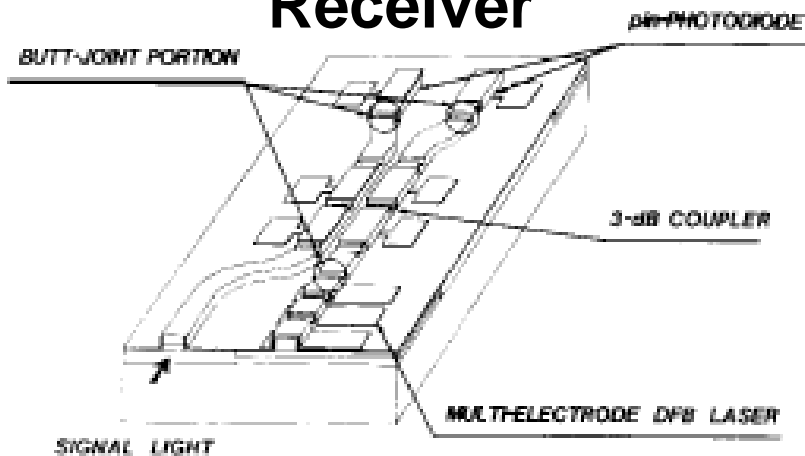
[-110] Direction



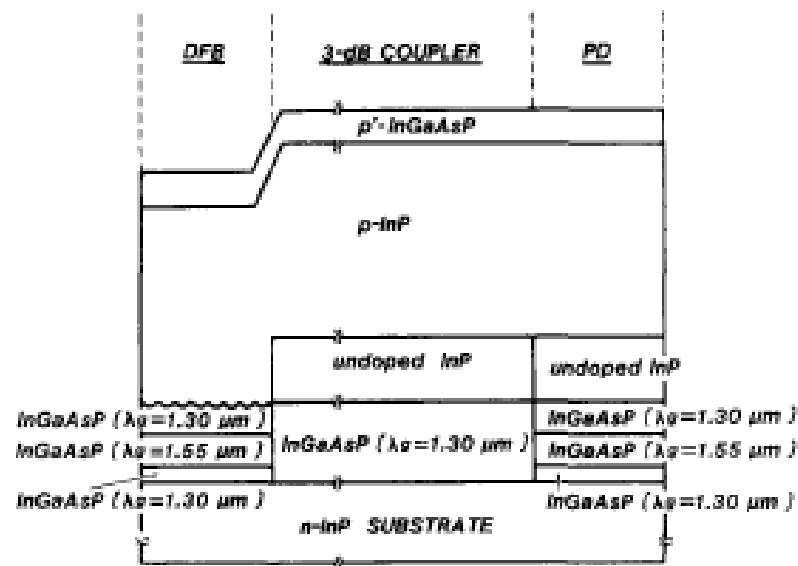
Binsma, et al., JDS Uniphase

Example BJG InP PIC

Monolithic Coherent Receiver



Device Structure

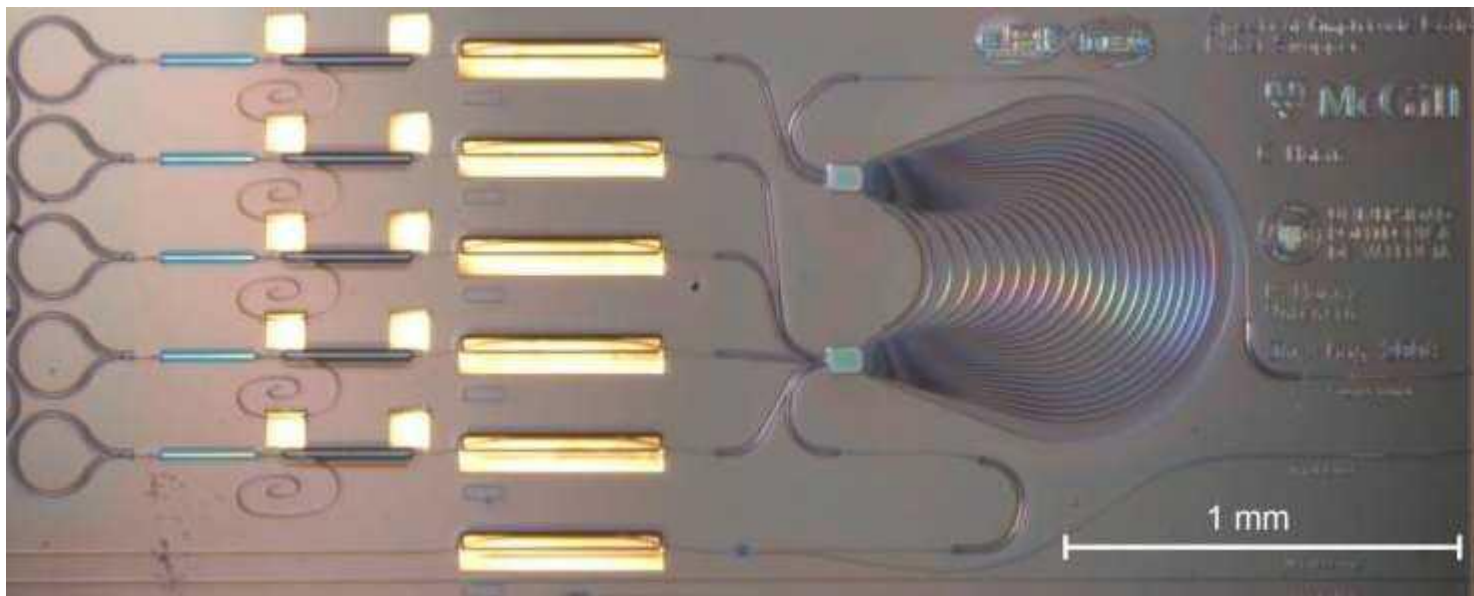


- Three-step growth process to integrate DFB laser, passive coupler, p-i-n photodiode

Takeuchi, et al., PTL 1(11), 1989

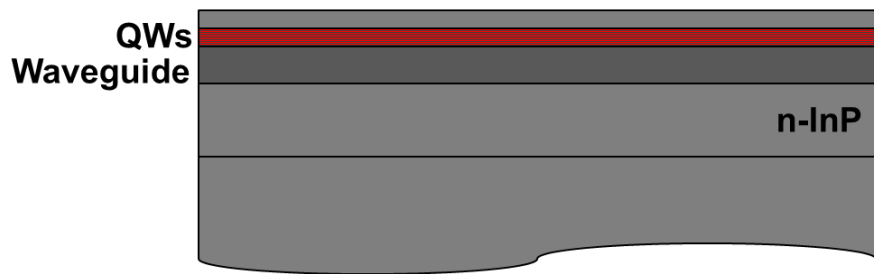
Example BJG InP PIC

Multi-Wavelength Laser

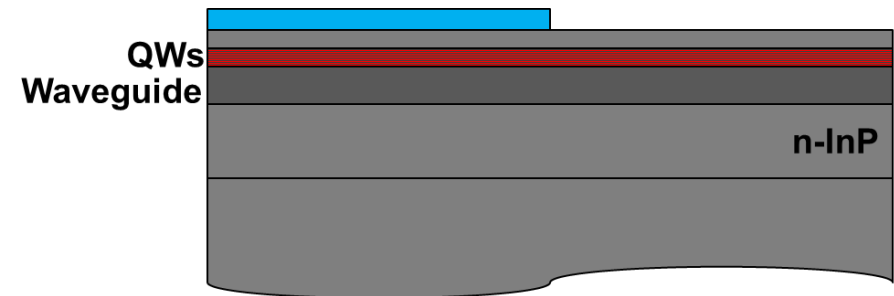


ECIO, 2010, Paper WEF2

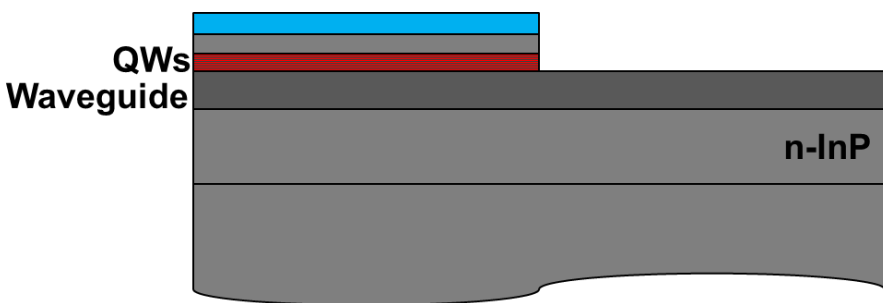
Offset Quantum Well (OQW)



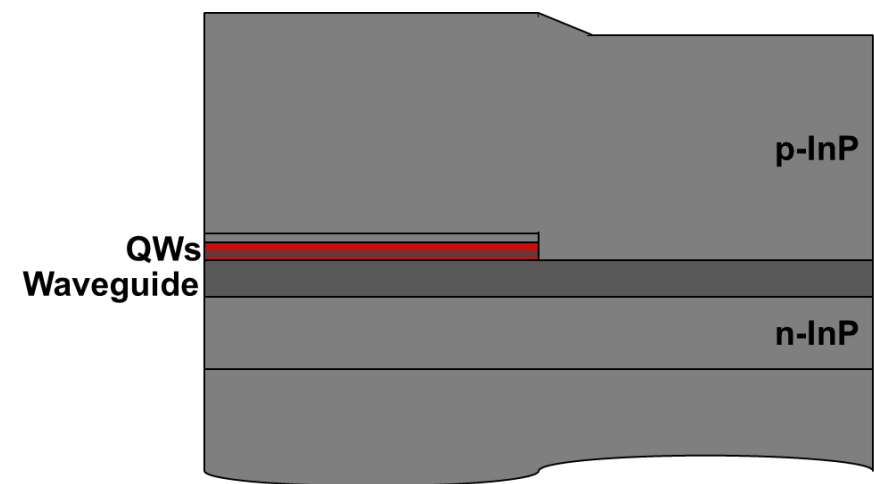
1. Waveguide and QW growth



2. Mask formation



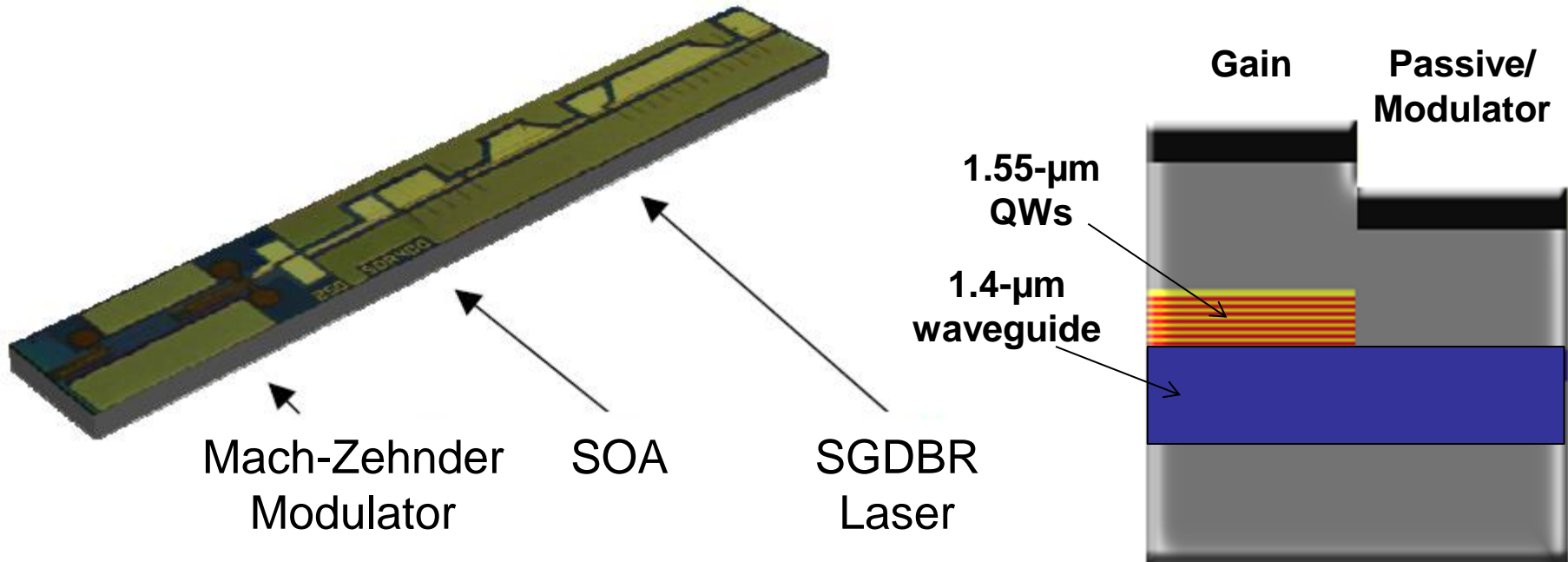
3. QW etch



4. Mask removal and upper cladding growth

OQW InP PIC

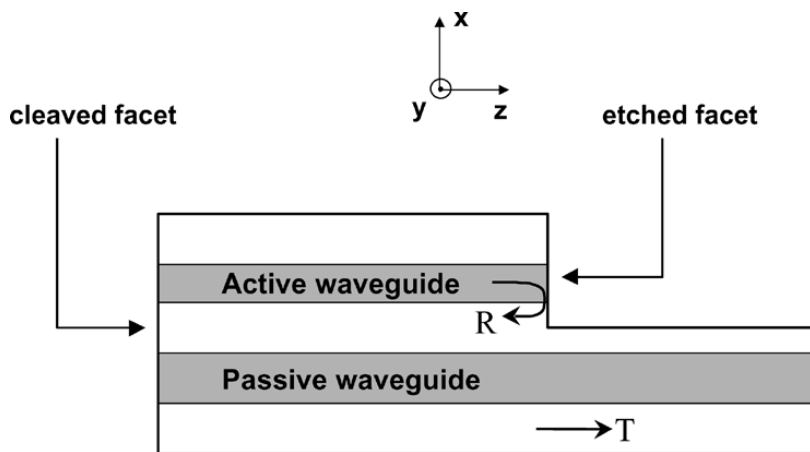
Widely-Tunable Laser Modulator Transmitter



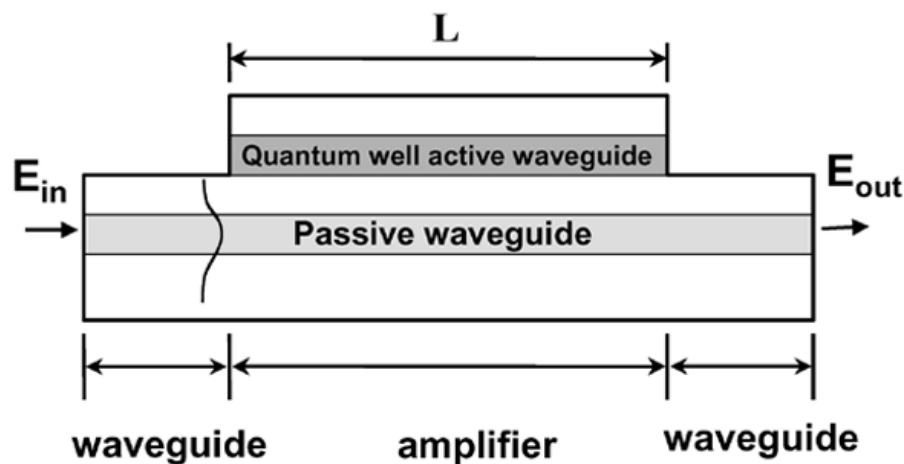
J. Barton, et al., JSTQE 9(5) 2003

Asymmetric Twin Guide (ATG)

Laser-Fed Passive Waveguide

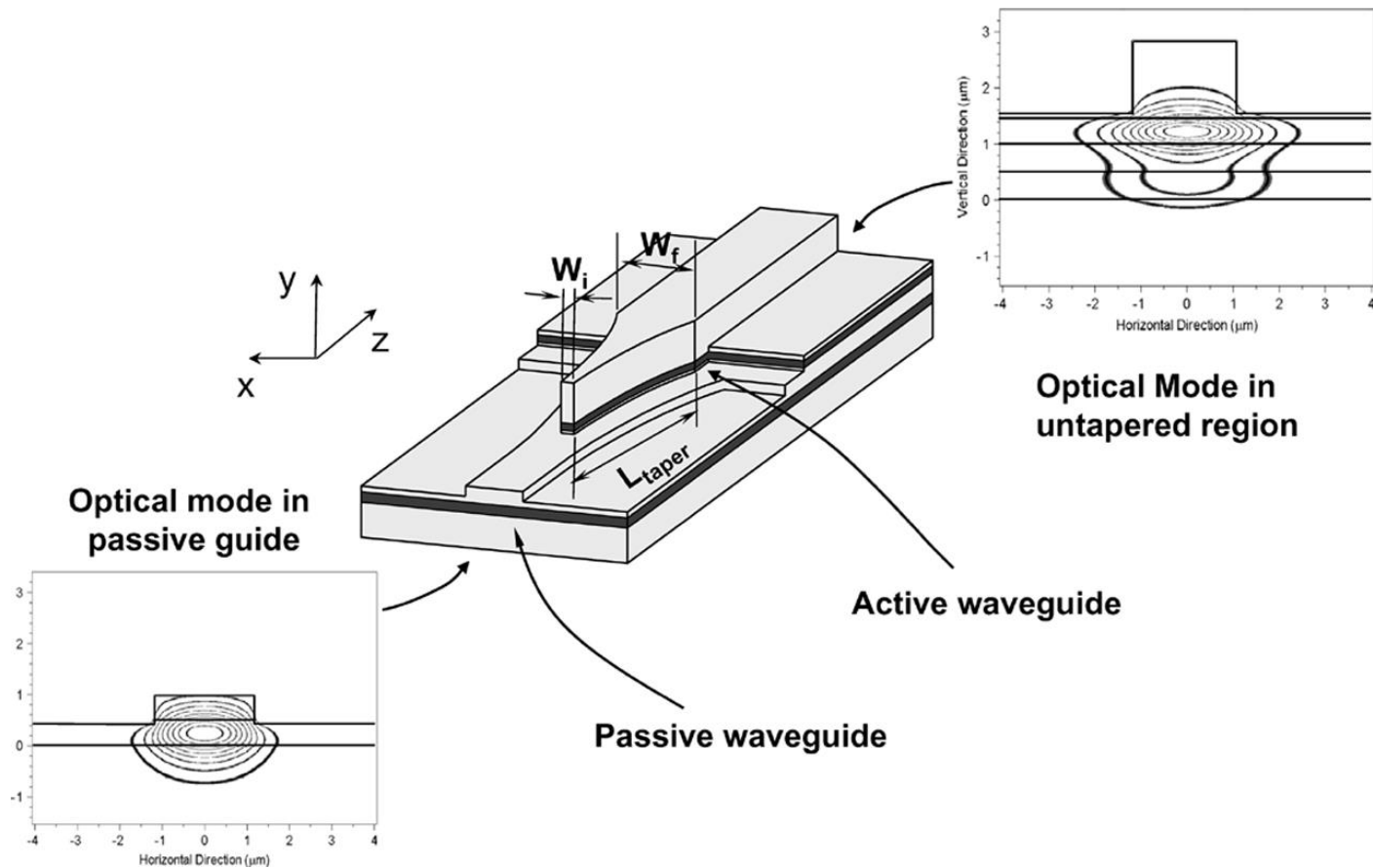


Amplified Waveguide



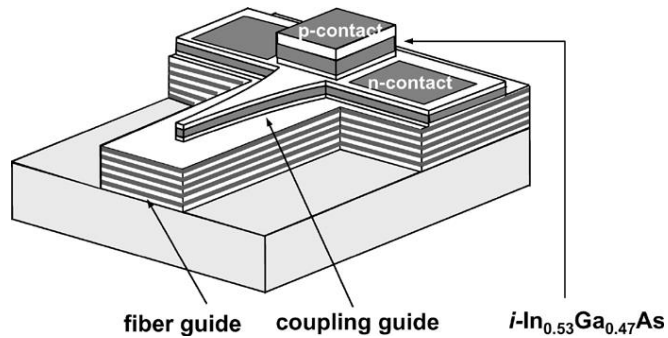
Xia, et al., JSTQE 11(1) 2005

- Active and passive waveguides are vertically displaced
- Light is transferred between waveguides using lateral taper mode transformers
- No regrowth required

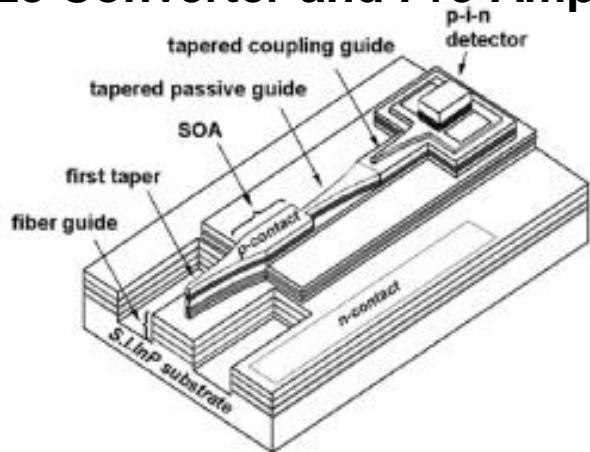


ATG Devices

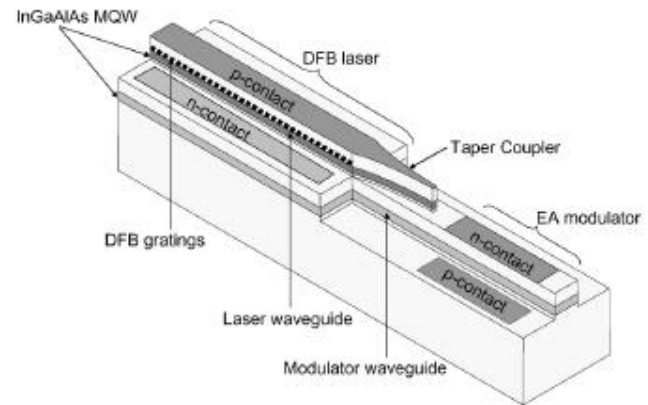
Photodiode with Integrated Spot-Size Converter



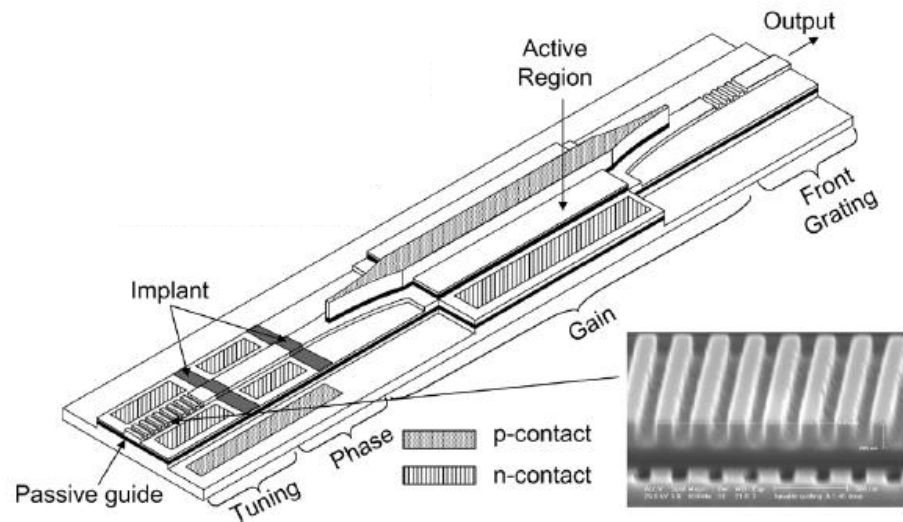
Photodiode with Integrated Spot-Size Converter and Pre-Amplifier



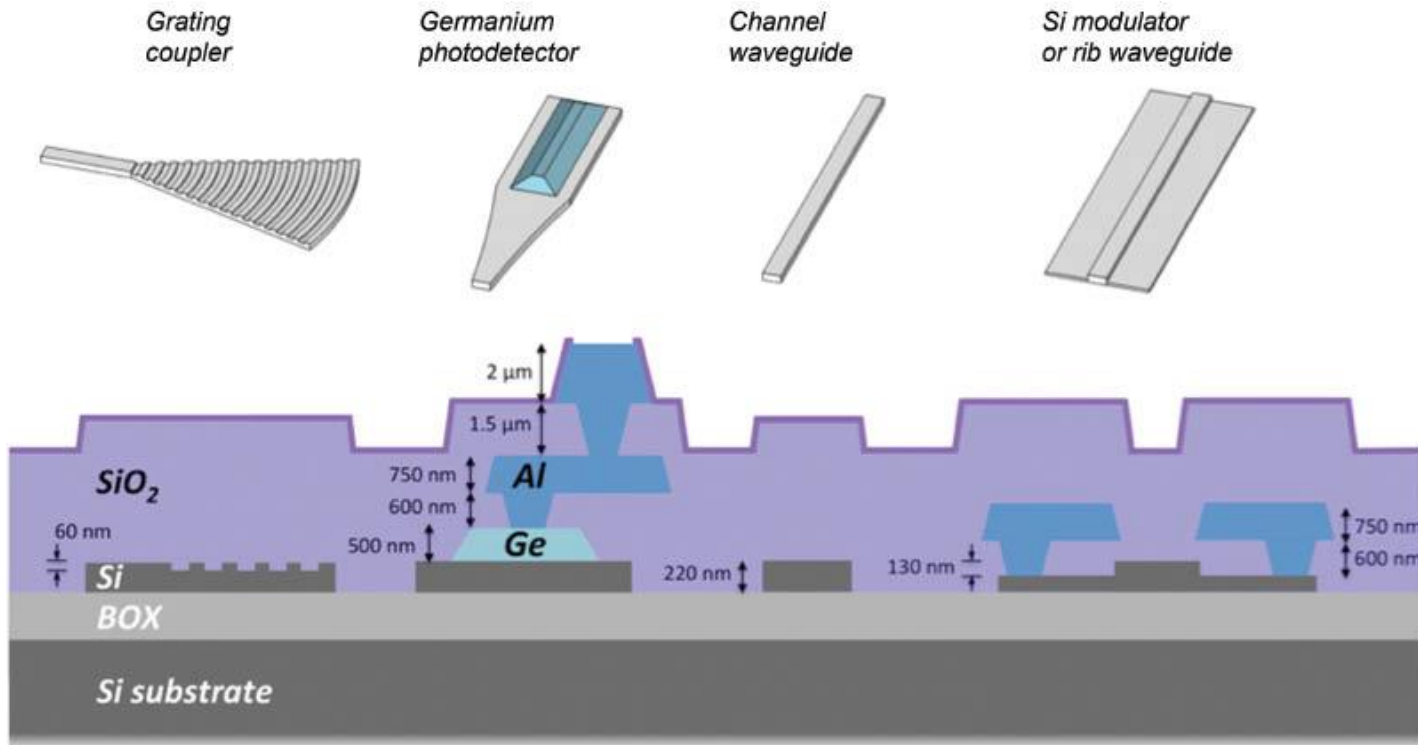
Wavelength Tunable DFB Laser



Wavelength Tunable DBR Laser



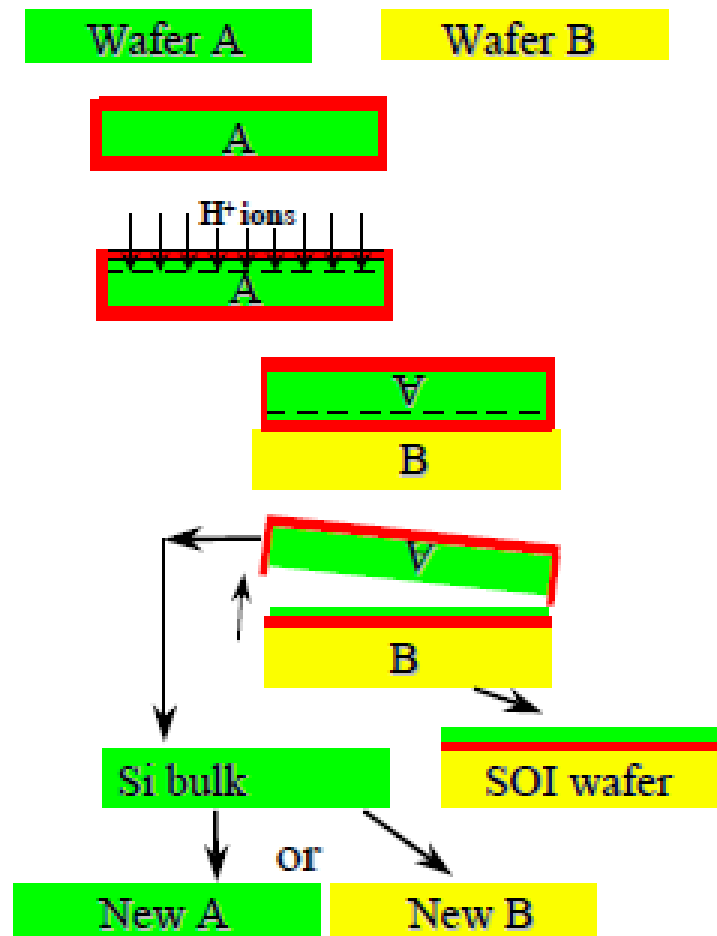
Silicon Photonics (SiPh)



A. Novack et al., Nanophotonics, 2014

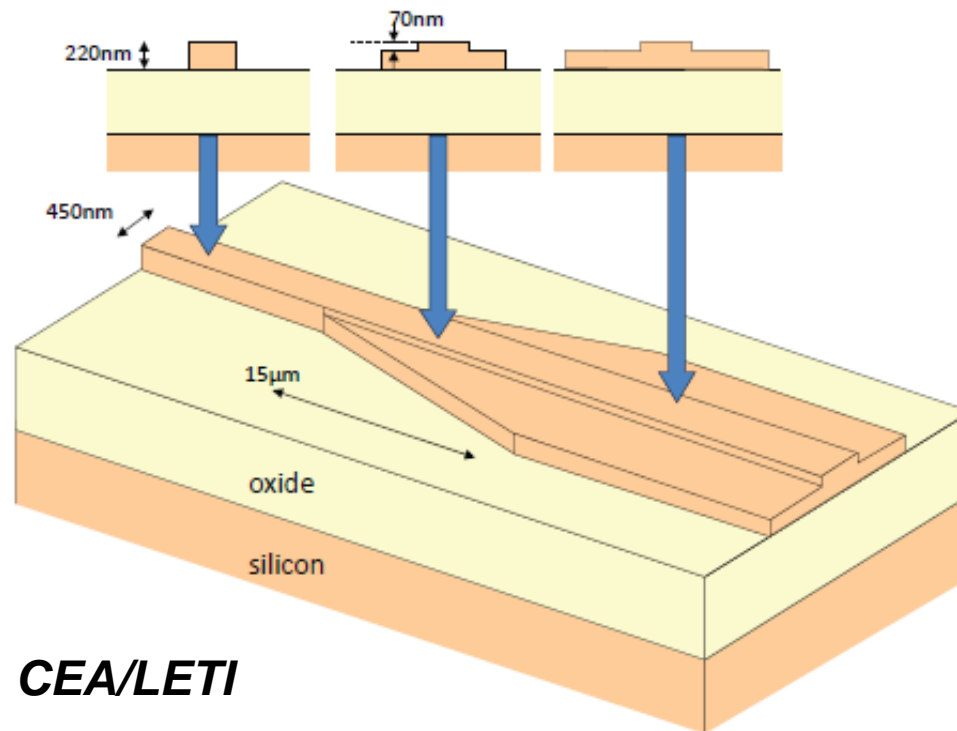
Silicon on Insulator (SOI)

- 1 Initial silicon wafers A & B
- 2 Oxidation of wafer A to create insulating layer
- 3 Smart Cut ion implantation induces formation of an in-depth weakened layer
- 4 Cleaning & bonding wafer A to the handle substrate, wafer B
- 5 Smart Cut - cleavage at the mean ion penetration depth splits off wafer A
- 6 Wafer B undergoes annealing, CMP and touch polish => SOI wafer complete
- 8 Split-off wafer A is recycled, becoming the new wafer A or B



***SOITEC**

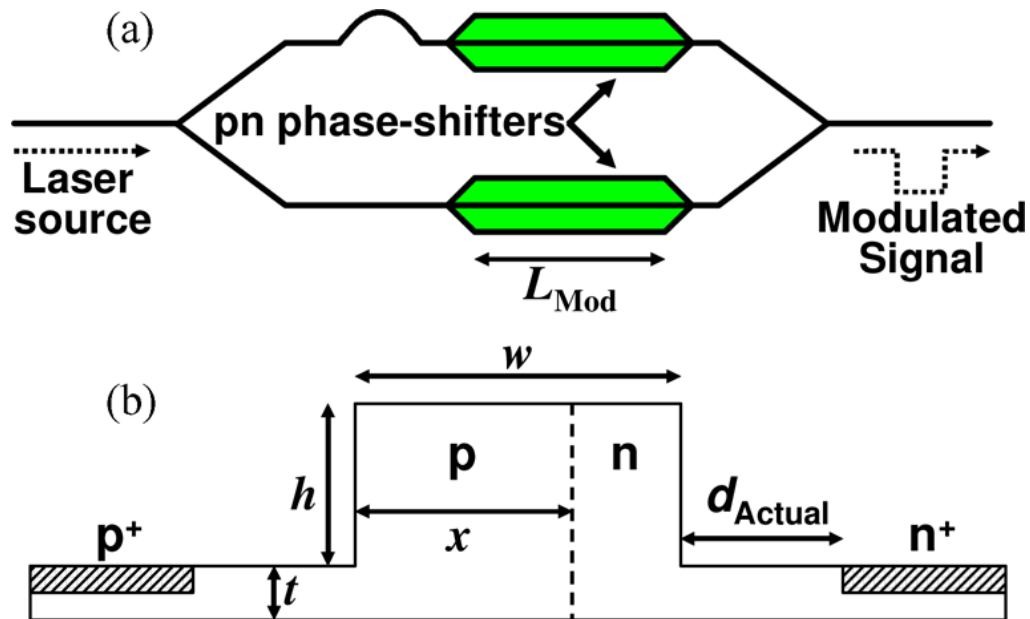
SOI Integrated Passives



CEA/LETI

- **Strip waveguides typically have loss of 2 dB/cm and can achieve very tight bending radius**
- **Rib waveguides typically have loss of 0.3 dB/cm**

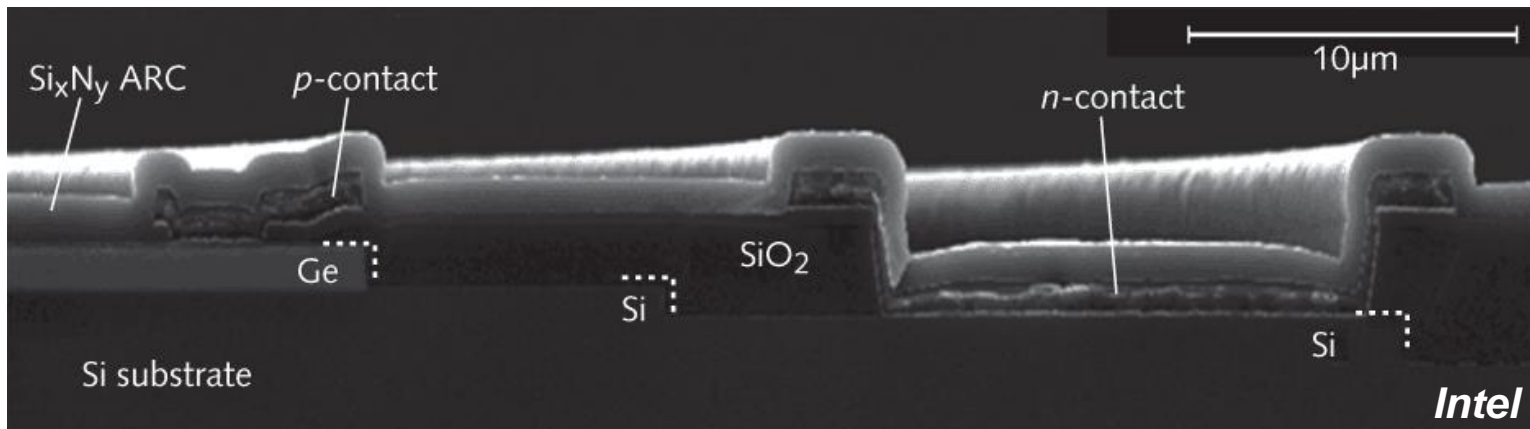
SOI Integrated Actives



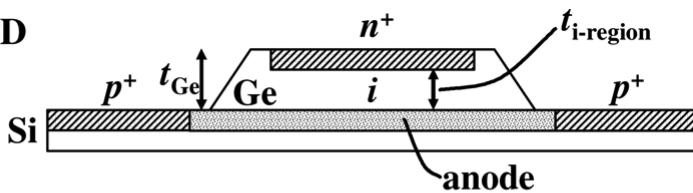
Liow, et al., JSTQE 16(1) 2010

- Modulator structures typically rely on plasma dispersion (carrier injection or depletion)
- p-n junction formed using ion implantation
- Junction location optimized for overlap of mode with carriers

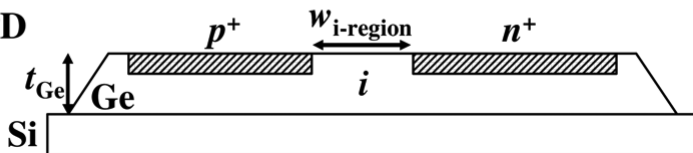
SOI Integrated Actives



(a) VPD



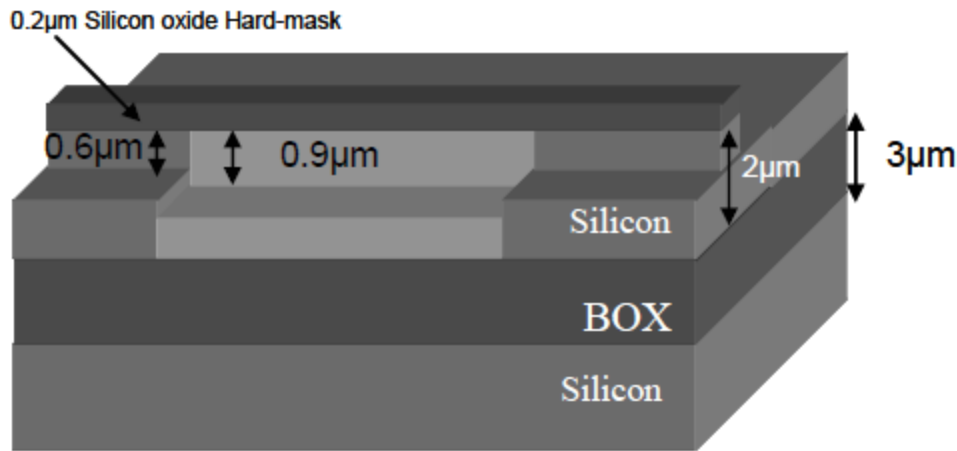
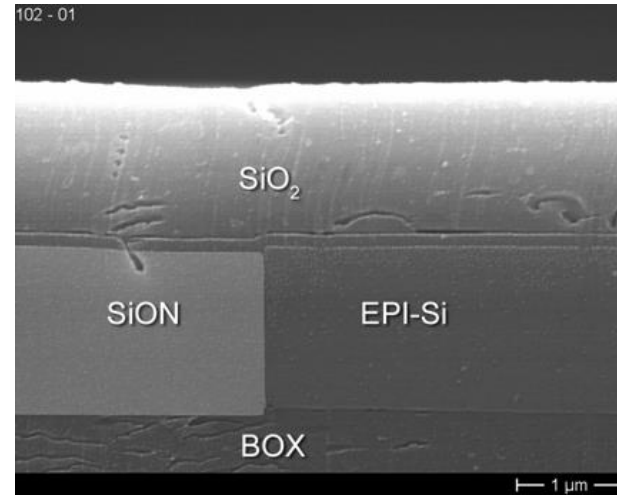
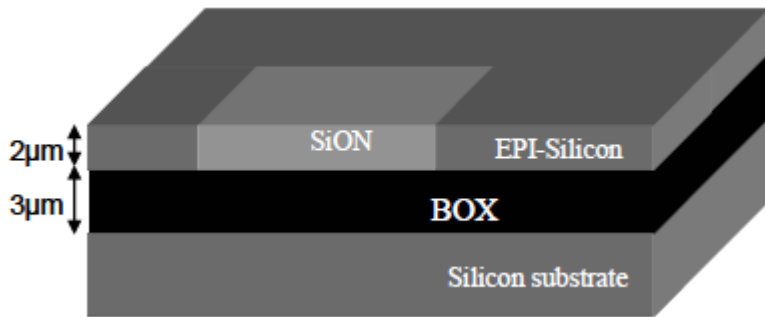
(b) LPD



Liow, et al., JSTQE 16(1) 2010

- Ge for photodetection at 1.55- μm
- Ge typically grown on Si using CVD techniques
- Challenging because lattice mismatch is 4%

SOI and SiON Waveguides

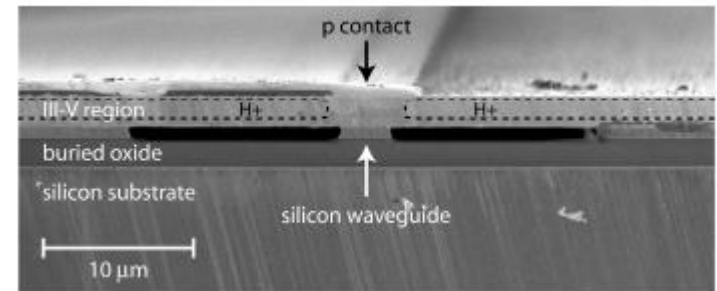
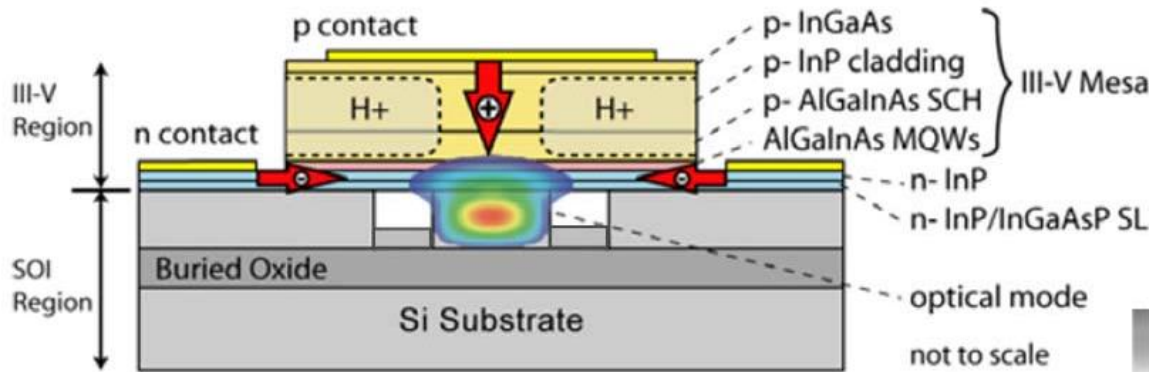


- **SOI waveguides ideal for sharp bends**
- **SiON waveguides yield lower loss and also less susceptible to thermal drift**

Cohen et al., Intel

III-V/Si Wafer Bonding

Si/InP Evanescent Devices

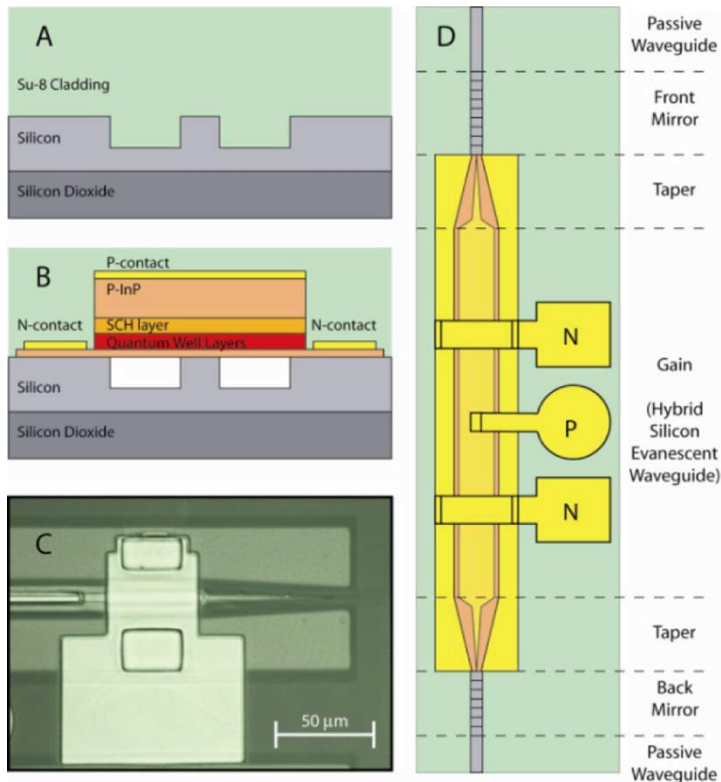


Fang et al., Optics Express 14(20) 2006

- Direct wafer bonding of InP to processed SOI wafer
- Following bond, remove InP substrate and fabricate III-V structure

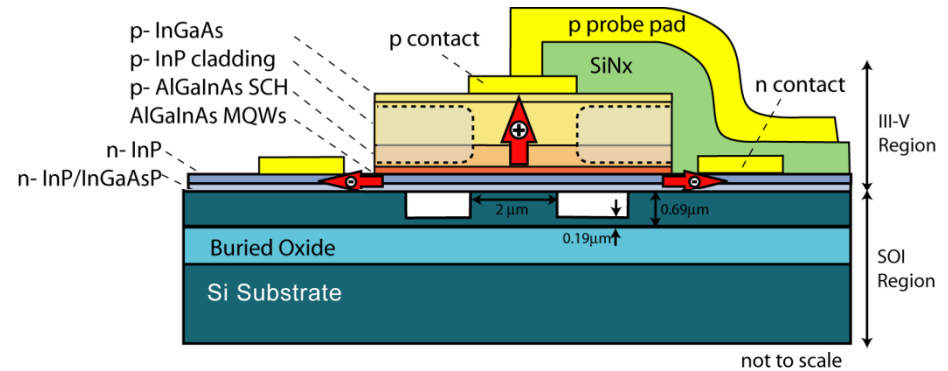
III-V/Si Wafer Bonding

DBR Laser



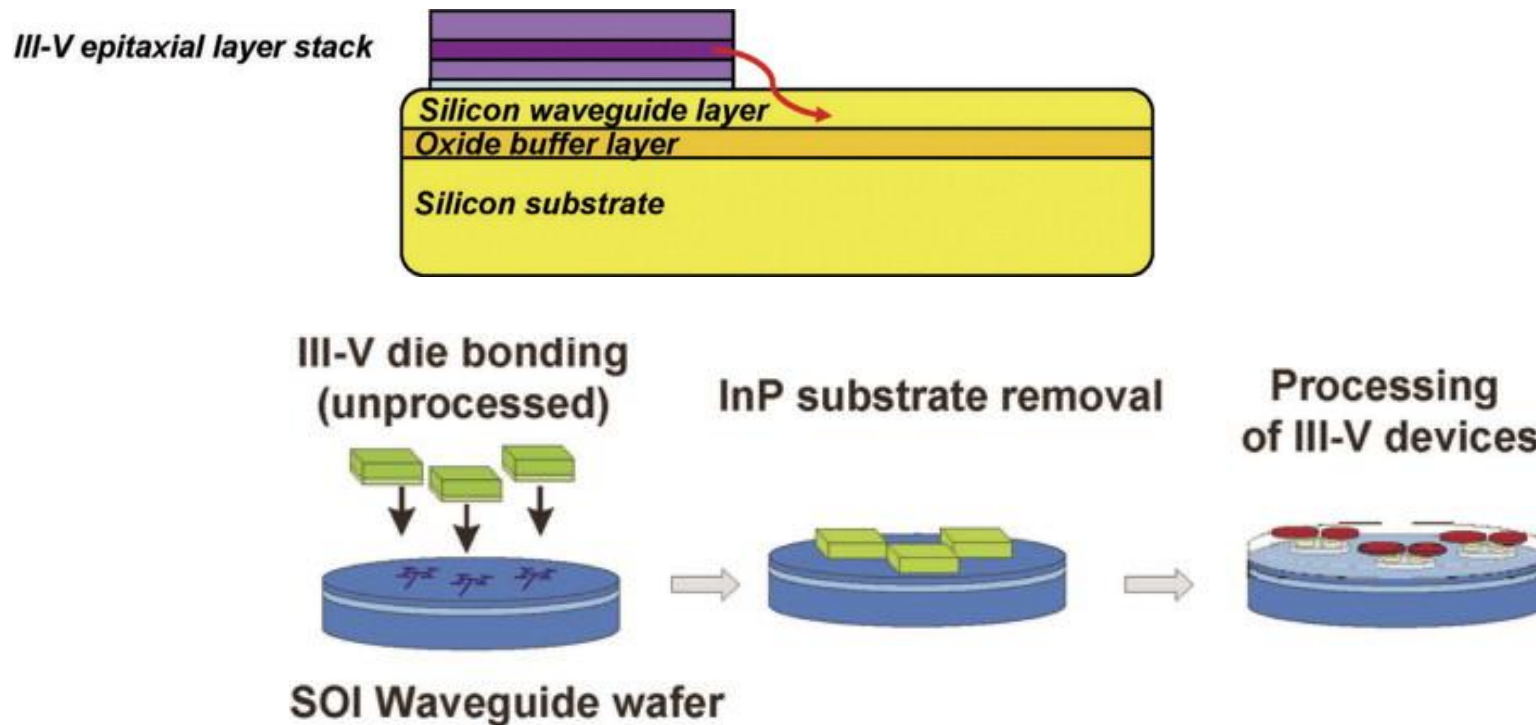
Fang et al., PTL 20(20) 2008

Waveguide Photodiode



Park et al., Optics Express 15(10) 2007

III-V/Si Adhesive Bonding

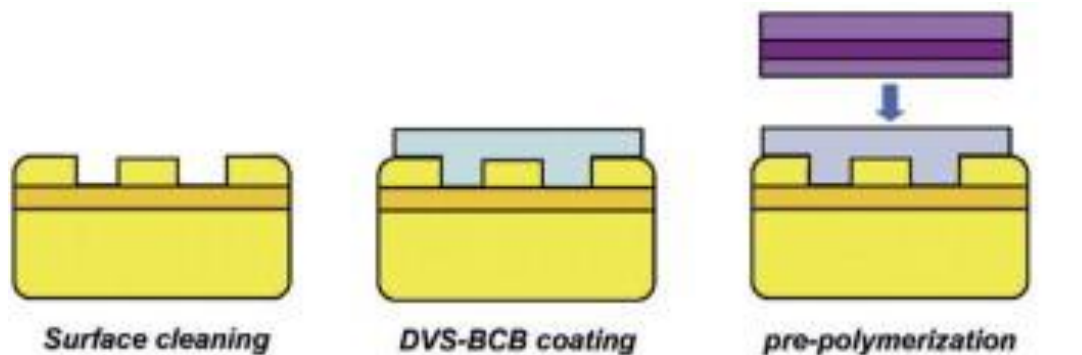


Roelkens et al., Materials Today, 20(7-8) 2007

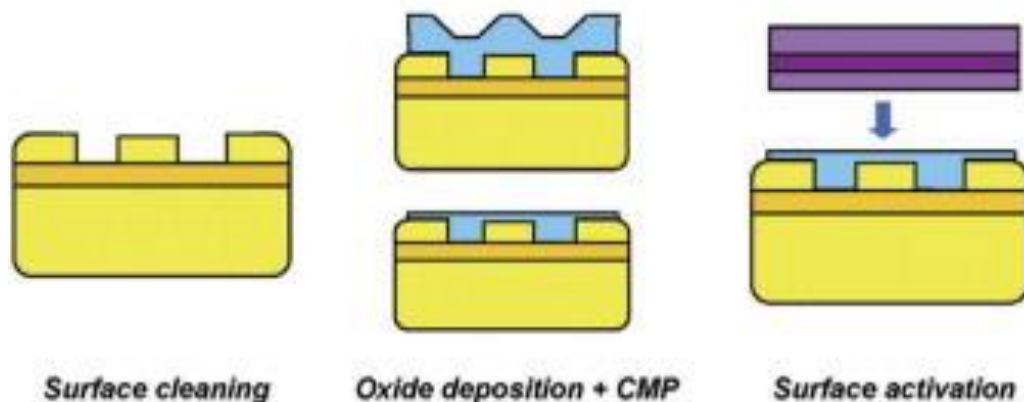
- **Local integration of III-V chips for efficient use of material**
- **Use of adhesive material for more forgiving process**

III-V/Si Adhesive Bonding

Adhesive Bonding using DVS-BCB

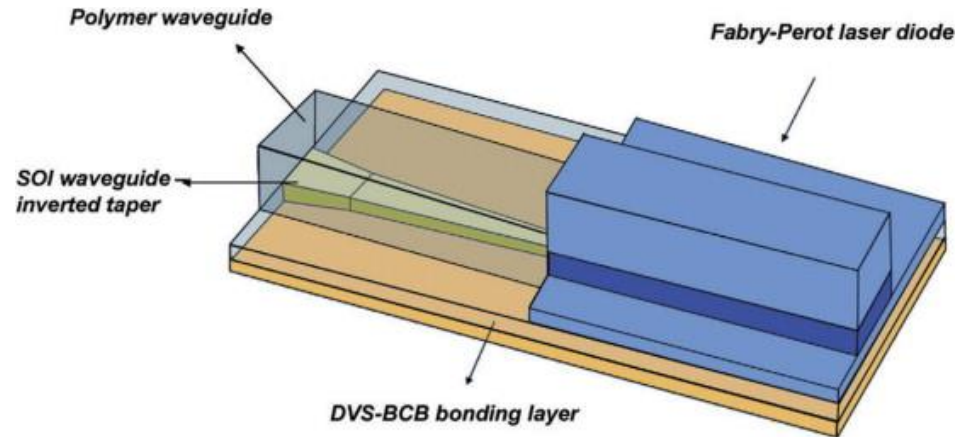
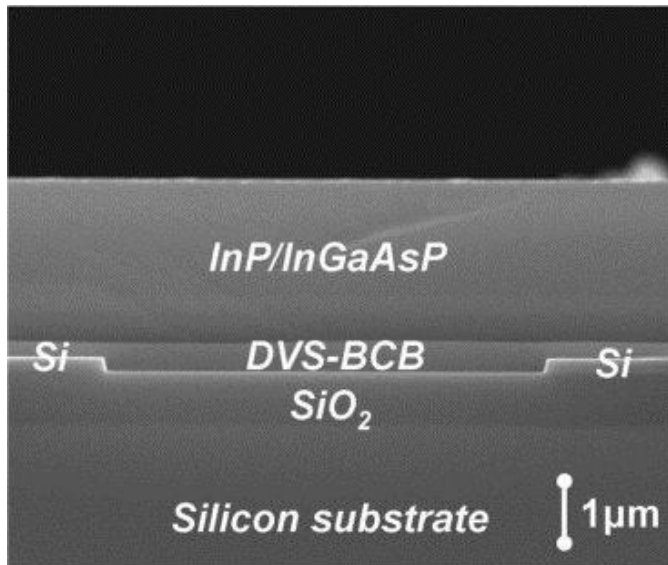


Direct molecular wafer bonding

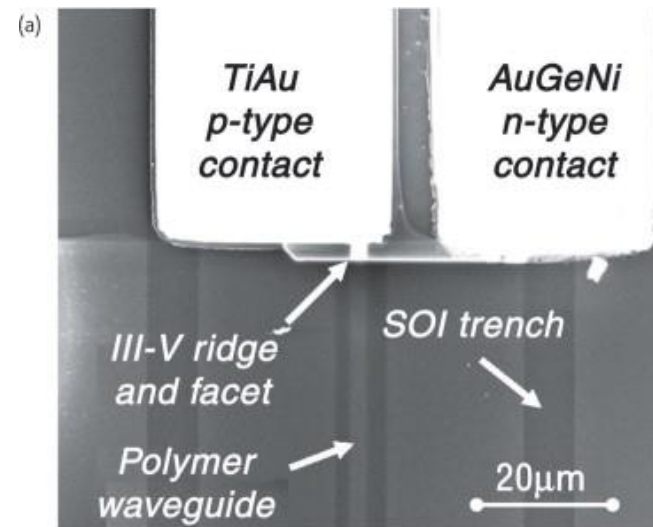


- DVS-BCB spin-coated on processed SOI wafer and partially cured
- III-V dies are attached and stack held at temperature to polymerize BCB
- Process more forgiving with regard to surface quality requirements and surface roughness

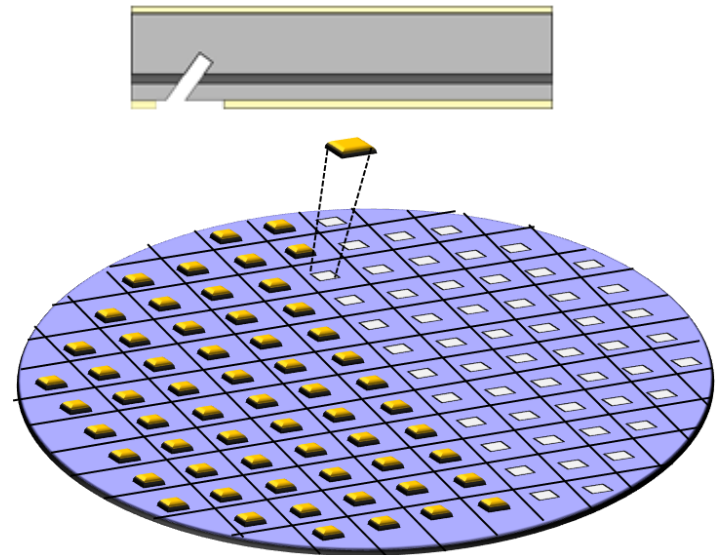
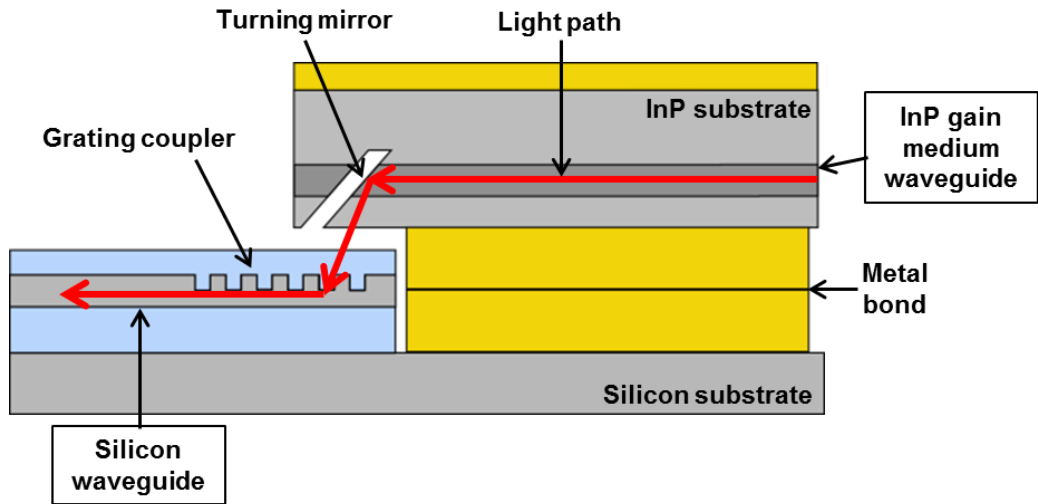
III-V/Si Adhesive Bonding



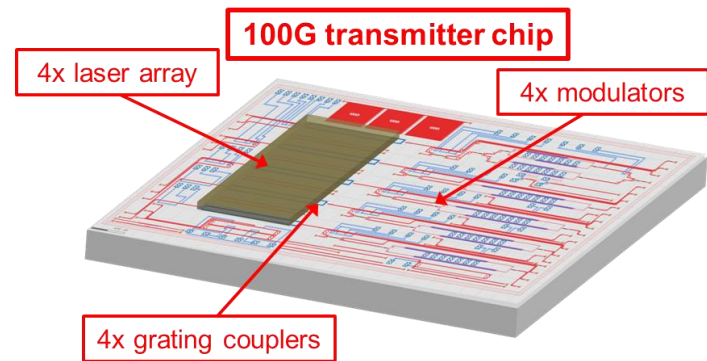
- After attachment of III-V chip, polymer waveguide is formed into an inverted taper structure for coupling from III-V to Si waveguide



3D Hybrid Integration



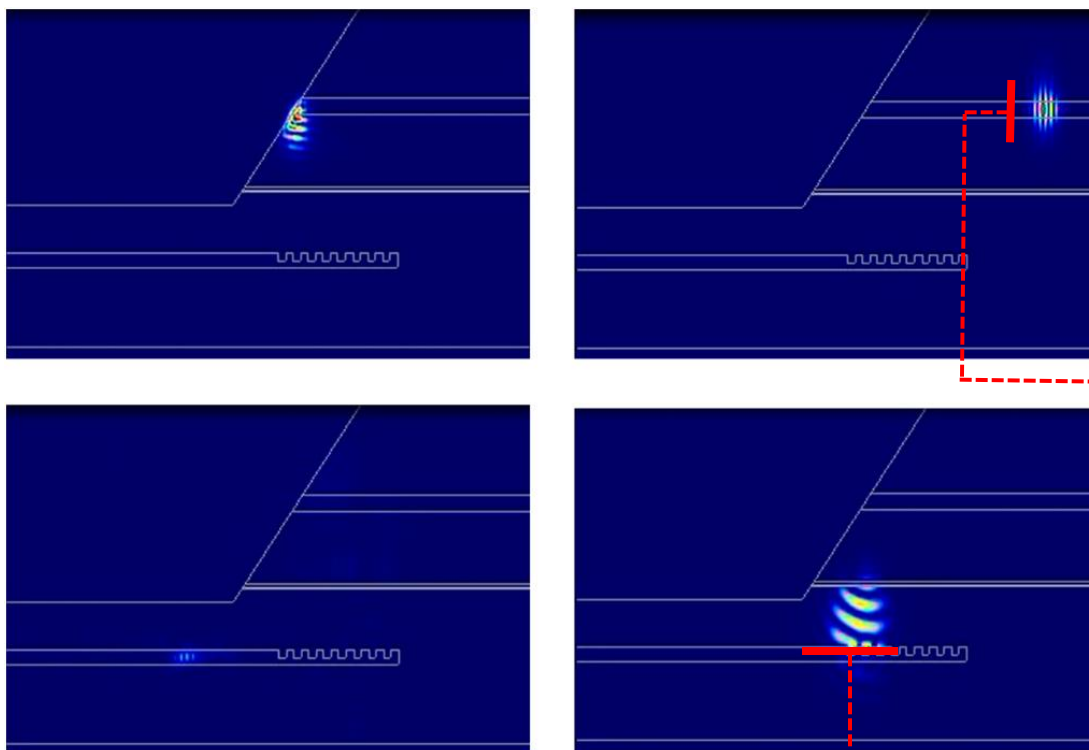
- Laser or gain with integrated **total internal reflection (TIR) turning mirror** coupled to Si with **grating coupler**
- Chips attached with standard IC bonding techniques
- Could be carried out at wafer level in backend step
- P-side down bond to Si substrate for heat removal



B. Song, et al., ECOC 2015

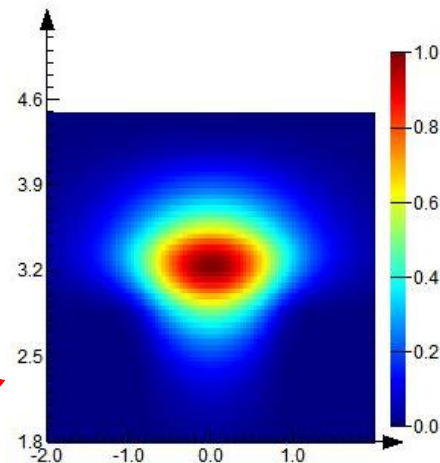
3D Hybrid Integration

Light propagation and coupling

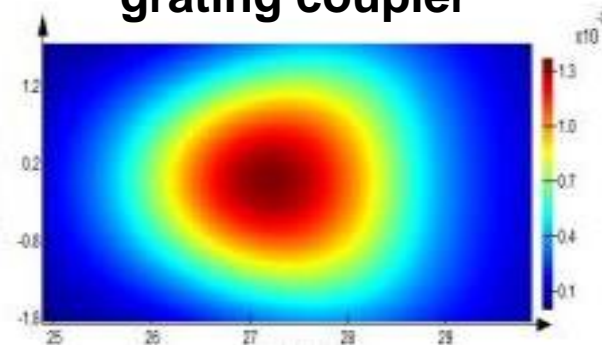


TIR mirror for **surface emission** and grating coupler for **surface coupling**

Mode in InP waveguide

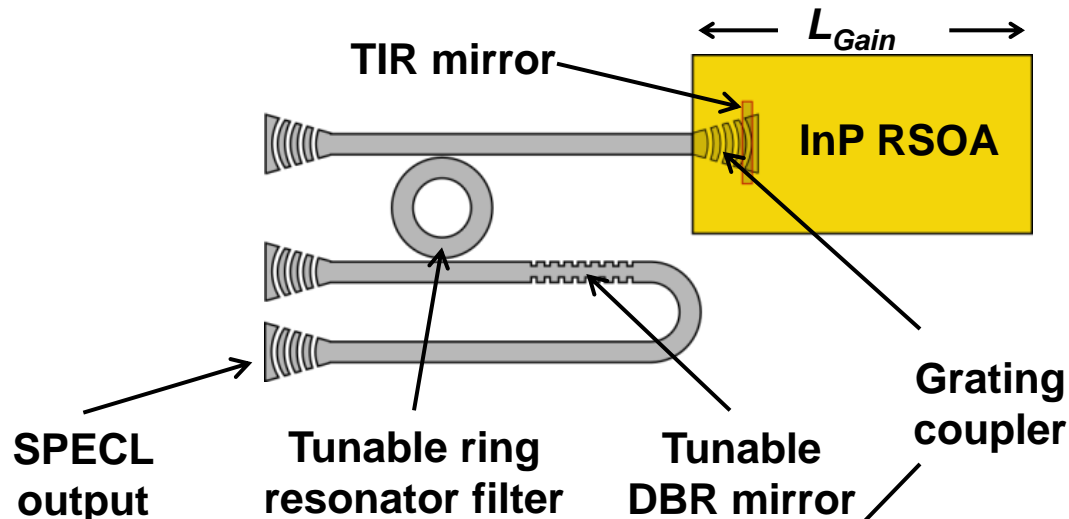


Mode incident on grating coupler

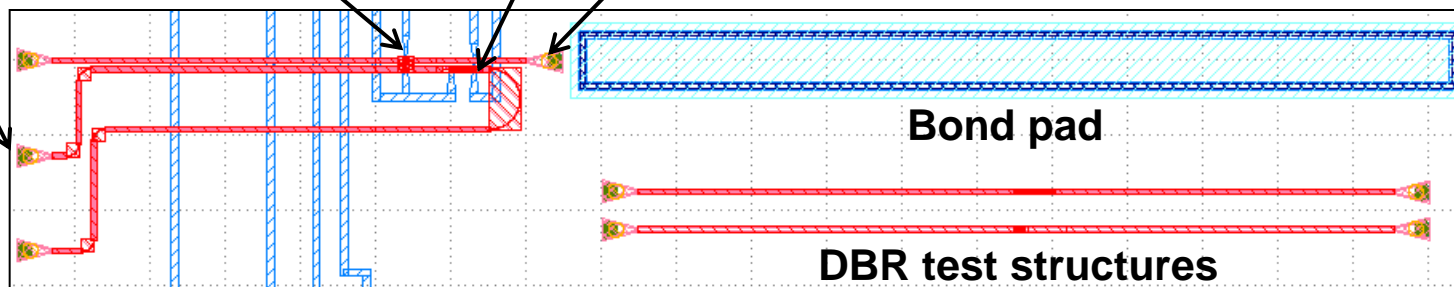
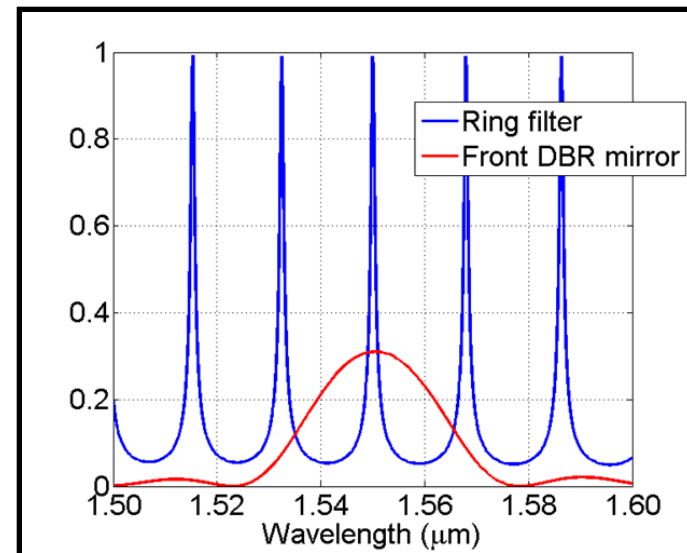


Silicon Photonic External Cavity Laser (SPECL)

SPECL schematic



SPECL concept

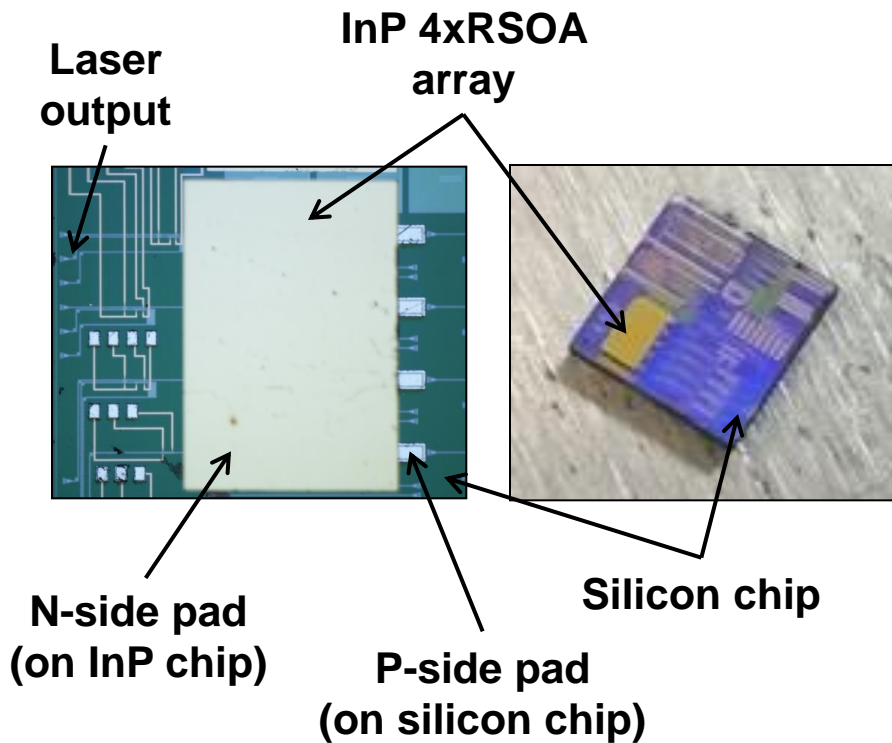


Silicon layout

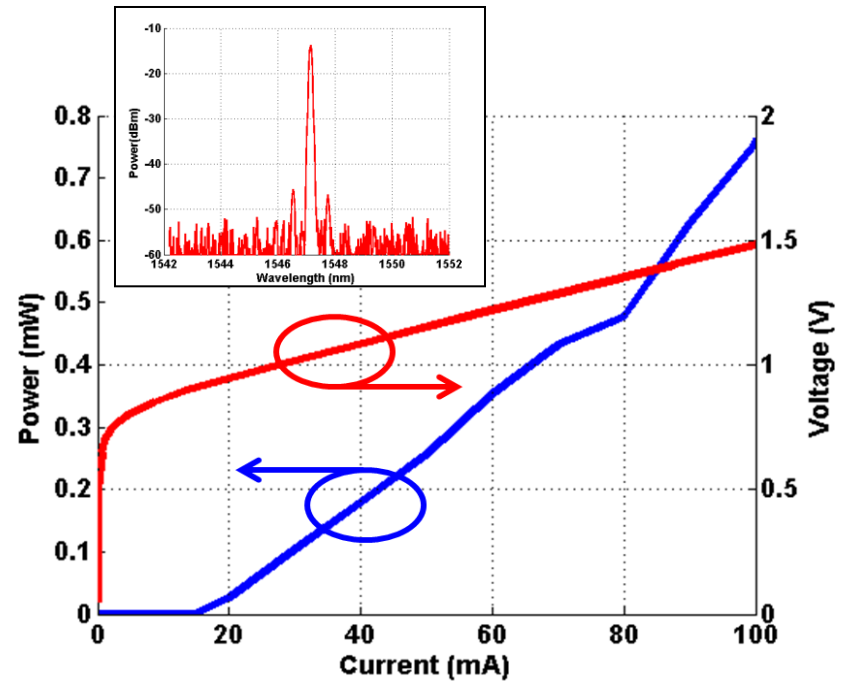
P. Contu et al., IPC 2013

3D SPECL Demonstration

Bonded chips

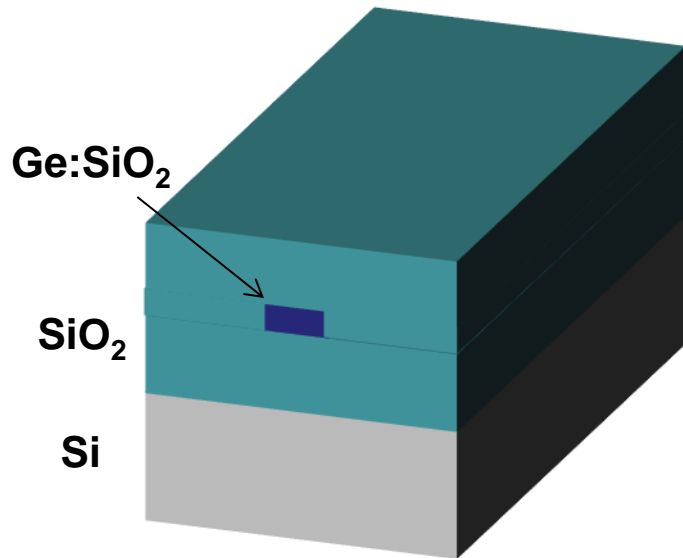


Lasing characteristics



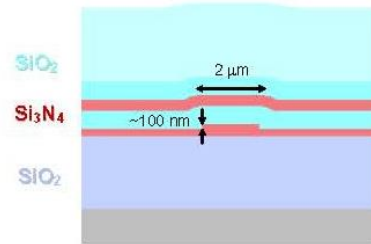
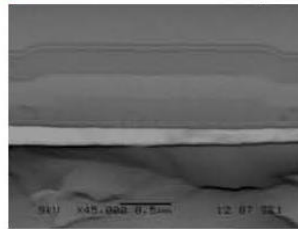
Planar Lightwave Circuit (PLC)

PLC waveguide

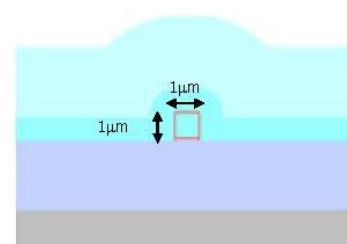
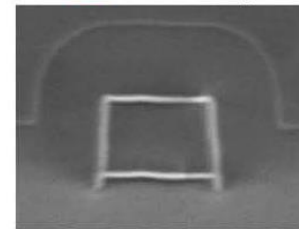


Lionix waveguides

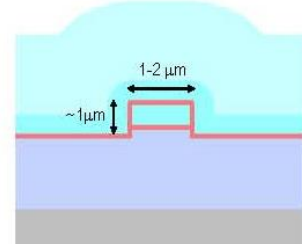
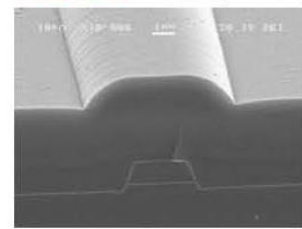
covered I'-shape



box-shape



A-shape



- **Low index contrast photonic materials system: SiO₂, SiON, SiN, ... (large devices, low loss)**
- **Cladding material: SiO₂**
- **Core materials: doped glass (Ge:SiO₂), SiON, SiN**

InP/PLC Hybrid Integration

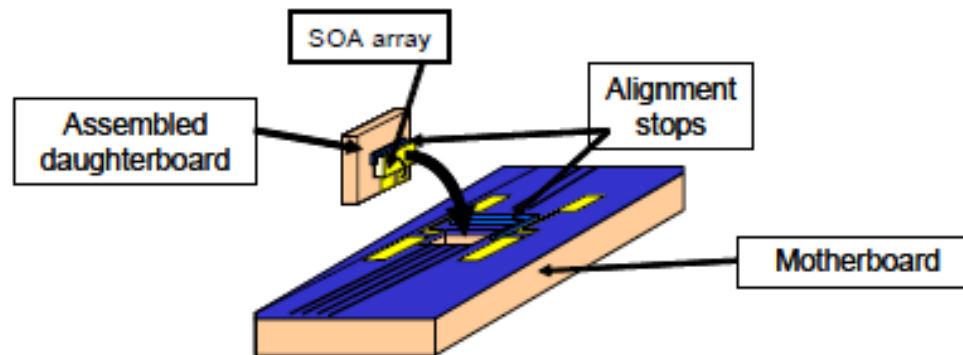


Figure 1: Schematic diagram of the CIP hybrid integration platform with passive assembly.

Poustie et al., CIP

- InP active chip is flip-chip bonded to daughter board
- Daughter board is inserted into micromachined hole in silica on silicon motherboard
- InP chips are butt-coupled to silica passive waveguides

InP/PLC Hybrid Integration

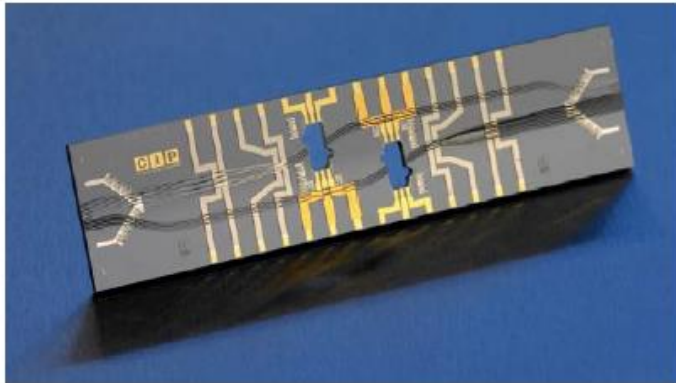


Figure 4: Photograph of a 4 channel SOA-MZI motherboard PLC.

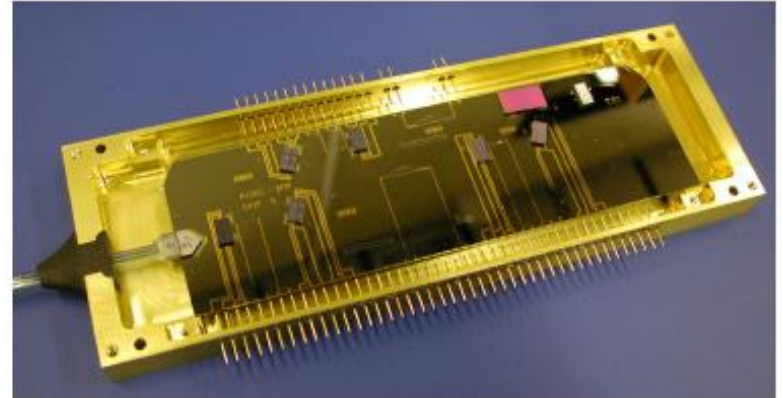
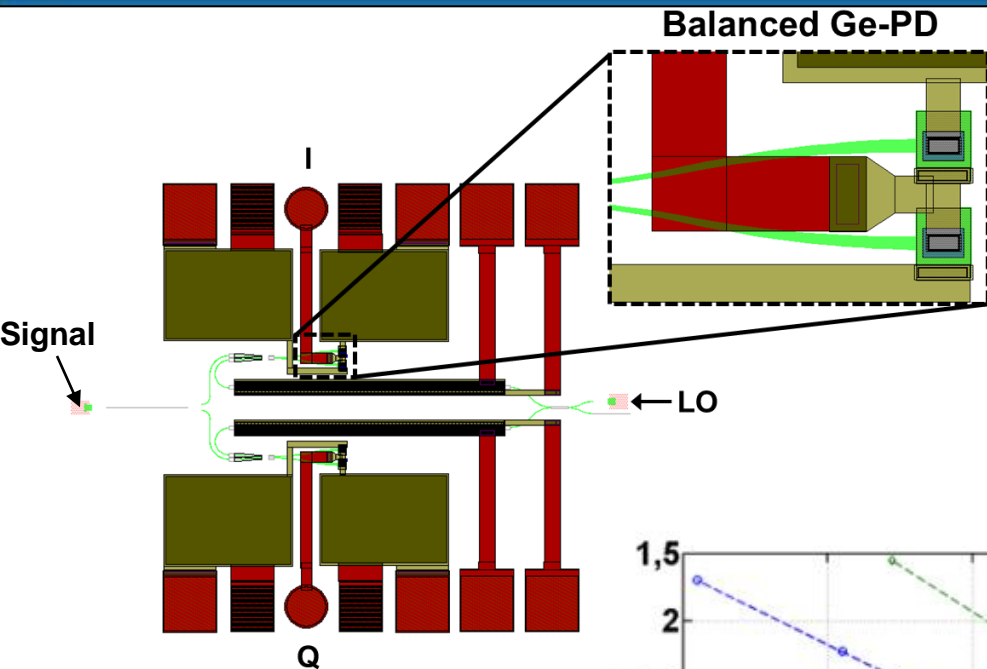


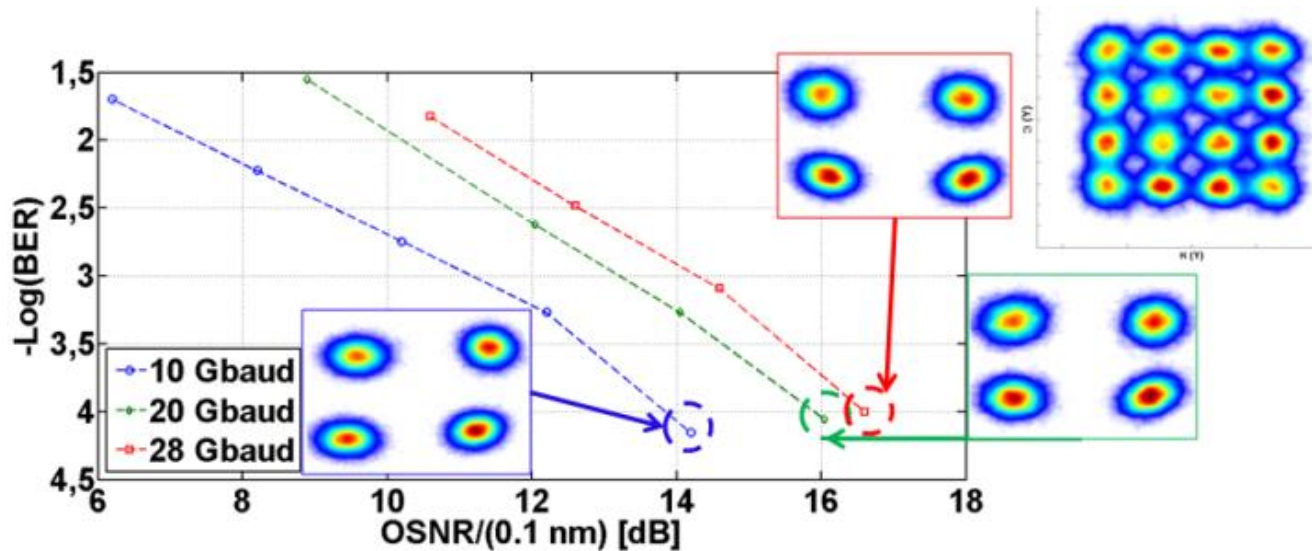
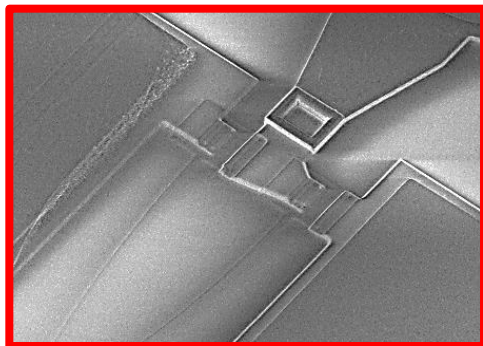
Figure 7: Photograph of the fabricated 40Gb/s BMR circuit.

Poustie et al., CIP

SiPh Coherent Receiver

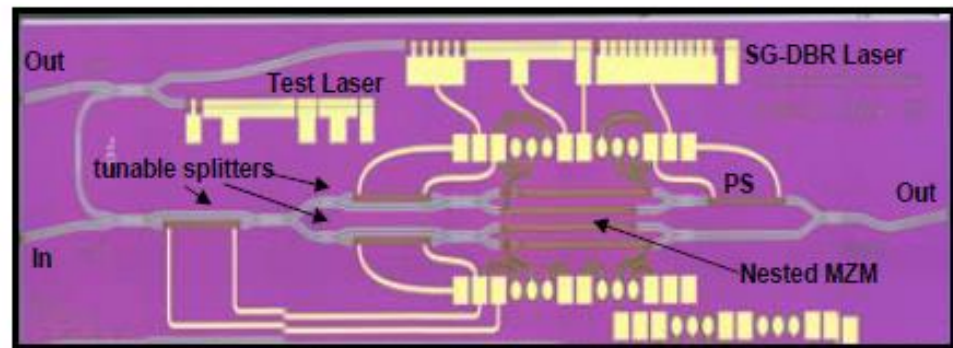
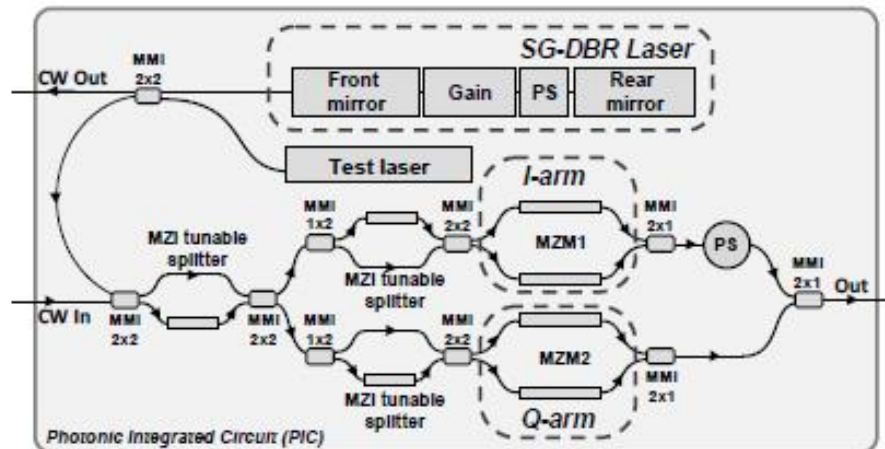


- Coherent receiver with optical hybrid free of waveguide crossings
- Compact ($0.8 \times 1.0 \text{ mm}^2$)
- Integrated on-chip MIM capacitors for DC decoupling
- **56-Gb/s QPSK and 80-Gb/s 16-QAM**



F. Gambini, et al., Group IV Photonics 2014

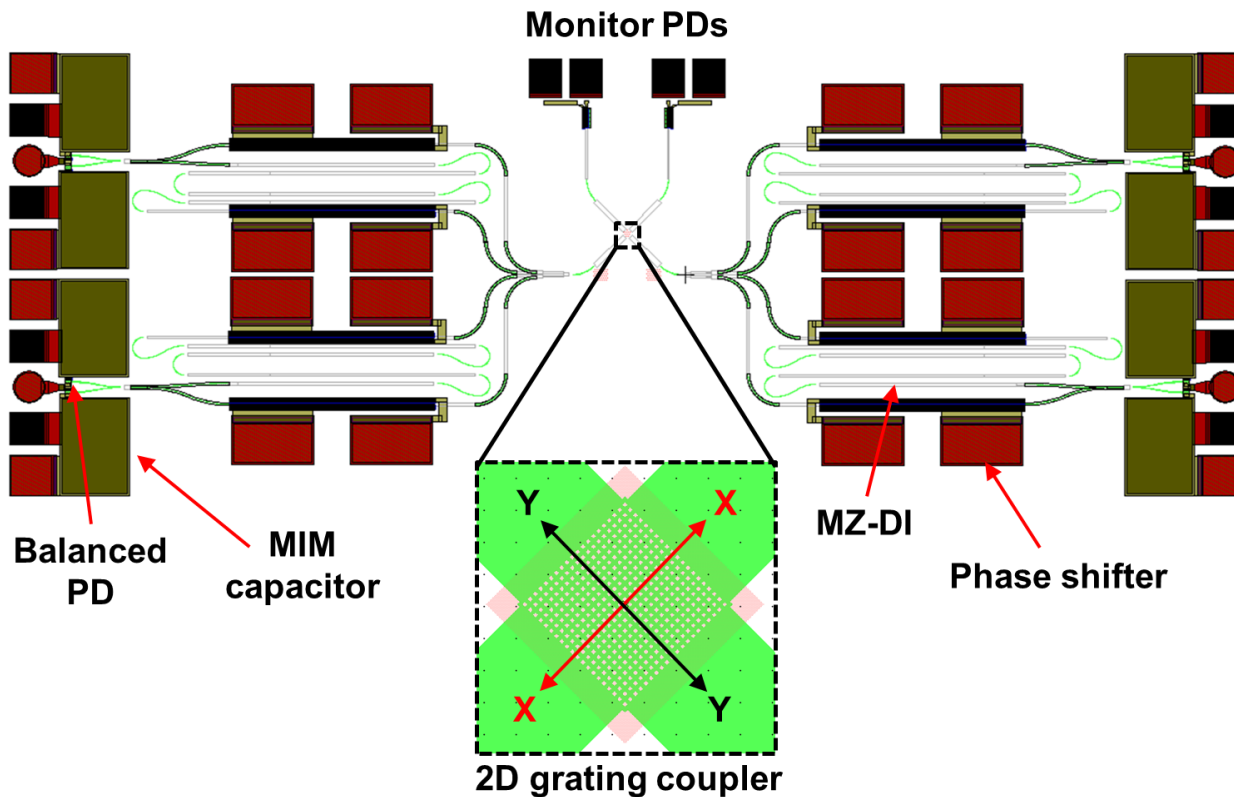
InP Coherent Transmitter



N. Andriolli, et al., Optics Express, 2015.

- Dual-parallel Mach-Zehnder structure with integrated lasers, phase shifters and couplers
- Fabricated in multi-step epitaxial foundry process at Oclaro (through Jeppix)
- Designed with flexibility of discrete-component system

100-Gb/s Noncoherent SiPh Receiver



- Dual polarization and phase modulation for high bit rate
- Mach-Zehnder delay interferometers for phase to intensity conversion
- Small footprint (3 x 1 mm²), no LO laser, simpler DSP → **low power**

J. Klamkin, et al., Optics Express 2014